AUSTRALIA'S NATIONAL SCIENCE AGENCY
www.csiro.au

Groundwater balance in northwest Bangladesh – modelling and scenario analyses

A project of the South Asia Sustainable Development Investment Portfolio (SDIP)

Sreekanth Janardhanan [J], Md Monirul Islam[2], Md Tohidul Islam[2], Mohammad A Mojid[3], Jorge Peña-Arancibia[1], Geoff Hodgson[1], Trevor Pickett[1], Fazlul Karim[1], Mohammed Mainuddin[1], Santosh Aryal[1], Md Tarikul Islam[2], Md Atiqur Rahman[2]

[1] CSIRO, Australia
[2] Institute of Water Modelling, Bangladesh
[3] Bangladesh Agricultural University

November 2021

Citation

Janardhanan S, Islam MM, Islam MT, Mojid MA, Peña-Arancibia JL, Hodgson GA, Pickett T, Karim F, Mainuddin M, Aryal SK, Islam MT, Rahman MA (2021) Groundwater balance in the northwest Bangladesh – modelling, uncertainty and scenario analyses. South Asia Sustainable Development Investment Portfolio project. CSIRO. pp180

This groundwater study was undertaken as part of the Sustainable Development Investment Portfolio (SDIP) project for Bangladesh from 2016 to 2020. The study was collaboratively undertaken by CSIRO researchers and engineers of the Institute of Water Modelling (IWM), Bangladesh.

Acknowledgements

The authors acknowledge support from the Department of Foreign Affairs and Trade (Australian government) for the Sustainable Development Investment Portfolio II program which, together with CSIRO, funded this study. We also acknowledge the cooperation of all SDIP partners in supporting the program. We also thank Susan Cuddy CSIRO for her support in its preparation for publication We also thank Susan Cuddy and Russell Crosbie for their constructive and comprehensive review of this report.

Copyright CSIRO 2021

Important disclaimer

Ethics

The activities reported herein have been conducted in accordance with CSIRO Social Science Human Research Ethics approval 030/17.

Sustainable Development Investment Portfolio

This report designed and implemented by CSIRO contributes to the South Asia Sustainable Development Investment Portfolio and is supported by the Australian aid program. Further details on CSIRO SDIP projects are available from http://research.csiro.au/sdip.

SDIP's goal is increased water, food and energy security in South Asia to support climate-resilient livelihoods and economic growth, benefiting the poor and vulnerable, particularly women and girls

SDIP 2020 objective: Key actors are using and sharing evidence, and facilitating private sector engagement, to improve the integrated management of water, energy and food across two or more countries - addressing gender and climate change.

Gender statement

All CSIRO SDIP projects consider gender. In this report, we have assumed that an improved, quantitative understanding of groundwater balance in northwest Bangladesh is of benefit to all, regardless of gender and other social factors. Excluding gender analysis, however, can lead to 'gender blind' tools, findings and decisions that reinforce existing gender inequities. This gap should be borne in mind when interpreting this report, and any application of its findings will need to integrate gender-specific and other social considerations to ensure benefits are distributed equitably.

EXECUTIVE SUMMARY

In this report we describe the development and application of numerical groundwater models for the 16 districts of the northwest Bangladesh region. These models were developed to simulate and analyse the impacts of historical and other groundwater development and climate scenarios on the groundwater balance and storage capacity within the region.

Four MIKE SHE models covering the northwest region were updated and calibrated to observed groundwater levels for the period 2005 to 2016. These models were used for the simulation of overall water balance and scenarios in the districts of northwest region by integrating catchment, river, unsaturated and saturated zones in a single modelling framework. Topography, precipitation, evapotranspiration, land use, vegetation, river flow and groundwater level data were used for updating and calibrating these models.

While the MIKE SHE model simulations gave a comprehensive representation of integrated water balance in the northwest Bangladesh, having them as four different computationally complex models limited the prospects of doing a comprehensive analysis of saturated zone water balance and especially storage changes in the aquifers.

A computationally faster, single-layer numerical groundwater model based on the MODFLOW code spanning the entire region was also developed and calibrated to investigate the long-term (1985 to 2016) groundwater balance in the region. The groundwater balance components simulated by the simpler MODFLOW model were compared to the corresponding values from the MIKE SHE models at the district scale to gain insights into the process details represented by these models.

The simpler MODFLOW model was constrained by the information available from the companion studies on water balance analysis, surface water modelling and remote sensing in addition to the groundwater level observations. The MODFLOW model was used for a probabilistic simulation and predictive uncertainty analysis of groundwater balance and long-term storage changes in the northwest. The probabilistic model simulation comprising thousands of model runs for model calibration and uncertainty analysis enabled to evaluate the groundwater balance changes corresponding to a wide range of plausible combinations of model inputs and parameters. This enabled better quantification of groundwater balance and storage change calculations accounting for prediction uncertainties.

The calibrated MIKE SHE models were used to analyse short-term groundwater responses corresponding to 2-year (50% dependable), 5-year (80 % dependable) and 25-year (dry) meteorological and hydrological conditions and considering expected irrigation water demand corresponding to future cropping patterns dominated by Boro rice.

Likely impact of increased abstraction on groundwater levels

The simulation analyses indicated that:

- increased abstraction results in deepening of water table in the dry season although it is likely to recover fully if the rainfall corresponds to 80% dependable or higher values for most areas.
- increased abstraction together with drier conditions (rainfall with 95% dependability or exceedance probability of 0.95) will result in groundwater mining or unsustainable use in larger areas predominantly in districts in the southwest including Nawabganj, Rajshahi, Naogaon and Joypurhat and some parts of the western districts including Dinajpur.

Likely impact of future climate on groundwater levels

Climate change can potentially cause significant change to groundwater resources by affecting the recharge and discharge processes. Five climate change scenarios were developed to simulate a range of possible future climates. This comprised 5 combinations of low, average and high rainfall and potential evapotranspiration (PET).

MIKE SHE simulations indicated that the short-term (annual) changes in groundwater levels are small among the 5 climate change scenarios. The analyses showed that groundwater levels in the alluvial aquifer are very responsive to meteorological and hydrological conditions and agricultural water use. If rainfall should fall below average and groundwater use is not adjusted to this, it is likely to result in lower groundwater levels in the summer season which could restrict groundwater access by suction pumps in large areas within the northwest. This does not necessarily indicate unsustainable use as groundwater levels recuperate through recharge in the monsoon season. However, simulations indicate that continued groundwater use combined with less than average rainfall in dry years (1-in-25-year rainfall) could result in large areas where groundwater levels do not recover after the monsoon recharge. The analyses indicated that:

- climate change combined with increased areas of Boro rice cultivation could exacerbate unsustainable use of groundwater.

Long-term groundwater balance changes

Long-term groundwater balance analysis was undertaken using the probabilistic MODFLOW model. The analysis indicated that in the long-term period between 1985 and 2016, an average of 20% of the rainfall entered the aquifer as gross recharge annually. In addition to this, a significant amount of water entered the aquifer through recharge from rivers. Owing to the shallow groundwater level in most areas, a significant share of that gross recharge contributed directly to actual evapotranspiration (ETa) by means of uptake from the root zone or shallow pumping.

The long-term average net recharge from rainfall was estimated as 9% of the annual average rainfall.

Gross and net recharge were estimated to be significantly higher than average in districts like Nawabganj, Naogaon and Rajshahi where groundwater extractions have been high. This is likely because of the lowering of water levels due to pumping, inducing additional recharge than occurring under pre-development conditions. While parts of these districts may have achieved potential maximum recharge, other areas may have potential opportunity for more induced recharge.

Groundwater contribution to ETa was estimated as high in the region with an average of 37 % of the ETa contributed by groundwater either as direct uptake from the root zone or pumping from shallow or deep wells.

Groundwater storage changes

The MODFLOW model simulation indicated that, across the northwest region:

- groundwater storage is likely declining at a small rate of –1.5 mm/year resulting in a likelihood of decline of groundwater levels at an average rate of –19 mm/year across the region.

An alternate conceptual model, representing net recharge and pumping, indicated that:

- the average groundwater storage loss could be potentially as much as –6.4 mm/year corresponding to an average groundwater level decline of –85 mm/year across the region.

The rate of groundwater depletion is relatively small in northern districts and higher in the southern districts, especially around the Barind tract area . This is indicative of the state of development and vulnerability of the system, especially when factors such as climate change or increasing demand put additional stress on the system in future.

The highest rates of groundwater storage decline were simulated for the districts of Nawabganj, Rajshahi and Naogaon with groundwater level declines in Nawabganj as high as –250 mm/year in pockets where specific yield is low. Such levels of decline have actually been observed in several bores in these districts. Current groundwater use is likely to be unsustainable in such pockets.

While pockets of over-exploitation exist, simulation analysis showed that increased pumping did not cause long-term groundwater storage depletion consistently in all areas within the northwest. In areas where the maximum recharge potential was achieved, pumping could directly result in groundwater mining and storage loss. This could be true in areas, especially in the Barind tract, within the districts of Nawabganj, Naogaon and Rajshahi where long-term storage depletion is relatively high. The modelling study could be extended at a finer scale to identify the hot spots of over-exploitation and other areas where further development is possible.

Management implications

Simulation analysis showed that

- reducing groundwater use with potential replacement using surface water where possible can decrease the long-term storage depletion.
- increased pumping could potentially increase recharge from the rivers (to groundwater) in many districts.

Such responses indicate that:

- pumping management and conjunctive surface water / groundwater management strategies could be adopted for more sustainable management.

Identifying conjunctive management strategies would require further analyses. The data sets and models developed in this study could be extended to do scenario analyses for evaluating management strategies.

CONTENTS

FIGURES

TABLES

TERMS AND ABBREVIATIONS

TERM/ABBREVIATION	DESCRIPTION
bgl	Below ground level
DTW	Deep tube well
ET	evapotranspiration
ETa	Actual evapotranspiration
ETg	Evapotranspiration from groundwater
EVT	Evapotranspiration package in MODFLOW (groundwater model)
GW-SW	Groundwater to surface water
IES	**I**terative **E**nsemble **S**moother approach, available in the PEST++ software suite
Kh	Hydraulic conductivity
MAE	Mean Absolute Error
MIKE II	River Modelling software suite MIKE 11
MIKE SHE	Integrated Hydrological Modelling software MIKE SHE
Mm^3	Million metres cubed (volume measure)
MODFLOW	Groundwater flow modelling software MODFLOW
OL	Overland flow
PEST	**P**arameter **Est**imation software
RMSE	Root mean square error
STW	Shallow tube well
SW-GW	Surface water to groundwater
SY	Specific yield
SZ	Saturated zone
UZ	Unsaturated zone

1 INTRODUCTION

During the last few decades, changes in cropping and planted area in northwest Bangladesh are widely considered to have impacted the volumes of groundwater withdrawn for irrigation. Quantifying the groundwater balance under current stresses and investigating the effects of evolving climate, hydrology and agricultural water use are crucial for understanding the sustainability of groundwater use for irrigation in the northwest region of Bangladesh, and to develop management and mitigation strategies.

Groundwater models can be used to understand the status quo and predict the effects of natural and anthropogenic stresses on the resource. While perfect prediction of the future is impossible, models underpinned by available data and thoroughly assessed for their predictive uncertainties can be used to make reliable estimation of groundwater resource and impacts caused by current and future stresses. The knowledge generated can be used with greater confidence for informing policy decisions to increase food security and economic prospects regarding sustainable use of groundwater for irrigation especially amongst the poorest who are most vulnerable to changes in the availability of water resource.

1.1 BACKGROUND

The northwest region of Bangladesh has the largest cropping areas in Bangladesh which rely on availability of fresh groundwater for irrigation, especially during the dry seasons (Mainuddin et al. 2019, Mainuddin et al. 2014). Declining groundwater levels, especially in the Barind area (Hodgson et al. 2014, 2021; Kirby et al. 2015; Mojid et al. 2019: Peña-Arancibia et al. 2020), have necessitated development of policy and management measures for the sustainable use of water resources.

To address this challenge, the Australian Government, through its Department of Foreign Affairs and Trade (DFAT) Sustainable Development Investment Portfolio (SDIP-II), have funded a project involving CSIRO and several Bangladesh partners.

Groundwater modelling is undertaken as part of this initiative to assess the current status and predict future changes of water resource in the 16 districts and its availability subject to natural and anthropogenic stresses, the most important being the use of water for irrigation. Other works under this initiative include surface water modelling and water balance analysis (Karim et al. 2021; Mainuddin et al. 2021), groundwater trend analysis (Hodgson et al. 2021), historical trends in land-use change and crop water requirements (Mojid et al. 2021a; Peña-Arancibia et al. 2020; 2021a,b), the impacts and interactions between these on the socio-economic aspects around livelihoods and poverty, especially relating to gender-specific issues (Al-Amin et al. 2019; Rahman et al. 2020, 2021).

Groundwater modelling activity in SDIP-II also focuses on addressing challenges of predictive uncertainty and model complexity by making use of two modelling approaches. First, an integrated modelling of the surface and groundwater flow and water balance was undertaken using MIKE SHE (Refsgaard and Storm, 1995) models. Subsequently, a simple numerical model for the saturated zone (aquifer) was developed using the MODFLOW code (Harbaugh, 2005) to undertake probabilistic analysis of district-scale groundwater balance. Simulation analyses using these models together with other companion activities in the project including surface water, crop simulation and water balance studies were used to reliably quantify the regional scale groundwater balance and evaluate the sustainability of current levels of use.

1.2 MODELLING OBJECTIVES

The following specific objectives were considered in the groundwater modelling study in conjunction with water balance and surface water modelling studies and other studies that are part of the project:

1) Update and calibrate the IWM MIKE SHE models that cover the northwest region with all available data sets pertaining to climate and hydrology and undertake short-term simulation and predictive analysis of groundwater flow, water levels and water balance accounting for the major recharge and discharge components.
2) Develop a computationally viable numerical model using the MODFLOW code for the saturated zone that enables probabilistic quantification of groundwater storage changes over the simulation period of 1985–2016.
3) Account for the predictive uncertainty in the simulation of groundwater levels and estimate the long-term groundwater balance to investigate trends and sustainability of groundwater use in the Northwest districts.
4) Scenario analyses to investigate groundwater levels and water balance corresponding to potential future climate and management option analysis.

Accounting for the predictive uncertainties can help inform the reliability and confidence levels of such prediction in practical decision-making contexts. Also, the development of simpler models using freely available modelling codes like MODFLOW can help improve accessibility of such models to practitioners and groundwater managers in the northwest region. The uptake of scientific tools by water resources engineers and managers would facilitate application of these tools for practical decision making.

2 MODELLING METHOD OVERVIEW

Coupled surface water–groundwater interaction models are ideally the best choice of models to simulate complex hydrological processes in regional river basins. The Institute of Water Modelling (IWM), Dhaka had developed four integrated MIKE SHE/MIKE 11 models that covers the northwest region of Bangladesh. These models were developed using extensive data sets of the topography, climate, hydrology and agricultural and other water use in the region and have a detailed representation of surface water and groundwater flow processes in the region. As such, these models, can provide a thorough understanding of the surface water (SW) and groundwater (GW) flow dynamics in the region.

The modelling approach used in this study makes use of these existing four MIKE SHE models to evaluate the overall water resources across the unsaturated and saturated zone of the subsurface together with rainfall, overland flow and evapotranspiration and river-aquifer interaction. Detailed representation of processes like rainfall, evapotranspiration, unsaturated zone flow and river-aquifer interaction enable these models to provide detailed simulation of land use changes and related changes in water fluxes across pertaining flow domains.

Predictions obtained from environmental models can be largely uncertain (Doherty, 2015). The use of such models in practical decision-making contexts should be accompanied by a thorough analysis of the predictive uncertainties to ensure the reliability of the predictions. One drawback of such fully integrated models is that they are less tenable with comprehensive parameter sensitivity and non-linear prediction uncertainty analysis workflows that require numerous runs of the simulation model. This limits the application of these models for the probabilistic analyses of water balance and groundwater storage changes especially when uncertain parameters can affect the prediction variables.

For this reason, the modelling community, in the recent times, have used the philosophy of building models as simple as possible but as complex as necessary. Simpler models often have computational advantage over complex ones and are better suited for computationally intensive sensitivity and uncertainty analyses. However, it is important to acknowledge that oversimplification could result in salient features being omitted from being analysed.

In this study we use a workflow that can overcome the challenges of simple and complex numerical models by a combined application in a unique way. We proposed to overcome the limitations by the paired use of an approximate and fast-running surrogate model constrained by the quantitative and qualitative knowledge of process details from the complex integrated model of the SW-GW system. While the complex model focuses on process dynamics as much possible as underpinned by available data, the surrogate model is purpose-built for the predictions of interest with approximation of the system dynamics and scale supported by parameterisation schemes that are suitable for predictions of interest. We used a low-fidelity groundwater model together with a complex integrated surface water and groundwater model built for the northwest region of Bangladesh to assess district scale water balance and groundwater storage changes under historical and future stresses. The integrated surface water and groundwater models are built using MIKE SHE and are underpinned by detailed conceptualization of the alluvial aquifer and channel bathymetry, simulation of the catchment processes and flow routing by the MIKE 11 routine and calibrated to observed water levels and flow data. The computationally simpler groundwater model was built using MODFLOW. The MODFLOW model approximates the groundwater flow processes in the saturated zone with simplified representation of recharge and discharge using appropriate parameterization and was subjected to calibration and uncertainty using the PEST suite to improve the match to observed water levels. The major recharge and discharge fluxes obtained from the calibrated MODFLOW model were further compared with

corresponding components of the integrated MIKE SHE model aggregated at the district scale. The fast-running MODFLOW model was then used to probabilistically quantify the groundwater balance and storage changes. Both models were then also used for climate change and pumping scenario analyses. The workflow adopted in this study is described in the following section.

2.1 MODELLING WORKFLOW

The modelling workflow is illustrated in Figure 2.1. It comprises:

1. Development, updating and calibration of existing integrated MIKE SHE models for the northwest region that incorporates detailed representation of the catchment and river flow processes, unsaturated and saturated zone flow.
2. Develop a simplified groundwater model using the free and computationally simpler modelling platform MODFLOW.
3. History matching of the simplified MODFLOW model to the observed time series groundwater levels data additionally constrained by the information regarding deep drainage obtained from the 1D water balance models (Mainuddin et al, 2021), river stage data simulated by the surface water models and unsaturated and saturate zone exchange simulated by the MIKE SHE models.
4. Undertake model uncertainty analysis with the surrogate MODFLOW model to quantify confidence level in the predictions using the models to inform management decisions.
5. Reconcile district scale groundwater balance estimates between the MIKE SHE and MODFLOW model medians. Also reconcile the flux estimates from other activities like SW modelling, crop water usage and district-wise water balance.

The IWM and CSIRO groundwater team of the project undertook the MIKE SHE and MODFLOW modelling activities in close coordination with the broader project activities including SW modelling, crop modelling and district-scale water balance analysis.

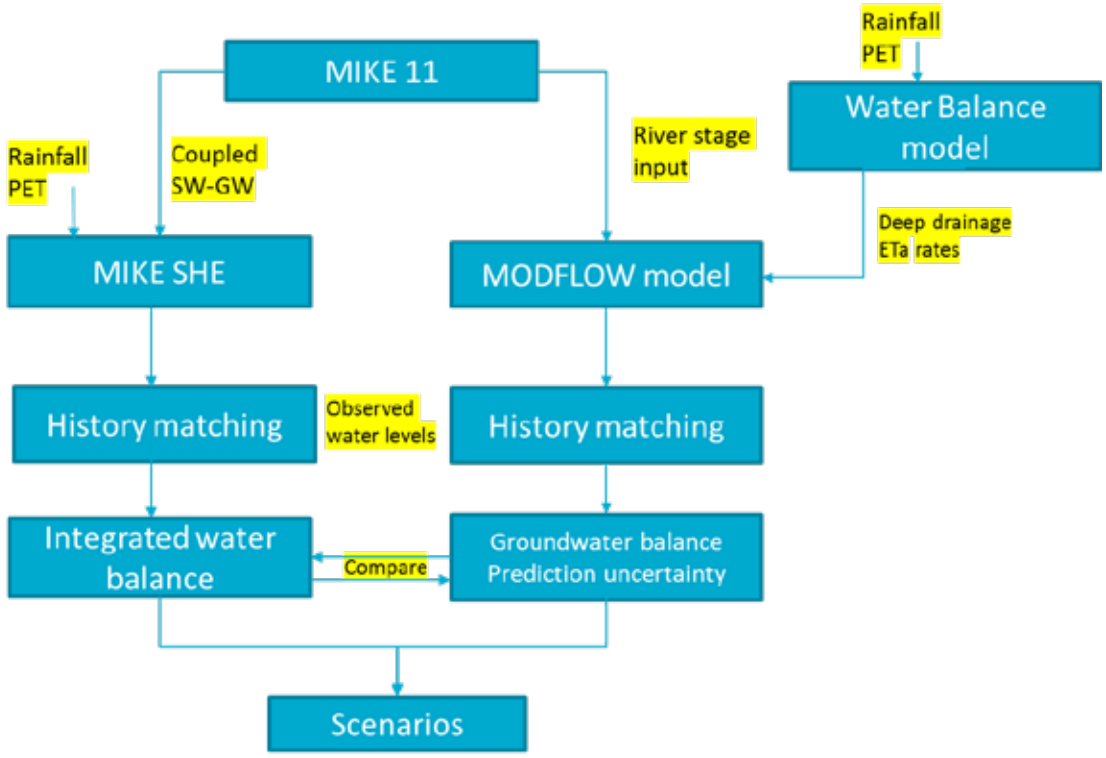

Figure 2.1: Modelling workflow

3 DYNAMICS OF GROUNDWATER RECHARGE AND DISCHARGE

The dynamics of groundwater recharge and discharge in the northwest region are analysed in this section using available data prior to the development of numerical groundwater models.

The material in Section 3.2 through to Section 3.4 has been extracted from an earlier paper by the authors, published in the Journal of Groundwater for Sustainable Development (Mojid et al. 2021b).

3.1 DYNAMIC AND RENEWABLE NATURE OF GROUNDWATER

The quantity of groundwater stored in an aquifer depends on recharge into and extraction from the aquifers and natural discharge into rivers, streams and other aquifers. Prior to widespread groundwater extraction from the mid-1980s and onwards, water levels/levels in the aquifers in Bangladesh were shallow with a weak seasonal fluctuating trend. With increasing utilization of groundwater, water levels fall during the dry season, when pumping for various usages and discharge to the rivers depletes the aquifers (Hodgson et al. 2021). The deepest groundwater conditions are found from April to mid-May, whereas the shallowest water levels are found in November. More than 90% of the annual recharge to the unconfined aquifers occurs during the monsoon, between May and September (MPO, 1987; WARPO, 2000). During this season, water level rises across Bangladesh since high rainfall and an associated inundation recharge the aquifers.

Groundwater recharge in Bangladesh mainly occurs by monsoon rainfall and flooding in addition to the contribution from irrigated crop fields. On the other hand, groundwater discharge occurs through pumping of water by well or by means of natural discharge from subsurface to the rivers, lakes, oceans and other wetlands. Sometimes, the discharge rate of groundwater becomes equal to the recharge rate. Hence, equilibrium is attained between the outflow and inflow into the subsurface. Rainfall is the most predominant source of recharge. Therefore, it is important to know the dynamic reserve of groundwater from rainfall for its sustainable usage. Groundwater level responses to rainfall when rainfall meets all requirements of surface depressions and soil moisture. There is a time difference between the occurrence of rainfall and groundwater response. This time for which infiltrated rainwater first reaches the aquifer from ground surface represents the response time/lag time of rainfall to groundwater. The lag period mainly depends on the geology of the aquifer and varies from a few days to several weeks or even longer period. In the analysis of recharge from rainfall, lag period of rainfall to recharge allows selecting the rainfall duration such as daily, weekly, monthly or annual. In some cases, the amount of water extracted from the aquifer is not recovered even after a long period of time, indicating groundwater deficit of the aquifer. Further extraction of water from that aquifer may lead to declining water levels, hydrostatic pressure reductions, water quality deterioration and other related problems such as land subsidence (Rose, 2009). There is also a possibility of rejection of recharge to groundwater. When rainwater is rejected from recharging into the aquifer in the form of runoff, the aquifer is safe for the extraction of more water.

This section of the study was planned to mainly determine the dynamic behaviours of the aquifers in the northwest region of Bangladesh. The specific objectives were:

- to understand rainfall-induced recharge-dynamics, i.e. determination of the lag/response period of rainfall to groundwater recharge
- identification of the locations and magnitude of recharge deficit/rejection.

3.2 METHOD

For analysing the rainfall-induced recharge dynamics, the region is divided into 3 sub-regions based on the hydro-geological characteristics. The Barind Tract is at higher elevation than the adjoining floodplain and there are two terrace levels – one at 40 m above mean sea level, known as High Barind, and the other between 19.8 m and 22.9 m, known as Level Barind (Figure 3.1). Approximately 47% of the Barind Tract is classified as highland, 41% as medium highland, and the rest as lowland (Zahid et al. 2016). For this study, the whole NW region was therefore divided into three sub-regions: High Barind, Level Barind and Other area.

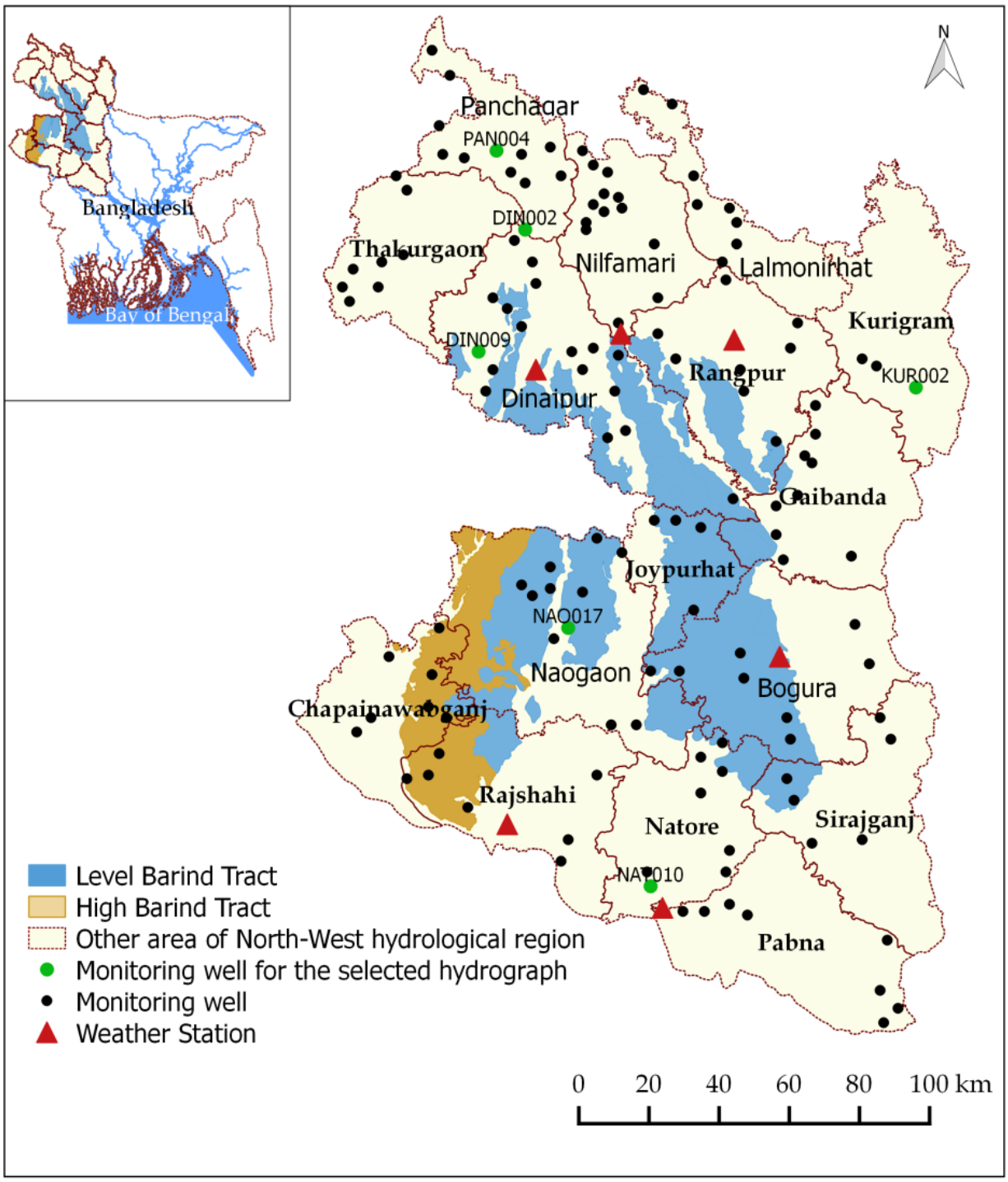

Figure 3.1: Map of the North-West (NW) region of Bangladesh showing 16 administrative districts, 3 sub-regions (High Barind, Level Barind, and Other area) and locations of 137 groundwater level (GWL) monitoring wells under investigation

Both GWL and rainfall data were used for assessing the rainfall-groundwater recharge dynamics. The weekly GWL and daily rainfall data of 1985 to 2016 period were collected and trained before objective-oriented analysis. To synchronize with GWL, weekly rainfalls were calculated from the daily rainfall data and cumulative weekly rainfall was calculated therefrom. Considering huge time-requirement for manual analysis and interpretation of data, 5 wells from the High Barind, 19 from Level Barind and 113 from the remaining area of the NW region were selected; the wells are distributed fairly uniformly over the entire NW region (Figure 3.1). The GWLs reached the maximum depths from ground surface at the end of dry season and the minimum depth occurred sometimes in the wet season. Both depths were identified on GWL hydrographs and noted separately for each monitoring wells. A typical GWL hydrograph is displayed in Figure 3.2(a).

3.2.1 DETERMINATION OF RECHARGE LAG-PERIOD

Recharge lag-periods were calculated from GWL hydrographs of the selected 137 monitoring wells for each year from 1985 to 2016. GWL hydrographs were prepared by plotting GWLs of each monitoring well against time (week) of the data period. Rainfall hydrographs were prepared by plotting cumulative weekly total rainfall against weeks (Figure 3.2(b)). For each monitoring well, rainfall hydrographs of the nearest meteorological station (Figure 3.1) were assigned for that well. For both hydrographs, January was taken as the starting month since dry season irrigation starts at this month and it is also starting of large-scale extraction of groundwater for irrigation. The irrigation period continues up to April and GWL continues dropping due to extraction by irrigation wells without reflecting any effect of recharge from irrigation fields although some recharge might occur (Rushton et al. 2020; Mainuddin et al. 2020). Since there is no measured data on the contribution of irrigation fields to groundwater recharge, we considered only the effect of rainfall in determining the response time of GWL to rainfall. The week of seasonal first rainfall was identified on the rainfall hydrograph at each monitoring well for each year. Some rainfall events with small quantity did not contribute recharging the aquifer since the unsaturated soil layer overlying the aquifer needed to be saturated before infiltrating water to the aquifer. When percolated water from rainfall reached the aquifer, GWL started rising. Figure 3.2(b), for example, elucidates that GWL responded one week after rainfall had occurred. The week at which GWL responded to rainfall was recorded in each year during 1985 to 2016 period for the 137 monitoring wells. The difference between the week at which rainfall started and the week at which GWL responded (lag-period of recharge from rainfall) was determined.

In Bangladesh, large-scale development of groundwater started in early 1980s and continued expanding rapidly almost to reach its full potential at around 2010 after which extraction of groundwater mostly remains unchanged or it declines because of continuous decline in GWL in many parts of the country, including the NW region. Taking this into account we divided the GWL data set into 3 time segments: 1985–1994, 1995–2004 and 2005–2016 periods to effectively capture the temporal variation of the recharge–rainfall mechanism. Therefore, the average lag-period of recharge for each monitoring well was calculated for these three different time periods by taking average of lag-periods of each year for each time period.

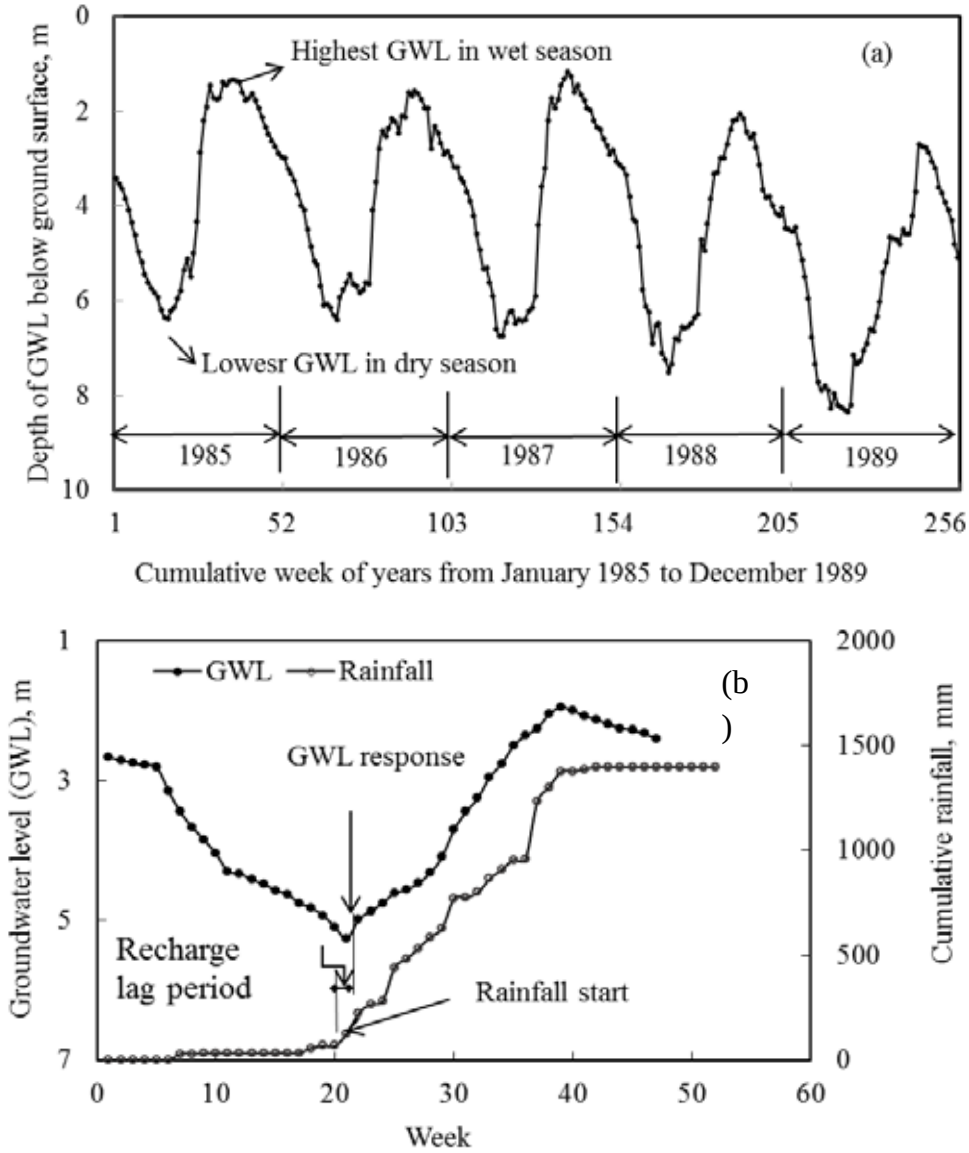

Figure 3.2: (a) A typical groundwater level (GWL) hydrograph of monitoring Well No. NAO017 (green solid circle in Naogaon district, Figure 3.1) from 1985 to 1989 period showing the highest GWL (minimum depth from ground surface) in wet season and lowest GWL (minimum depth from ground surface) in dry season, and (b) rainfall and groundwater level (GWL) hydrographs at monitoring Well No. PAN004 (green solid circle in Panchagar district, Figure 3.1) showing first recharge-generating rainfall, GWL response and recharge lag-period

3.2.2 DETERMINATION OF THE PERIODS AND QUANTITIES OF RECHARGE DEFICIT AND REJECTION

The amount of water, which percolates through the vadoze zone and joins the aquifer causing eventual rise (or reduction in the fall) of GWL, is the actual (net) recharge. On the other hand, the quantity of water, which could reach the aquifer hypothetically, is the potential recharge. When an aquifer has been fully recharged and GWL has reached its possible highest level (aquifer full condition) cannot accept any more water. So, water available on the ground surface but unable to move to groundwater because of aquifer full condition is the rejected recharge. Thus, the status of groundwater recharge at any monitoring well site can be explained in terms of one of three states of recharge: recharge deficit, recharge rejection or recharge balance. Deficit in recharge occurred when the amount of water withdrawn from the aquifer in dry season was not fully replenished during subsequent monsoon. In this case, GWL continued rising during whole monsoon period but did not reach the previous year's highest peak as illustrated in Figure 3.3(a). The amount of recharge deficit was determined from the difference between the highest peaks of GWL (minimum depth from ground surface) of two successive years. Recharge balance condition was observed

when cessation of rainfall and the highest peak of GWL occurred almost at the same time and GWL reached the previous year's highest peak. If GWL reached the highest peak well before cessation of rainfall, there was rejection of recharge. For example, Figure 3.3(b) shows the highest peak of GWL in 38th week and the occurrence of seasonal last appreciable rainfall event in 42nd week, revealing that the rainfall occurring after 38th week could not contribute to recharging the aquifer and hence was rejected, mainly, as runoff. The difference of times at which GWL reached the highest peak and rainfall ceased was the recharge rejection period. This time period was calculated from the difference between the times of occurrence of the two events (Figure 3.3(b)). The amount of rejected recharge was calculated from the difference between cumulative rainfall on the week when rainfall ceased and cumulative rainfall on the week when GWL reached the highest peak. Figure 3.3(b) demonstrates that the end-of-rainfall and arrival of GWL to its highest peak occurred at the same week (39th week); also the GWL was at the previous year's highest peak. There was neither deficit of recharge nor additional scope for recharge, implying that the aquifer was at 'recharge balance' condition. Similar to lag period, recharge deficit and rejection periods and their quantities were determined for the three time periods. The locations of recharge deficit, rejection and balance were identified from the identification number and associated locations of the monitoring wells.

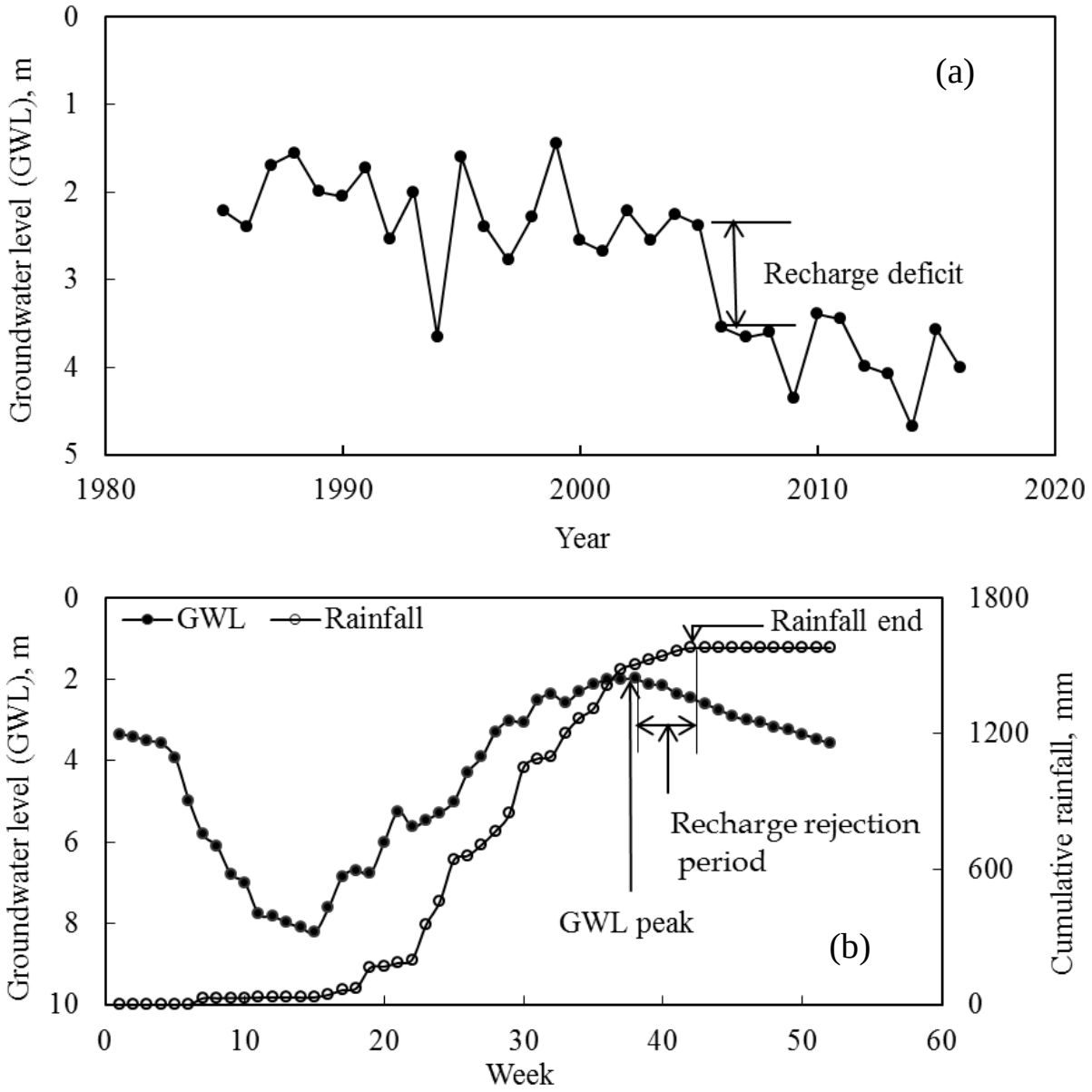

Figure 3.3: (a) Groundwater level (GWL) hydrograph representing the annual highest peak (lowest depth of GWL below ground surface) and amount of recharge deficit at monitoring Well No. DIN009 (green solid circle in Dinajpur district, Figure 3.1), and (b) rainfall and groundwater level (GWL) hydrographs showing period of recharge rejection and amount of rejected recharge at monitoring Well No. DIN002 (green solid circle in Dinajpur district, Figure 3.1)

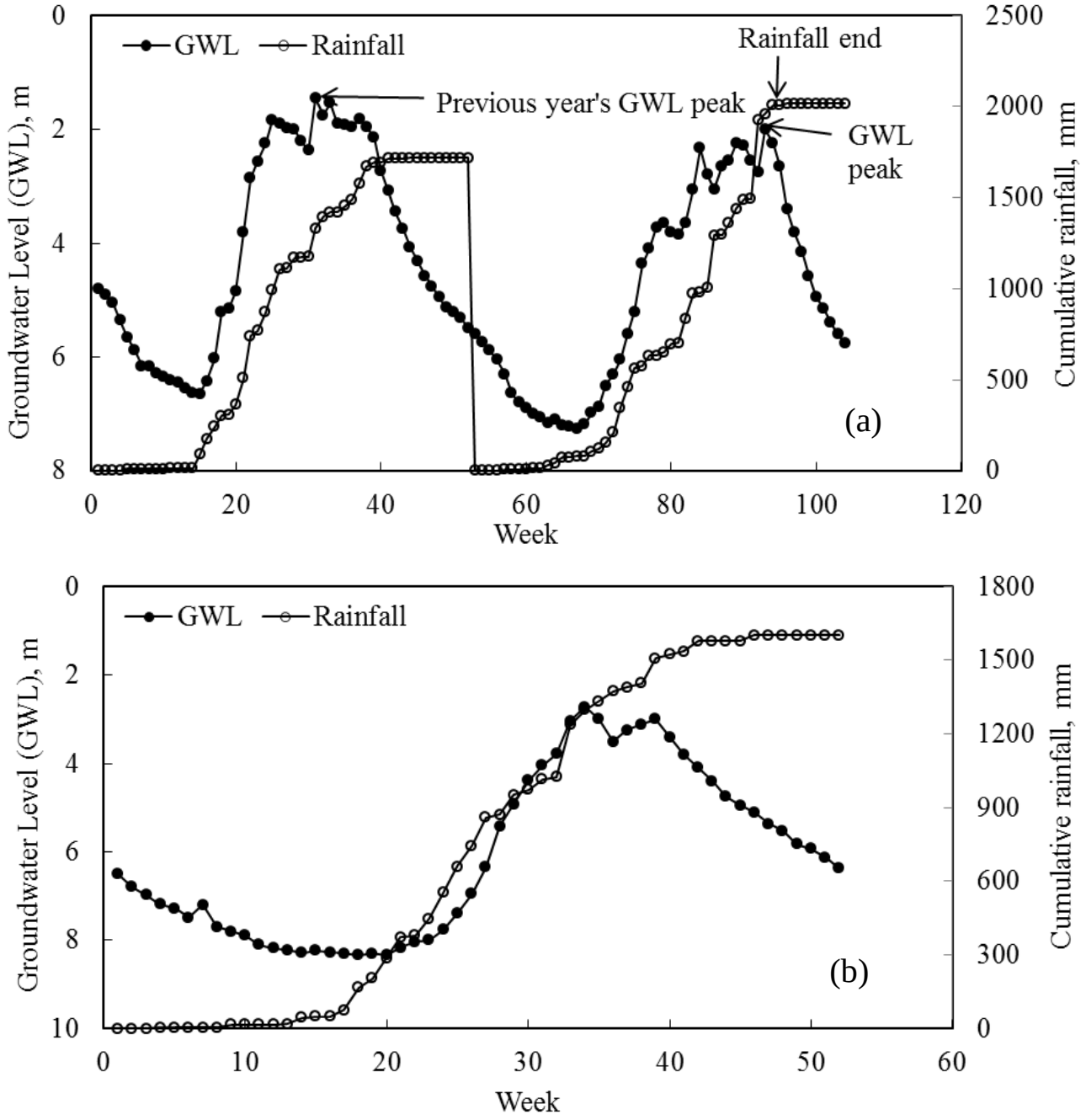

Figure 3.4: (a) Rainfall and groundwater level (GWL) hydrographs showing rainfall end, GWL peak and recharge balance condition at monitoring Well No. KUR002 (green solid circle in Kurigram district, Figure 3.1; data period 2000–2001), and (b) weekly total rainfall hydrograph and weekly groundwater level (GWL) hydrograph in 2002 at monitoring Well No. NAT010 (green solid circle in Natore district, Figure 3.1)

3.3 RESULTS

3.3.1 RECHARGE LAG-PERIOD AND THRESHOLD RAINFALL

GWL hydrographs of the monitoring wells reflected response of the aquifers to recharge from rainfalls; the responses were more vigorous in other areas than in High and Level Barind. Figure 3.4(b) (as an example) demonstrates that total 50 mm rainfall occurring during 8th to 16th weeks (8 weeks) before onset of monsoon (March–April) at a monitoring well site in Natore district within Other area (Figure 3.1) had no influence on GWL. The rise in GWL was first evident in 21st week after 26-mm rainfall had occurred in 17th week. The previous 50-mm rainfall, distributed over 8 weeks, was used partly for surface evaporation and

partly for wetting the vadoze zone. The previous weeks' total rainfall (50 mm) and 17th week's rainfall (26 mm) was the required threshold amount to start recharging the underlying aquifer in 21st week after satisfying surface evaporation and soil-moisture requirement of the vadoze zone. Since a large proportion of the crop acreage was under irrigated rice, the vadose zone within the irrigated area might remain saturated or partially saturated. Consequently, some recharge might have occurred both from the irrigated rice fields through deep percolation and appreciable rainfall events, when there was any (Rushton et al. 2020). The irrigation return flow and induced recharge can play a major role in recharging the aquifer in the irrigated area compared to local rainfall in the dry season.

The average (of the monitoring wells) range of lag-period of recharge from rainfall varied widely among the three sub-regions (High Barind, Level Barind and Other area; Figure 3.1), the highest range being in High Barind and the lowest in Other area (Table 3.1). The minimum range was relatively narrow (between 1 week and 3 weeks) and remained consistent among the sub-regions and three time periods (1985–1994, 1995–2004 and 2005–2016), while the maximum range was wide (between 1 week and 13 weeks), the widest range being in Other area. The average minimum lag period was largest (1.5 to 1.8 weeks) in High Barind and smallest (1.0 to 1.2 weeks) in Other area, while the average maximum lag period was the largest (4.8 to 6.5 weeks) in Other area and smallest (2.7 to 3.9 weeks) in Level Barind. The overall average lag period varied from 2.1 to 2.9 weeks among the three time periods, with the largest value in High Barind and smallest value in Other area. Comparison of spatial distributions of the average lag periods for the three time periods (Figure 3.5) reveals that the lag periods increased over time at several monitoring well sites. This observation is a clear indication of increasing depth of dry season GWLs over time in those sites.

Table 3.1: Range and average lag periods of recharge from rainfall at 5 monitoring well locations in High Barind, 19 monitoring well locations in Level Barind and 113 monitoring well locations in Other area of NW region

Time period	Range of lag period for individual well (week)			Average lag period for individual well (week)			
	Minimum	Maximum	Average	Minimum	Maximum	Average	SD
High Barind							
1985–1994	1–3	2–7	1.2–5.0	1.8	4.7	2.9	1.1
1995–2004	1–2	3–7	1.4–4.8	1.5	4.2	2.9	1.1
2005–2016	1–2	1–13	1.0–5.8	1.5	5.7	2.9	1.7
Level Barind							
1985–1994	1–3	1–7	1–5	1.3	2.7	2.1	0.37
1995–2004	1–3	2–8	1–5	1.6	3.4	2.5	0.56
2005–2016	1–3	1–7	1–5	1.6	3.9	2.6	0.6
Other area							
1985–1994	1–2	1–10	1.1–4.7	1.2	5.7	2.4	0.8
1995–2004	1–1	2–13	1–4.5	1.0	6.5	2.3	0.8
2005–2016	1–2	1–13	1–4.5	1.0	4.8	2.3	0.7

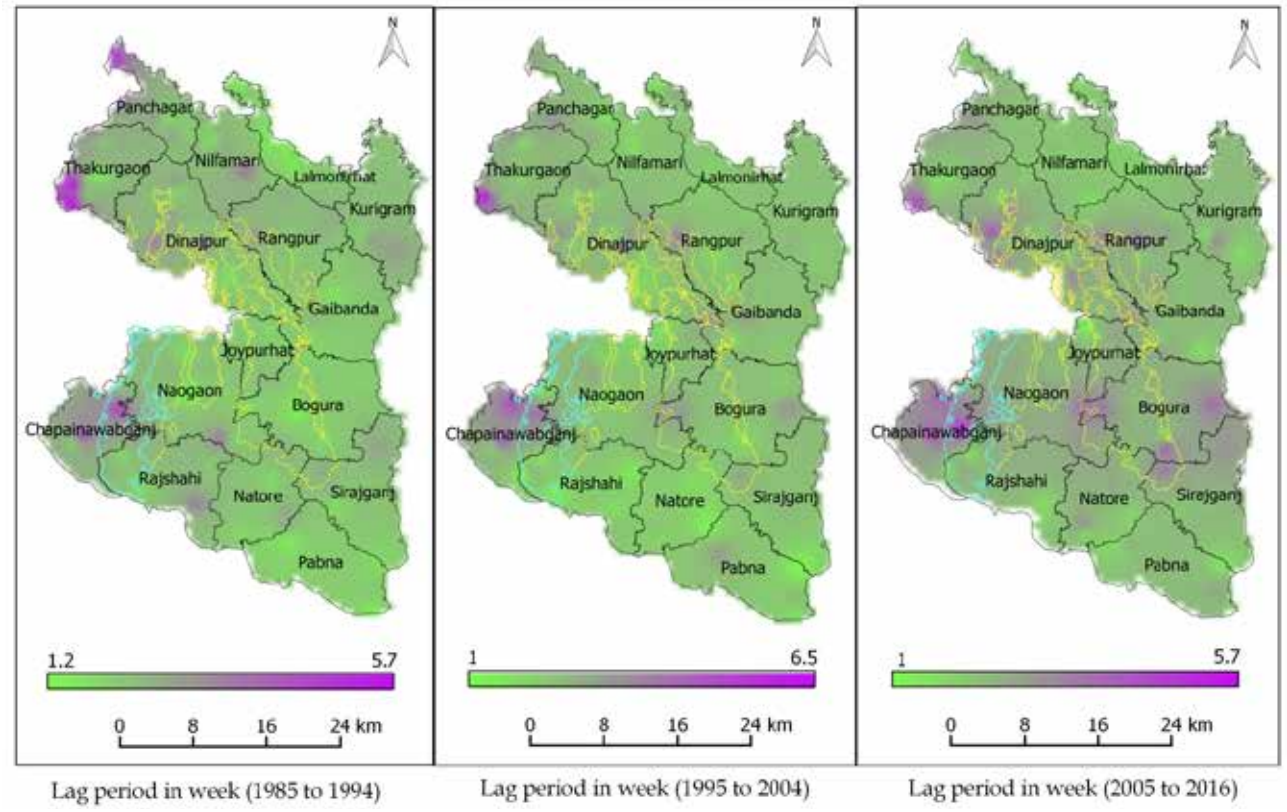

Figure 3.5: Spatial distribution of average lag period in High Barind (enclosed by aqua line), Level Barind (enclosed by yellow line) and Other area for 1985–1994, 1995–2004 and 2005–2016 time periods

The threshold rainfall to initiate rising of GWL varied widely among the three sub-regions and the three time periods. The minimum threshold rainfall was the largest (24–36 mm) in High Barind and smallest (11–13 mm) in Other area, with consistently increasing values over the three time periods in High Barind due to continuously declining GWL. The maximum threshold rainfall varied inconsistently both among the sub-regions and the time periods (Table 3.2). The average threshold rainfall was 39–75 mm in High Barind, 34–43 mm in Level Barind and 35–41 mm in Other area, with no consistent variation among the three time periods except in High Barind where it increased over time.

Table 3.2: Amount of threshold rainfall at which groundwater level responds at 5 monitoring well locations in High Barind, 19 monitoring well locations in Level Barind and 113 monitoring well locations in other area of NW region

Time period	Threshold rainfall at individual well site (mm)			
	Minimum	Maximum	Average	SD
High Barind				
1985–1994	24	66	39	16
1995–2004	33	56	44	10
2005–2016	36	180	75	60
Level Barind				
1985–1994	13	79	35	17
1995–2004	18	92	43	21
2005–2016	14	91	34	20
Other area				
1985–1994	11	98	37	20
1995–2004	13	179	41	25
2005–2016	11	100	35	17

3.3.2 RECHARGE REJECTION PERIOD

At each monitoring well site, there was recharge deficit for some period in some years and recharge rejection for some period in the other years, thus providing a year-averaged recharge deficit period as well as recharge rejection period for the well site. Although the range of year-averaged minimum recharge rejection period was within 0 (nil) to 3 weeks in the three sub-regions that of maximum recharge rejection period varied widely (2 to 21 weeks), with consistently widening range over the three time periods in High Barind (Table 3.3). The average minimum recharge rejection period over the three time periods was 0 (nil) to 2 weeks both in High and Level Barind and 1.5 to 2.2 weeks in Other area. The average maximum recharge rejection period for the corresponding sub-region was 4.2 to 8.0 weeks, 8.6 to 12.5 weeks and 10.3 to 12.7 weeks. The overall average recharge rejection period over the three time periods was 2.2 to 3.6 weeks, 3.6 to 4.5 weeks and 4.7 to 5.6 weeks in High Barind, Level Barind and Other area, respectively, with consistently decreasing recharge rejection period in Level Barind. It is noted that despite continuous decline in GWL in most parts in the Barind region (Mojid et al. 2019) the rainfall–GWL relation revealed occurrence of some recharge rejection period. This might be due to that because of deeper GWL and larger recharge lag-periods the infiltrating water was lost through lateral flow and surface evaporation before reaching the aquifer. The year-averaged minimum recharge rejection year for the individual monitoring wells within the three time periods was 0 nil) to 1 year both in High and Level Barind and 1 to 3 years in Other area (Table 3.3). The year-averaged maximum recharge rejection year in the corresponding sub-regions was 4 to 7 years, 9 to 10 years and 10 to 11 years within the three time periods. The average of the year-averaged recharge rejection year within the three time periods was 2.0 to 4.8 years, 4.6 to 7.2 years and 7.8 to 8.2 years in High Barind, Level Barind and Other area, respectively.

Figure 3.6 demonstrates spatial distribution of year-averaged recharge rejection weeks for the three time periods. In general, recharge rejection period was higher in Other area than in Level Barind, which had higher recharge rejection period than High Barind. The larger proportion of monitoring well sites in Other area provided larger recharge rejection period compared to other two sub-regions in the three time periods. Figure 3.6 reveals that the number of weeks of recharge rejection at the monitoring well sites with larger recharge rejection period in Other area increased from 1985–1994 to 1995–2004 period after which it decreased during 2005–2016 period. There was wide variation in recharge rejection period over the years in the three time periods and three sub-regions; wide variation was also in the number of years of recharge rejection at the monitoring well sites (Table 3.3,Figure 3.7).

Table 3.3: Recharge rejection periods and number of years of recharge rejection at 5 monitoring well locations in High Barind, 19 monitoring well locations in Level Barind and 113 monitoring well locations in Other area of NW region

TIME PERIOD	RANGE OF RECHARGE REJECTION PERIOD (WEEK)			AVERAGE RECHARGE REJECTION PERIOD (WEEK)				YEARS OF RECHARGE REJECTION (NO.)			
	MIN	MAX	AVG	MIN	MAX	AVG	SD	MIN	MAX	AVG	SD
High Barind											
1985–1994	0–2	2–7	0.4–2.8	0.0	4.2	2.2	1.5	1.0	6.0	2.0	2.3
1995–2004	0–2	2–10	1.8–6.2	2.0	5.2	3.6	1.6	1.0	7.0	4.8	2.3
2005–2016	0	3–13	1.3–4.8	0.0	8.0	3.6	2.9	0	4.0	2.2	1.8
Level Barind											
1985–1994	0–2	2–16	1.6–8.7	2.0	8.6	4.5	1.7	1.0	10.0	7.2	2.2
1995–2004	0	2–15	1.5–7.1	0	9.3	4.0	2.3	0	10.0	4.9	3.1
2005–2016	0	7–18	1.6–6.3	0	12.5	3.6	2.9	0	9.0	4.6	3.0
Other area											
1985–1994	2–3	3–19	1.9–10.0	2.2	10.4	5.2	2.1	2.0	10.0	8.0	1.7
1995–2004	1–3	2–19	1.7–10.8	1.8	12.7	5.6	2.9	3.0	10.0	8.2	1.6
2005–2016	0–2	2–21	1.7–9.1	1.5	10.3	4.7	1.8	1.0	11.0	7.8	2.2

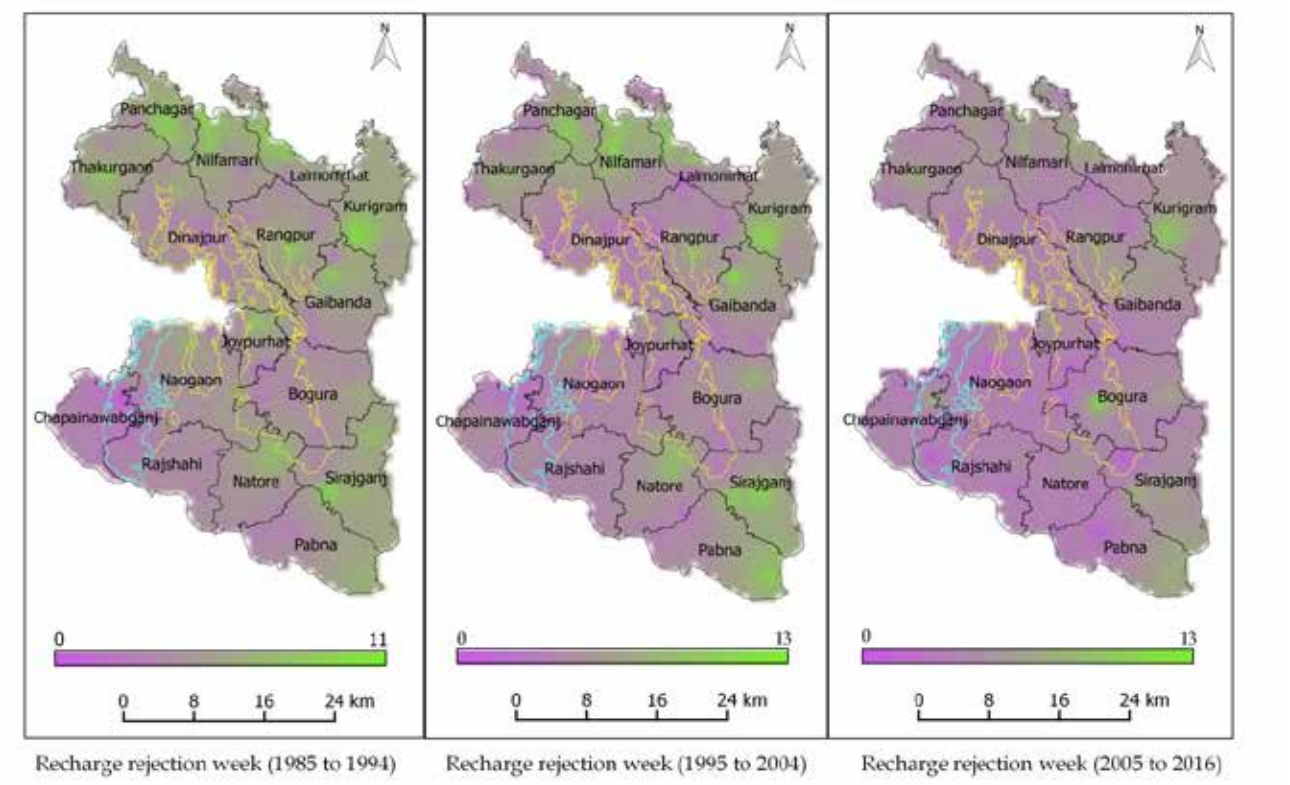

Figure 3.6: Spatial distribution of year-averaged recharge rejection period (week) in High Barind (enclosed by aqua line), Level Barind (enclosed by yellow line) and Other area during 1985–1994, 1995–2004 and 2005–2016 periods for the NW region

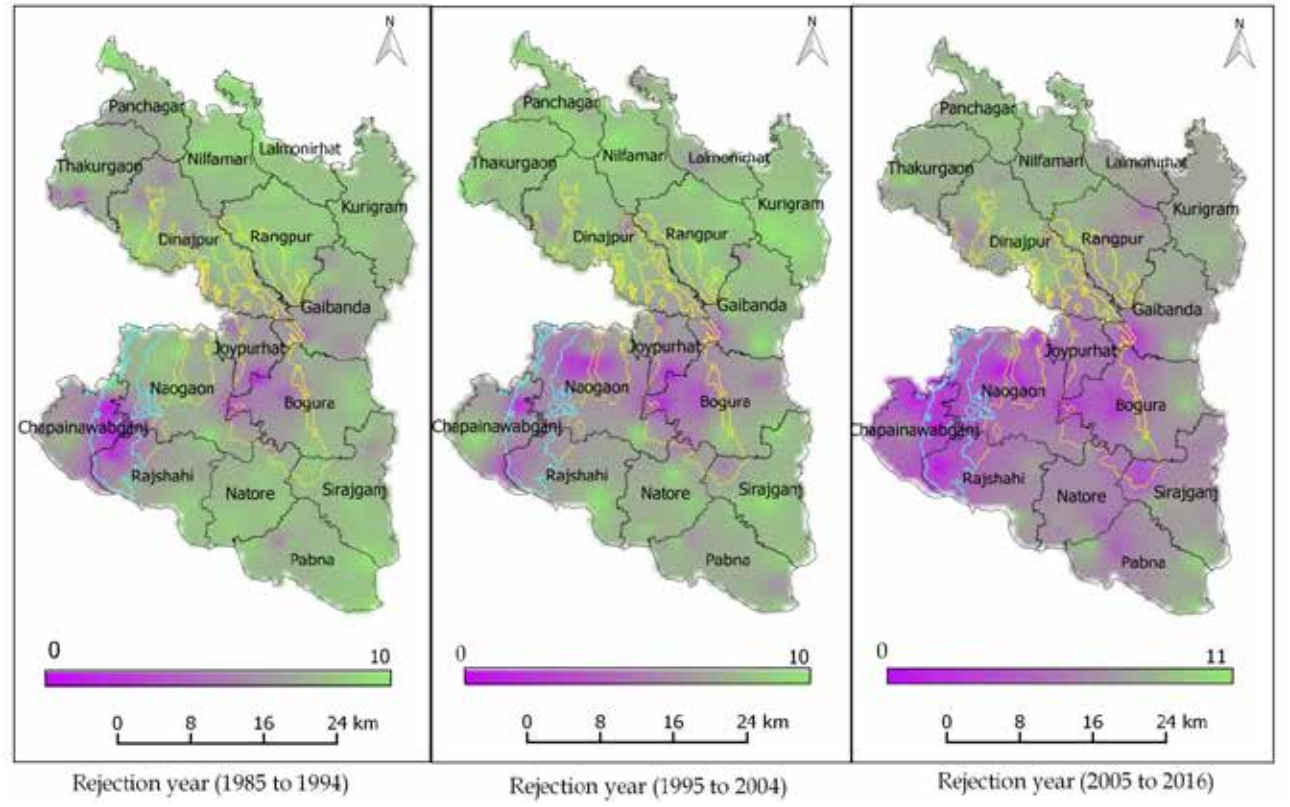

Figure 3.7: Spatial variation in recharge rejection year in High Barind (enclosed by aqua line), Level Barind (enclosed by yellow line) and Other area during 1985–1994, 1995–2004 and 2005–2016 periods for the NW region

3.3.3 QUANTITY OF RECHARGE DEFICIT

The annual quantities of recharge deficit in terms of depth of aquifer (for unconfined aquifer) or pressure head (for confined aquifer) at the monitoring well sites are provided in Table 3.4 for the three time periods for the three sub-regions. The average annual recharge deficit remained practically unchanged (87–90 cm) in High Barind during 1985–1994 and 1995–2004 but increased enormously (415 cm) during 2005–2016 due to wide variations in recharge deficit (21–1730, 108–1990 and 165–1105 cm) in 3 monitoring wells at Nachol upazila in the High Barind. The wide variation in recharge deficit is also reflected in the maximum and average range of recharge deficits (21–1730 and 65–1272 cm, respectively) for this sub-region (Table 3.4). The recharge deficit varied over a narrow range (107–122 cm) over the three time periods in Level Barind but decreased significantly (from 180 to 99 cm) from 1985–1994 to the latter periods in Other area. Figure 3.8 shows spatial variation of this recharge deficit over the NW region for the three time periods. A large proportion of the monitoring wells in Other area shows larger quantity of recharge deficit during 1985–1994 period compared to the latter periods. Recharge deficit increased significantly both in High and Level Barind and at some parts in Other area over the time periods. However, in some northern parts of Other area it increased during 1985–1994 to 1995–2004 period but decreased during 2005–2016 period.

Table 3.4: Recharge deficit in terms of aquifer's depth at 5 monitoring well sites in High Barind, 19 monitoring well locations in Level Barind and 113 monitoring well locations in other area of NW region

TIME PERIOD	RANGE OF RECHARGE DEFICIT (CM)			ANNUAL AVERAGE RECHARGE DEFICIT (CM)			
	MINIMUM	MAXIMUM	AVERAGE	MINIMUM	MAXIMUM	AVERAGE	SD
High Barind							
1985–1994	19–96	3–400	16–240	50	116	90	31
1995–2004	2–155	35–255	17–208	63	114	87	21
2005–2016	21–648	21–1,730	65–1,272	182	544	415	142
Level Barind							
1985–1994	8–19	5–439	40–190	13	220	113	58
1995–2004	4–14	18–856	35–259	9	333	122	88
2005–2016	25–65	21–877	17–314	48	223	107	42
Other area							
1985–1994	3–22	16–1,954	51–393	13	879	180	209
1995–2004	3–5	22–1,312	68–770	3	613	101	127
2005–2016	4–15	55–1248	24–238	9	531	99	88

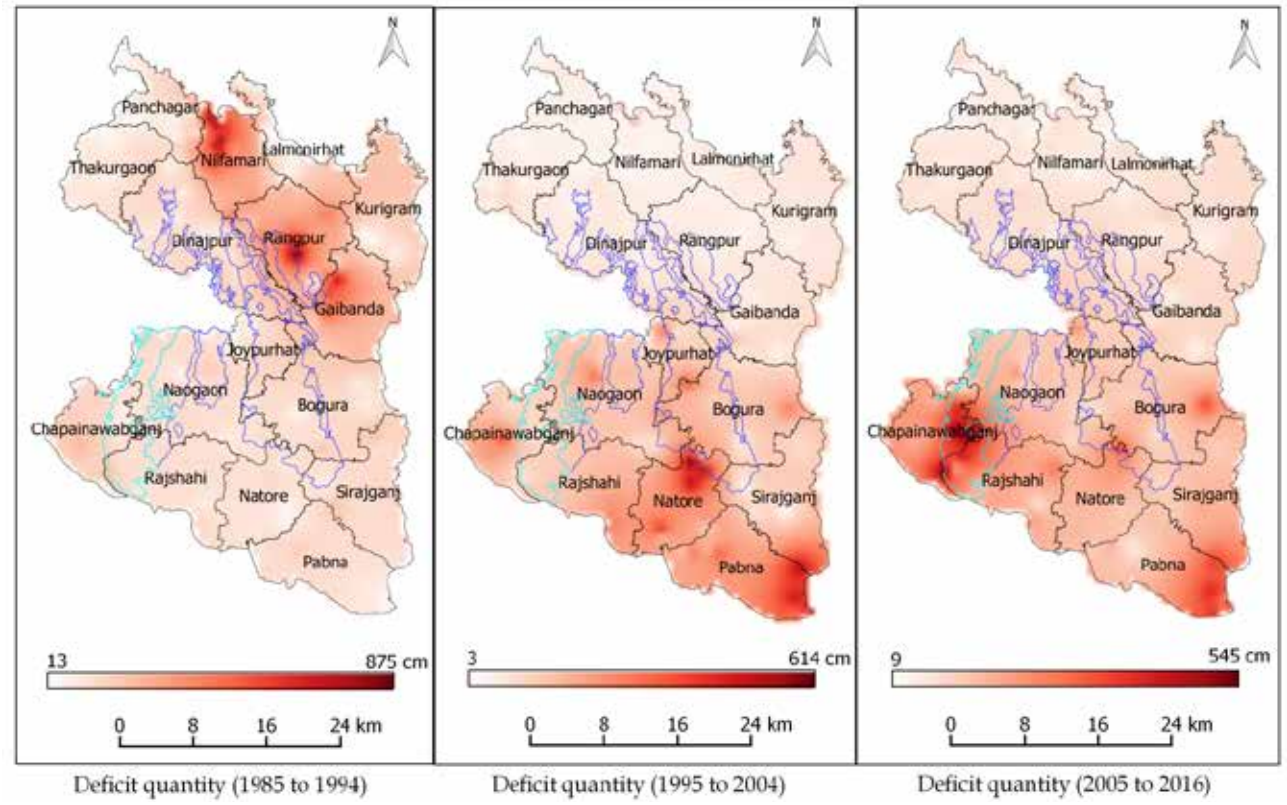

Figure 3.8: Spatial variation of the quantity of year-averaged recharge deficit at the monitoring well sites in High Barind (enclosed by aqua line), Level Barind (enclosed by blue line) and Other area for (from left to right) 1985–1994, 1995–2004 and 2005–2016 periods for the NW region

3.3.4 QUANTITY OF RECHARGE REJECTION

The annual quantities of recharge rejection in terms of rainfall depth at the monitoring well sites are provided in Table 3.5 for the three sub-regions for three time periods. The average annual recharge rejection was the smallest (65–149 cm) in High Barind; the other two sub-regions showed mostly similar average annual recharge rejection (between 314 cm and 336 cm) during 1985–1994 and 1995–2004 periods but decreased significantly (to 243 cm in Level Barind and 265 cm in Other area) during 2005–2016. Figure 3.9 illustrates spatial variation of this recharge rejection for the three time periods for the NW region. Recharge rejection was significantly larger in Other area than in High and Level Barind; High Barind showed significantly lower recharge rejection than the other sub-regions. A large proportion of monitoring wells in Level Barind and Other area showed smaller quantity of recharge rejection during 2005–2016 period compared to 1985–1994 and 1995–2004 periods.

Table 3.5: Recharge rejection in terms of quantity of rainfall at 5 monitoring well sites in Level Barind, 19 monitoring well locations in Level Barind and 113 monitoring well locations in other area of NW region

Time period	Range of recharge rejection (mm)			Annual average recharge rejection (mm)			
	Minimum	Maximum	Average	Minimum	Maximum	Average	SD
High Barind							
1985–1994	0	51–602	20–198	0	224	89	87
1995–2004	3–105	105–819	45–358	56	301	149	105
2005–2016	0	78–236	33–104	0	146	65	53
Level Barind							
1985–1994	0–104	239–1,391	49–822	74	793	320	173
1995–2004	7–84	113–1,375	54–499	51	1375	320	315
2005–2016	15–40	1,080–1,647	110–421	29	1339	243	322
Other area							
1985–1994	1–5	506–2,141	57–722	5	1158	314	271
1995–2004	2–44	467–2,205	68–770	30	1079	336	280
2005–2016	2–26	285–2,390	59–597	23	913	265	171

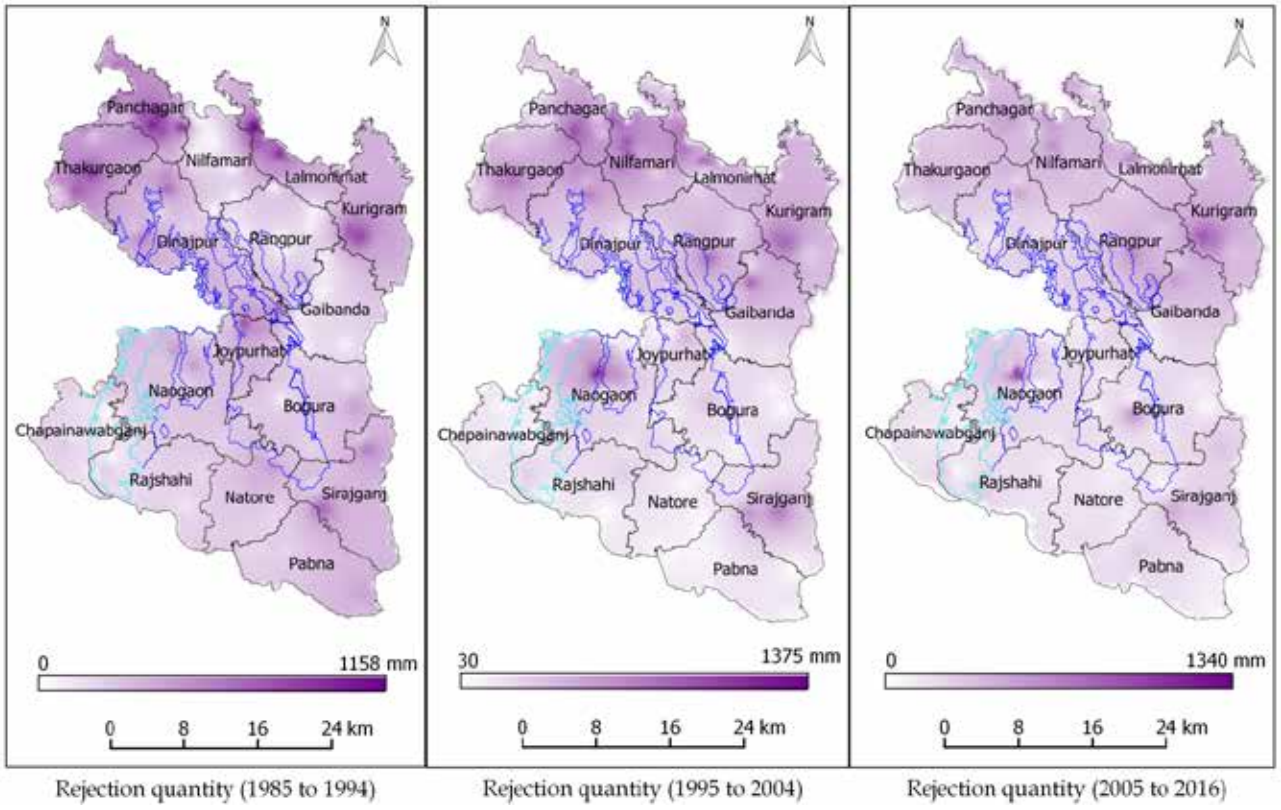

Figure 3.9: Spatial variation of the quantity of year-averaged recharge rejection at the monitoring well sites in High Barind (enclosed by aqua line), Level Barind (enclosed by blue line) and Other area during 1985–1994, 1995–2004 and 2005–2016 periods for the NW region

3.4 Conclusion

The hydrological interaction between rainfall or surface sources of recharge and groundwater can reveal spatial heterogeneity in the distribution of groundwater. This can guide making measurements at the appropriate scale and developing proper management policies for groundwater resources. Interpretation of long-term (in this study 32 years) GWL hydrographs of monitoring wells (total 137) revealed crucial information on recharge–discharge dynamics of the aquifers. GWL responded to a threshold minimum rainfall that varied both spatially and temporally. At each monitoring well sites, recharge deficit occurred in some years and recharge rejection in the other years. The threshold rainfall was greater and lag-period was

longer in areas with thick clay layers overlying the aquifers (e.g. in Barind Tract). In the years with recharge rejection, most of the rainfall occurring during monsoon (July to September) was rejected since the aquifers got fully replenished before rejection of recharge had started except in the clay-overlain Barind Tract. At many locations of the study region, recharge rejection occurred in most of the years, indicating further potential of groundwater withdrawal from the aquifers in the dry season. Despite clear evidence of continuously declining GWL, the Barind Tract exhibited recharge rejection period in some years with considerable quantity of recharge rejection. These incongruent results from the GWL's response to rainfall are in contrast to field-observed recharge dynamics of the aquifer and clear indications of the presence of dominant recharge process(es) in the area other than from local rainfalls. The results, based on locally observed GWL data, provide information on duration and quantity of recharge deficit and recharge rejection and their spatial and temporal variations. Such information, derived for any groundwater basin, is crucial in updating groundwater development program for the concerned region. This procedure provided information on real-time measured data without any assumption or approximation. The weak point was that the response of GWL was identified by considering only rainfall (the major source of recharge for the study region) although irrigation return flow and interflow had some contributions in recharging the aquifers.

4 INTEGRATED MIKE SHE MODELS FOR THE NORTHWEST DISTRICTS

The groundwater resources of northwest districts of Bangladesh are intimately connected with the surface water resources. The annual dynamics of the groundwater resource is influenced by the recharge processes comprising, inflow from diffuse recharge following rainfall, irrigation and flooding, exchanges with rivers and discharge through pumping for irrigation and other uses, contribution to natural evapotranspiration and draining into rivers. To understand groundwater dynamics in this region, it was important to undertake integrated assessment of water resources using appropriate modelling tools. MIKE SHE models were used for this purpose.

4.1 STUDY AREA

The study area comprises the whole Northwest region of Bangladesh which covers 16 districts namely Rajshahi, Chapai Nawabganj, Naogaon, Natore, Pabna, Sirajganj, Bogra, Gaibandha, Kurigram, Rangpur, Nilphamari, Lalmonirhat, Joypurhat, Dinajpur, Thakurgaon and Panchagarh districts (Figure 4.1). The area lies approximately between $23^0 40'$ to $26^0 51'$ N latitudes and $87^0 44'$ to $90^0 10'$ E longitudes. The area is bounded by Indian territory on the west and North, Ganges River on the South, and Brahmaputra-Jamuna River on the east. The gross area of the study area is about 37,000 square kilometres.

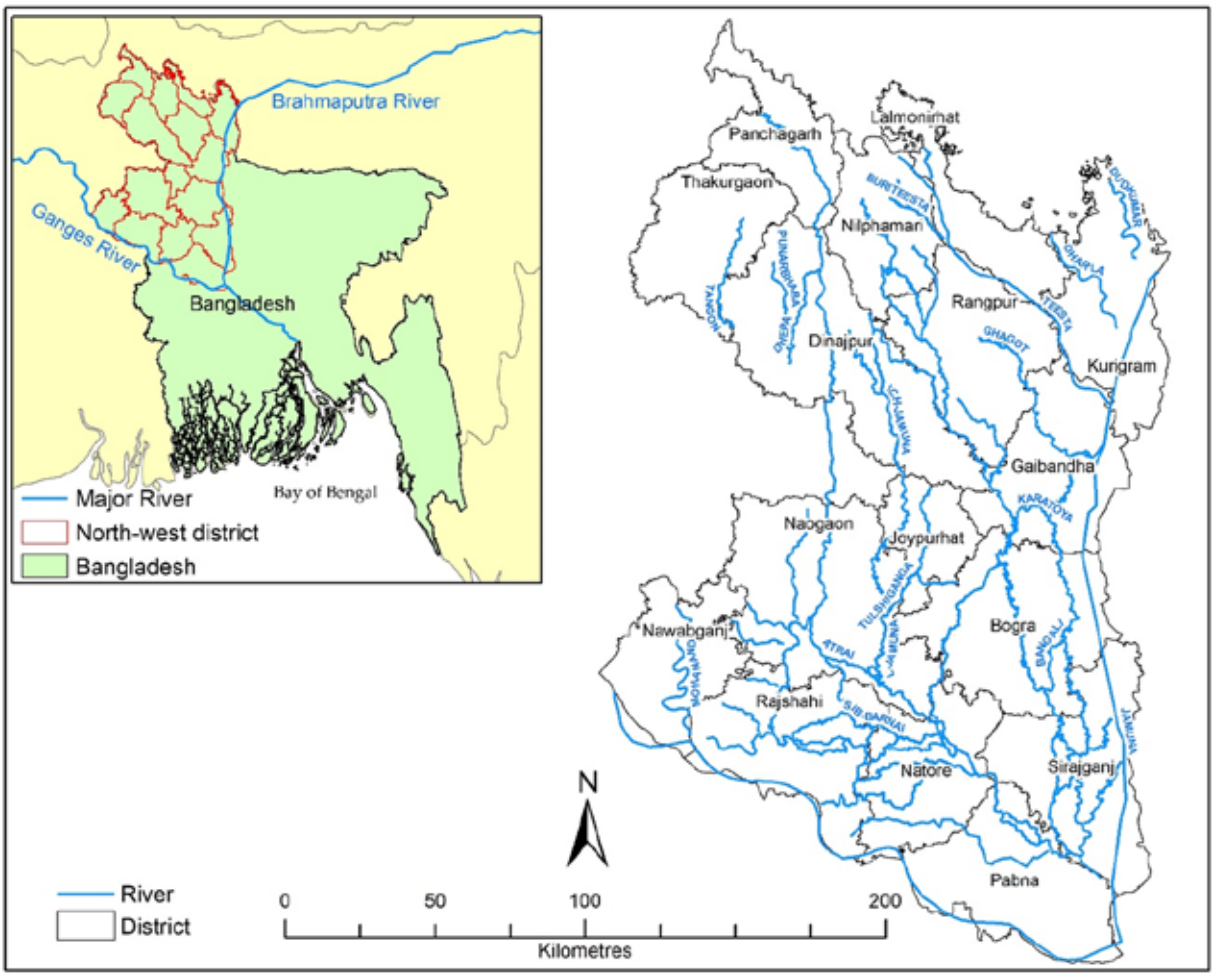

Figure 4.1: Location of the study area

4.1.1 CLIMATE

The study area experiences a tropical humid monsoon climate. In summer the mean maximum temperature is well above 35^0C whereas in winter the mean minimum temperature is below 10^0C. The cool weather begins in October and continues up to the end of March. The High Barind area in Rajshahi, Nawabganj and Naogaon districts is the driest part of the study area where annual rainfall varies from minimum of 1,250 mm and to a maximum of 2,080 mm. In the rest of the study area annual rainfall varies with a range of 1,800 mm to 2,600 mm. Almost 80% of the rainfall occurs during June to October. The relative humidity in the study area varies from 46% to 83%.

4.1.2 TOPOGRAPHY

Topography of the area varies from a maximum 94 m PWD (Public Works Datum) in Panchagarh District to a minimum 4 m PWD in Pabna District area. The study area is relatively flat, sloping towards southeast. However, the land slope is steeper in the northern part while the slope is gentle in the southern part.

4.1.3 RIVERS

The study area is drained mainly by Atrai, Sib-Barnai, Mohananda, Karatoya, Tangon, Kulik, Dhepa, Punarbhaba, Little Jamuna, Ichamati-Jamuna, Tulshiganga, Ghagot, Buriteesta, Chikly, Dudkumar, Dharla, Teesta, Bangali and Jamuna rivers. Among these rivers, Atrai, Buriteesta, Chikly, Dudkumar, Dharla, Teesta, Bangali and Jamuna rivers are the perennial rivers which cross the international boundary also. Dudkumar, Dharla and Teesta are the tributaries of the river Jamuna. The Jamuna flows along the eastern side of the study area. The study area appears to be well drained because of these major rivers and a number of small rivers, which criss-cross the study area. However, there are some low-lying areas and beels in the study area. Most of these low-lying areas and beels dry up during dry season.

4.1.4 GEOLOGY AND HYDROGEOLOGY

The study area has two major distinct physiographic units, the high relief Barind terraces and the low relief floodplains. Pleistocene Barind clay floors the Barind tract area whereas younger and older alluvium floors the rest of the study area (Figure 4.2). The study area is formed of a broad river-valley of the River Jamuna Teesta Atrai Dharala Dhudkumar and Hurasagar in the recent times. Towards the eastern region, the river-valley gradually widens up and ultimately merges into vast floodplain of the Ganges River further to the recent deltaic plains in the south and southeast. There are two types of floodplains in the area, the young flood plain of the river Ganges or Padma as well as Jamuna and older floodplain of the rivers Atrai. The Young Alluvium of Holocene (Recent) age consists of unconsolidated deposits of active channel, active floodplain and modern deltaic deposits. It is composed of sand, silt and clay. The older floodplains are a complex of abandoned channels and 'beels' or depressions.

The Pleistocene deposits are termed as Older Alluvium that forms the terraces. It is believed that the raised terraces are formed due to tectonic uplift. The terraces are composed of calcareous and lateritic residual clays and designated as Madhupur Clay Residuum. It is evident from the geological setting that during the Late Pleistocene to Early Holocene the sea was at low level, which caused erosion and incision of the exposed Pleistocene sediments through the fractured and sheared zones of the study area.

The geomorphology of the area appears to be simple due to easily recognizable physiographic units like the terraces and the floodplains. However the geomorphic processes acting in the area are controlled by the subsurface basin configuration. Four distinct units are present in the study area, namely Barind Terrace, Teesta Floodplain, Jamuna Floodplain and Atrai Floodplain.

The landforms of the study area are mostly level. The Jamuna, Atrai, Buriteesta, Teesta, Jamuneswari, Ghagot, Dudkumar, Dharla and Chikly are the major rivers to carry most of the drainage water in the study area. In the eastern part, most of the drainage water flows through the river Jamuna. The depressions in the Teesta and Atrai floodplains remain watery almost throughout the year due to steady water flow from upland river systems of the rivers Atrai, Teesta and the Jamuna.

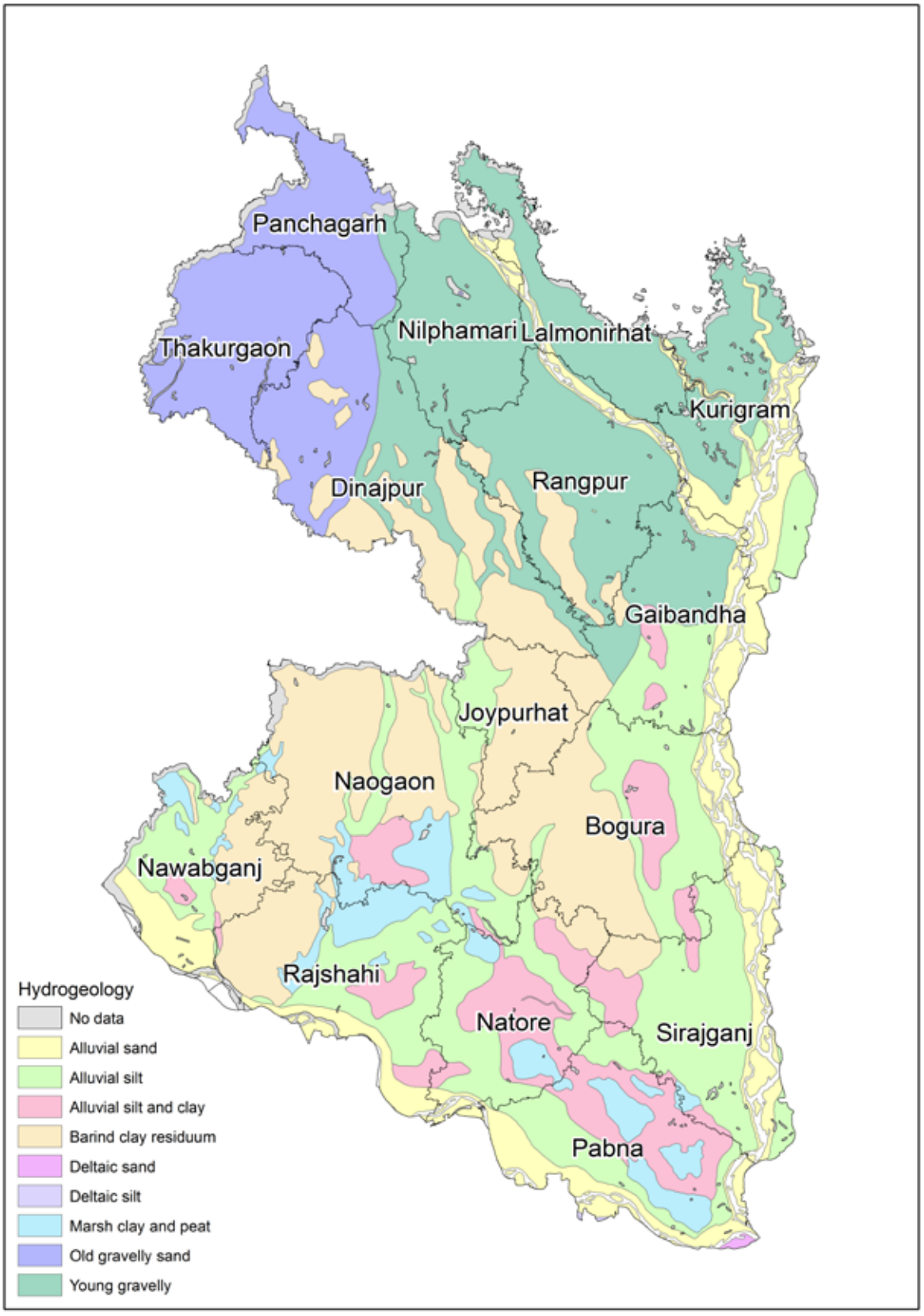

Figure 4.2: Hydrogeology of northwest Bangladesh

4.2 INTEGRATED MODELLING APPROACH

4.2.1 MIKE 11-MIKE SHE INTEGRATED MODELLING

Integrated surface water–groundwater numerical models enable better understanding of the river-aquifer interaction, as well as, providing a tool that can be used to manage the water resources in the best possible way considering the relative contribution of the components on the water balance in the area. The best option of future surface water and groundwater developments which will effectively utilize all available water resources with no or minimum of negative environmental impacts maybe explored using integrated surface water groundwater modelling technique. Integrated MIKE 11-MIKE SHE modelling system has been adopted in this study for this reason.

The MIKE 11 hydrodynamic module uses an implicit, finite difference scheme for the computation of unsteady flows in rivers and estuaries. MIKE SHE is a comprehensive mathematical modelling system that covers the entire land-based hydrological cycle. It is a finite difference model, which solves systems of equations describing the major flow and related processes in the hydrological system and simulates surface flow, infiltration, flow through the unsaturated zone, evapotranspiration and groundwater flow. The technical details of the MIKE SHE model including the underpinning equations are given in Appendix A.

4.2.2 SURFACE WATER MODEL

The physically based hydrodynamic modelling using MIKE11 tools was used to develop the surface water model. The MIKE 11 model was coupled with the groundwater model of the study area to simulate the groundwater and surface water interaction. The surface water model covers the entire study area incorporating the existing river systems with updated cross-sections.

MIKE 11 modelling system requires large amount of high-quality data including river channel bathymetry, water level and discharge measurements. After a model is developed, it requires a calibration phase. This is done to determine its ability to reproduce phenomena observed in the field. This is a trial-and-error process in which any deficiencies in the model setup and input data are rectified and model elements fine-tuned until a reasonable agreement between simulation and observation is achieved. After the model is calibrated, it is verified against known recent events to ensure that the model can simulate various hydrological scenarios correctly.

In this study a surface water model has been developed and calibrated with river water level and discharges taking data from northwest regional model developed by IWM. Then the model was coupled with a groundwater model. Details of the surface water modelling are described in the surface water modelling report (Karim et al. 2021).

4.2.3 GROUNDWATER MODELS

The MIKE SHE groundwater models were developed to understand the groundwater resources, to assess integrated water balance, and to undertake scenario analysis. The numerical models were developed with a grid size of 1000m×1000m. The spatial extents of these models are shown in Figure 4.3.

The models were updated for the period from 2005 to 2016 and were calibrated using observed groundwater levels. To improve the reliability, the calibrated models were also subjected to validation using a separate data set.

4.2.4 MODEL AREAS

Both surface water (MIKE 11) and groundwater (MIKE SHE) models were coupled and run dynamically. Four separate models cover the northwest region:

- DTW Installation Project Model (High Barind model), covers Rajshahi, Nawabganj, Naogaon districts
- BMDA Phase 2 Project Model (8-district model), covers Pabna, Sirajganj, Bogra, Gaibandha, Rangpur, Kurigram, Nilphamari, Lalmonirhat districts
- BMDA Unit 2 Project (4-district model), covers Panchagarh, Thakurgaon, Dinajpur, Joypurhat districts
- HYSAYA Project Model (Natore model), covers Natore district.

The models cover an area of 37,000 sq km; the extent of each model is shown in Figure 4.3.

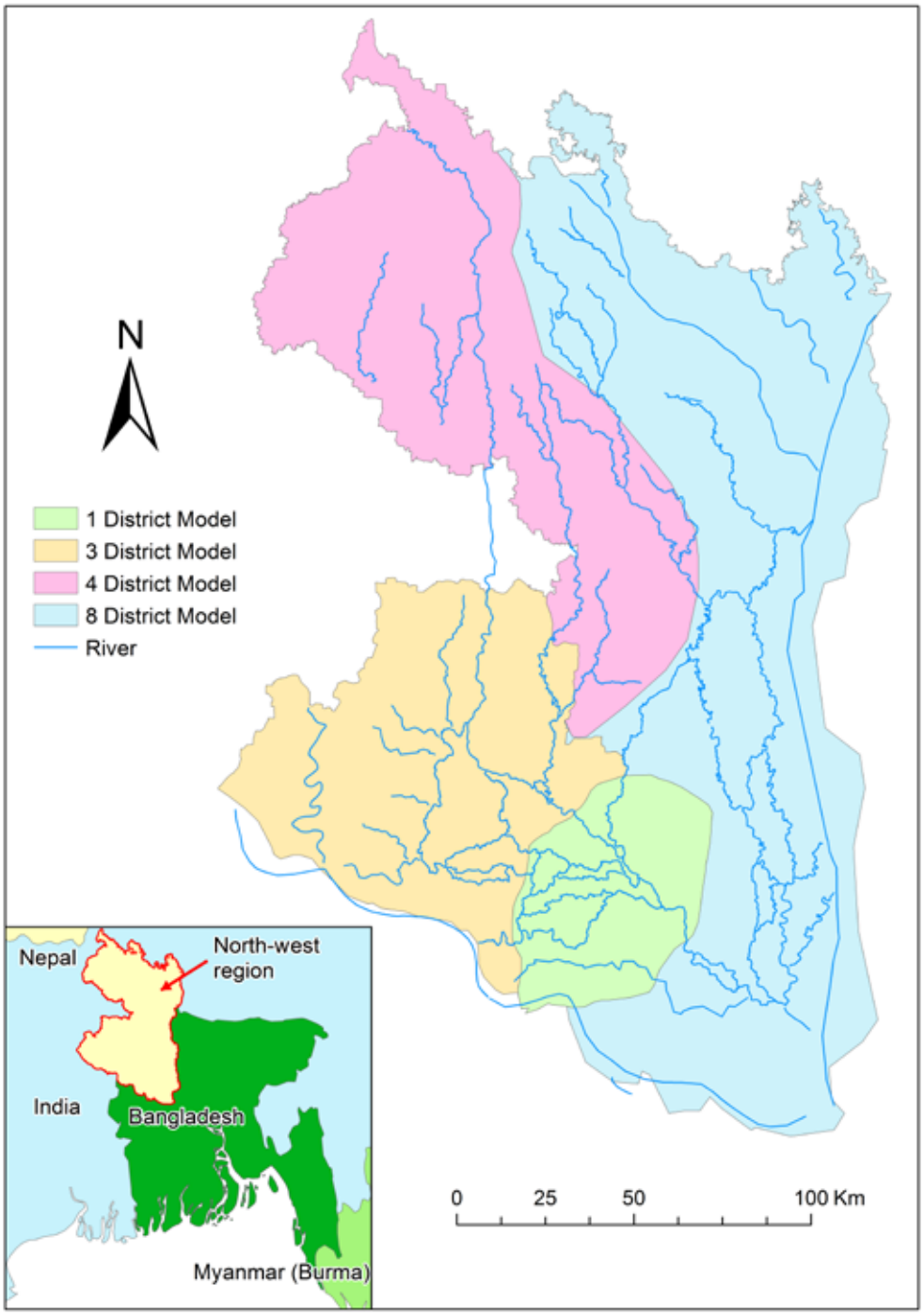

Figure 4.3: Spatial extents of the four MIKE SHE models that cover the Northwest region that were used in this study

4.2.5 MODEL SETUP

The major components of the model setup comprised representation of precipitation, evapotranspiration, unsaturated zone, saturated zone, overland flow and river systems in the spatially and temporally discretised model grid.

The default time step control and computational control parameters for Overland Flow (OL), Unsaturated Zone (UZ) and Saturated Zone (SZ) have been used for the entire simulation period. However, simulation periods of the calibration and validation models were different and user specified.

The model area was discretised into 1000m square grids as shown in the horizontal plan of the Figure B.1 to Figure B.4 in Appendix B. The Barind model has 8,030 grid cells, where 432 grids are the boundary cells (red cells) and the rest are computational cells. The 8-district model has 20,067 grid cells, where 865 grids are the boundary cells (red cells) and the rest are computational cells. The 4-district model has 9,799 grid cells, where 582 grids are the boundary cells (red cells) and the rest are computational cells. The Natore model has 2,983 grid cells, where 193 grids are the boundary cells (red cells) and the rest are computational cells. The grid cells are the basic units to provide all the spatial and temporal data as input and to obtain corresponding data as output. The computational layers define the vertical discretization of the 3-D groundwater model. Special consideration was given to the unsaturated zone, where the vertical resolution is as fine as 0.05 m, 0.1 m and 1 m towards the increasing depths.

4.2.6 TOPOGRAPHY

A well-prepared digital elevation model (DEM) is essential for visualizing the floodplain topography and for accurate modelling. A DEM of 300 m resolution has been developed using the topographic database available at IWM to define the topography of the study area. The DEM has been further updated using the surveyed data of different projects done by IWM in the area. Figure C.1 to Figure C.4 (Appendix C) show DEM of the study area. Elevation of the Barind model area varies from 8.86 m PWD to 46.88 m PWD. Elevation of the 8-district model area varies from 4.96 m PWD to 69.30 m PWD. Elevation of the 4-district model area varies from 14.60 m PWD to 103.16 m PWD. Elevation of the Natore model area varies from 7.09 m PWD to 17.79 m PWD.

4.2.7 PRECIPITATION

Rainfall data is needed as input to the model. Seventy-seven (77) rainfall stations are available in the region which have consistent time series data for development of the models. Table D.1 (Appendix D) shows the name, ID and location of rainfall stations used in the model for the study area.

To account for the spatial variation in rainfall, the time series data for each station have been associated with an area. This area has been estimated by Thiessen Polygon Method. The rainfall data for the relevant stations have been collected from BWDB office. After checking the consistency of these data, the time series input files for precipitation have been computed and incorporated in the model. Thiessen polygons for each rainfall stations are shown in Figure D.1 to Figure D.4 (Appendix D).

4.2.8 EVAPOTRANSPIRATION

The actual evapotranspiration is estimated in the model based on potential evapotranspiration rates, the root depths and leaf area indices of different crops over the seasons. Model uses Kristensen and Jensen formula (1975) for calculation of actual evapotranspiration. Time series data of the potential

evapotranspiration for 16 districts (Mainuddin et al. 2021; Mojid et al. 2021a) of the northwest region are given as input to the model.

4.2.9 LAND USE AND VEGETATION

Land use and vegetation are used in the model to calculate actual evapotranspiration depending on the actual crops grown in the project area. The major part of the study area is agricultural land, and includes homestead and water bodies. Under the present study, spatial distribution of crops has been determined from remote sensing data and field survey data available with IWM. However, for the model input, these cropping types and cropping pattern have further been simplified considering the major crops that require irrigation water. A crop database for each crop, which defines leaf area index, root depth and other properties of each crop have been developed based on FAO Irrigation and Drainage Paper 24 (Doorenbos and Pruitt, 1984) and previous analysis done by IWM in the study area and used in the model.

In the study area, crops are grown both in rain-fed and irrigated condition. Boro, wheat, potato, maize and Rabi vegetables are the main crops. Sugarcane is the yearly crops. Vegetable seed production is also becoming a popular practice in the recent years. The major cropping patterns that prevail within the project area, based on secondary data, are:

1. High Yielding Variety (HYV) Aman followed by potato followed by maize
2. HYV Aman followed by potato followed by HYV Boro
3. HYV Aman followed by mustard followed by HYV Aus
4. HYV Aus / Jute followed by HYV Aman followed by wheat
5. HYV Aman followed by HYV Boro
6. HYV Aman followed by wheat
7. HYV Aman followed by potato
8. HYV Aman followed by rabi vegetables
9. HYV Aman followed by maize
10. HYV Aman followed by pulses
11. Local variety Aman followed by wheat/potato/maize
12. Sugar cane
13. Fruit trees.

4.2.10 RIVER SYSTEMS

The river systems of the study area have been included in the model using MIKE 11 modelling tools as described in the companion surface water modelling report (Karim et al, 2021). The river model was coupled with the groundwater model for integrated simulation of surface and groundwater balance.

4.2.11 OVERLAND FLOW

When the net rainfall rate exceeds the infiltration capacity of the soil, water gets ponded over the ground surface. This water is then called surface runoff, and it is to be routed down-gradient towards the river system. Overland water starts flowing when it exceeds the specified detention storage. Detention storage can be specified either as spatially distributed or a constant value. Initial water depth on the ground surface

is also required as input data that can also be distributed or constant. The usual practice of paddy field band height is in range of 100 mm to 200 mm. A detention storage of 100 mm has been considered in the model. Overland flows are governed by the roughness of topography. A lower value of roughness has been considered in the model since the area is mainly agricultural land. A Manning number (n) has been specified describing the surface roughness. Since the area is dominantly agricultural, a constant value has been considered for the entire area. Exchange of overland flow and groundwater flow occurs when a soil becomes completely saturated and at the same time there is ponding water on the ground surface. Like river-aquifer exchange, leakage coefficient along with hydraulic conductivity is taken for overland-groundwater exchange.

4.2.12 UNSATURATED ZONE

The unsaturated zone (UZ) extends from the ground surface to the groundwater table. There are two unsaturated soil functions required for all soil types characterizing the individual soil profiles of the model area. The functions are the relationships on soil potentials (suction) versus soil moistures and the hydraulic conductivities. The vertical distribution of soil in the project area is highly heterogeneous. Due to high heterogeneity, soil parameters of different textures in different locations have been adjusted during calibration.

The unsaturated zone (UZ) extends from the ground surface to the groundwater table. UZ controls overland flow and percolation to groundwater. The flow through UZ is estimated using one-dimensional Richards' equation. It is based on input on soil-moisture due to rainfall, evapotranspiration and upward movement of capillary flux from groundwater table.

There are two unsaturated soil functions required for all soil types characterizing the individual soil profiles of the study area. The functions are the relationships on soil potentials (suction) versus soil moistures and the hydraulic conductivities as shown in Figure 4.4. In the study area, a field survey of soil relating to its physical and hydraulic properties viz, texture, moisture content and infiltration rate were performed. Most commonly occurring textures found in the study area have been found are: loamy sand, sandy loam, silty loam, silty clay and clay loam. The vertical distribution of soil in the project area is highly heterogeneous.

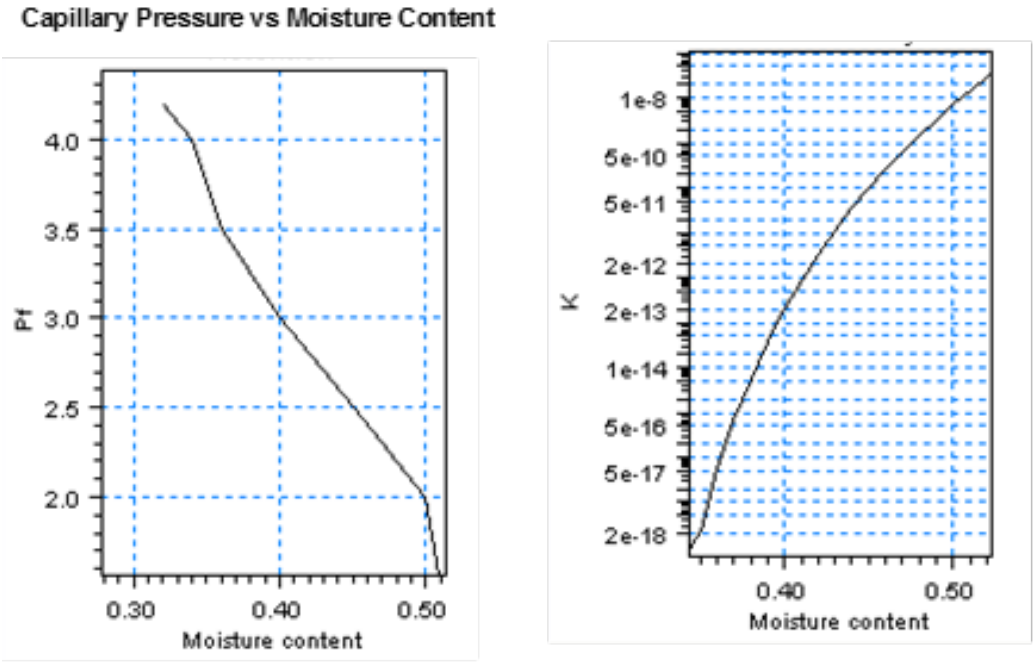

Figure 4.4: Soil moisture retention and hydraulic conductivity curve (m/s) for clay soil

4.2.13 SATURATED ZONE

The saturated zone component of MIKE SHE Water Movement Module accounts for the water exchange with other components and estimates the saturated subsurface flow in the catchment. MIKE SHE allows a full three-dimensional flow in a heterogeneous aquifer with switching conditions between unconfined and confined situations. The spatial and temporal variations of the potential heads are described mathematically by the non-linear Boussinesq equation and solved numerically by an iterative implicit finite difference technique. Setting up the saturated zone includes defining the computational layers from geological layers, hydrogeological characteristics, initial and boundary conditions, drainage, pumping wells and abstractions.

The available lithologs have been collected from IWM and other secondary sources. Based on the collected data, geological layers were established for the models of the study area and used as input. After analysing and simplifying, the model layers used in the models are: Top Layer, Aquitard and Aquifer. The hydraulic properties obtained from aquifer tests, IWM data bank and other reliable sources were used in the model as initial estimates of these parameters. Sample hydro-stratigraphic cross sections are shown in Figure E.1 to Figure E.3 (Appendix E).

Within the study area, the aquitard is not continuous and thus the different layers are not interconnected in nature. Computational layers were defined following the geological layers of the study area. Three computational layers (top layer, aquitard and aquifer) obtained from geological layers have been used as computational layers in the models.

4.2.14 INITIAL AND BOUNDARY GROUNDWATER LEVELS

Initial conditions of a model refer to distributions of hydraulic heads and/or concentrations in the model domain at the start of the simulation runs. The specification of the initial conditions is required for transient simulations, but not necessary for steady state simulations. Based on available observation wells data in and around the model area, a groundwater head map, by interpolation method, for January 2005 was prepared and used in the model. Figure F.1 to Figure F.4 (Appendix F) show the potential head map at the start of simulation.

Boundary condition must be specified for all layers along the boundary of the model area. A total of 127 monitoring wells was available along the boundary line of the four models. Available river water levels along boundary of the model were also used as boundary. A time series head boundary condition file was prepared for each boundary cell using the observed groundwater level and river water level. As the layers are leaky in nature in most of the area, the same boundary condition was applied in all layers. The location of the boundary wells used to generate the prescribed head boundary conditions for the numerical models are shown in Figure F.5 to Figure F.8 (Appendix F).

4.2.15 DRAINAGE

Drainage representation in the model covers natural drainage as well as drainage through man-made channels. It was not feasible to individually represent smaller channels and ditches in the regional model. Drain flow is simulated by a linear routing of water. Drain water could be routed to overland water, rivers or model boundaries. In this study, drain water is routed to the respective rivers and natural drainage channels.

4.2.16 PUMPING WELLS AND ABSTRACTIONS

Water demand and abstraction data for the period of 2005 to 2016 were needed for model calibration and verification. The total abstraction from the model area comprises irrigation, domestic and industrial water

use components. Water abstraction for the period of 2005 to 2016 was estimated and used in the model. The irrigation demand was computed using crop water requirements using the crop coefficient approach and compared with the estimates from the companion studies in the project (Mainuddin et al. 2021, Peña-Arancibia et al. 2021a). The demand for domestic & industrial purposes was calculated considering per capita consumption as well as relevant population data.

4.2.17 SURFACE WATER–GROUNDWATER INTERACTION

The aquifers are often fed by seepage from rivers, ponds and other water bodies. Groundwater also discharges through seepage to feed rivers, ponds and water bodies. Two conditions may exist that determine how groundwater use has an effect on the surface water resources. These conditions are:

- An interconnected river and aquifer, where the river is losing water to the aquifer and
- An interconnected river in which the river is gaining water from the groundwater.

In the first condition, river losses will increase in response to groundwater pumping. In the second condition, river gains will decrease in response to groundwater pumping. In either case, groundwater pumping will result in a depletion of surface water. All these conditions may exist in the same river at different locations or times of the year.

In the study, the GW-SW interaction mainly deals with the interaction between river and aquifer at the river-aquifer interface. It has been incorporated through coupling of river model with groundwater model.

The coupling of surface water with groundwater model involves a number of specifications. The river reaches where the coupling will occur are defined in the river model. In the study, all major rivers within the model area have been coupled with groundwater. Type of river-aquifer exchange and the flooding condition have also been defined. The exchange of flow between the saturated zone component and the river component is mainly dependent on head difference between river and aquifer and properties of riverbed material such as leakage coefficient. For this study, the leakage coefficient is specified as 1.0e-6/s**.** For river-aquifer exchange, leakage coefficients along with the hydraulic conductivity of the saturated zone are taken into account for most of the river reaches.

In the present study, SW-GW interaction models developed in the previous studies covering the whole northwest region of Bangladesh have been updated incorporating the recent data. The models have been updated from January 2005 to December 2016. The models were updated with the data of groundwater levels, river water levels and river flows.

4.2.18 MODEL CALIBRATION

The purpose of model calibration is to achieve an acceptable agreement with measured data by adjusting the input parameters within acceptable range. As a coupled surface water groundwater model contains huge number of input data, the parameters to adjust during the calibration could be numerous. During the calibration, it is therefore important to adjust the parameters within the acceptable range. Model runs were completed for the time period from January 2005 to December 2016. First two year were kept as 'warm-up' period of simulation. Accordingly, model calibration was undertaken for the period from January 2007 to December 2013. In the present model, calibration was done against observed groundwater levels. The remainder of the data from 2013 to 2016 was used for model validation

ADJUSTED PARAMETERS

The calibration of the coupled model follows a computationally demanding and repetitive procedure. Calibration of one parameter has influence on the others. The controlling parameters for groundwater flow

in the aquifers were adjusted, so that the simulated groundwater level matches the observed level. While there are some minor parameters to influence the groundwater calibration, initial tests revealed that the hydraulic conductivity is the main parameter for groundwater model calibration. Evapotranspiration and unsaturated zone parameters, and drainage levels also influence the fluctuations of the observed groundwater heads. The controlling parameters for river flow were adjusted so that the simulated river water levels and discharges corresponds to observed data. Then the controlling parameters for river-aquifer interaction were adjusted. The main parameters for river-aquifer interaction are the river leakage coefficient and the conductivity of the upper layer. During calibration, overland leakage coefficient, hydraulic conductivity and storage coefficient were also adjusted. The final calibration of parameters for the aquifer layer of different models are given in Table 4.1.

Table 4.1: Adjusted calibration parameters for the aquifer layer in four MIKE SHE models

Name of the Model	Horizontal Hydraulic Conductivity, Kx & Ky (m/day)			Vertical Hydraulic Conductivity, Kv (m/day)			Specific Yield (Sy)			Specific Storage (Ss)
	Max	Min	Avg.	Max	Min	Avg.	Max	Min	Avg	Average
Barind	90.98	8.74	34.21	18.23	1.73	6.91	0.131	0.012	0.050	0.000020
8-district	94.78	12.96	51.75	18.32	2.59	10.37	0.142	0.015	0.064	0.000899
4-district	99.96	8.64	36.80	19.95	1.75	7.34	0.25	0.05	0.132	0.00009
Natore	98.05	10.47	46.31	23.80	2.09	9.30	0.188	0.025	0.069	0.00005

Overland leakage coefficient

The overland leakage coefficient was also adjusted during calibration. The overland leakage coefficient is used when the soil becomes fully saturated. If, at the same time, there is ponded water on the ground surface, the exchange of water between overland flow component and groundwater component is calculated based on vertical hydraulic conductivity in upper layer of the saturated zone and hydraulic gradient between surface water level and groundwater table in the upper layer of the saturated zone.

However, often the vertical hydraulic conductivity of the upper layer in the saturated zone is not representative of the permeability of the top layer of the soil (the soil layers are usually described in more detailed in the unsaturated zone (UZ)model than in the saturated zone (SZ) model, but the UZ parameters is not used when UZ disappears).

To handle such situations a leakage coefficient can be specified. The exchange of water between the surface water and ground water is then calculated based on the specified leakage coefficient and the hydraulic head between surface water and groundwater. In other words, the UZ model is automatically replaced by a simple Darcy flow description when the profile turns completely saturated.

Vertical hydraulic conductivity

This is one of the main parameters that determines vertical exchange of water across layers during model calibration. Vertical hydraulic conductivity describes the ability of soils to move water in the vertical direction. Hence a higher vertical hydraulic conductivity gives a higher ability to move water from one point to another. When vertical hydraulic conductivity is increased, the water movement increases and groundwater head rises. During the calibration, the vertical hydraulic conductivity has been used to control water movement towards downward and in that sense, control the groundwater table and fluctuation.

Storage terms

The storage terms, specific yield and storage coefficient, describe the storage potential of the aquifer during unconfined and confined conditions. For unconfined conditions the specific yield describes the amount of

water that could be drained from unit volume of the aquifer media. The specific yield is in many cases equal to the effective pore space. During unconfined conditions, drainage from the soil is mainly occurring by gravity driven processes as water table is lowered. During confined conditions the soil will be fully saturated at all times, and the storage release is then mainly driven by the change in water and soil pressure. For this reason the storage coefficient is much smaller than the specific yield. For MIKE SHE model the storage coefficient was used for all fully saturated computational layers, meaning for layers where the potential head is above the upper boundary of the layer. For layers, which are not fully saturated, the specific yield was used. During calibration, the storage terms was adjusted to control the fluctuations. A higher storage term increases the amount of water that can be stored in the aquifer and thereby decreases the water level fluctuations. The storage does not influence the general water movement significantly but has a significant effect on the water fluctuation during periods of vertical water movement.

RIVER LEAKAGE

The exchange of water between rivers and surrounding aquifers is controlled by the head difference between the surface water and groundwater schemes and hydraulic conductance. The head difference is simulated by MIKE SHE and MIKE 11 model, while conductance is described either by use of the parameters from the geological model or from a user specified leakage coefficient. The leakage coefficient is used to control the water exchange between the river and the aquifer and thereby also to regulate either the groundwater level or surface water level. As a general rule, the same leakage coefficient has been applied to the whole area, but in areas where a higher or lower leakage is expected the value has been changed.

4.2.19 CALIBRATION AGAINST GROUNDWATER LEVEL

During calibration of the models, a total of 257 monitoring wells were selected for calibration of the four models. The locations of the monitoring wells for observed data used in calibration process are shown in Figure G.1 to Figure G.4 (Appendix G). These monitoring wells were spatially distributed over the entire region ensuring that satisfactory calibration would represent good model performance over the entire study area. Sample calibration plots for the entire northwest region covering the 16 districts are given in Figure 4.5 to Figure 4.8. Maps of calibrated hydraulic conductivity and specific yield in the aquifer layers for the different model areas covering the whole northwest region of Bangladesh are shown in Appendix H.

There is no single metric that completely describes the goodness of calibration. Some simple measurements could be the mean error (ME) and a guideline could be ME/Dh £ b1; Dh is the difference between maximum and minimum potential head in the areas. The value of b1 for an acceptable model could be, for example, specified as 0.05. The mean error should be less than b1 times the total difference in potential head. Within the area, an acceptable mean error may be specified as 1.0 m. Choice of such metrics should be carefully chosen considering the main objectives of model development.

It was found that 75% of the observation wells had a mean error less than one meter. It indicates that model represents the yearly fluctuation and the change in head over the model area reasonably well. In some areas, the mean error was greater than 1.0 m. There are several reasons for this, and these are explained in more detail below.

REASONS FOR DEVIATION BETWEEN SIMULATED AND OBSERVED GROUNDWATER LEVEL

In general, the overall calibration of the present model was acceptable, but there is scope for further improvement. Some of the reasons for the deviation between observed and simulated groundwater levels are.

- insufficient irrigation information; the conceptual description of the irrigation abstraction could be further improved by using cropping patterns identified using high resolution remote sensing data

- missing description of pumping or drainage systems close to the observation wells
- observation wells close to the river and the groundwater are connected to the river water level
- for a model with large grid size, it is often challenging to obtain a good agreement between observed and simulated values
- there is considerable uncertainty in the crop water demand and the actual abstraction in the field.

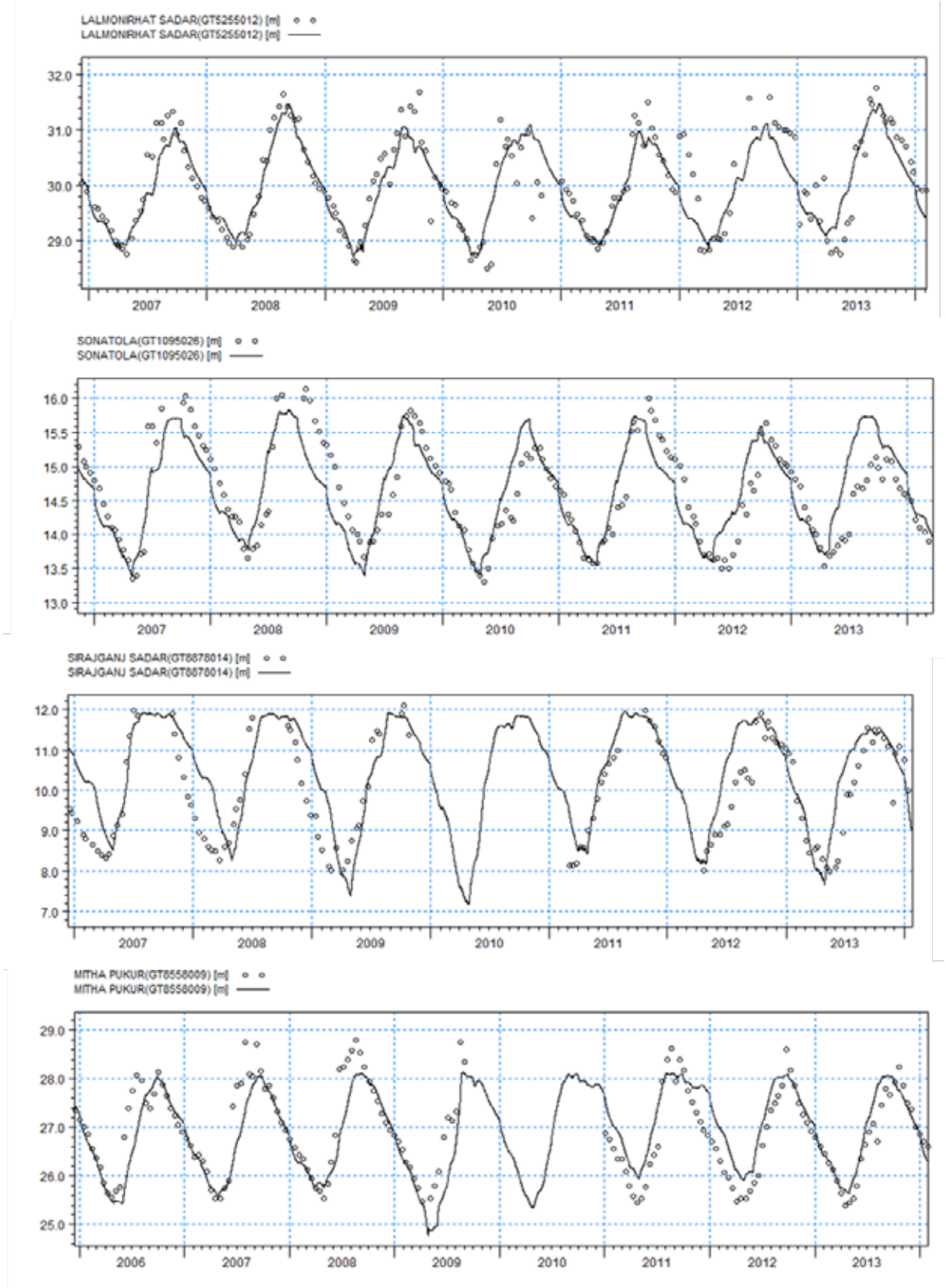

Figure 4.5: Calibration plots against groundwater levels for Lalmonirhat, Bogra, Sirajganj, Rangpur districts area

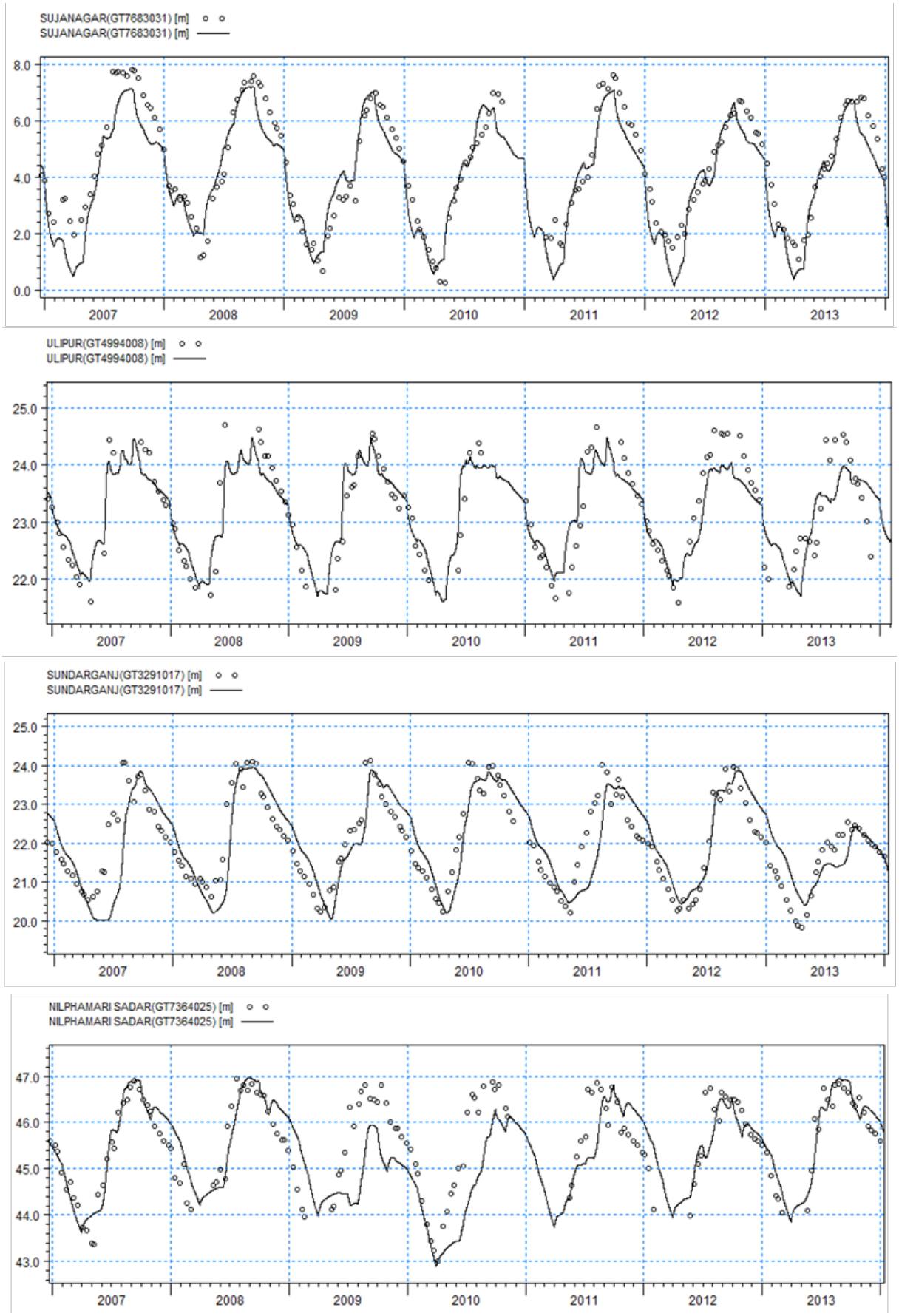

Figure 4.6: Calibration plots against groundwater levels for Pabna, Kurigram, Gaibandha, Nilphamari districts area

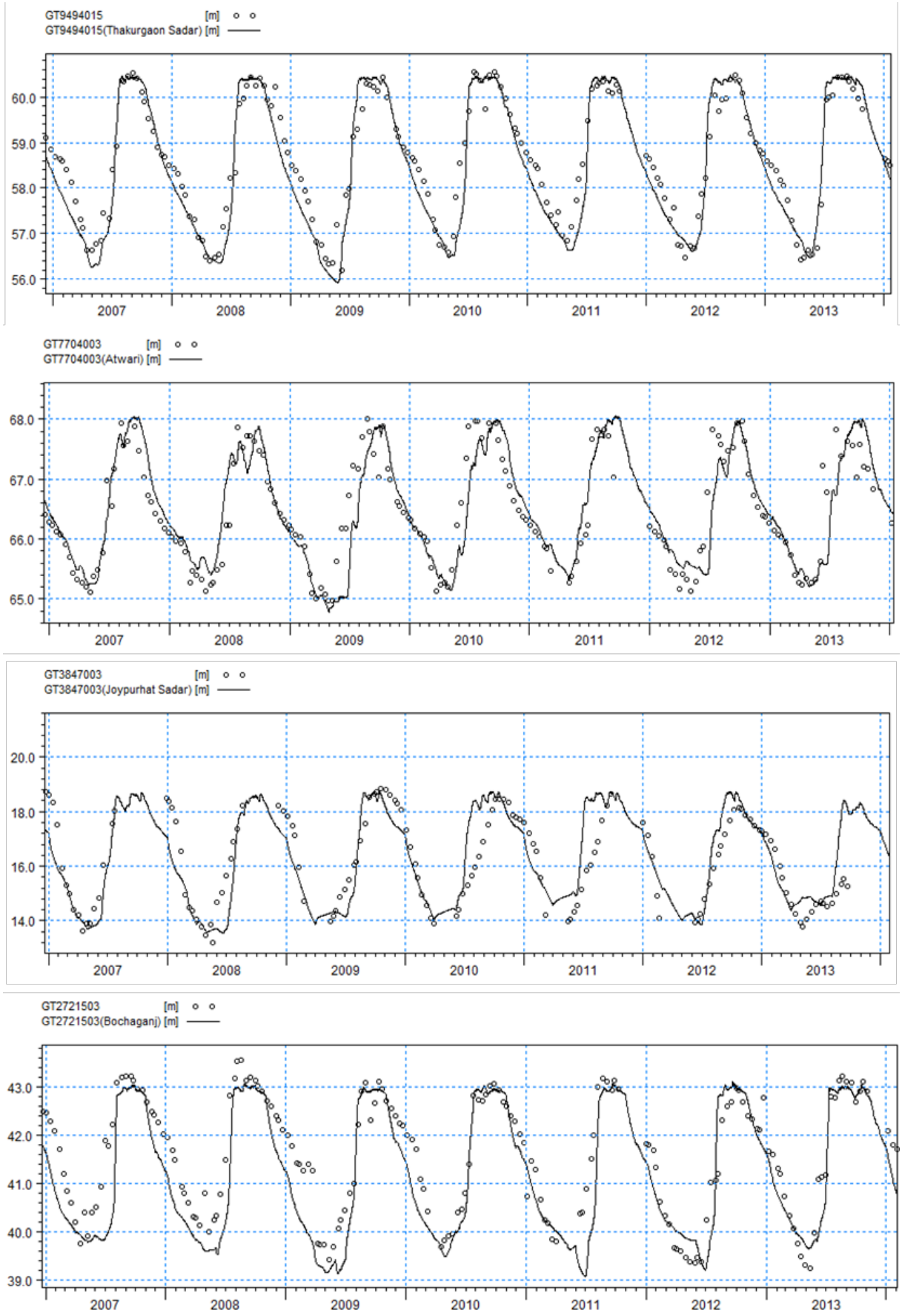

Figure 4.7: Calibration plots against groundwater levels for Thakurgaon, Panchagarh, Joypurhat, Dinajpur districts area

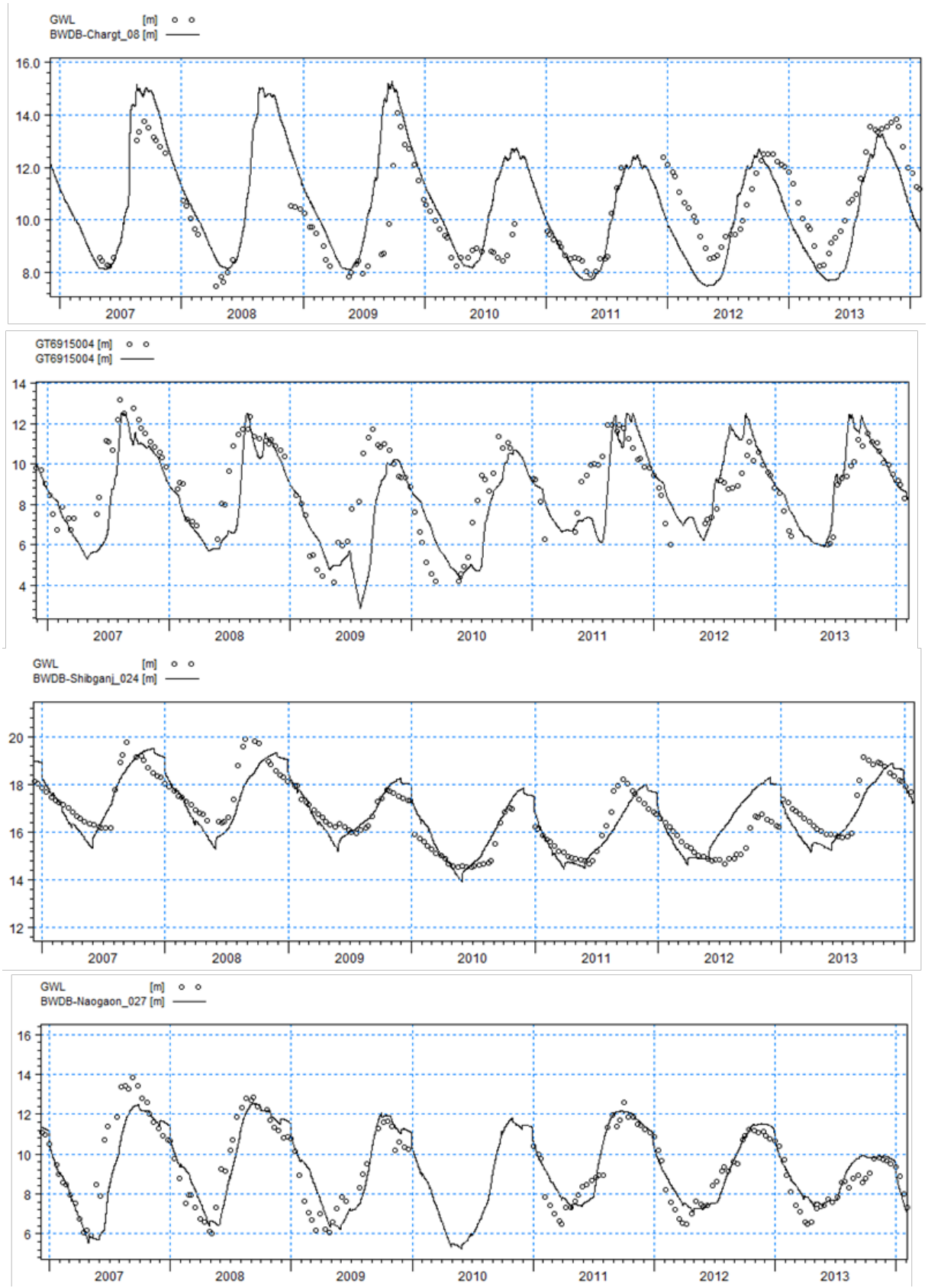

Figure 4.8: Calibration plots against groundwater levels for Rajshahi, Natore, Chapai Nawabganj, Naogaon districts area

LIMITATIONS IN CALIBRATION DUE TO LACK OF ABSTRACTION DATA

The abstraction for irrigation is one of the controlling parameters when simulating the groundwater fluctuation in Bangladesh. Even though the main irrigation withdrawal is during the dry period, it affects the groundwater resource and change in groundwater level during the whole year. In the study area, there are many Deep Tube Wells (DTWs), Shallow Tube Wells (STWs) and other infrastructure used for irrigation. Due to non-availability of their position, screen depth, and operating hour, the abstraction has been specified by considering land use, cropping pattern and demand. Consequently, even if the overall water balance is constrained by groundwater levels, ETa and other estimates, in some areas, the local drawdown may not be simulated correctly. In areas with a high density of DTW or STW the simulated drawdown may be underestimated and in areas with a low density of DTW or STW the drawdown may be overestimated. The hydrological responses to a DTW and a STW are very different. As a DTW has higher capacity than a STW, the localized impact from a DTW is more likely to be higher than the impact from even a number of STWs. Such localised drawdowns around DTWs are difficult to be represented in regional scale models with coarse grid resolution. The calibration may be improved if the DTW abstraction is handled as an actual groundwater abstraction, meaning that water from DTW will be withdrawn at the actual location with actual volume.

CALIBRATION PROBLEMS CONCERNING THE MODEL DISCRETIZATION AND SPATIAL HETEROGENEITY

Another reason for the discrepancy is the model grid discretization. The study area has been discretised into 1,000 m square grids. The models have total 40,879 grid cells, where 2,072 grids are the boundary cells and the rest are computational cells. The grid cells are the basic units to provide all the spatial and temporal data as input and to obtain corresponding data as output. As many local features can influence the observed values, it is often challenging to obtain a good accordance between observed and simulated values with large grid size.

Another important factor aiding better model calibration is improved representation of spatial heterogeneity in hydraulic characteristics like the hydraulic conductivity and specific yield. For the MIKE SHE model, it was not possible to take a computationally intensive calibration approach given the licence conditions and available resources in this study.

MODEL VALIDATION

Calibrated models are sometimes validated by using data beyond the calibration period. In this study validation was done for the period 2014 to 2016. Model validation was undertaken by comparing the simulated groundwater levels to observed ones at the same observation locations which are considered for calibration. Some examples of validation results against groundwater levels for the period 2014 to 2016 are shown in Figure 4.9 and Figure 4.10. Overall, validation results show similar trend of groundwater fluctuation of groundwater levels between observed and simulated values.

From the results of the model validation, it could be concluded that the parameters used in the calibrated model are acceptable, thus the model can be used for prediction purposes.

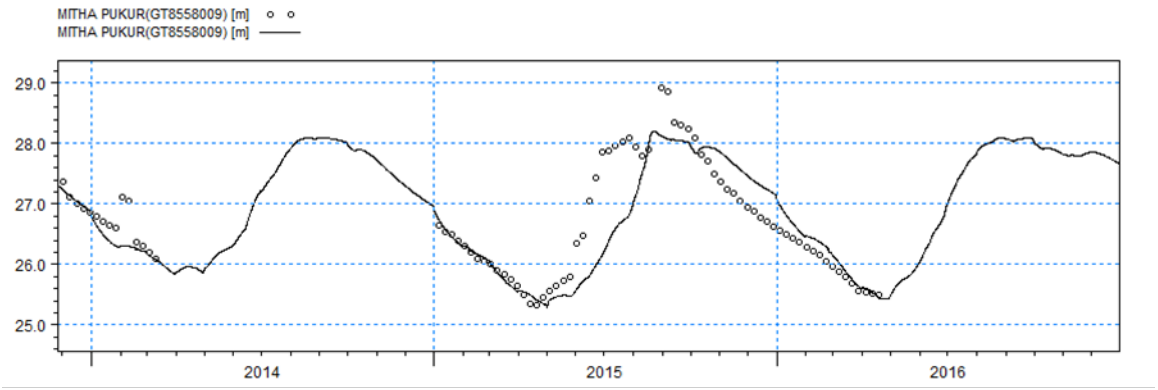

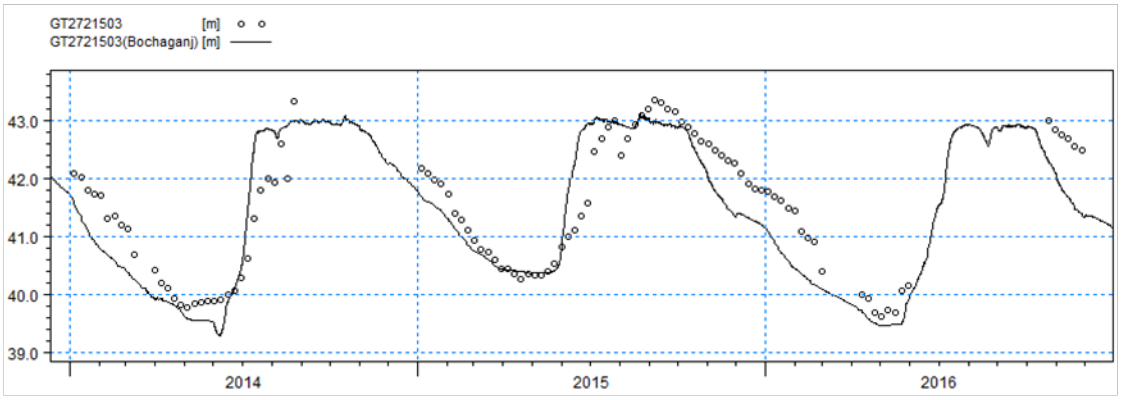

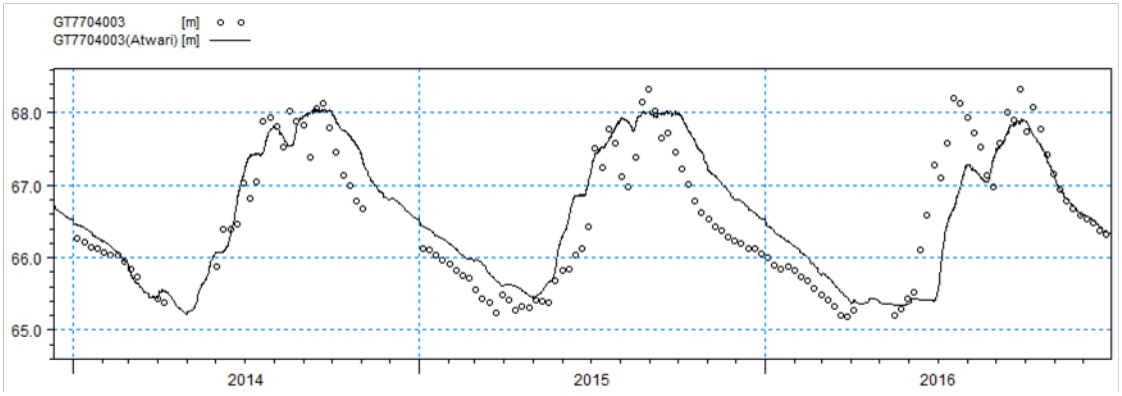

Figure 4.9: Groundwater level validation plots for bores GT8558009, GT2721503, GT7704003

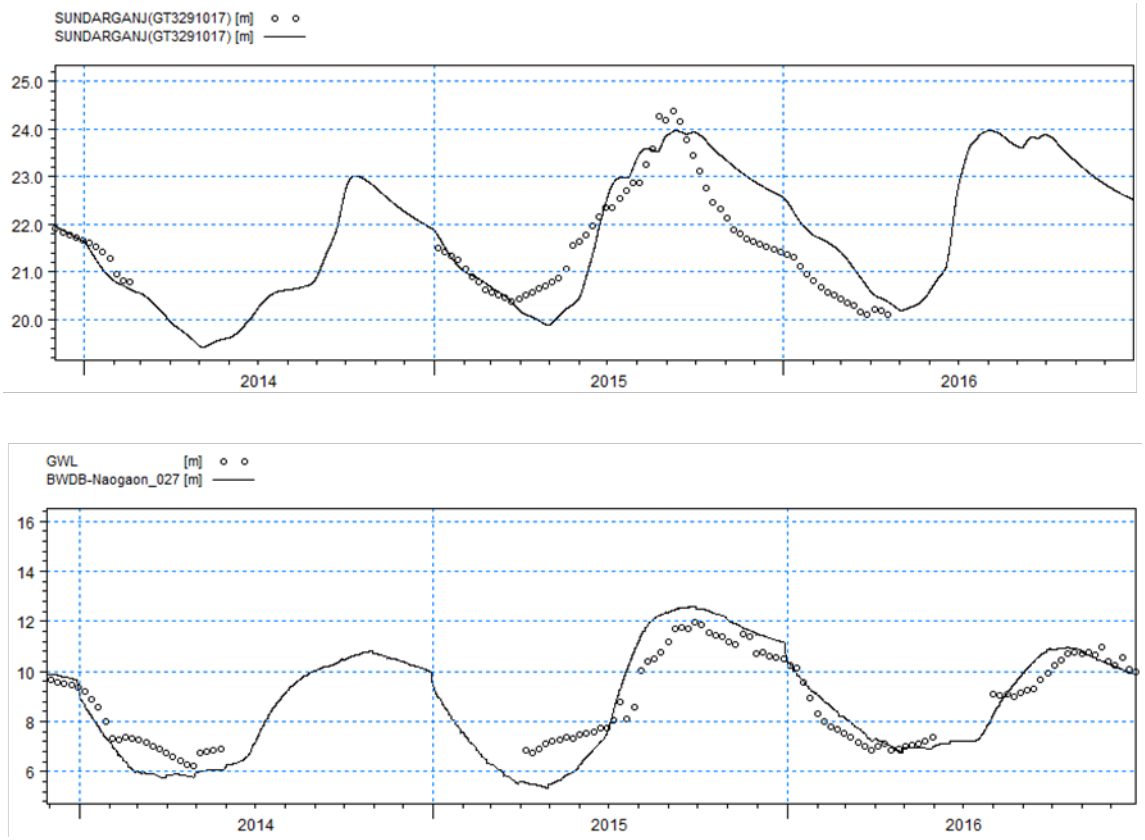

Figure 4.10: Groundwater level validation plots for bores GT3291017, and BWDB-Naogaon_027

4.2.20 SENSITIVITY ANALYSIS

Sensitivity analysis is a procedure for quantifying the impact on an aquifer's simulated response due to an incremental variation in a model parameter or a model stress. The purpose of sensitivity analysis is to identify those parameters which are most important in determining the aquifer behaviour.

The parameters can be ranked in order of importance, and then priorities set for focusing field investigations on key parameters to reduce model uncertainty. Sensitivity analysis was carried out for the horizontal hydraulic conductivity, detention storage, boundary condition and subsurface drainage. Processes like recharge are often sensitive informing the groundwater levels and storage changes. In this study recharge is simulated using the complex interaction of unsaturated and saturated zone flow and hence was not included in the sensitivity analysis. The hydraulic conductivity values were multiplied by 2 and 0.5 times to its base condition whereas detention storage has been considered as 50 mm instead of 100 mm as in base condition. The bias induced due to the boundary condition was checked by considering no flow boundary condition in all the layers. The sensitivity of the above-mentioned are presented in Figure I.1 to Figure I.16 in Appendix I.

The sensitivity analysis shows that subsurface drainage has a great influence followed by horizontal hydraulic conductivity in the model calibration. However it is noteworthy that these parameters would be correlated when calibrating to groundwater heads and the sensitivity analysis approach using one parameter at a time may not reveal the actual sensitivities.

The sensitivity plot also indicates that the detention storage and boundary do not have a significant influence on model calibration. As the boundary condition does not have much influence on model simulation so it can be concluded the model is unbiased with respect to boundary condition.

4.2.21 RECHARGE CHARACTERISTICS FOR THE STUDY AREA

Recharge means the replenishment of groundwater storage that is depleted by withdrawal of groundwater with tube wells and by natural processes. The sources of groundwater replenishment of the study area are deep percolation of rainwater and irrigated water from the crop fields, seepage from the rivers, khals, ponds and other water bodies, and horizontal flow of groundwater from the surrounding areas. Recharge to groundwater depends on different physical and climatic conditions as well as hydraulic properties related to soil, aquifer and water. Recharge to groundwater begins with the rainfall from late May and continues up to October while recharge from irrigated crop field occurs from December to the end of March.

The aquifer becomes full in the months of August/September but excess rains are available to recharge till October, if there is room for recharge. By creating additional storing space the magnitude of annual replenishment of groundwater may be increased but it depends on the availability of water and the percolation rate of soil. Direct percolation occurs during the rains from naturally submerged fields and un-submerged lands. Excess rainwater is also stored within the bund that surrounds the paddy field and in the depression areas. This water is also available for recharging the groundwater after meeting the demand of evapotranspiration. When sufficient groundwater development occurs to attain the recharge potential, the long-term average of annual replenishment of groundwater may be considered as safe yield. Groundwater storage reduces due to withdrawal for irrigation and domestic uses and outflow to rivers, canals, ditches, ponds and other water bodies. The loss of groundwater due to evaporation from water table and transpiration by plants also attributes to depletion of groundwater storage.

4.2.22 DEPTH TO PHREATIC SURFACE/GROUNDWATER TABLE FOR THE STUDY AREA

Spatial distribution maps of maximum and minimum depth to groundwater tables were prepared for 01.05.2016 (pre-monsoon) and 01.11.2016 (post-monsoon). Sample maps for Barind model area for maximum and minimum depth to groundwater tables are shown in Figure 4.11.

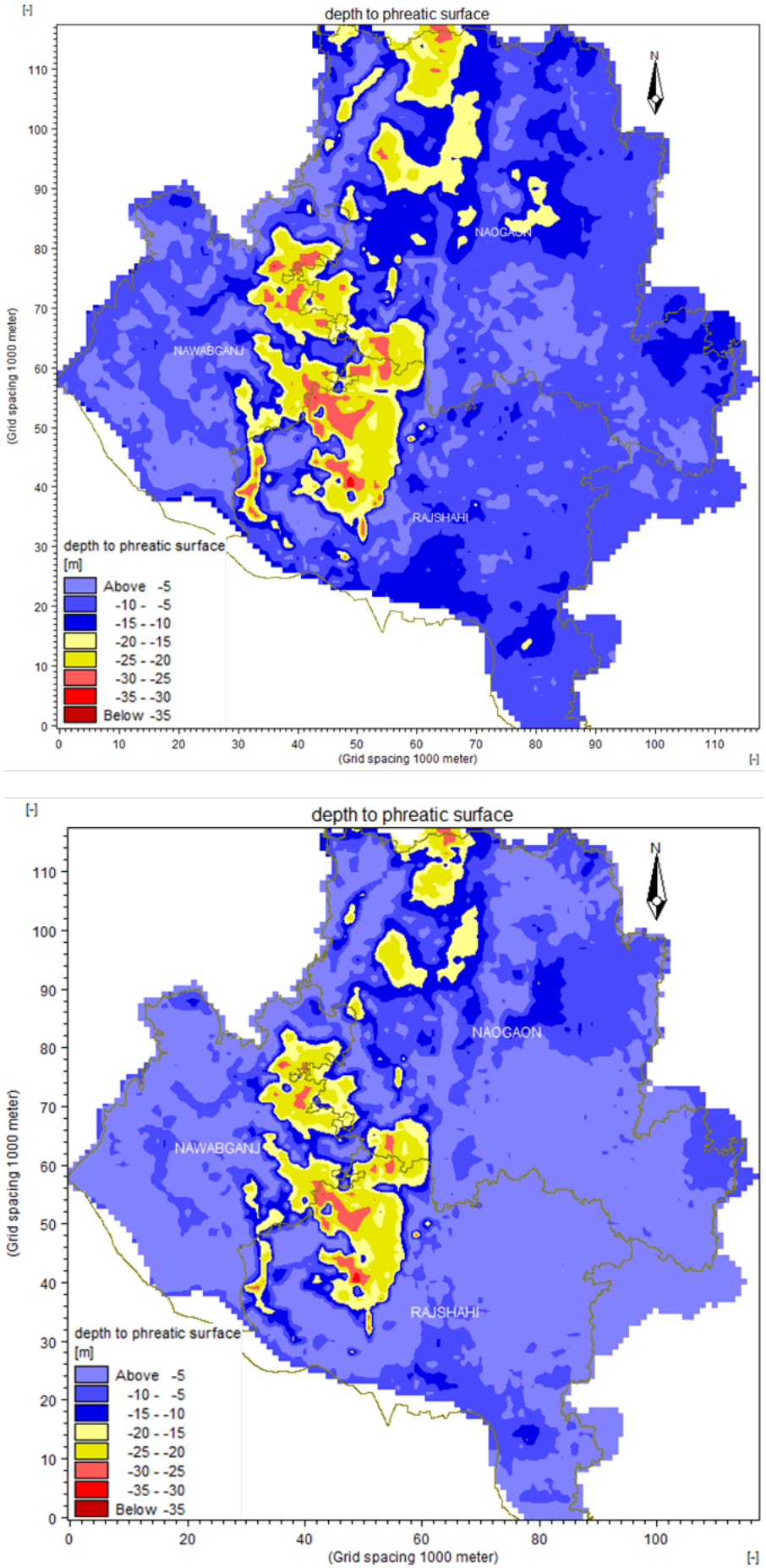

Figure 4.11: Depth to groundwater table for Barind area a) maximum depth (pre-monsoon) and b) minimum depth (post-monsoon)

Maps for maximum and minimum depth to groundwater tables were prepared to see the effect of pumping during irrigation season and also to see whether the groundwater table regains to its original positions or not. It can be seen that maximum depth to groundwater table remains within (–) 2.5 m to (–) 35.0 m in most of the areas on 1 May. From Figure 4.11, it is observed that in the dry season (pre-monsoon) the groundwater table goes beyond the suction limit (approximately 7 m below ground level) in major part of the Barind area. Suction mode tube wells will not operate in the areas where the groundwater table goes beyond the suction limit. At the end of October, due to recharge from rainfall, the groundwater table remains below (–) 2.5 m to (–) 30.0 m (Figure 4.11b), in most of the Barind area. Negative sign indicates below ground surface.

4.2.23 WATER BALANCE

The average water balance for the northwest region obtained by combining the district scale water balance for the 16 districts is shown in Figure 4.12.

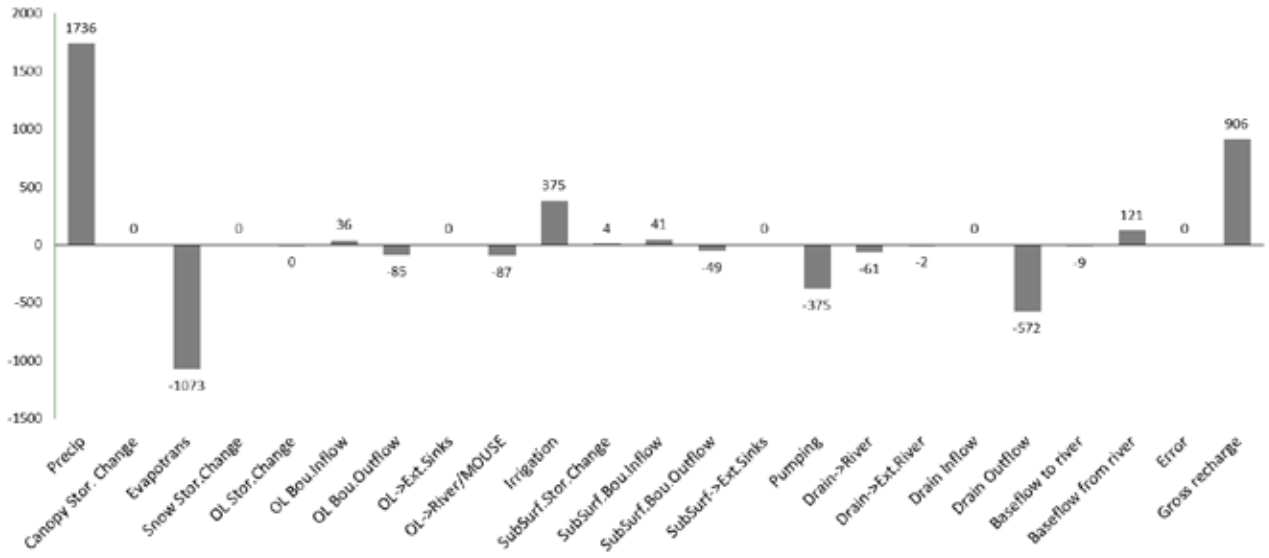

Figure 4.12: Average water balance for the northwest region based on district scale water balance between 2005 and 2016 obtained from MIKE SHE models

To assess the recharge characteristics, water resources and component wise contribution, a water balance of the study area has been made considering all the physical processes in saturated and unsaturated zones and rivers systems in an integrated way. In general, water balance includes the hydrological components which come as inflow to or outflow from the system. The difference between inflow and outflow is the net storage change within the system. Water balance of the calibrated model is used to understand the overall recharge characteristics of the study area. Recharge means the replenishment of groundwater storage that has been depleted by the withdrawal of groundwater with the irrigation wells, and by the natural processes. The losses are due to outflow to rivers, canals, ditches, ponds, beels (depression areas) and other water bodies. The loss of water for evaporation from the water tables and transpiration by plants also contributes to depletion of groundwater storage. Recharge to groundwater depends on different physical, climatic and hydraulic properties related to soil and aquifers.

In the study, the calibrated models were used for simulation of the historical water balance in the districts in NW Bangladesh over the period 2007–2016. Detailed analysis of saturated and unsaturated zone and recharge and discharge components for each district is presented in Appendix J.

An average of 2,111 mm of water enters into the northwest region mainly from rainfall and irrigation applied to the field from both groundwater and surface water sources while a total of 1,073 mm of water goes out of

the system mainly as evapotranspiration (ET). It is noteworthy that this is the gross water balance for the complete surface and groundwater system. The components of groundwater balance are much smaller compared to this as only a smaller fraction of the water reaches the aquifer after runoff and other discharges related to the surface water.

Groundwater enters and leaves the system through lateral flow and exchange with the rivers. The percentage of ET is about 50% of applied water (rainfall and irrigation application). Annually an average of 375 mm is pumped out for irrigation from the northwest region. These vertical components comprising rainfall, ET, irrigation, pumping and exchange with river dominates the water balance of the northwest region, while other smaller components comprise lateral inflows and outflows across and within the boundaries.

5 PROBABILISTIC GROUNDWATER MODEL

While the MIKE SHE model simulations gave a comprehensive representation of integrated water balance in the northwest Bangladesh, having them as four different computationally complex models limited the prospects of doing a comprehensive analysis of saturated zone water balance and especially storage changes in the aquifers. To overcome this constraint, we developed a simple numerical model for the saturated zone. This chapter reports the development and calibration of the numerical groundwater model based on the MODFLOW code for the northwest Bangladesh region. This model was designed to represent the recharge and discharge components that are spatially and temporally variable in the model at the district scale with the objective of undertaking probabilistic analysis of groundwater storage changes in the aquifer and identify districts where groundwater storage decline is likely and quantify the rate of decline.

5.1 MODEL DEVELOPMENT

The popular USGS code for groundwater modelling, MODFLOW-2005 was used to build the model using structured finite difference grids. The model area comprising the northwest Bangladesh region was discretised into cells with size of 1500 m × 1500 m in a single layer and monthly stress periods The plan view of the model grid and the river network are shown in Figure 5.1. The eastern and southern boundaries of the model area are bounded by the Jamuna (Brahmaputra) and Padma (Ganges) rivers respectively. The study area is part of the regional Ganga-Brahmaputra Basin – it has no natural groundwater boundaries and hence head dependent flux boundary conditions represented by the MODFLOW General Head Boundary condition were used for the western and northern boundary of the model.

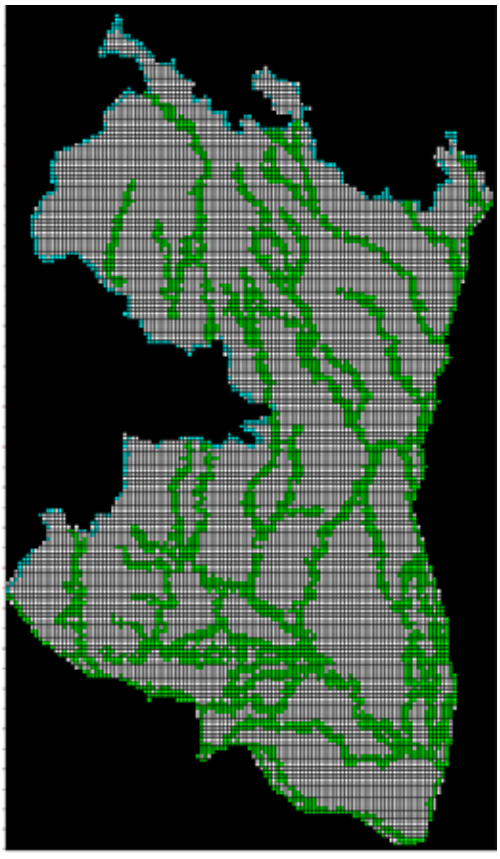

Figure 5.1: Plan view of the model grid showing the river network and the general head boundaries on the north and west boundaries

5.2 BOUNDARY CONDITIONS

5.2.1 RECHARGE

Groundwater recharge and its spatial and temporal patterns in the northwest region is influenced by rainfall and irrigation pattern as described in Chapter 4. Another major component of recharge occurs from rivers and flooding. The pattern of diffuse recharge was assumed to follow the spatial and temporal pattern of deep drainage estimated for the region by the companion water balance study (Mainuddin et al. 2021). The recharge characteristics also vary based on other factors like soil properties, groundwater use resulting in induced recharge, clay content etc. which vary across the region. As the focus of water balance and storage change simulations in this study pertain to the district-scale, separate parameters were assigned for each of the 16 districts in the region to estimate the fraction of deep drainage that becomes groundwater recharge. A wide range was assigned for the prior distribution of these parameters. The posterior distribution of the parameters and estimates of groundwater recharge were then derived during model calibration and uncertainty analysis.

5.2.2 RIVERS

The major rivers and tributaries in the northwest region were represented in the MODFLOW model using MODFLOW river package. The flows in these rivers or tributaries were modelled as part of the companion activity of SW modelling in this project using the MIKE 11 model (Karim et al. 2021). Time series of river stages simulated at 1500 m intervals were obtained from that analysis to provide the river stages corresponding to the river cells in the MODFLOW model for the simulation period between January 1985 and December 2015. The river package represents the two-way surface water–groundwater interaction in the model using a head-dependent flux boundary condition:

- when the river stage is above the groundwater level in the model cell, river loses water into the aquifer
- when the groundwater level is above the river stage in the model cell, the river gains water from groundwater.

Other inputs in addition to the river stage time series are the bottom elevation of the river and river conductance. Because of the large uncertainty in the SW-GW interaction process, we considered hydraulic conductance of the riverbed as an uncertain parameter. Including it as uncertain parameter enables the quantification of prediction uncertainty in the groundwater balance resulting from this.

5.2.3 GROUNDWATER CONTRIBUTION TO EVAPOTRANSPIRATION AND PUMPING

Owing to the shallow groundwater table across most of the region, groundwater contributes to the actual evapotranspiration resulting from the direct uptake of water from within the vegetation root zone. In addition to this, groundwater also contributes to the consumptive water use by being pumped for irrigation. These two components were represented in the MODFLOW model using the EVT and well packages respectively. In the absences of metered data of groundwater use, these components were assumed to be proportional to the estimated actual evapotranspiration.

During the monsoon season, water table is very close to the land in most of this region, and hence contributes directly to evapotranspiration as the groundwater contribution to evapotranspiration (ETg). In the drier season, the water table is lower and direct contribution of groundwater to ETa will be less. However, groundwater is pumped to irrigate Boro rice and other crops and indirectly contributes to evapotranspiration (Mainuddin et al. 2019; 2020). District-scale evapotranspiration was estimated by two different approaches in the companion activities of this project a) crop water modelling and b) using MODIS

data set and CMRSET algorithm (Mainuddin et al. 2021; Mojid et al. 2021a, Peña-Arancibia et al. 2020, 2021a,b). We used the spatial and temporal pattern of ETa estimates from the crop water modelling approach to constrain groundwater contribution to evapotranspiration.

By using the EVT package spatially and temporally, variable ET rates were input into the model with parameters governing this rate for different zones in the model. ET rate multipliers and extinction depths were considered as model parameters, the posterior distribution of which were obtained by constraining the model using observed groundwater levels. Similarly, the groundwater pumping rates within the districts were also considered spatially variable in proportion to the estimated ETa. Parameters were assigned to adjust the pumping rate in each district and were constrained during the model calibration process. In addition to these vertical boundaries, the lateral boundaries other than in the east and south were defined by general head boundaries.

5.3 MODEL PARAMETERISATION

The model was parameterised in a particular way to facilitate probabilistic analysis of groundwater balance and long-term storage changes in the aquifer. Hydraulic properties of the aquifer comprising hydraulic conductivity and storage characteristics are two critical properties that determine groundwater flow and storage in the aquifer. These properties are spatially variable and are largely uncertain; however the uncertainty can be constrained by model calibration to observed groundwater levels. These properties were included as model parameters in this study. Hydraulic conductivity and specific yield were included as spatially varying model parameters in this study.

The spatial parameterization device called pilot points was used for representing spatial variability in hydraulic properties. Uniformly distributed cells in the model were chosen as pilot points where hydraulic property values are estimated during model calibration. The hydraulic characteristics of other cells in the model are calculated by interpolating from pilot points using ordinary Kriging. Spherical variogram with a nugget or 0.100, sill of 0.764 in the log domain and a range of 70 km were used. These variogram parameters were chosen to represent spatial heterogeneity in the parameters given the absence of pump tests of pump tests or other estimates to optimise the variogram parameters. Hydraulic property estimates from across the region were not available, hence the variogram parameters were not fitted to observed data; rather a sill value above 0.5 was used to represent the likelihood heterogeneity in such alluvial aquifer system. This variogram model underpinned the spatial covariance structure for characterising prior uncertainty in hydraulic properties.

With the objective of investigating groundwater balance in the district of northwest region, 16 zones were demarcated within the model area corresponding to the 16 districts. The district boundaries were used as distinct zones for the parameters for which the zonation approach was used. It may be noted that these district boundaries do not always conform to natural boundaries like rivers – however, assignment of parameters corresponding to district-based zones gives the opportunity to explore and represent predictive uncertainties of water balance for each district. Other activities in this project, such as the water balance modelling (Mainuddin et al. 2021), focus on each district, and this approach makes it convenient to compare the groundwater modelling results with those analyses.

Zonation approach was adopted for parameters pertaining to recharge, evapotranspiration and SW-GW interaction. Spatial and temporal variability of groundwater recharge was assumed to be proportional to the deep drainage estimated using the district-scale water balance model (Mainuddin et al. 2021). Each recharge zone was assigned a multiplier to determine the fraction of spatially and temporally variable deep-drainage that reaches groundwater table as groundwater recharge. The prior range for this parameter was determined by assuming that groundwater recharge could be between 10% and 80% of deep drainage. An additional parameter was used to distinguish between the proportion of recharge between monsoon and

non-monsoon months. This was done considering the possibility that, depending on the antecedent moisture condition and water table depth, fraction of deep drainage resulting in recharge in the monsoon can be considerably different from that of non-monsoon months.

Hydraulic conductance of the riverbed was also parameterized using the zonation approach. A wide range spanning 4 orders of magnitude was used considering that the vertical conductivity may vary over 1e-3 m/d to 10 m/d. A relatively high value of vertical conductivity (10 m/d) was included considering the vast floodplains which can significantly contribute to river recharge during high flows.

Other parameters that used the zonation approach were those pertaining to evapotranspiration. Two sets of parameters were used for this. The first one is the ET rate multiplier. Groundwater use for irrigation was assumed to be proportional to estimated actual evapotranspiration. The ET rate multiplier parameter determines the fraction of actual ET that is contributed by groundwater either naturally because of a water table within the root zone or indirectly because of groundwater use for irrigation.

Table 5.1: Parameter groups and prior distribution

PARAMETER TYPE	PARAMETER UNIT	NUMBER OF PARAMETERS	TRANSFORM	UNIFORM PRIOR DISTRIBUTION RANGE
Recharge multiplier	Zone	16	Relative	0.1 – 0.8
Recharge monsoon	Zone	1	Relative	0.1 – 1.0
ET rate multiplier	Zone	16	Relative	0.1 – 1.5
ET extinction depth multiplier	Zone	16	Relative	0.04 – 1.0
Pumping rate multiplier	zone	16	Relative	0.1 – 1.5
River conductance multiplier	Zone	16	Relative	10 – 1.0e+05
Hydraulic conductivity	Pilot points	310	Log	5 – 200
Specific yield	Pilot points	310	Log	0.05 – 0.15
Total		**701**		

The model parameterisation that combines parameter zones for recharge and discharge fluxes together with spatially variable parameterisation for hydraulic properties facilitates to capture the correlation between model inputs and hydraulic property parameters. The spatial representation of model parameterisation is shown in Figure 5.2 and the number of parameters in each parameter type and their prior range is shown in Table 5.1. The model was parameterized in such a way that predictive uncertainty in groundwater balance owing to uncertainty in the model inputs and parameters could be quantified during model calibration and uncertainty analysis.

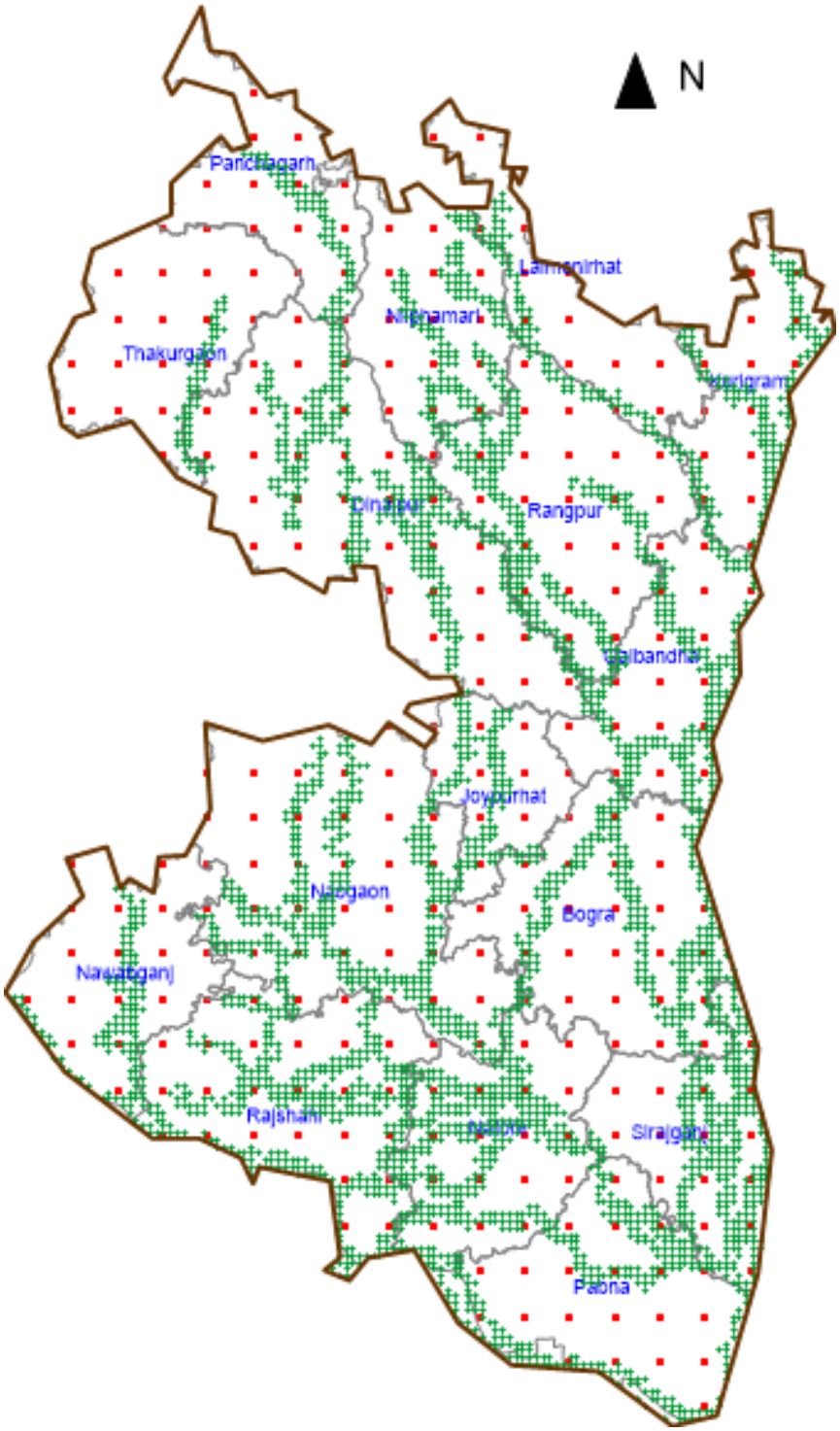

Figure 5.2: Distribution of hydraulic property pilot points (red) and river cells (green) within the model area. River cells within each district have separate hydraulic conductance parameter

5.4 OBSERVATIONS

Groundwater head observations from 351 observation wells between the period 1985 to 2010 (refer to Hodgson et al. (2021) for their location and trends in observed water levels) were used to constrain the groundwater flow simulation by the MODFLOW model. Weekly groundwater level observations were available for these bores. Simulation analyses was undertaken for the whole period of 1985 to 2016.

5.5 CALIBRATION AND UNCERTAINTY ANALYSIS

Calibration and uncertainty analysis was undertaken using the PEST++ software utility. The uncertainty analysis approach we implemented is based on the Iterative Ensemble Smoother (IES) approach (White, 2018) that is available in PEST++ software suite. This method implements the Gauss-Levenberg-Marquardt algorithm for the minimisation problem using the ensemble smoother form in this tool. The PEST-IES software utility has built-in parallel run manager and model run failure tolerance. This makes it suitable for our study to implement probabilistic modelling considering a wide range of plausible parameter sets. In this approach, the number of model runs undertaken for the inversion is directly proportional to the number of model parameters and poses a significant challenge when used in highly parameterised models like that used in this study.

A total of 701 adjustable parameters were included in the calibration and uncertainty analyses. This included 310 pilot points for hydraulic conductivity and specific yield; 16 zonal parameters for recharge, river, pumping and ET rate and ET extinction depth; and one additional parameter to govern the monsoon recharge. During each iteration of the model calibration, these parameters were adjusted to populate the Jacobian Matrix that represents the sensitivity of observations to the parameters. PEST-IES uses an empirical approach for populating the Jacobian matrix using an ensemble of random parameter sets using the formulation proposed by Chen and Oliver (2012). Using this formulation, the model needs to be run only as many times as the size of the ensemble chosen, thus eliminating the computational burden induced by the large number of parameters. In this study we used an ensemble size of 500. Since an ensemble of parameters are propagated through the algorithm until acceptable objective function values are attained, the calibration process ends up with an ensemble of model parameter sets that can all calibrate the model. This provides an estimate of the posterior parameter distribution constrained by the available observations (White, 2018). This enables quantification of model prediction uncertainty.

5.6 RESULTS OF CALIBRATION AND UNCERTAINTY ANALYSIS

The prior and posterior uncertainty in model parameters and results of calibration with groundwater head observations are described in this section.

5.6.1 PRIOR AND POSTERIOR PARAMETER UNCERTAINTY

The prior uncertainty in model parameters was specified by using a range for the parameter bounds and sampling parameter realisations randomly from that range. Model calibration using the PEST-IES framework resulted in adjustment of parameter values to minimise the squared error of simulated groundwater heads. This resulted in the posterior distribution of parameters that gives minimum values for the calibration objective function.

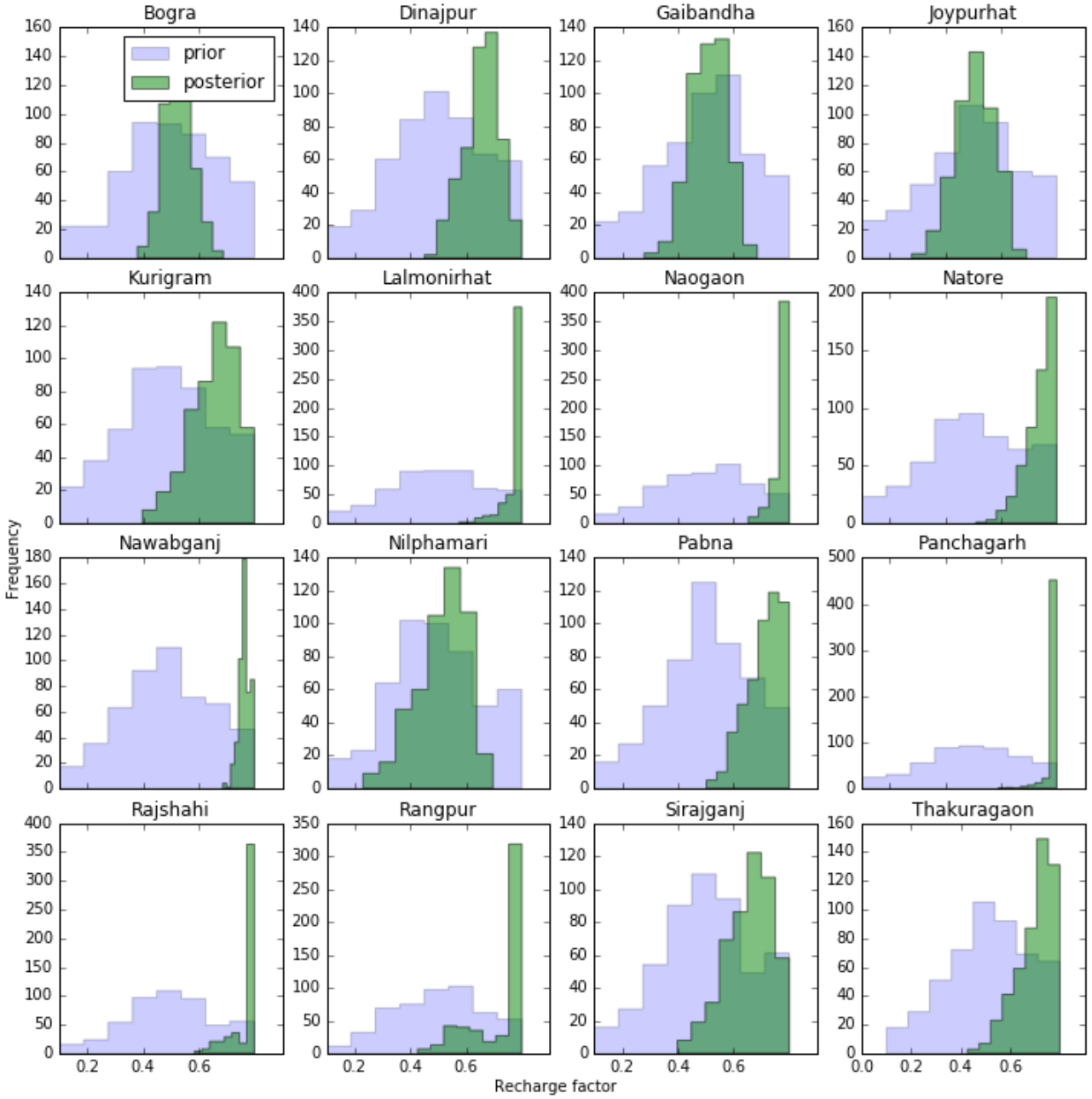

Figure 5.3: Prior and posterior distribution of recharge parameters

The prior and posterior distributions of the river hydraulic conductance parameter for all districts are shown in Figure 5.4. There is a wide range for the prior distribution of these parameters. A wide range was chosen because vertical hydraulic conductivity of the riverbed is a very uncertain parameter and can range over a few orders of magnitude. It can be seen that the base of the posterior distribution is also considerably wide, although there is uncertainty reduction achieved by history matching. This is because groundwater heads is the only type of data set used in the calibration. If other data types like river flow especially that of dry spells were available, more reduction in parameter uncertainty could be achieved.

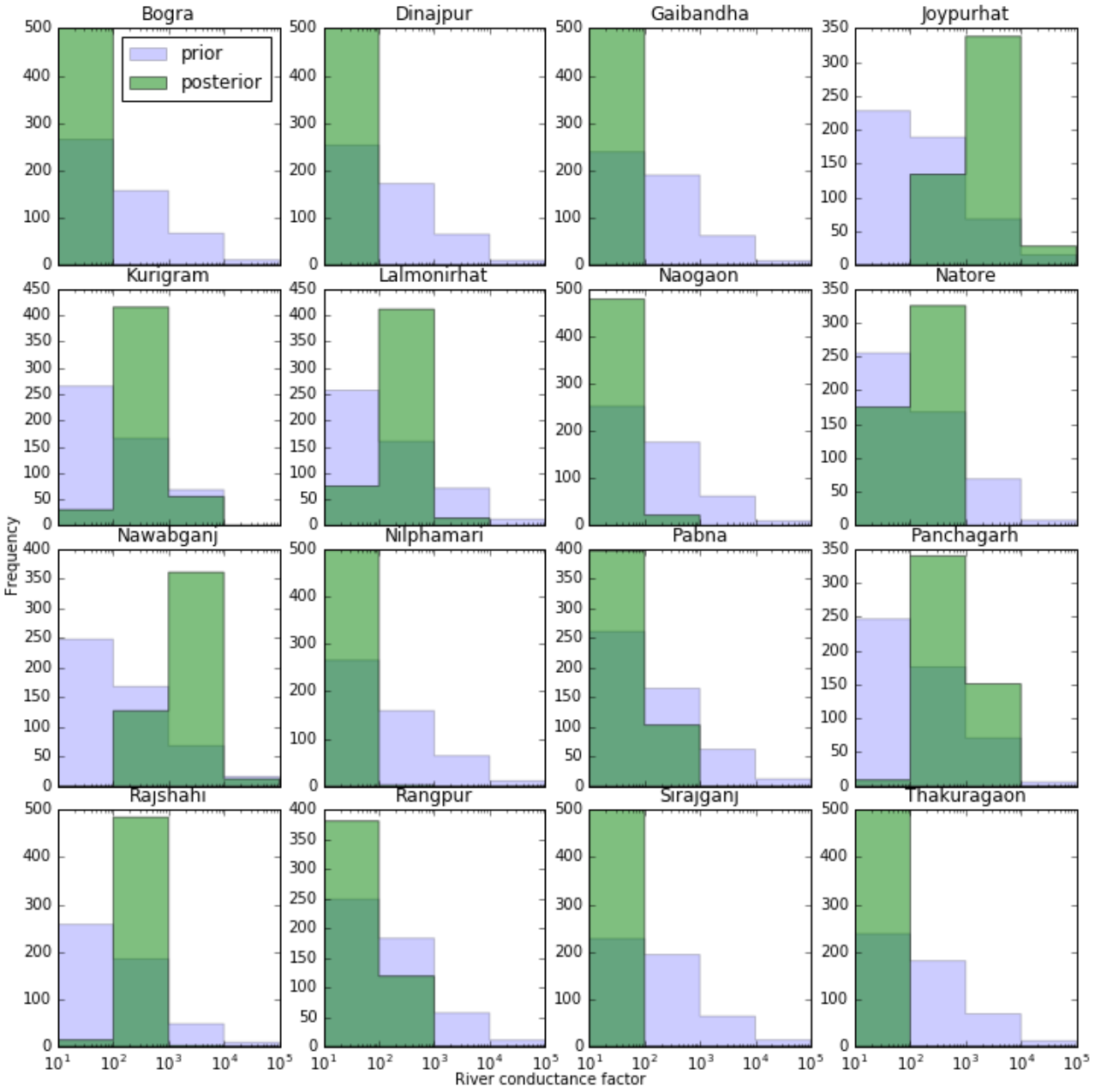

Figure 5.4: Prior and posterior distribution of river hydraulic conductance factor

Similar distributions of district-scale parameters controlling groundwater contribution to ET (groundwater ET rate factor) and ET extinction depth factor are shown in Figure 5.5 and Figure 5.6 respectively. Shallow pumping was also represented as part of ET in the model set up. Hence the maximum extinction depth was considered to be 30 m to account for shallow pumping and the groundwater ET rate factor was assigned values between 0.04 and 1 so that ET extiction depth assumes values between 1.2 m and 30 m.It may be observed that these parameters are constrained to varying degrees after the calibration exercise.

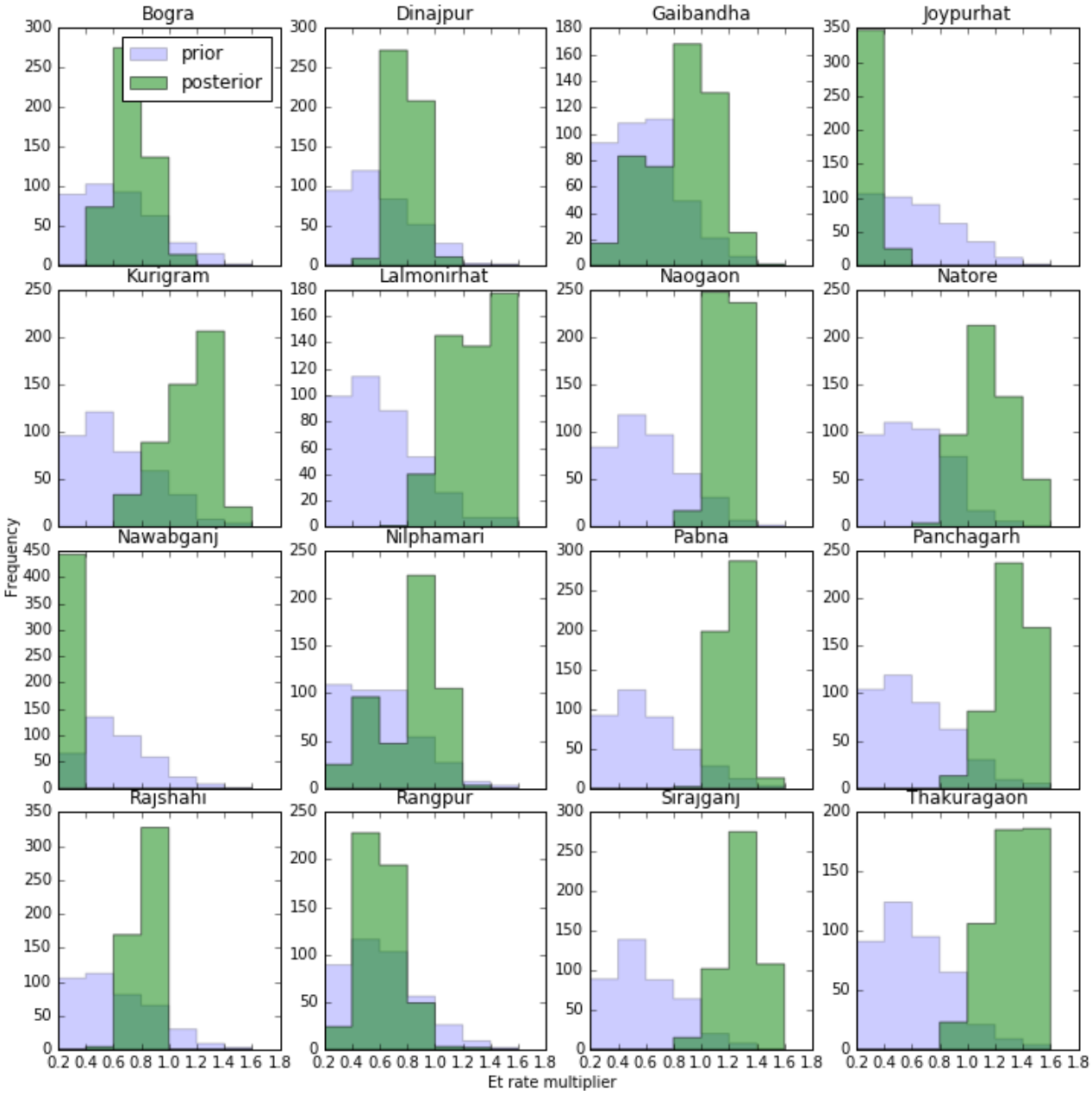

Figure 5.5: Prior and posterior distribution of groundwater ET rate factor

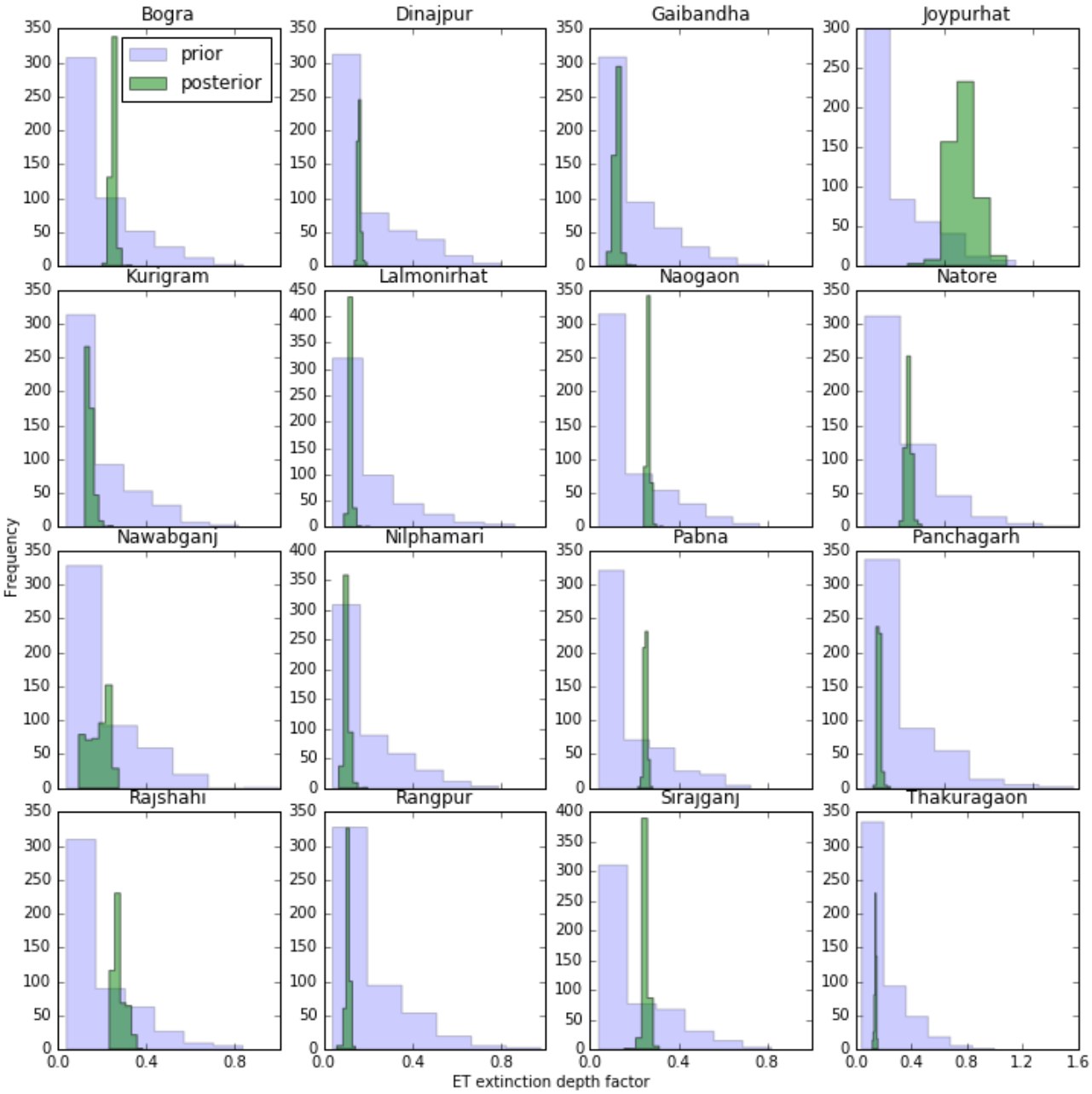

Figure 5.6: Prior and posterior distribution of ET extinction depth factor at the district scale

Figure 5.7 shows the prior and posterior distribution of hydraulic properties. Posterior distribution of hydraulic conductivity (Kh) and specific yield (SY) across all pilot points have the same range as the prior distribution. However, at individual pilot points the posterior distribution is constrained by groundwater head observations around the location as can be seen in plots Figure 5.7c and Figure 5.7d.

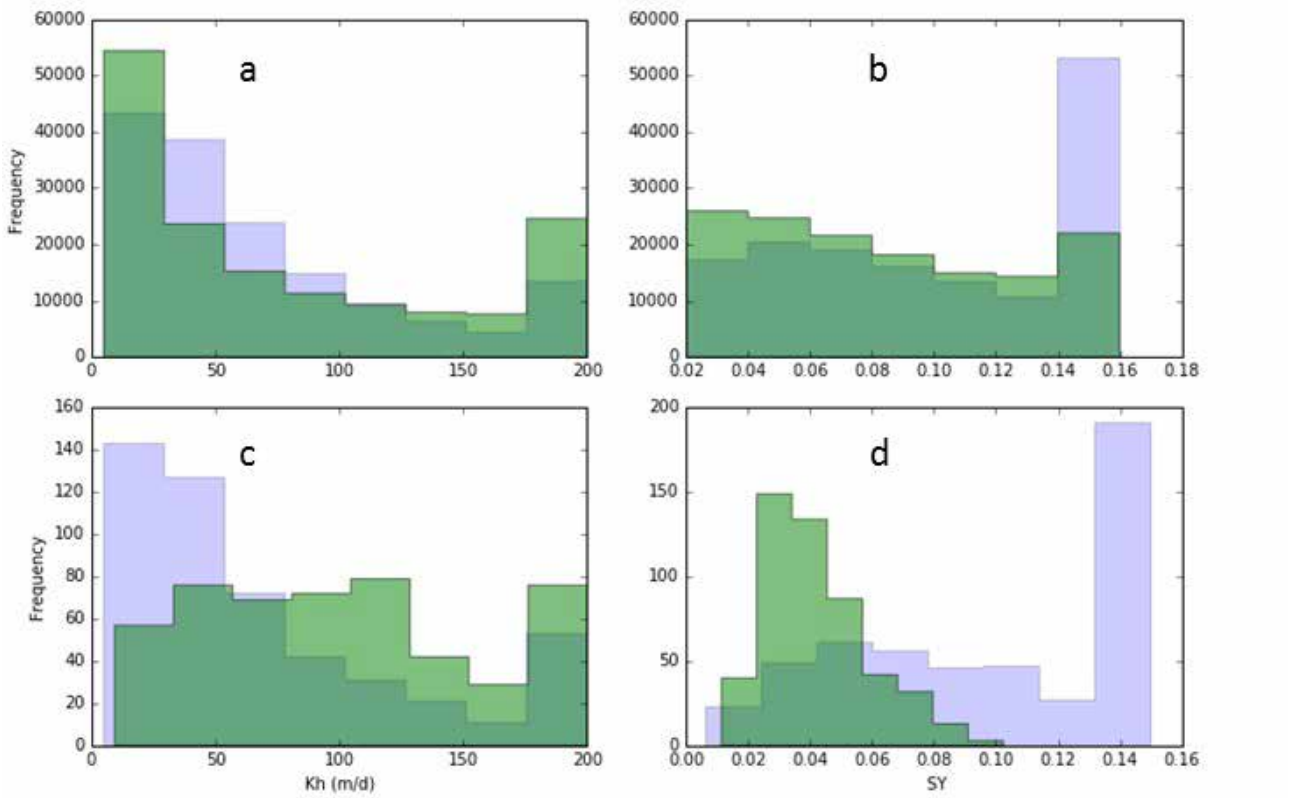

Figure 5.7: Prior and posterior distribution of hydraulic properties at pilot points. The plots a) and b) show the distributions of hydraulic conductivity (Kh) and specific yield (SY) respectively across all pilot points and c) and d) show the distributions at one pilot point

5.6.2 HISTORY MATCHING

The scatter plot of observed and simulated groundwater heads and the distribution of error in groundwater head simulation are shown in Figure 5.8. After history matching, simulated groundwater heads had a mean absolute error (MAE) of -0.05 m and a root mean square error (RMSE) of 2.4 m.

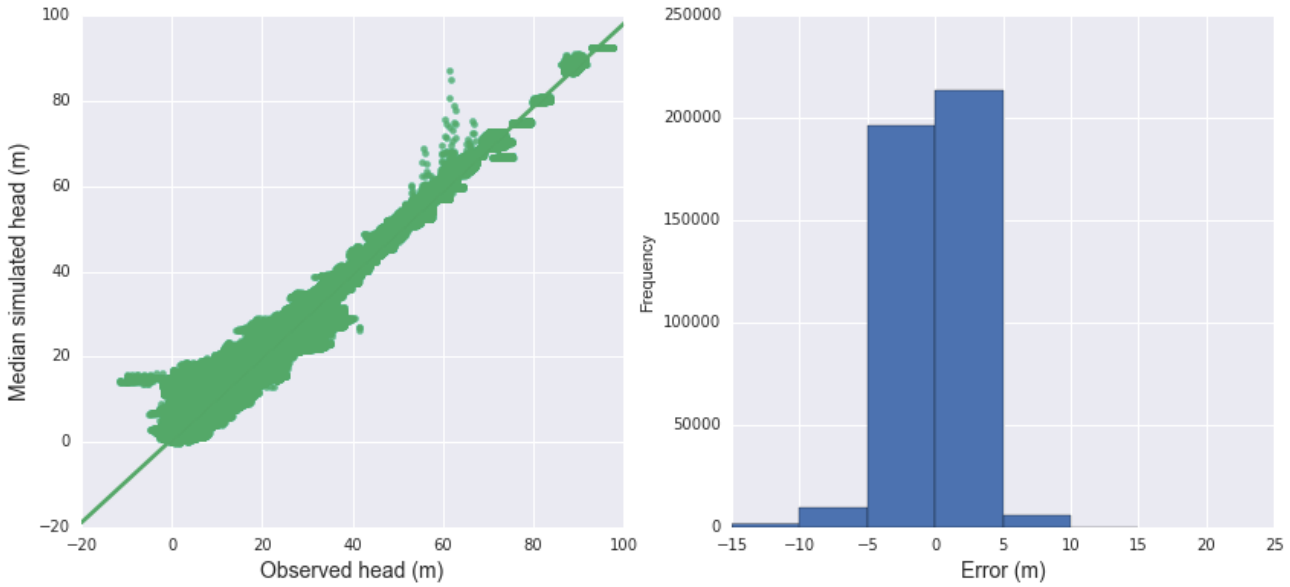

Figure 5.8: Scatter plot of observed and simulated groundwater head and histogram of error in groundwater head simulation

Comparison of the observed and simulated median groundwater head for example bores in the different districts of the northwest Bangladesh are shown in Figure 5.9 to Figure 5.11. It may be noticed that declining trends in groundwater head, as indicated by the descending broken lines in the plots, are comparable between the observed and simulated values in this region. A good match between observed and simulated heads is achieved for many observation bores as the highly parameterised approach enabled adjustment of the model parameters in the vicinity of each bore to match observed values. It was observed that calibration achieved good match between the simulated and observed trends in groundwater levels where as maximum and minimum groundwater levels are often not matched. This could be an artefact of the coarsen grid used in the regional model. In the northwest region where large number of tube wells are present, the groundwater levels in the observation bores are likely to be affected by local pumping which is not aadequately represented in the MODFLOW model. Future efforts to refine the model with better representation of local pumping may help improve the simulation of minimum and maximum water levels. It is important to note that the MODFLOW model uses a rather simplified representation of the aquifer geometry with a single model layer. While that is sufficient for the district scale groundwater balance analysis, the model conceptualisation and parameterisation may need to be re-visited if the model is to be used for other purposes.

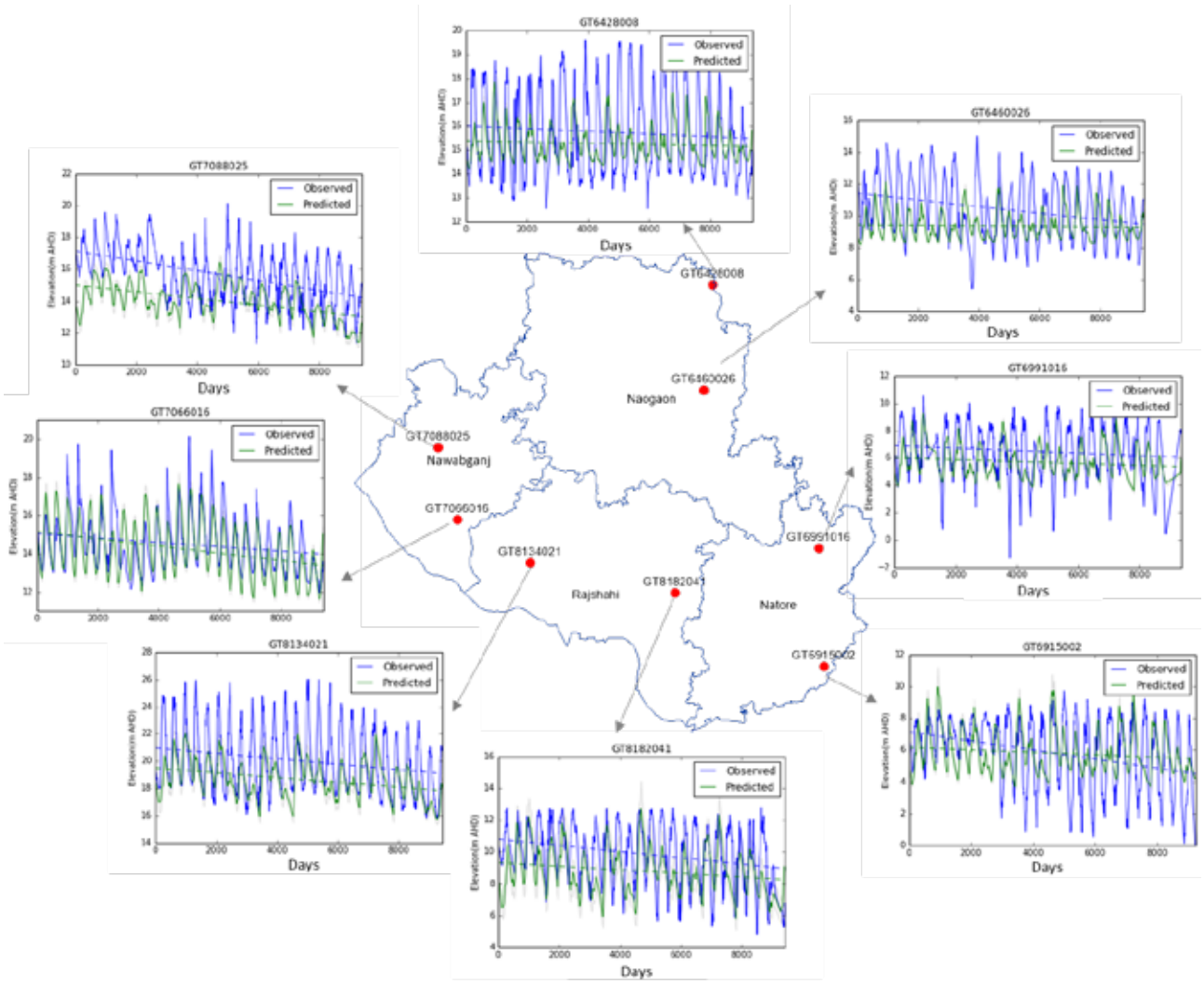

Figure 5.9: Time series of observed and predicted (median simulation) groundwater head elevation (m AHD) at selected bores in the districts in and around the Barind tract area

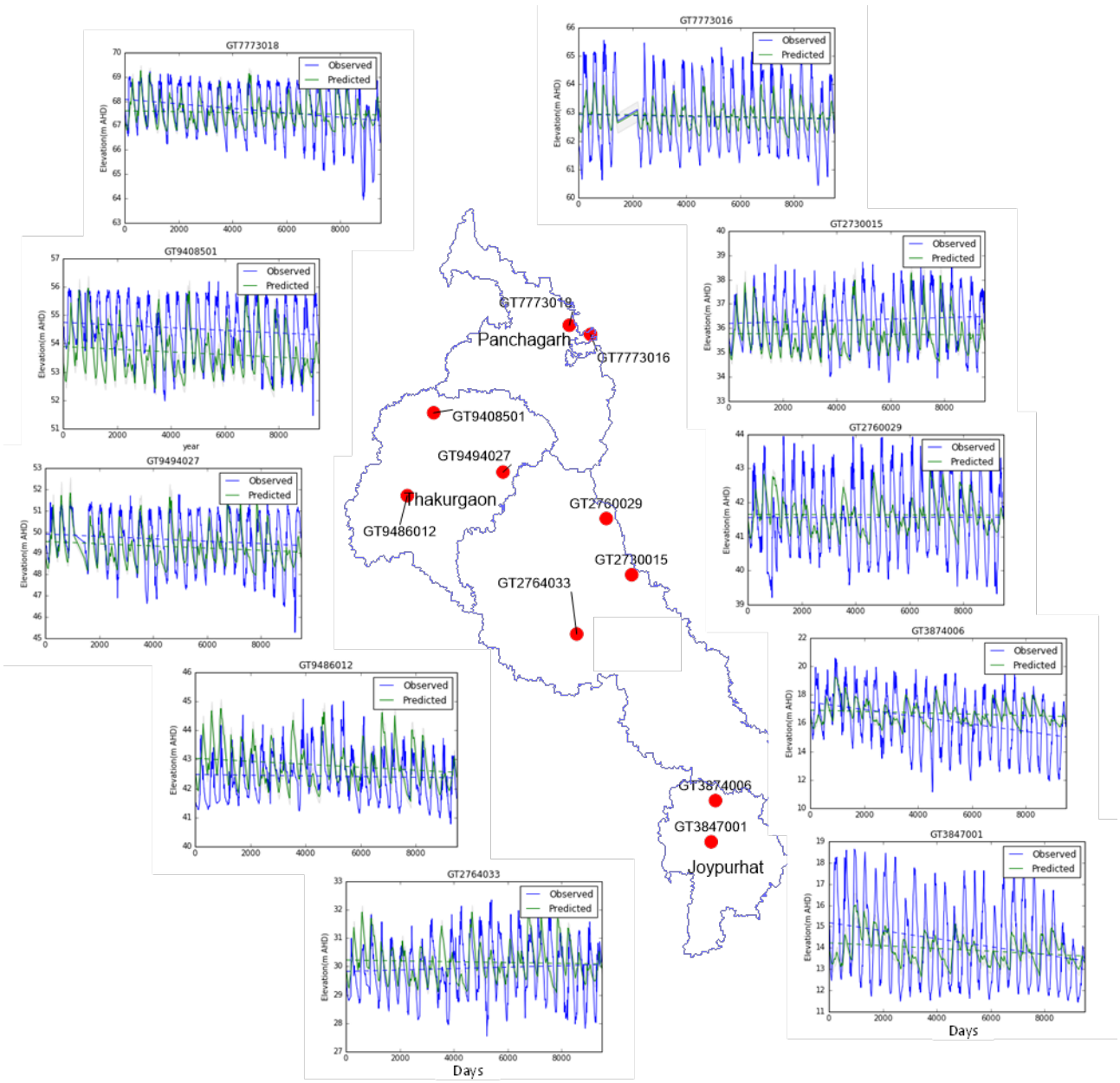

Figure 5.10: Time series of observed and predicted (median simulation) groundwater head elevations (m AHD) at selected bores in the Panchgarh, Thakuragaon, Dinajpur and Joypurhat districts

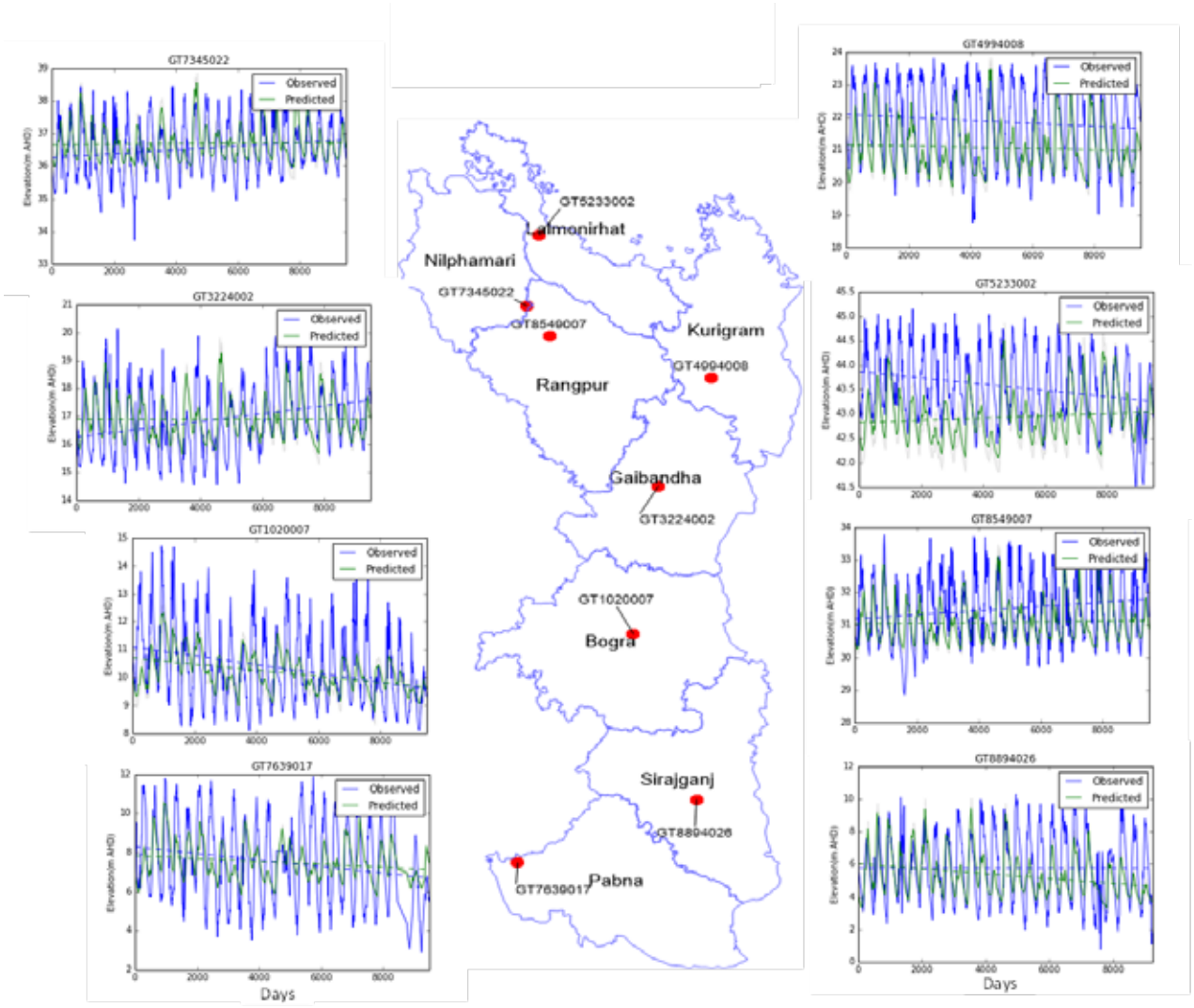

Figure 5.11: Time series of observed and predicted (median simulation) groundwater head elevations (m AHD) at selected bores in the eight districts toward the east of the northwest region

5.7 GROUNDWATER BALANCE

The groundwater flow simulation for the period 1985 to 2016 was used to compute long-term groundwater balance in the districts of northwest region.

A probabilistic approach was used to analyse groundwater balance using the MODFLOW model. The calibration of the model using the PEST-IES approach resulted in many realizations of the model parameters that produced similar objective function values for history matching. An ensemble comprising 500 parameter realizations, all of which calibrate the model equally well, was used for groundwater balance analysis. Groundwater balance was assessed at the northwest regional scale as well as at individual district-scale. The groundwater balance for the northwest region and the districts computed as the median of the 500 simulations is shown in Table 5.2. The last column of this table represents the long-term average rate of storage changes in the region. The negative sign for these numbers indicates that there is a net decline in the rate of groundwater storage change over the 30-year simulation period. The average storage loss across the northwest region is -1.5 mm/year. It should be noted that this storage loss is the estimated average value for the whole region for the period between 1985 and 2016. The storage loss is generally higher in the southern districts of the region and during the recent decades when increased use of deep tube wells occurred for Boro rice cultivation. For example, the probabilistic simulations show that in the district of Nawabganj the

water level drawdown could be in the range of 58 to 174 mm/y (Table 5.3), implying decline in groundwater level up to 5.2 m across the district in the 30-year period.

Table 5.2: Annual average groundwater balance for northwest region based on the median of 500 simulations

	Water balance component (mm/y)											
District	Recharge	River in	Lateral in	Storage in	Total in	ETg	wells.1	Storage out	River out	Lateral out	Total out	Storage change
Bogra	297.4	28.5	14.9	111.4	452.2	255.4	73.6	110.3	0.0	12.9	452.2	−1.1
Dinajpur	290.7	9.8	18.8	96.6	415.9	151.8	116.2	95.9	14.5	37.6	415.9	−0.7
Gaibandha	249.2	12.2	20.2	88.2	369.8	36.7	232.3	87.1	0.3	13.4	369.8	−1.2
Joypurhat	259.0	114.2	48.4	122.5	544.1	188.8	155.5	121.5	42.2	36.1	544.1	−1.0
Kurigram	335.2	75.2	27.0	98.2	535.7	253.9	103.7	97.8	7.8	72.6	535.7	−0.5
Lalmorihat	333.3	59.1	13.3	98.5	504.2	260.5	24.9	97.9	4.2	116.7	504.2	−0.5
Naogaon	387.4	64.4	28.0	130.1	610.0	405.8	62.2	128.7	1.6	11.7	610.0	−1.4
Natore	434.7	167.9	19.8	172.6	795.0	515.0	73.6	171.0	5.9	29.5	795.0	−1.5
Nawabganj	431.6	140.8	56.1	262.4	891.0	40.4	438.1	253.7	101.2	57.5	891.0	−8.7
Nilpharmari	217.6	12.8	24.6	66.2	321.1	106.1	108.5	65.7	3.7	37.1	321.1	−0.4
Pabna	416.5	220.5	32.0	168.9	837.9	525.6	131.8	167.4	0.3	12.9	837.9	−1.5
Panchagarh	398.8	13.2	9.3	91.4	512.7	201.4	49.8	90.6	55.1	115.8	512.7	−0.8
Rajshahi	513.7	172.6	15.9	211.9	914.0	320.3	340.7	209.3	15.5	28.3	914.0	−2.5
Rangpur	373.8	27.2	17.8	109.6	528.4	57.6	333.5	109.1	11.4	16.9	528.4	−0.5
Sirajganj	417.2	102.4	28.8	146.1	694.5	494.4	45.4	144.8	0.2	9.6	694.5	−1.3
Thakurgaon	409.7	13.0	13.0	117.0	552.7	282.3	45.6	116.2	3.3	105.2	552.7	−0.8
Northwest	360.4	77.1	24.2	130.7	592.5	256.0	146.0	129.2	16.7	44.6	592.5	−1.5

It may be observed that the vertical components of flux comprising recharge, groundwater contribution to evapotranspiration (ETg), pumping and river fluxes dominate the groundwater balance. The recharge represented in this way is the gross amount of deep drainage that reaches the water table. ETg represents the groundwater contribution to evapotranspiration occurring because of the direct uptake of water from the root zone by crops or shallow pumping. The wells represent the deep groundwater pumping although specific well-screening depth was not prescribed in the model. While ETg and pumping wells were not constrained separately, together they represent the total consumptive groundwater use plus the irrigation (pumping) excess that is returned to the groundwater table.

It should be noted that as the model is constrained only by observed groundwater levels, there is significant uncertainty in the estimates of these water balance components. The parameters governing recharge and ETg can be directly correlated resulting in significant prediction uncertainty. For example, the box plot of groundwater balance inflow and outflow components for the Rajshahi district shown in Figure 5.12 illustrate the uncertainty in these fluxes. However, the uncertainty in the storage change (storage in – storage out) is much less because it is better constrained by the groundwater level observation data.

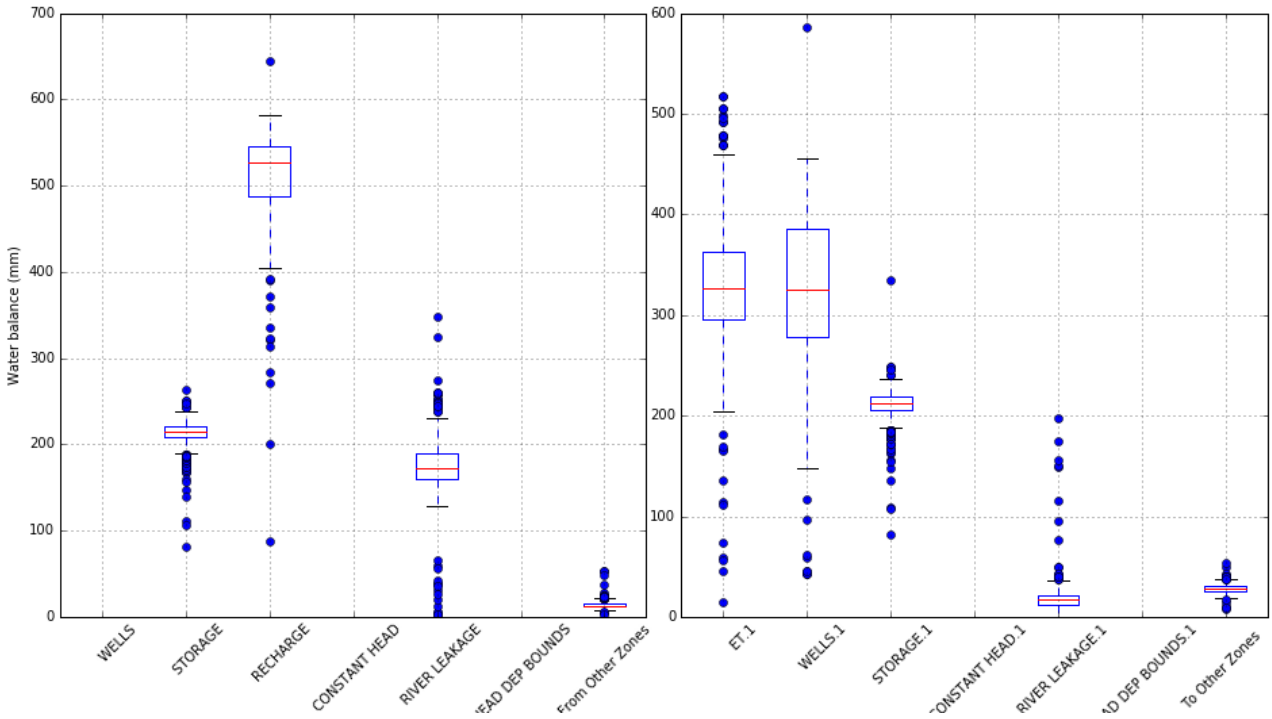

Figure 5.12: Probabilistic groundwater balance for Rajshahi district

Table 5.3: Predicted water level change corresponding to annual storage changes

District	Water level change (mm/y)			
	Storage change	SY = 0.075	SY=0.05	SY=0.15
Bogra	-1.1	−14	−22	−7
Dinajpur	−0.7	−9	−14	−5
Gaibandha	−1.2	−15	−24	−8
Joypurhat	−1.0	−13	−20	−7
Kurigram	−0.5	−6	−10	−3
Lalmorihat	−0.5	−6	−10	−3
Naogaon	−1.4	−18	−28	−9
Natore	−1.5	−19	−30	−10
Nawabganj	−8.7	−112	−174	−58
Nilpharmari	−0.4	−5	−8	−3
Pabna	−1.5	−19	−30	−10
Panchagarh	−0.8	−10	−16	−5
Rajshahi	−2.5	−32	−50	−17
Rangpur	−0.5	−6	−10	−3
Sirajganj	−1.3	−17	−26	−9
Thakurgaon	−0.8	−10	−16	−5
Northwest	−1.5	−19	−30	−10

The time series of mean monthly recharge, ETg and groundwater extraction and corresponding uncertainties are shown in Figure 5.13 to Figure 5.15. While ETg and groundwater pumping are shown as independent

variables, they are not individually constrained in the model. The long-term trends observable in monthly recharge and ETg in Figure 5.13 and Figure 5.14 respectively are directly proportional to the trends in input variables, respectively, deep drainage and ETa rates used from the companion study (Mainuddin et al. 2021). Small decreasing trends in recharge in several districts reflect the decreasing trend in rainfall in these districts. Declining trends in ETg could also be indicative of groundwater levels receding below the root zone in several districts over the long time period. Increasing and decreasing trends in groundwater pumping have also been reported in the recharge and discharge study reported in Chapter 3. Different types of trends in observed groundwater levels are discussed in detail in the companion report (Hodgson et al. 2021).

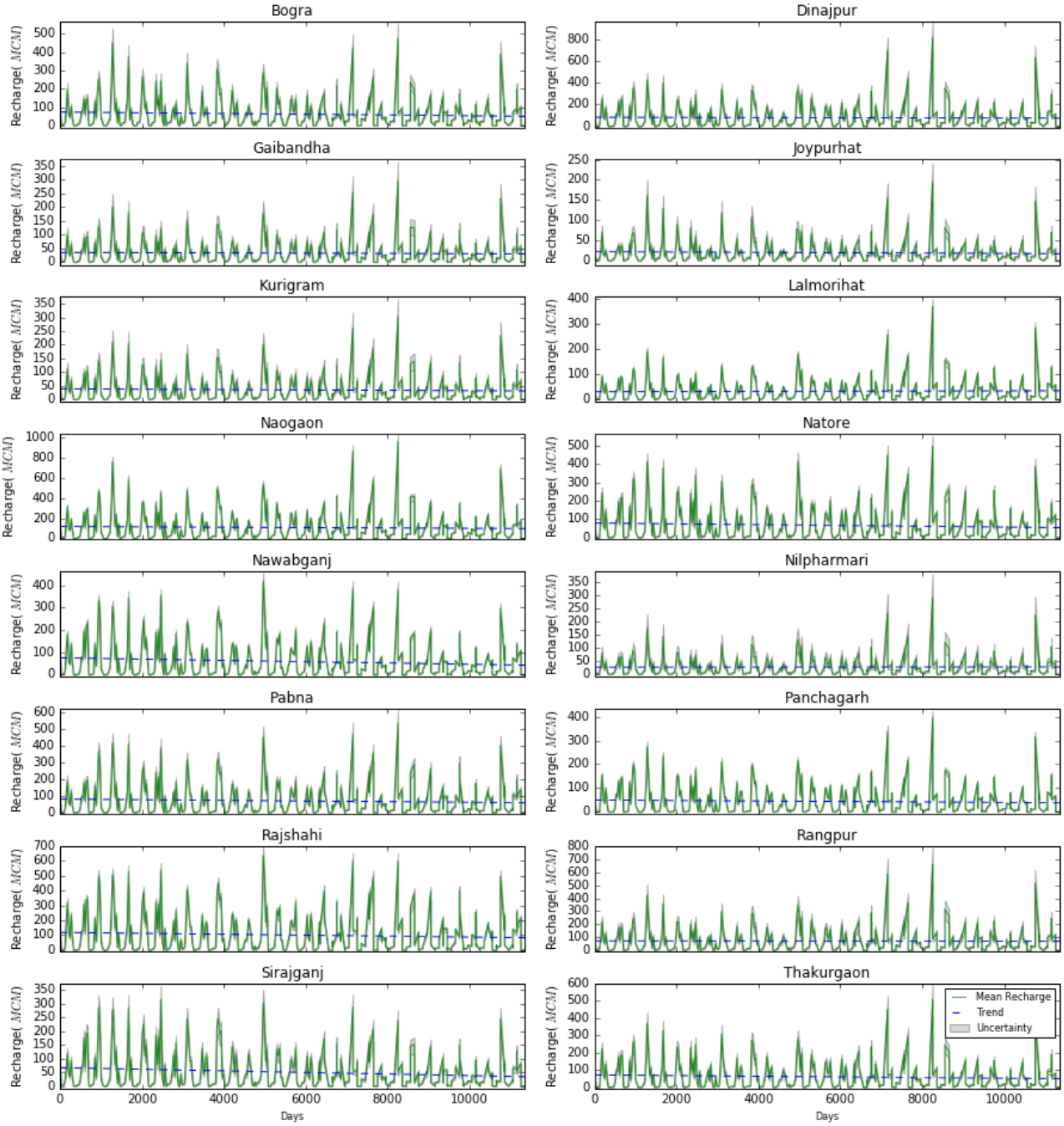

Figure 5.13: Mean monthly recharge fluxes simulated for the 16 districts of the northwest region

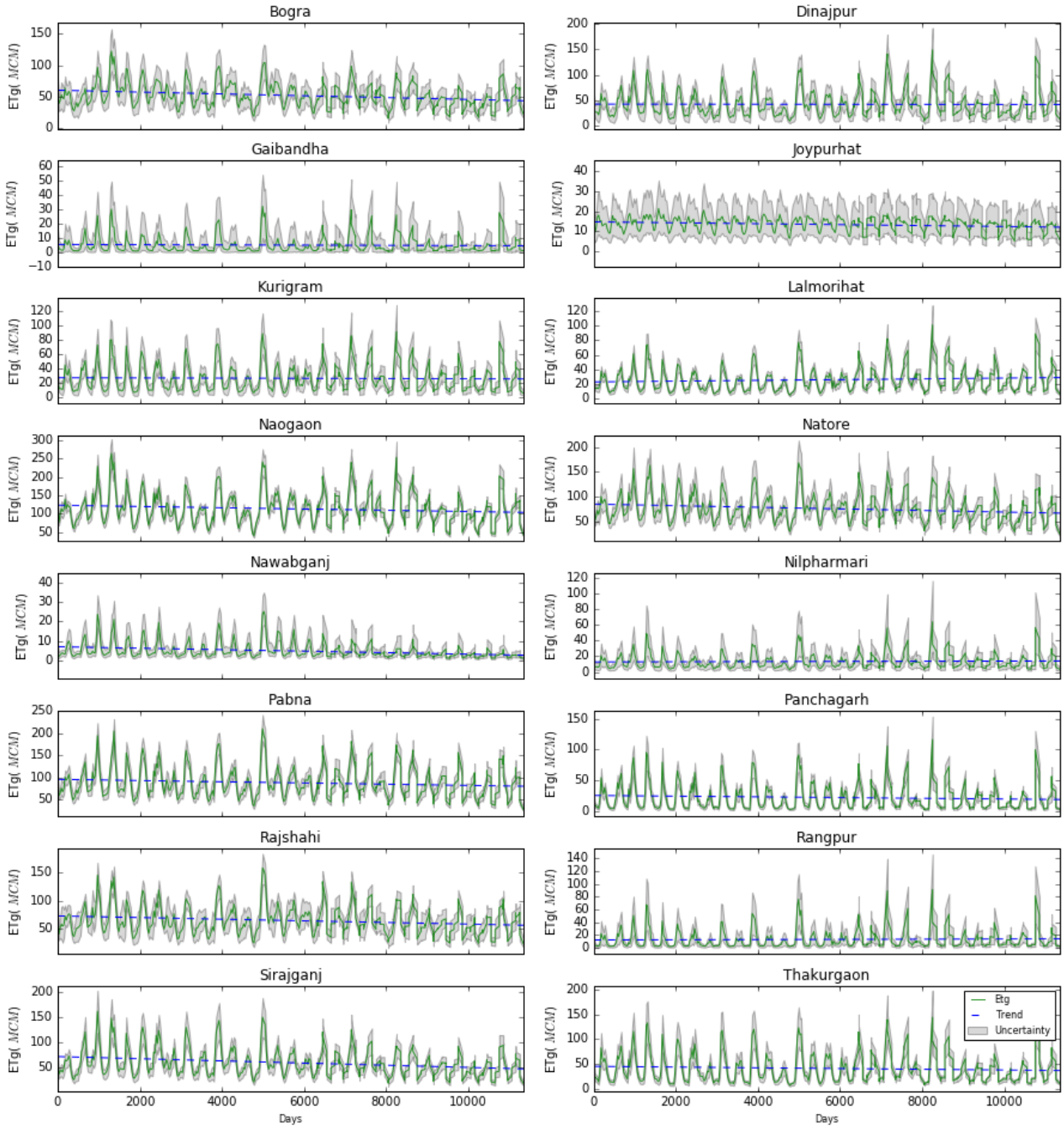

Figure 5.14: Mean monthly ETg fluxes simulated for the 16 districts of the northwest region

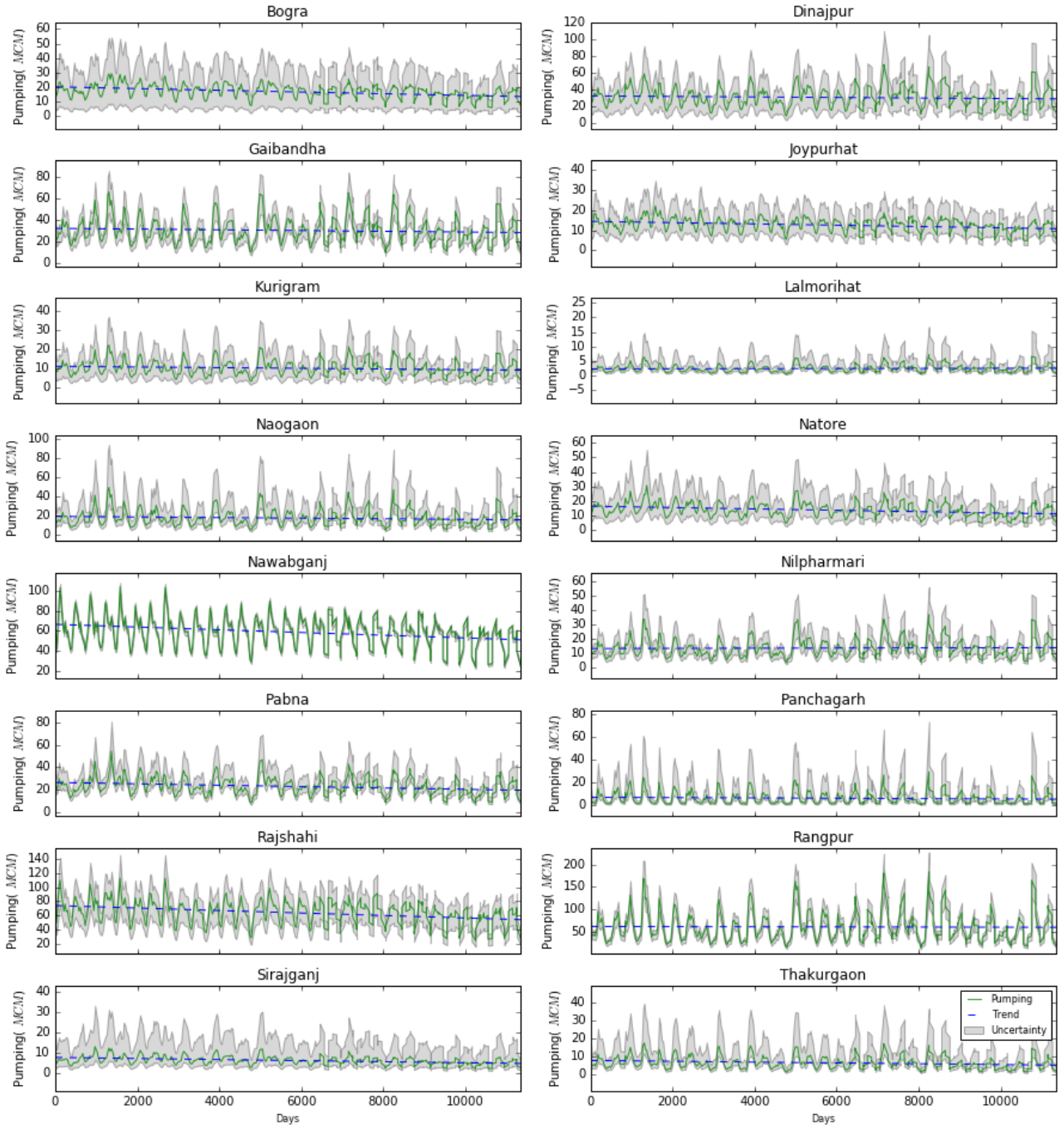

Figure 5.15: Mean monthly pumping simulated for the 16 districts of the northwest region

5.7.1 ALTERNATIVE MODEL SET UP WITHOUT MODFLOW EVT PACKAGE

The conceptualisation of the model with gross recharge and two components of vertical discharge (evapotranspiration and pumping) was found to be suitable for simulating the overall groundwater balance that was best comparable to the MIKE SHE estimates of groundwater balance. However, because the apportioning of groundwater discharge between the EVT and well package could result in inconsistent estimation of storage changes in some districts, another set of model calibration and probabilistic simulations was undertaken using a different conceptualization of the model. In this conceptualization the model was set up without the EVT package – net recharge (gross recharge minus ETg) was represented using the recharge package; and groundwater use for irrigation was represented with the well package. This conceptualisation is better suited for districts where groundwater table is deeper (southern districts) and hence natural groundwater contribution to ETa is smaller.

Table 5.4: Groundwater balance obtained from the alternative model conceptualization without EVT package

District	Recharge	River in	Lateral in	Storage in	Total in	Well	river out	Lateral out	storage out	Total out	Storage change
Bogra	77.4	20.6	12.1	36.8	147.0	104.4	1.0	13.5	28.0	147.0	−8.8
Dinajpur	116.9	5.6	18.9	43.6	185.0	104.6	10.6	31.9	37.9	185.0	−5.7
Gaibandha	62.4	64.7	13.1	60.8	201.1	100.1	27.8	15.3	57.8	201.1	−3.0
Joypurhat	216.5	42.0	35.3	79.9	373.7	270.9	15.6	13.8	73.5	373.7	−6.4
Kurigram	144.7	33.9	38.9	59.6	277.1	187.1	6.5	29.1	54.3	277.1	−5.3
Lalmorihat	179.3	59.0	23.4	76.1	337.7	115.7	40.5	108.8	72.8	337.7	−3.3
Naogaon	193.8	325.8	20.4	78.7	618.7	227.7	285.2	37.7	68.2	618.7	−10.6
Natore	248.3	191.1	33.9	115.5	588.8	425.0	18.6	33.2	112.0	588.8	−3.5
Nawabganj	198.5	173.5	70.7	155.0	597.8	242.1	140.0	73.1	142.6	597.8	−12.5
Nilpharmari	147.9	23.0	23.1	54.3	248.2	135.0	24.4	38.1	50.8	248.2	−3.5
Pabna	137.5	30.1	26.1	67.3	260.9	190.5	0.9	9.7	59.8	260.9	−7.5
Panchagarh	165.7	1091.4	17.6	53.9	1328.6	75.7	1090.8	112.1	50.0	1328.6	−3.9
Rajshahi	323.4	123.3	6.5	155.6	608.8	309.4	127.1	25.5	146.7	608.8	−8.9
Rangpur	263.9	24.7	25.0	80.7	394.2	299.1	10.1	12.8	72.1	394.2	−8.5
Sirajganj	196.4	81.1	27.3	84.4	389.1	302.4	2.7	7.1	76.8	389.1	−7.5
Thakurgaon	125.2	10.3	21.7	43.7	201.0	86.8	5.0	68.8	40.3	201.0	−3.4
Northwest	174.9	143.7	25.9	77.9	422.3	198.5	112.9	39.4	71.5	422.3	−6.4

As in the previous runs, groundwater pumping was simulated as a fraction of ETa and recharge was also estimated as a fraction of deep drainage. This type of model conceptualization is more suitable for areas where water table is deeper than the rootzone and is less likely to naturally contribute to ET, like in the Barind tract areas in districts like Rajshahi and Nawabganj. The model was re-calibrated using the same approach as described earlier and probabilistic simulation of long-term annual groundwater balance was carried out. This approach resulted in a model calibration with an RMSE and MAE values of 2.8 m and -0.3 m respectively.

Higher rates of declining storage were estimated for most districts with Nawabganj, Naaogaon and Rajshahi having the highest declining rates of -12.5 mm/y, -10.6 mm/y and -8.9 mm/y respectively. The average rate of decline for the whole of northwest region based on this conceptualization is -6.4 mm/y. The groundwater balance simulated by this model conceptualization is shown in Table 5.4. The median recharge values obtained by the calibration of this model is substantially less than the values obtained from previous calibration. This is because these are net recharge values.

Estimated rate of groundwater level decline for 16 districts and average for the whole region based on this alternative model conceptualization is shown in Table 5.5. Estimates based on median storage change indicate that groundwater levels could be declining at an average rate of -85 mm/y across the northwest region with highest rate of decline of -167, -141 and -119 mm/y in the districts of Nawabganj, Naogaon and Rajshahi. In areas where specific yield is lower groundwater level declines could be as high as -250 mm/y in Nawabganj. Such high rates of groundwater level decline has been observed in several bores in Nawabganj (Hodgson et al, 2021).

Table 5.5: Simulated water level change corresponding to annual storage changes based on the alternative conceptualization

District	Storage change	Simulated rate of groundwater level change (mm/y)		
		SY = 0.075	SY=0.05	SY=0.15
Bogra	-8.8	-117	-176	-59
Dinajpur	-5.7	-76	-114	-38
Gaibandha	-3.0	-40	-60	-20
Joypurhat	-6.4	-85	-128	-43
Kurigram	-5.3	-71	-106	-35
Lalmorihat	-3.3	-44	-66	-22
Naogaon	-10.6	-141	-212	-71
Natore	-3.5	-47	-70	-23
Nawabganj	-12.5	-167	-250	-83
Nilpharmari	-3.5	-47	-70	-23
Pabna	-7.5	-100	-150	-50
Panchagarh	-3.9	-52	-78	-26
Rajshahi	-8.9	-119	-178	-59
Rangpur	-8.5	-113	-170	-57
Sirajganj	-7.5	-100	-150	-50
Thakurgaon	-3.4	-45	-68	-23
Northwest	-6.4	-85	-128	-43

6 SIMULATION ANALYSES FOR MANAGEMENT OPTIONS AND CLIMATE SCENARIOS

Analyses of short-term (annual) changes in groundwater levels corresponding to three management options comprising different rainfall characteristics and different groundwater abstractions due to cropping pattern changeswere simulated using the MIKE SHE model. Simulation of differences in short-term groundwater level changes for 5 climate scenarios were also undertaken using the MIKE SHE model. Due to the smaller run times and longer simulation period, the MODFLOW model was used to analyse long-term changes in groundwater balance for historical and other pumping and climate scenarios. An ensemble of 500 parameter sets that provided similar calibration objective function values were used for these scenario simulations. The details of the scenarios are described in the following.

6.1 MANAGEMENT OPTIONS SIMULATION USING MIKE SHE

Rainfall events with different return periods together with future irrigation demand were considered to evaluate groundwater level changes and sustainability. MIKE SHE model management options were formulated based on crop coverage and irrigation demands in different hydrological situation of the study area. A sample analysis of the study area for the 4-district model is described below.

There are 24 rainfall stations which fall in and around the 4-district model areas. Rainfall data for these 24 stations for a period of 32 years (1985–2016) have been considered for statistical analysis. Rainfall data have been fitted to a Log Normal distribution to analyse and to identify the year which matches with different return period event. The statistical software HYMOS 4.0 has been used for this purpose. The results of the analysis for 2-yr, 5-yr, 10-yr and 25-yr return period are presented in Table 6.1. Due to the randomness of rainfall events, all rainfall events for each station will not represent a unique design year and it is necessary to select a design year on the basis of stations which represent a unique design year.

Table 6.1: Rainfall data corresponding to 2-yr, 5-yr and 25-yr return periods for the 4-district model area

Station Name	2 Yr	Matching Year	5 Yr	Matching Year	10 Yr	Matching Year	25 Yr	Matching Year
Badalgachi	1558	1984	1309	1985	1105	1989	1024	2007
Badarganj	2027	1983	1588	2010	1382	1992	1178	1994
Bithargarh	2766	1990	2149	**2007**	1787	1992	1388	2003
Boda	2358	1996	1927	1993	1686	**1994**	1198	2003
Ghoraghat	1743	2012	1381	2013	1138	2008	907	1997
Debiganj	2398	**2008**	1800	2009	1488	2008	940	2005
Dinajpur	2106	2004	1584	1992	1433	2000	1159	2013
Dubchanchia	1547	2009	1315	2006	1145	1997	1032	2003
Hilli (Hakimpur)	1876	2002	1442	2001	1212	2003	1005	1996
Khansama	3682	2010	3248	**2007**	2759	2012	2508	2004
Kantanagar	2076	1990	1445	2008	1129	2012	1015	2013
Khetlal	1950	1989	1599	2009	1371	2011	1129	2012
Noagaon	1516	**2008**	1277	1996	1143	**1994**	918	**2009**
Nazirpur (Patnitala)	1516	**2008**	1262	2011	1143	**1994**	918	**2009**
Nekmard	1949	2002	1591	2005	1292	2011	1237	2007
Nawabganj	1916	**2008**	1486	**2007**	1194	2006	942	2011
Panchagarh	2908	1990	2320	**2007**	1987	2006	1681	2013
Phulbari	1740	1991	1196	2006	963	**1994**	926	2010
Ruhea	2325	2002	1811	1990	1587	**1994**	1316	2008
Saidpur	2332	1997	1654	2006	1245	2007	1116	1994
Setabganj	1947	1990	1560	1996	1401	2008	1100	2007
Tentulia	3029	1983	2309	**2007**	1938	**1994**	1485	**2009**
Thakurgaon	2370	1991	1825	2012	1417	1996	1216	**2009**
Joypurhat	1777	1999	1459	2011	1331	2002	1057	2001

It was found that 4 stations match the year 2008 as 2-yr return period (50% dependable or exceedance probability of 0.5) event, 5 stations match the year 2007 as 5-yr return period (80% dependable or exceedance probability of 0.8) event and 4 stations match the year 2009 as 25-year return period (95% dependable or exceedance probability of 0.95) event. As such, 2008, 2007 and 2009 have been selected as the average year (50% dependable), design year (80% dependable) and dry year (95% dependable) respectively.

The scenario options are briefly described in Table 6.2:

Table 6.2: Brief description of the MIKE SHE management options

SCENARIO NAME	BRIEF DESCRIPTION
Option 0: Base option, i.e. average condition	· Hydrological condition for 2-Yr return period event (50% dependable rainfall) · Crop coverage for existing condition · Irrigation demand for the existing cropping pattern and crop coverage · Domestic (rural & urban) and industrial demands for existing condition etc · Water application: as per crop demand and irrigation coverage
Option I: Future option with 80% dependable rain (dry year)	· Hydrological condition for 5-Yr return period event (80% dependable rainfall) · Crop coverage for future condition (considering 90% area under HYV Boro) · Irrigation demand for future cropping pattern and crop coverage considering 90% area under HYV Boro · Domestic (rural & urban) and industrial demands for future condition · Water application: as per crop demand and irrigation coverage
Option II: Future option with 95% dependable rainfall (extreme dry year)	· Hydrological condition for 25-Yr return period event (95% dependable rainfall) · Crop coverage for future condition (considering 100% area under HYV Boro) · Irrigation demand for future cropping pattern and crop coverage considering 100% area under HYV Boro · Domestic (rural & urban) and industrial demands for future condition · Water application: as per crop demand and irrigation coverage

6.2 SIMULATION OF THE MANAGEMENT OPTIONS USING MIKE SHE MODELS

Hydraulic parameters comprising hydraulic conductivity, transmissivity, specific yield and storage coefficient obtained through calibration were kept unchanged throughout the simulation of management options. Number of geological and computational layers along with their top and bottom elevations, soil properties and soil moisture retention curves, DEM of the study area, crop data base (leaf area index, root zone depth, crop growth stages and growing season) of individual crops were also kept the same. Meteorological data (rainfall, evaporation, temperature, humidity etc), hydrological data (river water level and discharge at the boundary locations) and hydrogeological data (groundwater level at boundary locations) were provided according to the hydrological year considered for the three different management options . The initial conditions were kept as those corresponding to the beginning of the selected matching year (Table 6.2) for the respective option. Changes that were considered in different option simulations were:

- land use and crop coverage
- water abstractions.

With the above necessary changes, the calibrated and validated surface water–groundwater interaction model was used to complete the option simulations. Results of the option simulations were analysed, presented and compared with the base (current condition) as:

- groundwater level hydrographs
- spatial distribution map of depth to groundwater table.

6.2.1 OPTION O: BASE (I.E. AVERAGE) CONDITION

The base condition includes hydrological situation for the average year (2008) and all other existing situations that prevail in the field. The main purpose of this option is to understand the present state of the study area under base year in terms of volume of water presently being used and for comparison with future condition with changed water abstraction.

GROUNDWATER TABLE FOR OPTION 0

Hydrographs of simulated groundwater tables for selected locations showed that the maximum and minimum depth to groundwater table occur at the end of April and end of October respectively. Hydrographs of observed water table also support the above findings. Based on these findings, maps of maximum and minimum depth to groundwater tables were prepared for 1 May and 1 November respectively for the 16 districts of the Northwest (NW) area for base condition (Figure 6.1 and Figure 6.2) to see the effect of pumping during irrigation season and also to see whether the groundwater table regains to its original positions or not. The maximum depth to groundwater table remains within 1.50 m to 4.50 m in large parts of the northwest on 1 May. From Figure 6.2, it is also observed that during the peak time of monsoon (1 November), the groundwater table bounds back close to the ground surface in most of the areas except for some pockets in Rajshahi, Naogaon and Nawabganj District areas.

6.2.2 OPTION I: FUTURE OPTION

Option I explore a potential future development, which includes future cropping pattern, crop coverage and abstraction of water from groundwater to meet future irrigation demand. Water demand for crops has been estimated considering that existing 90% cropped area is covered by HYV Boro. Hydrological condition for 5-yr return period event (80% dependable rainfall) has been considered to simulate this option (relatively dry year). The purpose of this option is to assess the impact of future development on groundwater levels when rainfall is lesser than average.

HYDROGRAPH ANALYSIS

The hydrograph of simulated groundwater levels for this option is compared with simulated groundwater levels for the base condition (option 0) at selected locations. Sample comparison plots of hydrographs are shown in Figure 6.3 and Figure 6.4. These reveal that, in some places, groundwater level drops down by about 1 to 2 m compared to the groundwater level for base condition during irrigation period. This situation occurred due to higher abstraction in option I compared to the base case. However, groundwater level almost regains to its original position during the peak time of the monsoon in most of the areas. This indicates that increased abstraction in option I is compensated by increased recharge during the rainy season.

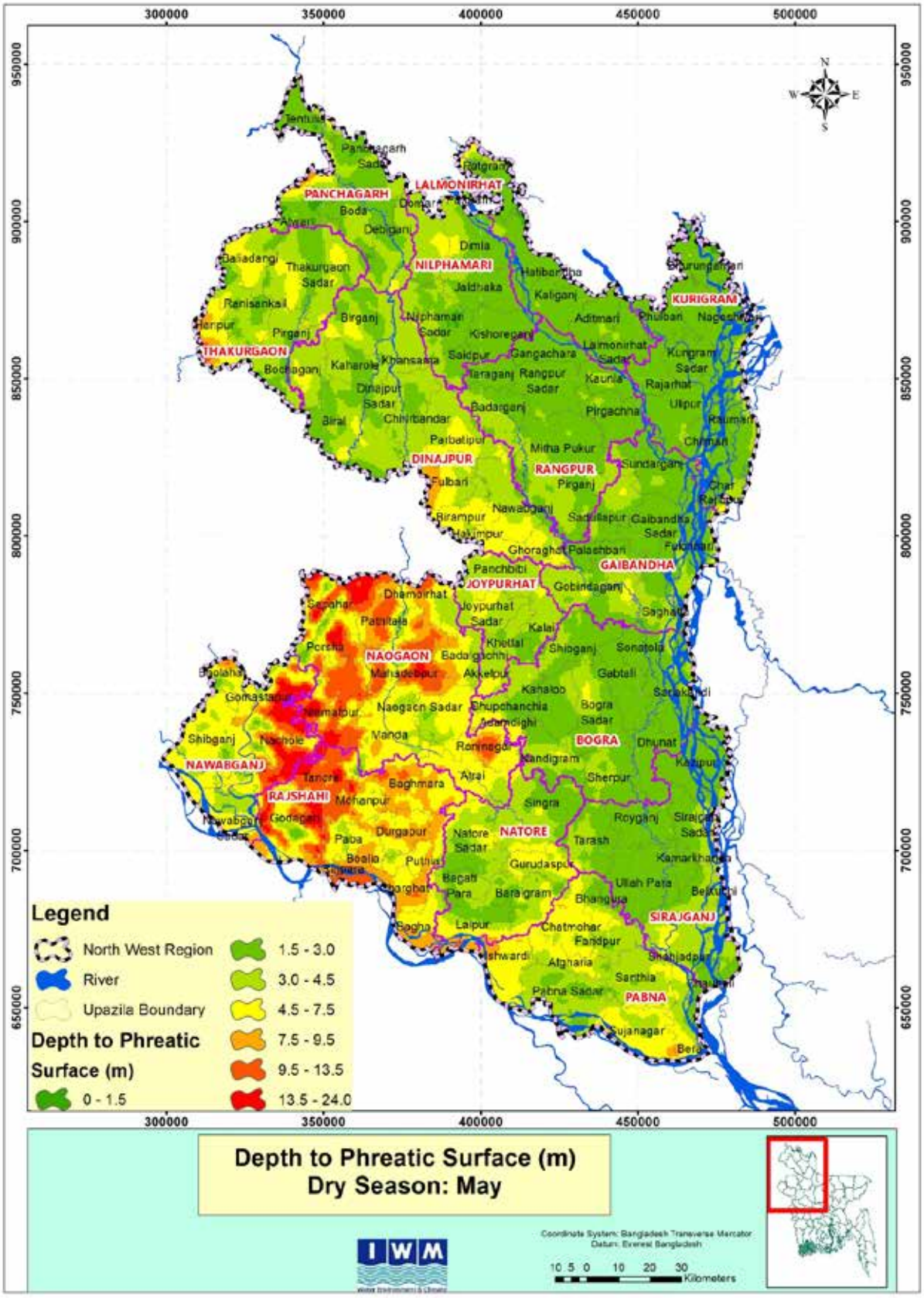

Figure 6.1: Maximum depth to groundwater table on 1 May under Option O (base condition)

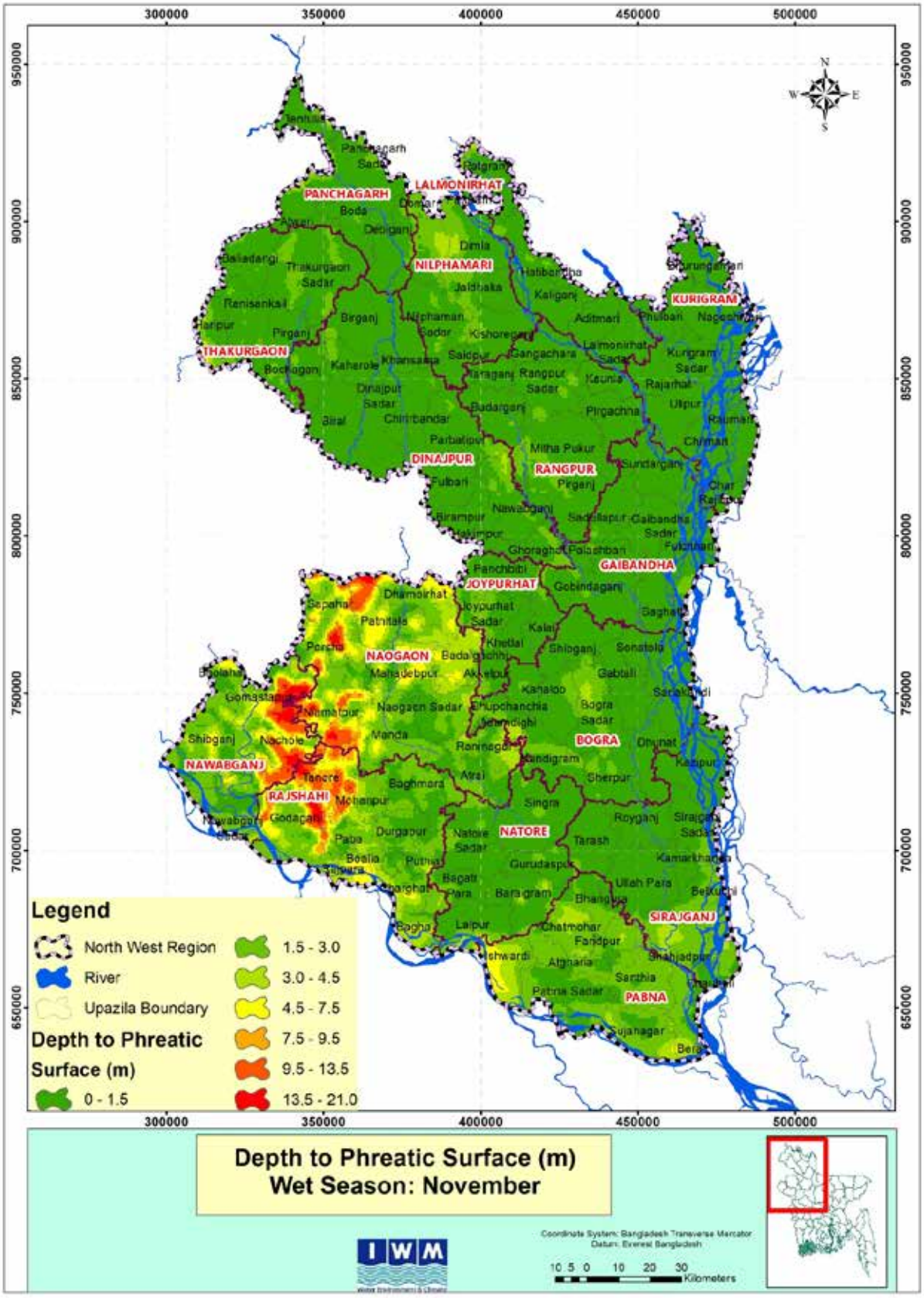

Figure 6.2: Minimum depth to groundwater table on 1 November under Option O (base condition)

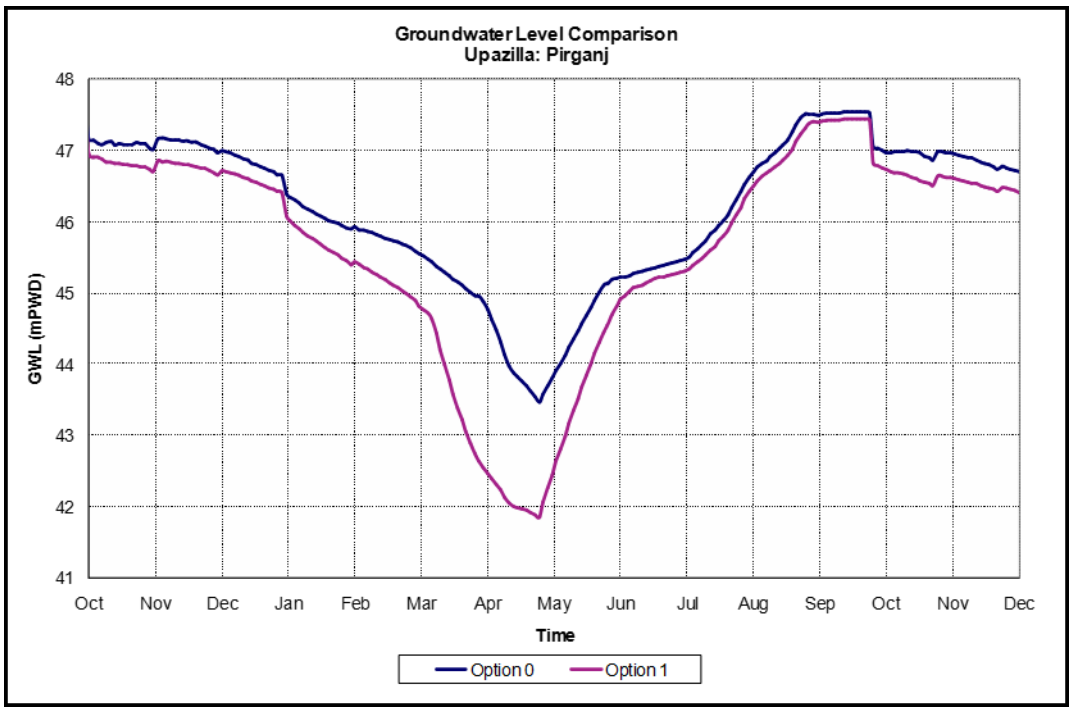

Figure 6.3: Groundwater Level Comparison; Option I & Option 0 for Pirganj of Thakurgaon District

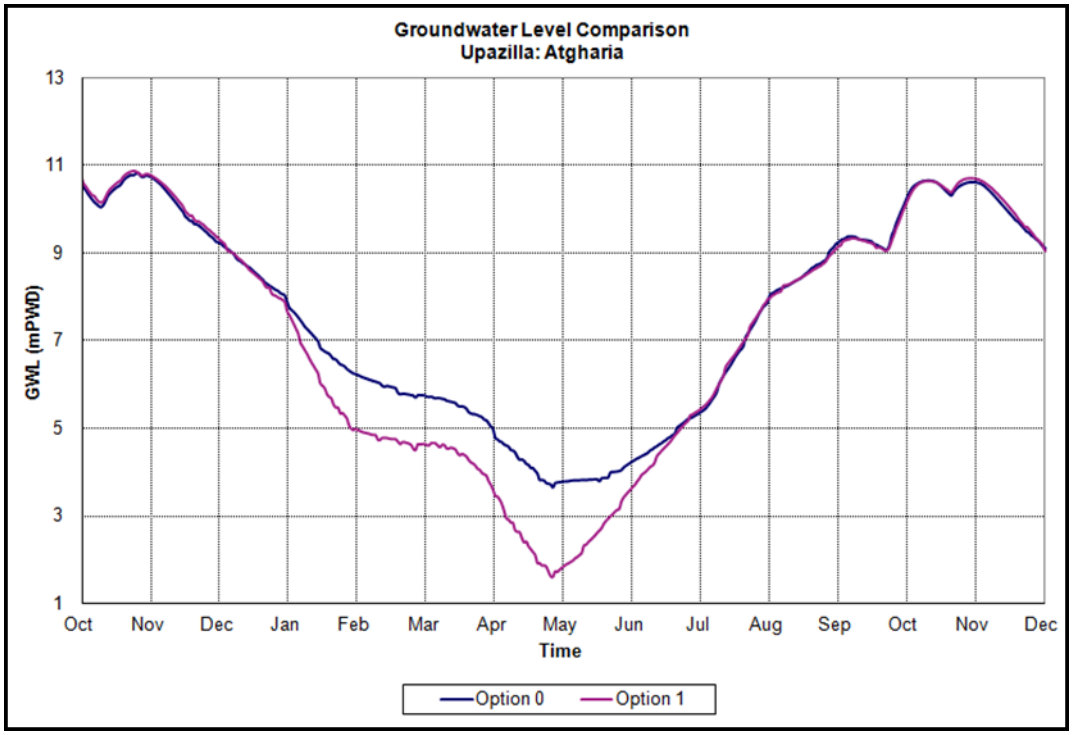

Figure 6.4: Groundwater level comparison; Option I & Option 0 for Atgharia of Pabna District

IMPACT ON DEPTH TO GROUNDWATER TABLES

To investigate the impact of increased abstraction on the study area, spatial distribution of impact maps (Option O – Option I) of maximum and minimum depth to groundwater tables were prepared for 1 May and 1 November as shown in Figure 6.5 and Figure 6.6 for the 16 districts of NW areas. It is observed from Figure 6.5 that in most of the areas, the groundwater table drops down by about 1.0 m to 3.0 m compared to the groundwater table in Option O. It is also observed that groundwater table drops down by about 3.0 m to 9.5 m in some pockets of the areas of NW region as shown in Figure 6.5. However, groundwater tables under Option I returns to its original position during the peak time of the monsoon in major part of the areas

except some part of Rajshahi, Naogaon, and Nawabganj Districts (Figure 6.6). As a major part of the NW area returns to its original position, it reveals that aquifer system has potentiality for further development for future condition i.e in Option I.

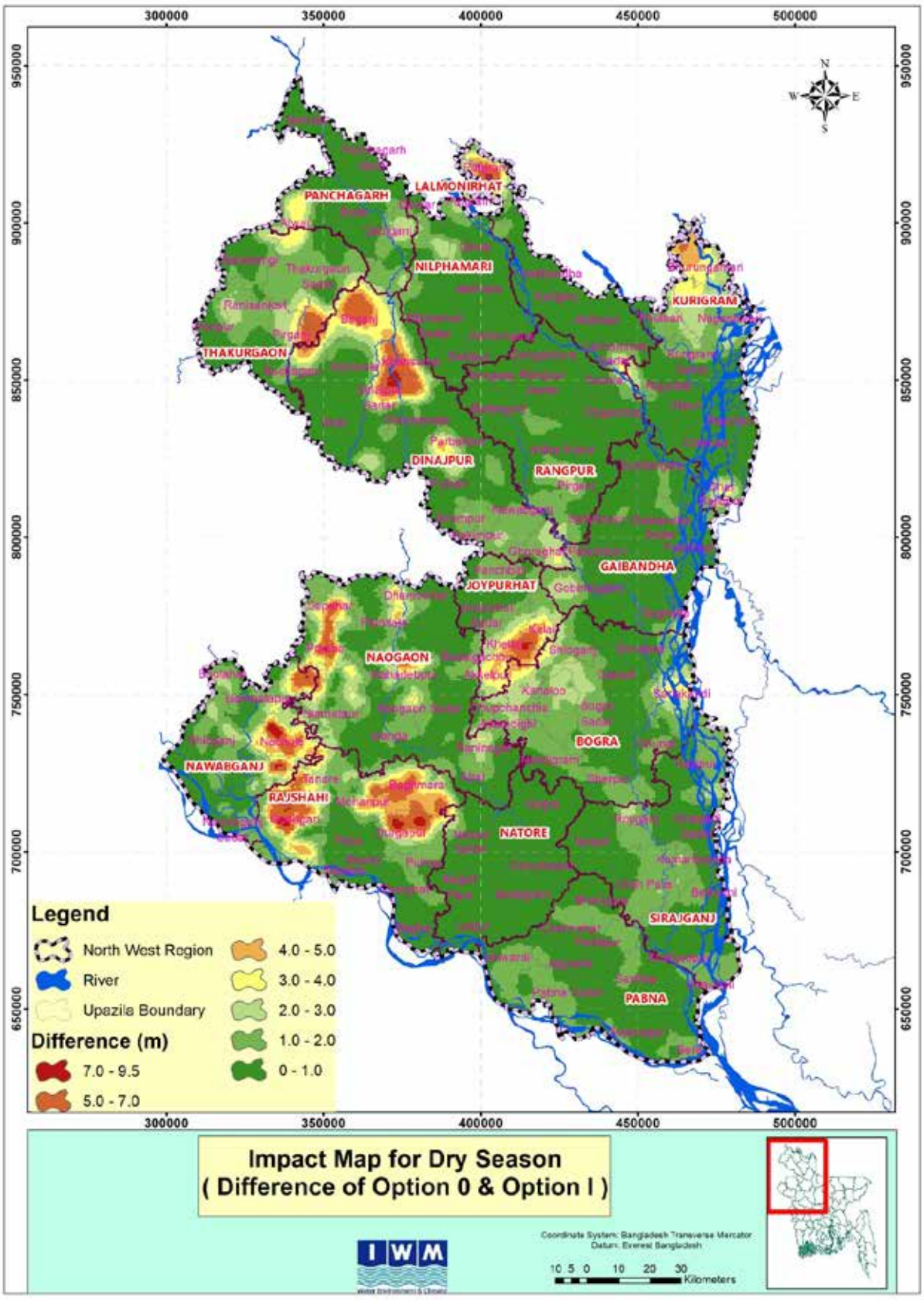

Figure 6.5: Impact map (Option O – Option I) of maximum depth to groundwater table for the dry season

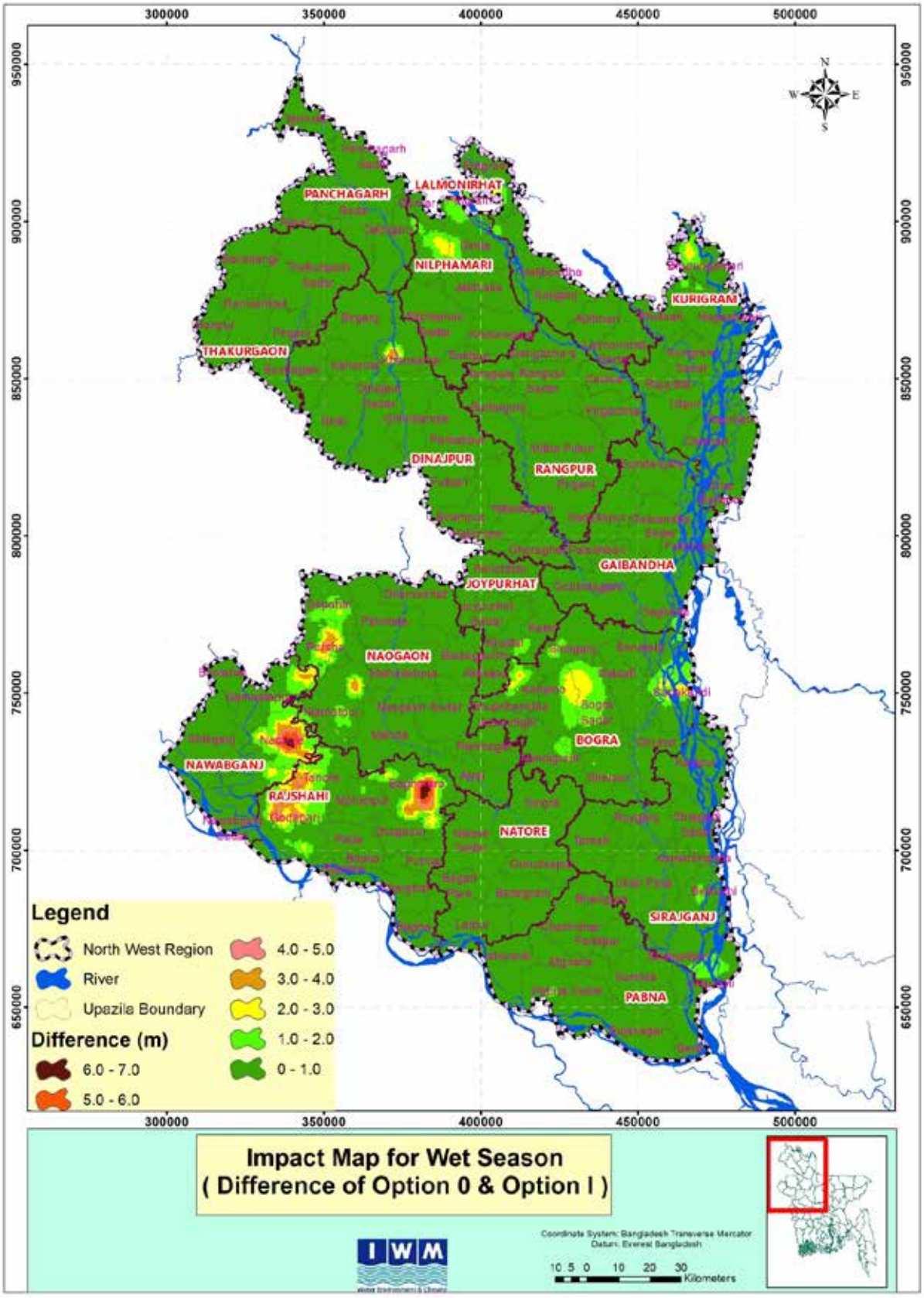

Figure 6.6: Impact map (Option O – Option I) of minimum depth to groundwater table for the wet season

6.2.3 OPTION II: FUTURE OPTION WITH EXTREME DRY YEAR

Option II was designed to evaluate the impact of drought on groundwater. Model simulation was carried out for dry year condition (2009, which is 1: 25 yrs extreme dry year) for this option. Hydrographs of simulated groundwater tables of Option II were compared with simulated groundwater tables of Options I and O at some pre-selected locations.

HYDROGRAPH ANALYSIS

Sample plots of hydrographs are shown in Figure 6.7 and Figure 6.8. Option II causes greater decline in groundwater level in the dry season than Option I and Option O. This situation occurred because in dry year the amount of rainfall is much less than that of the rainfall in Option I and Option O. The groundwater level is slightly lower than its original position in monsoon which indicates that continued groundwater use, despite the occurrence of dry years, can lead to groundwater mining. In such scenarios, management measures would be required to ensure long-term sustainability. Recurrence of such climatic conditions over the years may lead to slow decline in long-term average groundwater levels.

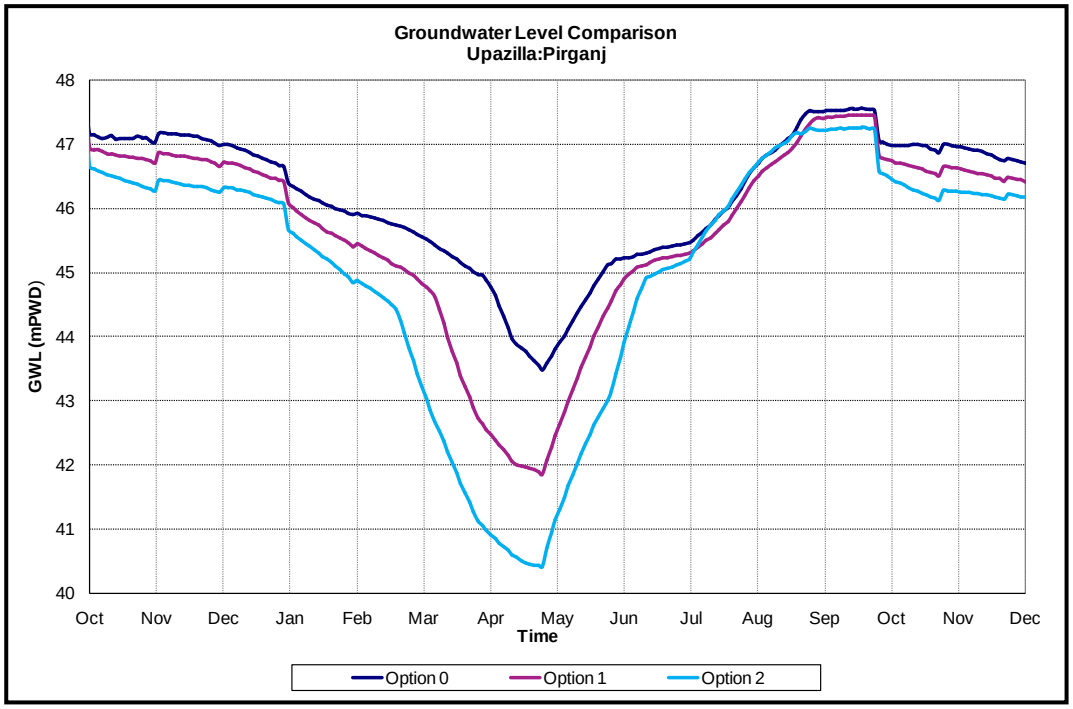

Figure 6.7: Comparison of hydrographs of Option II with Options I and O for Pirganj of Thakurgaon District

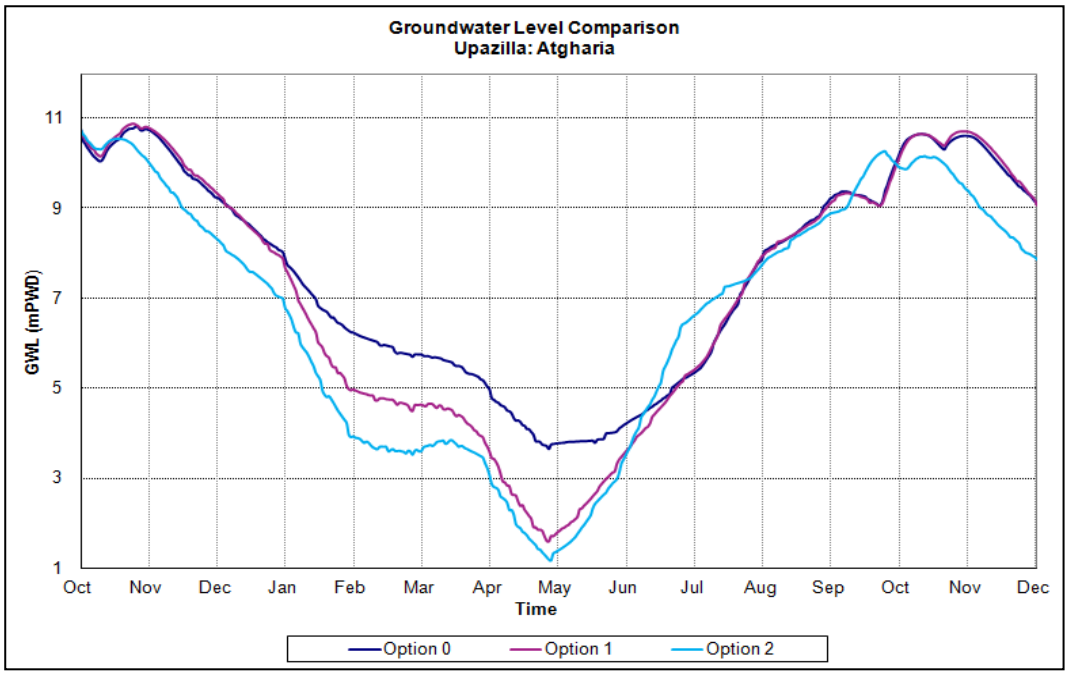

Figure 6.8: Comparison of hydrographs of Option II with Options I and O for Atgharia of Pabna District

IMPACT ON DEPTH TO GROUNDWATER TABLES

To investigate the impact of increased abstraction on the study area for Option II, spatial impact maps (Option O – Option II) of maximum and minimum depth to groundwater tables were prepared for 1 May and 1 November as shown in Figure 6.9 and Figure 6.10 for the 16 districts of NW area. It is noticeable from Figure 6.9 that in most of the areas, the groundwater table drops down by about 1.0 m to 4.0 m compared to the groundwater table of Option 0. It is also observed that groundwater table drops down by about 4.0 m to 10.0 m in some pockets of the NW area. However, groundwater tables under Option II returns to its original position during the peak time of the monsoon in the major part of the areas except some parts of NW areas especially in Rajshahi, Naogaon, and Chapai Nawabganj Districts shown in Figure 6.10.

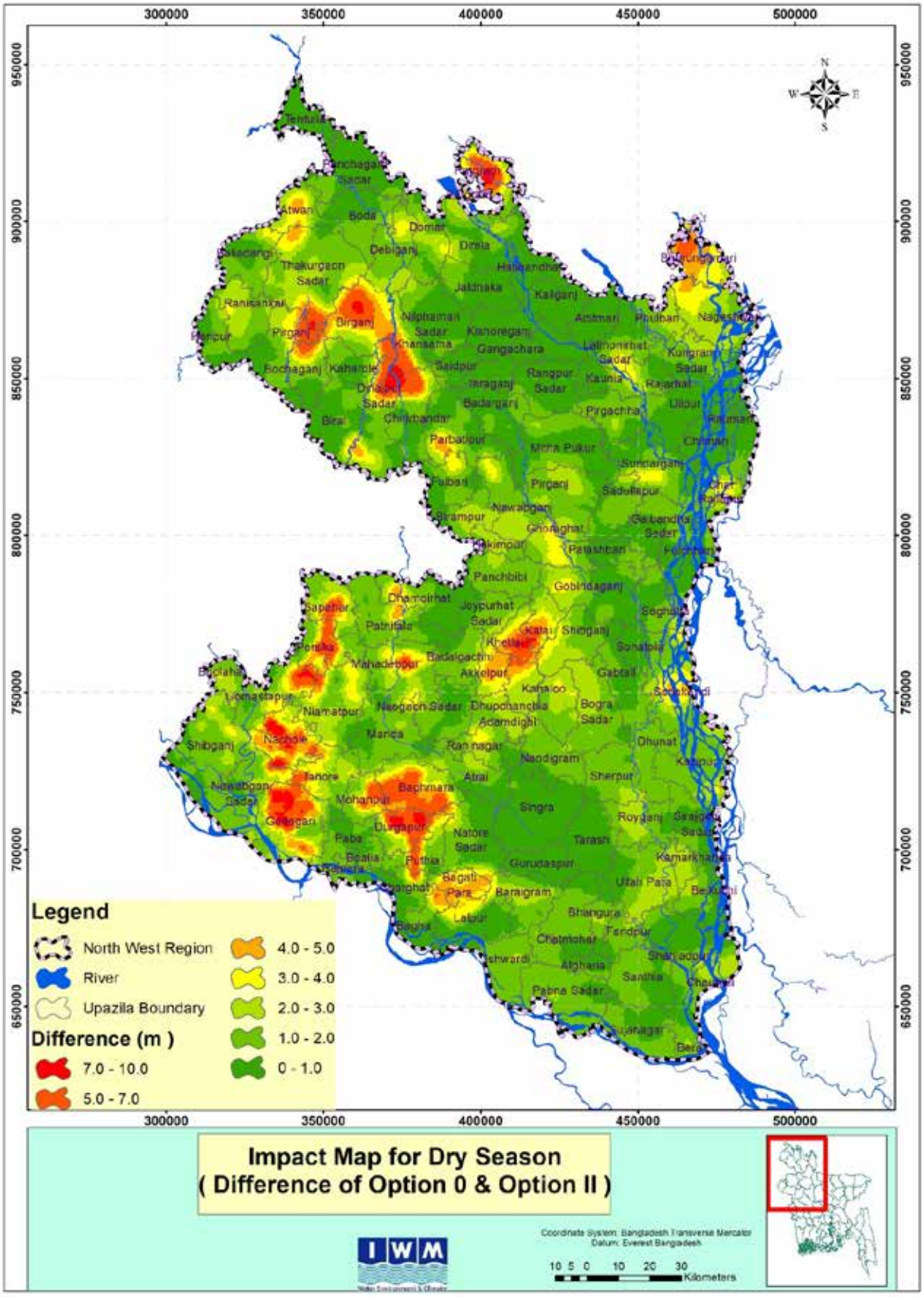

Figure 6.9: Impact map (Option O – Option II) of maximum depth to groundwater table

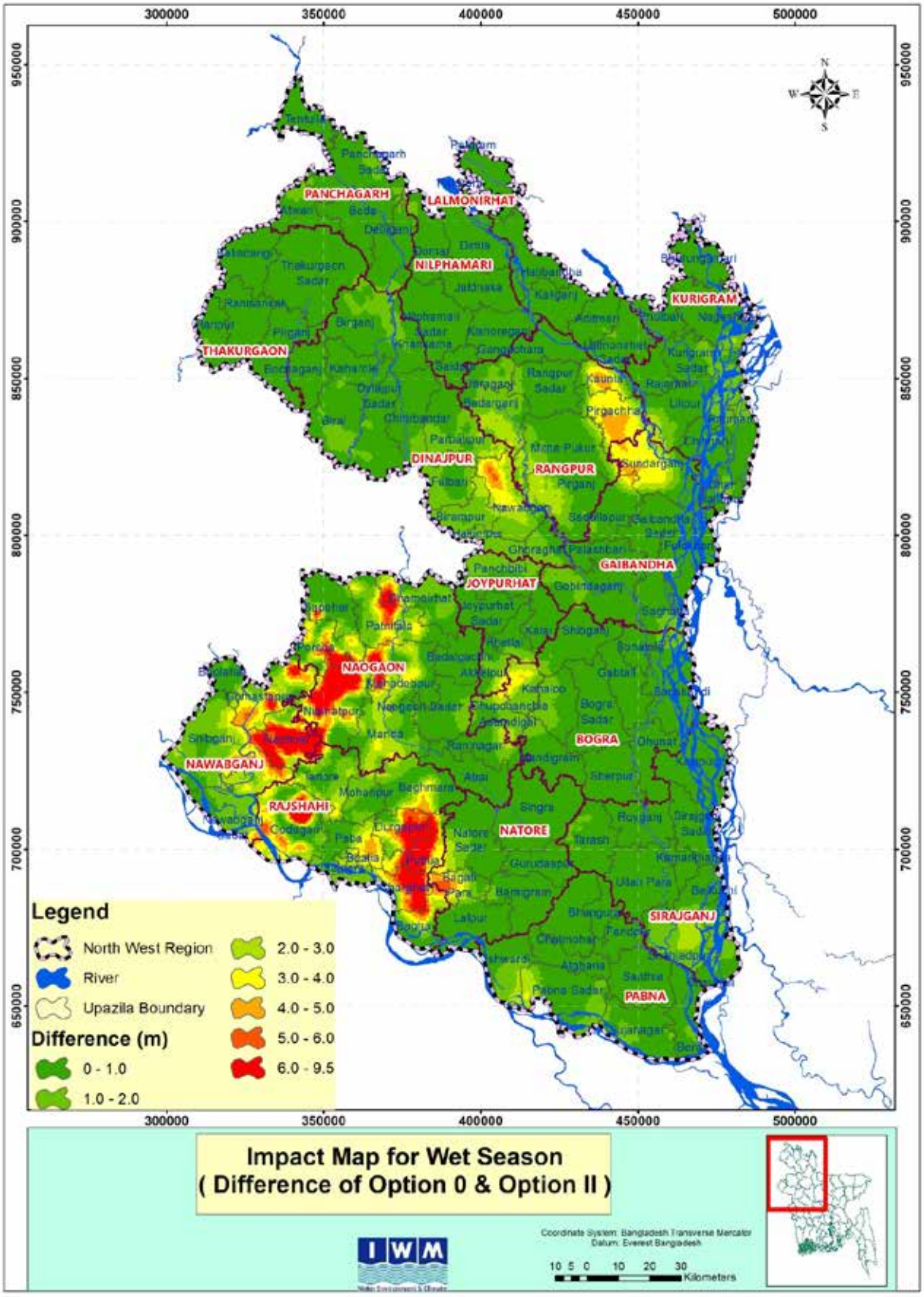

Figure 6.10: Impact map (Option O – Option II) of minimum depth to groundwater table

6.3 MIKE SHE CLIMATE CHANGE SCENARIOS

Bangladesh is a country which is highly vulnerable to climate change impact due to its geographical location (IPCC, 2014). With future changes in climate, temperature is projected to increase in the Ganges and Brahmaputra basins (Moors et al. 2011; Mulligan et al. 2011; Masood et al. 2015). The trend for precipitation is less certain (Jeuland et al. 2013; Moors et al. 2011; Mulligan et al. 2011; Masood et al. 2015). Masood et al. (2015) concluded that there will be an increasing trend of rainfall in the Ganges, particularly of wet season rainfall. Mainuddin et al. (2015) studied the spatial and temporal variations of, and the impact of climate change on, the dry season crop irrigation requirements in Bangladesh and found that crop evapotranspiration may increase up to 6.8% in the northwest region by 2050. The irrigation requirements of Boro rice is projected to increase by 3%.

Kirby et al. (2016) studied the impact of climate change on regional water balances in Bangladesh and found that the impact of change on water availability and use is greater in the Northwest region than elsewhere. As part of this project, Karim et al. (2021) assessed the potential impacts of climate changes on rainfall and evapotranspiration in the Northwest Region of Bangladesh using results from 28 global climate models (GCMs), based on IPCC's 5th assessment report (AR5) for two emission scenarios. They considered 5 scenarios of rainfall and PET jointly encompassing the range of projections to capture the full range of uncertainty. More details about the procedure is given in Karim et al. (2021). For determining the probable changes in future, 5 scenarios as described by Karim et al. (2021) have been considered to investigate climate impacts and uncertainty in predictions. Scenarios and scaling factors for rainfall and PET for these scenarios are given in Table 6.3.

Table 6.3: Five climate change scenarios – names, 2060 scaling factors, rainfall and PET factors

SCENARIO ID	SCENARIO NAME	SCALING FACTORS FOR 2060	RAINFALL	PET
1	AvPETLoR	Average PET and low rainfall	0.983	1.029
2	AvPETHiR	Average PET and high rainfall	1.220	1.039
3	AvPETAvR	Average PET and average rainfall	1.118	1.034
4	LoPETAvR	Low PET and average rainfall	1.096	0.991
5	HiPETAvR	High PET and average rainfall	1.019	1.075

Source: Karim et al, 2021

Using the scaling factors as shown in Table 6.3, the GW-SW interaction model (Option O) was run for the period between 2045 to 2075. To analyse and compare the climate change, the three options (Options O I, II) were run under each of the 5 climate scenarios listed in Table 6.3.

HYDROGRAPHS

Simulated hydrographs for these are shown in Figure 6.11 to Figure 6.15.

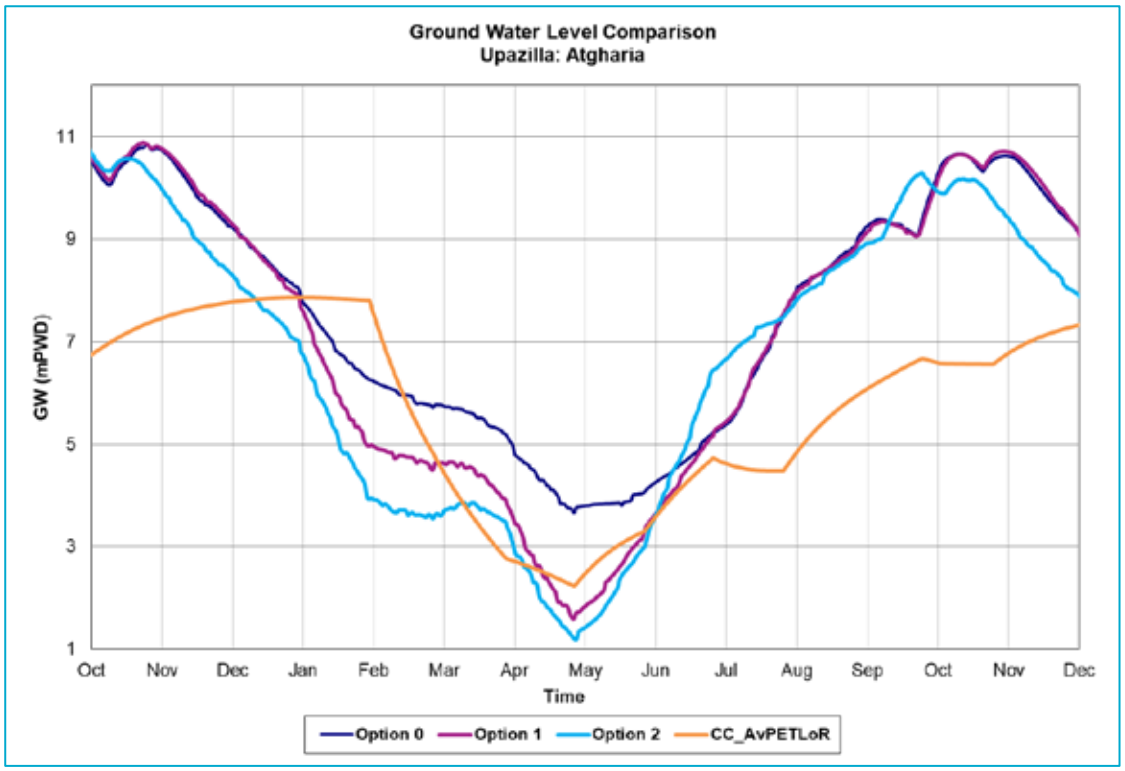

Figure 6.11: Comparison of hydrographs of Options O, I and II under climate change (CC) Scenario 1

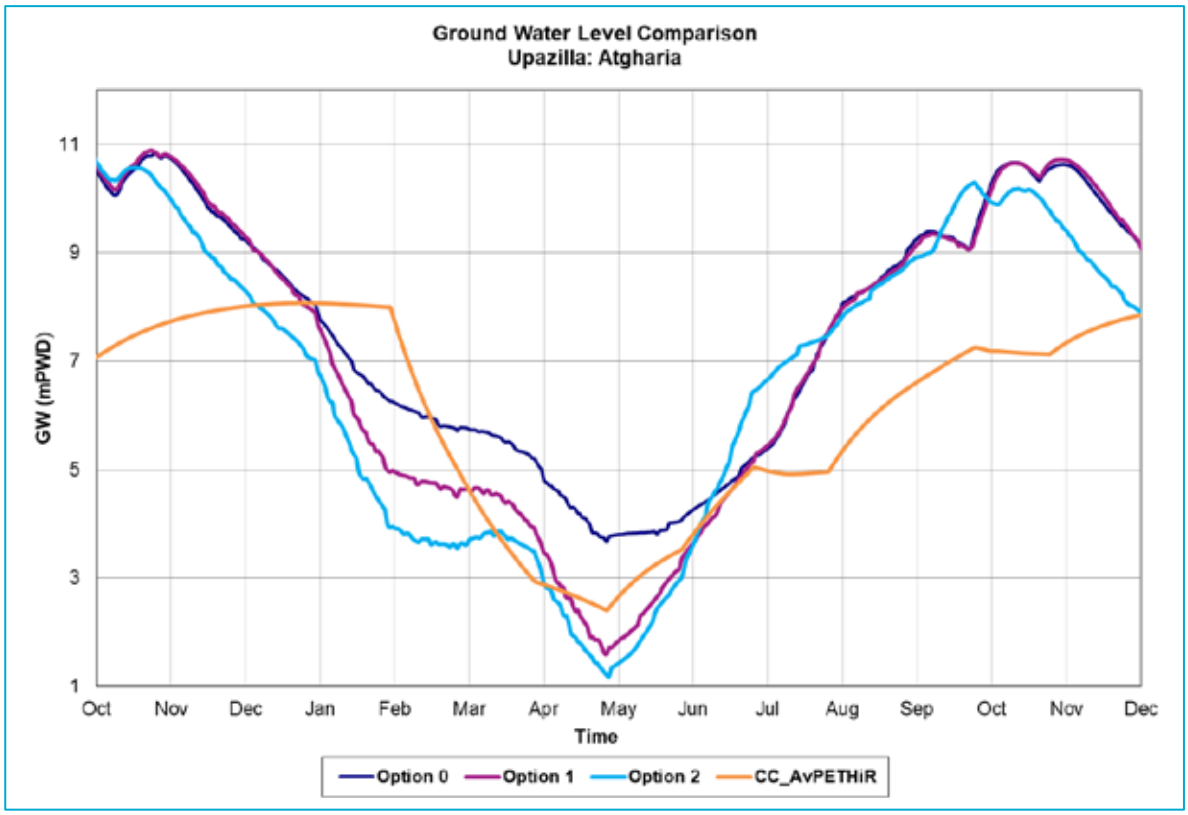

Figure 6.12: Comparison of hydrographs of Options O, I and II under climate change (CC) Scenario 2

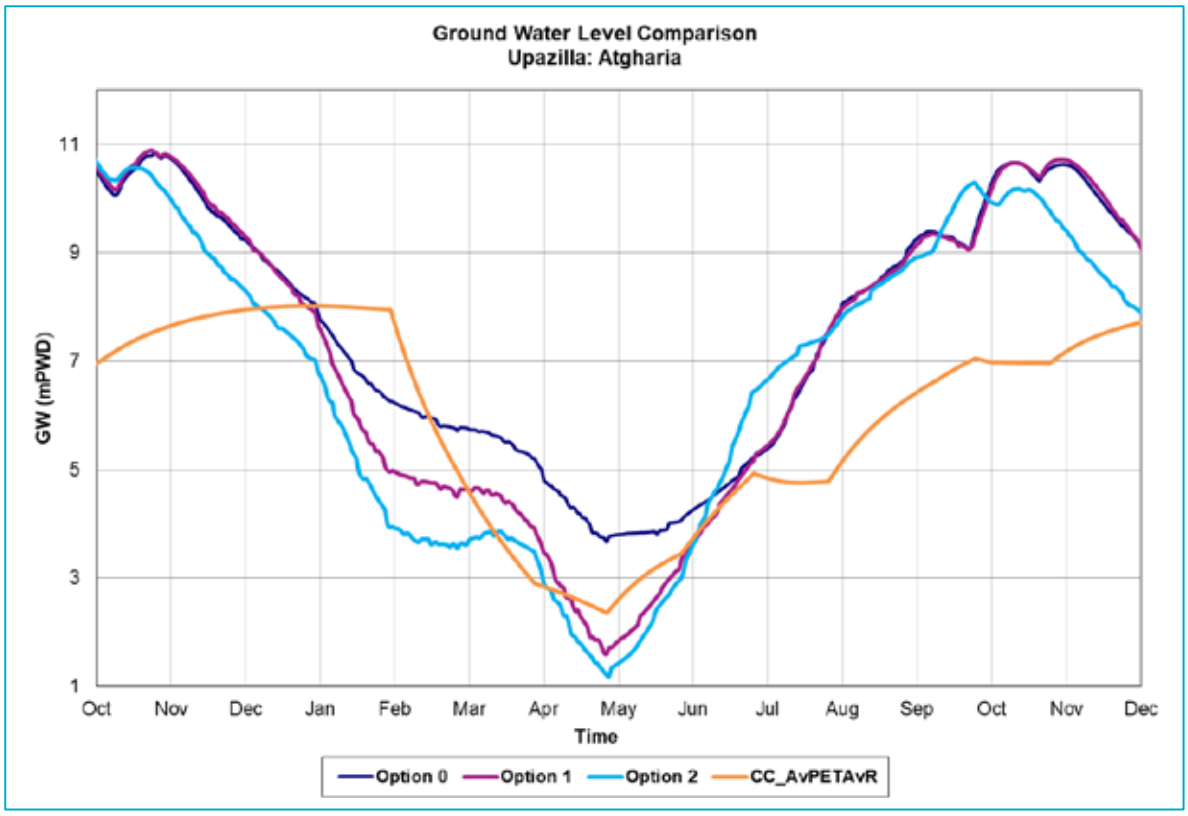

Figure 6.13: Comparison of hydrographs of Options O, I and II under climate change (CC) Scenario 3

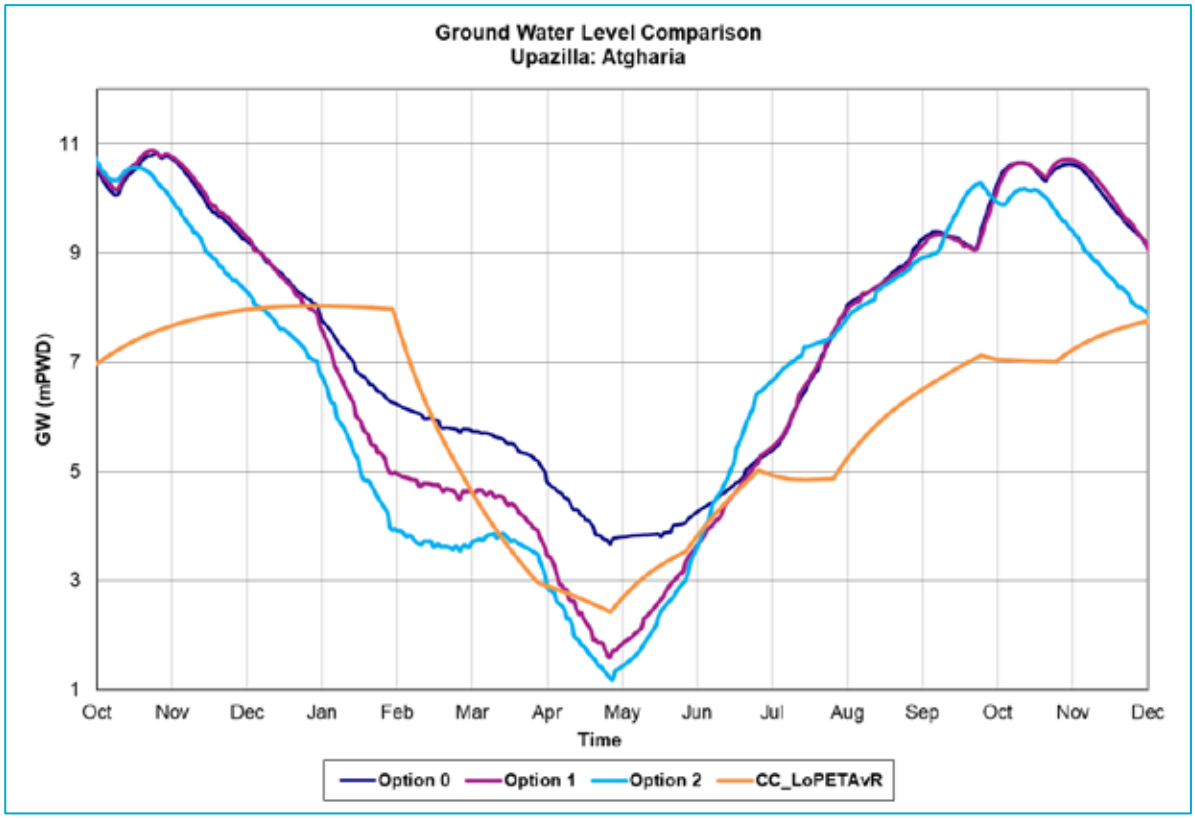

Figure 6.14: Comparison of hydrographs of Options O, I and II under climate change (CC) Scenario 4

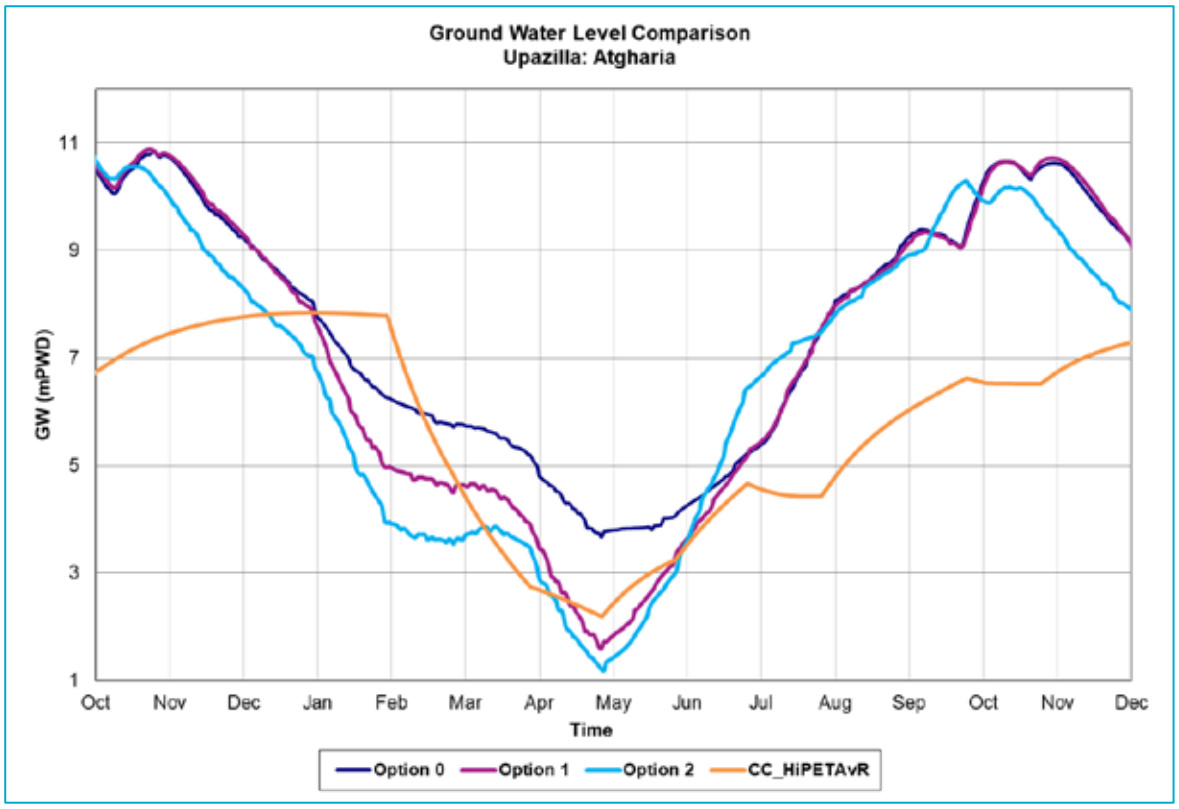

Figure 6.15: Comparison of hydrographs of Options O, I and II under climate change (CC) Scenario 5

Comparison of hydrographs in Figure 6.11 to Figure 6.15 reveals lower groundwater head in the summer months (March, April, May) for the climate scenarios compared to the baseline condition considered in Option). Changes in groundwater level across different climate scenarios are not significant in the annual time scale considered in the analysis. Climate change impact on groundwater levels may occur due to change in amount, distribution and/or duration of rainfall. The most important simulated effect is that the groundwater table fails to regain to its original position in monsoon and in post monsoon. This indicates that the groundwater table may drop about 1 m to 4 m due to the impact of climate change, although these are subject to uncertainties in the predicted rainfall. Considering these situations, the proper monitoring of groundwater level should be continued and initiatives should be taken accordingly. Overall these simulations indicate that groundwater levels will be immediately responsive to changes in rainfall and ET patterns.

There are important insights emerging from these analyses:

- Increased groundwater extraction for expansion of Boro rice may still be possible in some areas of the northwest when historical average rainfall conditions exist. In such conditions groundwater levels would recover by increased recharge during the monsoon season although recurrent occurrence of drought years with significantly lower than average rainfall conditions can result in the decline in long-term average groundwater levels. However, water table could be deeper during the dry season beyond the suction limit in many areas causing groundwater access issue, although this problem is different from unsustainable use
- Changes in pumping is quickly reflected in the groundwater levels under different management options. Under reduced rainfall conditions, increased groundwater use can quickly lead to unsustainable use, especially continued occurrence of reduced recharge due to drought years can result in significant groundwater storage loss.

6.4 MODFLOW PUMPING SCENARIOS

Four pumping scenarios were considered. Unlike the MIKE SHE scenarios, these scenarios explored long-term effect of pumping options on the storage changes in the aquifer. These are described in the following

SCENARIO NAME	DESCRIPTION
Scenario A – base case	Corresponds to the model set up used for the historical simulation over the period 1985–2016. The long-term average storage change in the aquifer for this scenario was computed based on model calibration analysis corresponding to the historical conditions between 1985 and 2016. The time series of pumping for this historical scenario was estimated as a fraction of the ETa through model calibration and uncertainty analysis
Scenario B – linearly increasing pumping over the 30-year period	Analysis of groundwater extraction trends (see section 7.1.4) showed increasing trend in 10 districts and decreasing trend in 6 districts between 1985 and 2016. As the extraction rates are not metered, these trends were not hard-wired into the model simulations. Instead, we simulated the scenario B that considered a gradual increase in the annual average groundwater extraction in proportion to linear increase in ETa up to 50% over the last 30 years in all districts. This scenario is intended to test the hypothesis that net groundwater extraction has increased significantly over the 30-year period owing to deep tube well use for Boro rice cultivation and urban and industrial use leading to declining groundwater levels
Scenario C – 20 % less pumping than the base case	Considers groundwater extraction reduced by 20% compared to the base scenario. This could correspond to a potential conjunctive water use option whereby 20% of groundwater use is offset by surface water use. Scenario C is considered to evaluate the effect of decreased pumping on mitigating the storage decline in the northwest districts
Scenario D – 20 % more pumping than the base case	Corresponds to a hypothetical scenario of increased pumping in all districts potentially arising from increased use of area for Boro cultivation, other cropping and industrial use. Scenario D is considered to evaluate the additional long-term storage decline that may be incurred due to increase in groundwater use

6.5 MODFLOW CLIMATE CHANGE SCENARIOS

The effects of overall water balance changes caused by climate change will also affect the groundwater balance. The effects of climate change on the overall water balance are reported in the companion report (Mainuddin et al. 2021). The water balance study used five climate change scenarios (Karim et al. 2021; as described earlier), each based on the RCP4.5 emissions scenario and each based on a single general circulation model (GCM). They were chosen to give contrasting changes in rainfall and potential evapotranspiration in northwest Bangladesh (Karim et al. 2021):

- average change in rainfall with average change in potential evapotranspiration (labelled CC_**AvPETAvR** in the figures in the next section)
- most negative (or least positive) change in rainfall with average change in potential evapotranspiration (CC_**AvPETLoR**)
- most positive change in rainfall with average change in potential evapotranspiration (CC_**AvPETHiR**)
- average change in rainfall with most negative (or least positive) change in potential evapotranspiration (CC_**LoPETAvR**)
- average change in rainfall with most positive change in potential evapotranspiration (CC_**HiPETAvR**).

We developed projections of changed climates for the period 2046 to 2075, for the districts based on an empirical downscaling or change-factor approach (Zheng et al. 2018), using seasonal scaling factors derived from the five GCMs. The effects of these climate change scenarios on the ETa and deep drainage were analysed in the water balance study. We used the time series of these variables as inputs in the groundwater model to estimate changes in ETg and groundwater recharge to compute changes in groundwater balance corresponding to these climate scenarios.

6.6 RESULTS

6.6.1 MODFLOW PUMPING SCENARIOS

The second conceptualisation of the model was used for simulation of pumping scenarios. The storage changes corresponding to the four pumping scenarios are compared in Table 6.4. Average storage changes simulated for the base case scenario indicate that groundwater storage in the northwest is likely declining at a rate of -6.4 mm/year as reported earlier.

The simulations for scenario B (which considered linear increase in groundwater pumping in all districts increased by 50% between 1985 and 2015), predicted an average groundwater storage decline at the rate of −11.9 mm/year. The likely rate of decline in different districts corresponding to this scenario is shown in Table 6.4. In the districts around the Barind tract, groundwater extraction could have actually increased significantly in the last 30 years and these predicted levels of groundwater storage as in scenario B are more likely to have occurred in those districts. The districts of Nawabganj, Naogaon and Rajshahi have average storage declines of −18.0 mm/year, −19.3 mm/year and −13.1 mm/year under this scenario. Considering the average specific yield of 0.075, this implies declining groundwater levels at the rates of -240 mm/year, −257 mm/year and −175 mm/year respectively in these districts. Such high rates of decline have been observed indicating the possibility of increased groundwater extraction is at least partly responsible for the enhanced decline in groundwater storage in this part of northwest Bangladesh. Thus, it is likely that the net groundwater pumping has increased by 50% in districts like Naogaon, Nawabganj and Rajshahi. The thick clay layer in the Barind district could be preventing proportional increase in induced recharge corresponding to dynamic changes in water levels caused by increased pumping leading to long-term storage decline.

On the other hand, Scenario B resulted in higher-than-observed rates of storage decline in northern districts like Rangpur, Kurigram and Dinajpur. For example, a very high rate of decline of storage of −20 mm/year was simulated for the Rangpur district for this scenario. This corresponds to an average long-term water level decline of 267 mm/year whereas the observed trend is −10 mm/year. This indicates that a significant increase in net groundwater pumping is very unlikely to have occurred in such districts. While the gross pumping may have increased, a significant portion of that would be returning to the water table as induced recharge and irrigation return.

Table 6.4: Average long-term storage decline in the 16 districts corresponding to the four pumping scenarios

	STORAGE CHANGE CORRESPONDING TO PUMPING SCENARIOS (MM/Y)			
DISTRICT	A. BASE	B. 50% INCREASE OVER 30 YRS	C. 20% DECREASE	D. 20% INCREASE
Northern districts				
Panchagarh	-3.9	-5.8	-3.3	-4.5
Thakurgaon	-3.4	-7.9	-1.9	-5.4
Nilpharmari	-3.5	-6.4	-2.8	-4.1
Lalmorihat	-3.3	-5.9	-2.7	-3.9
Dinajpur	-5.7	-11.0	-3.6	-7.7
Rangpur	-8.5	-20.3	-4.0	-13.0
Kurigram	-5.3	-11.2	-3.9	-6.2
Gaibandha	-3.0	-7.1	-2.5	-3.0
Southern districts				
Nawabganj	-12.5	-18.0	-10.9	-13.8
Naogaon	-10.6	-19.3	-7.9	-12.8
Joypurhat	-6.4	-12.1	-4.8	-6.9

District	Storage change corresponding to pumping scenarios (mm/y)			
	A. Base	B. 50% increase over 30 yrs	C. 20% decrease	D. 20% increase
Bogra	-8.8	-16.3	-6.0	-9.4
Rajshahi	-8.9	-13.1	-7.7	-9.8
Natore	-3.5	-7.2	-3.3	-3.0
Pabna	-7.5	-14.5	-5.7	-7.6
Sirajganj	-7.5	-15.1	-5.5	-7.3
Northwest	-6.4	-11.9	-4.8	-7.4

Scenario C considers a potential management option which envisages reduction in groundwater extraction. This could be affected by conjunctive management where surface water use offsets groundwater use in districts where it is possible. The simulation analysis shows that such intervention can yield positive results by reducing the storage loss rates in all districts. The scenario of 20% increase in extraction results in a higher rate of groundwater storage loss across the region. The groundwater level changes corresponding to these scenarios are compared in Figure 6.16.

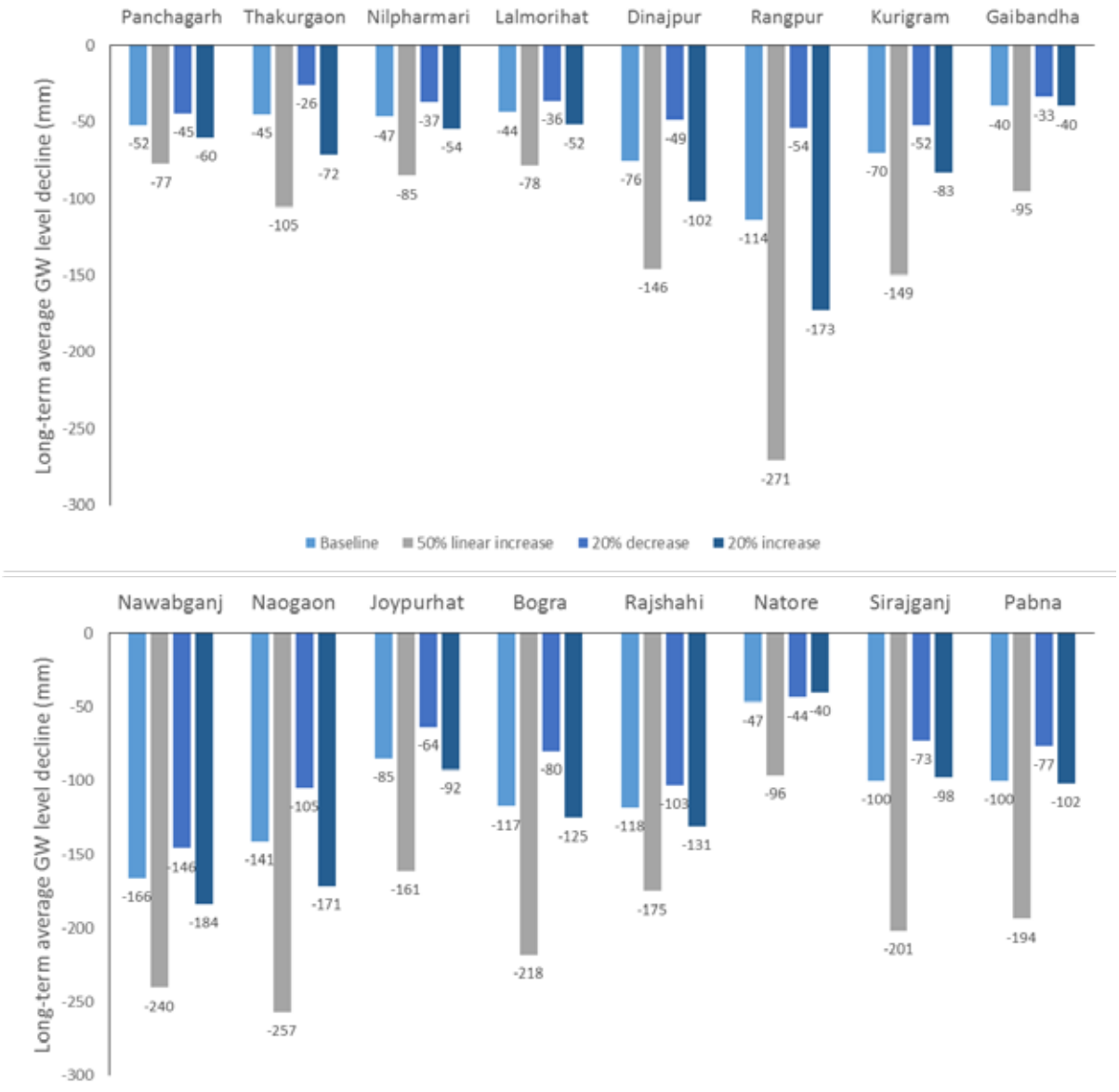

Figure 6.16: Long-term average groundwater level trend for the four pumping scenarios in the A) northern districts, B) southern districts

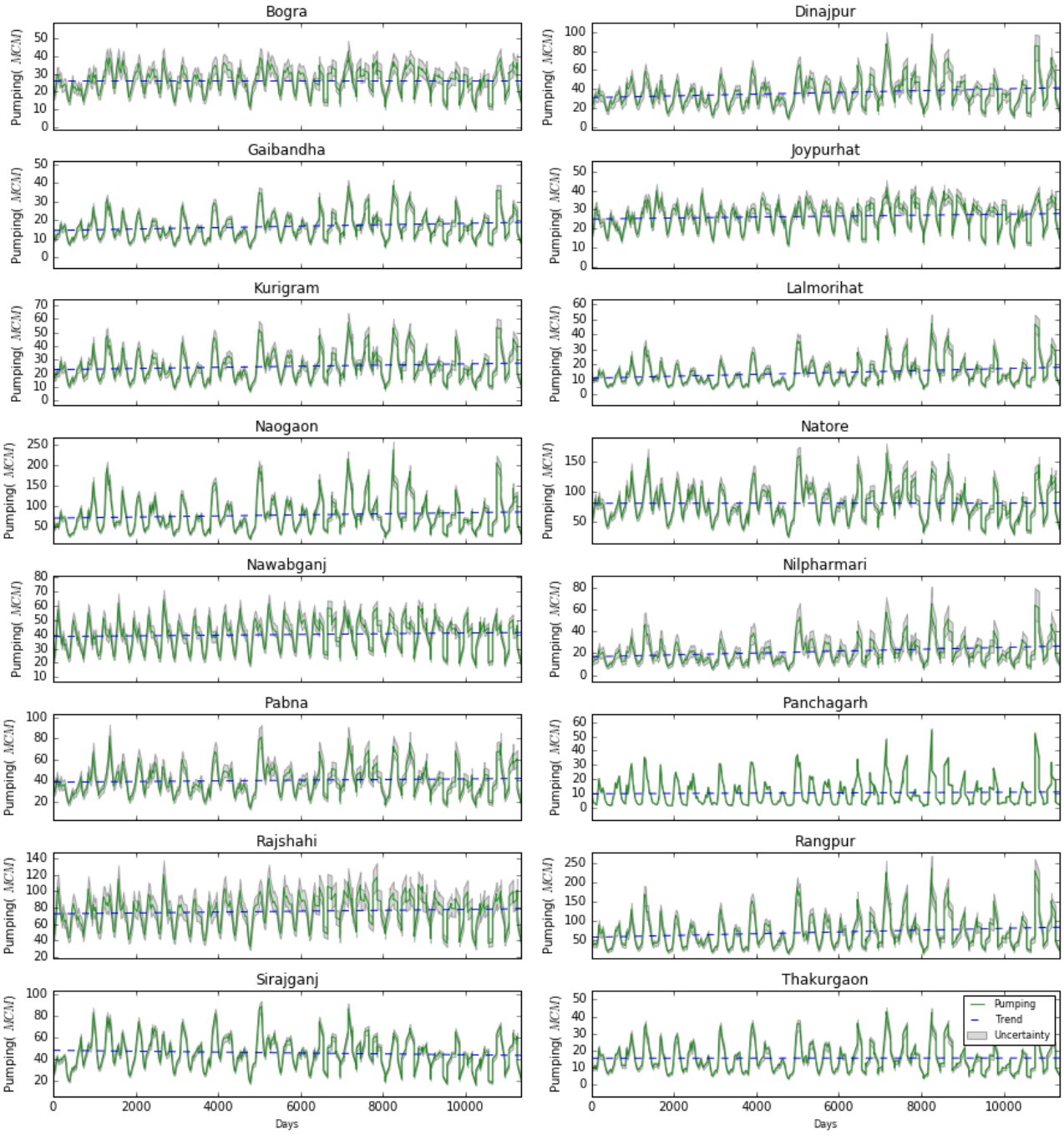

Figure 6.17: Groundwater pumping flux and trend simulated for pumping scenario B

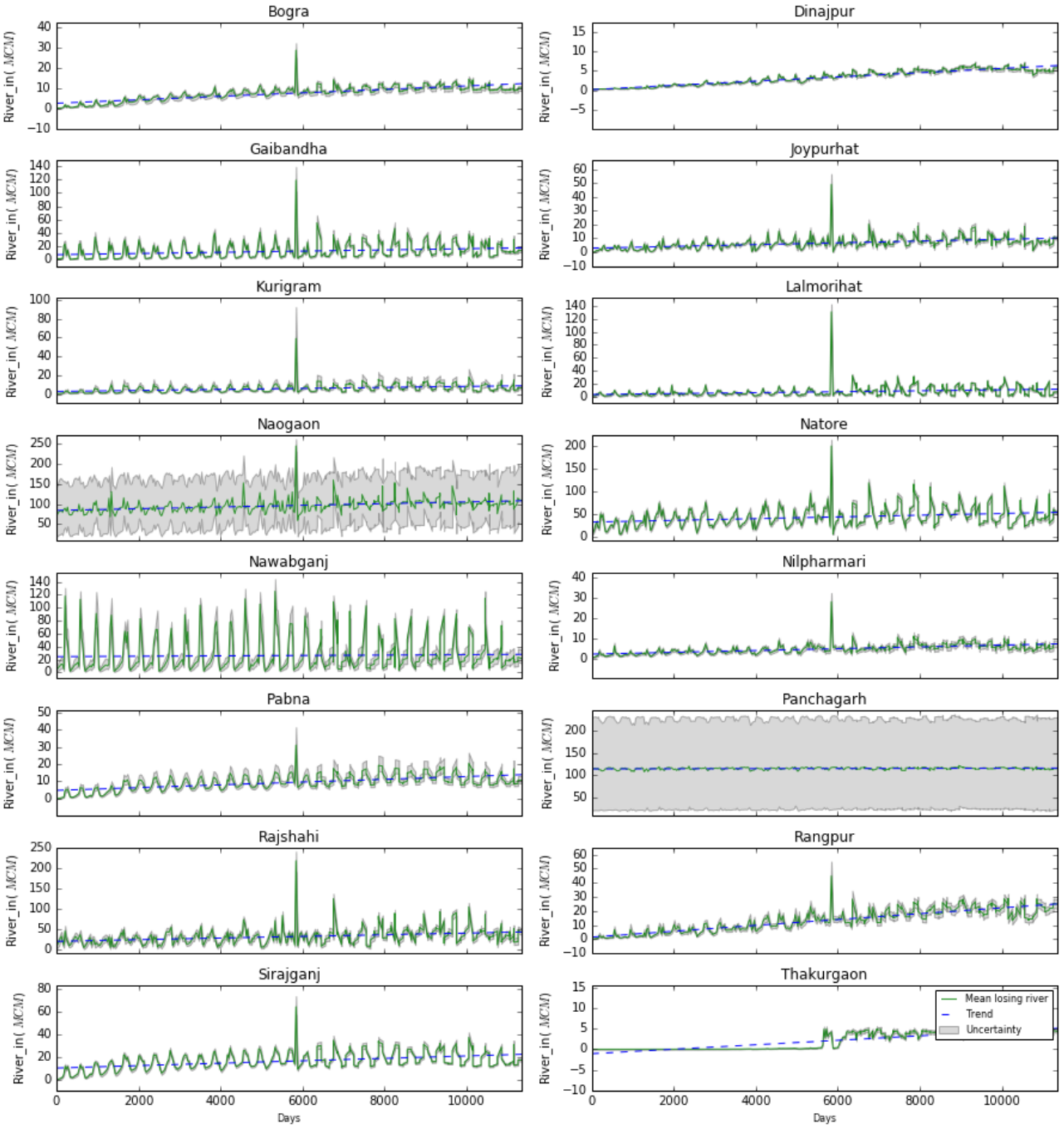

Figure 6.18: Losing river fluxes simulated for the districts corresponding to pumping scenario B

The trend in groundwater pumping flux simulated for scenario B is shown in Figure 6.17. The increasing trend in groundwater pumping considered in this scenario is notable from the trend line plotted for each district. A similar increasing trend over time is observable in the simulated river to aquifer flux shown in Figure 6.18. This is indicative that when there is increased groundwater pumping across the districts, it is likely to induce increased recharge from the losing stretches of the river. The simulated long-term average annual recharge of the aquifer from the losing river reaches for the 4 scenarios in shown in Figure 6.19.

The results consistently show that increased extraction results in a corresponding increase in the river recharge in most districts. Similarly, a decrease in groundwater extraction across the region will have a similar decrease in the river influx into the aquifer.

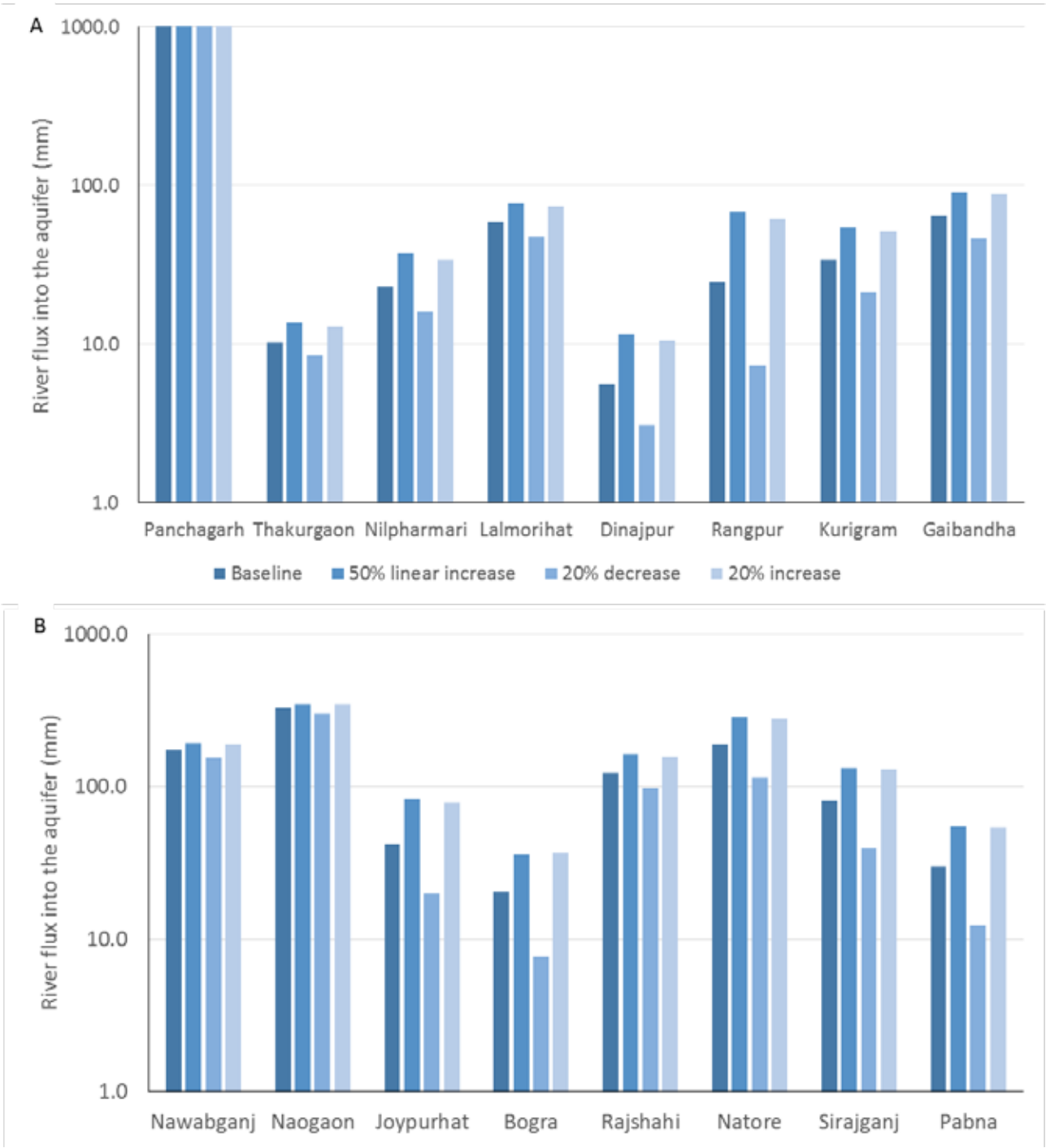

Figure 6.19: Simulated average flux into the aquifer from the river network for A) northern districts B) southern districts

As the groundwater model is constrained only by the observed water levels and simulated river flows, there is large uncertainty in the volume estimates of surface water–groundwater interaction. Especially very large fluxes estimated for Panchgarh district illustrate the unconstrained nature of these estimates from a broad range of relevant parameter combinations.

Nonetheless, the results clearly indicate that the shallow aquifer system is in a dynamic equilibrium with the surface water system and changes in the regional groundwater use will have an effect on this equilibrium. This also indicates that conjunctive management strategies could be explored for most of the districts.

6.6.2 MODFLOW CLIMATE SCENARIOS

The MODFLOW model runs used recharge as an input into the model. The fraction of deep drainage that becomes recharge in different districts was estimated as model parameters during model calibration using historical groundwater level observations. Thus these parameters are most relevant for the historical context and need not necessarily hold true in the context of future scenarios if the recharge regime changes significantly as in the case of climate scenarios. Hence, the climate scenarios explored using the current version of the MODFLOW model is of indicative nature and is used to explore the relative differences in groundwater level change across the five climate scenarios. It is not, as such, intended to predict groundwater storage or levels corresponding to any future state of the system. Considering the simulation of recharge and ET changes, the initial model set up that uses gross recharge and EVT packages is used for these climate scenario simulations.

The simulated groundwater level trend for the 5 climate scenarios is shown in Figure 6.20. Among the 5 climate scenarios, the one corresponding to low rainfall and average PET (AvPETLoR) resulted in the most declining trend in groundwater levels in most districts. While the high PET scenario also leads to increased declining trends, it is not as prominent as the former. This is because low rainfall has a more direct impact on groundwater levels by reducing the recharge. There was no remarkable difference found between the groundwater level change rates between the AvPETAvR and AvPETHiR scenarios. This potentially indicate that higher rates of rainfall than the average may not result in increased net recharge as it is likely to be drained through lateral drainage given the shallow water table in most districts during the monsoon season.

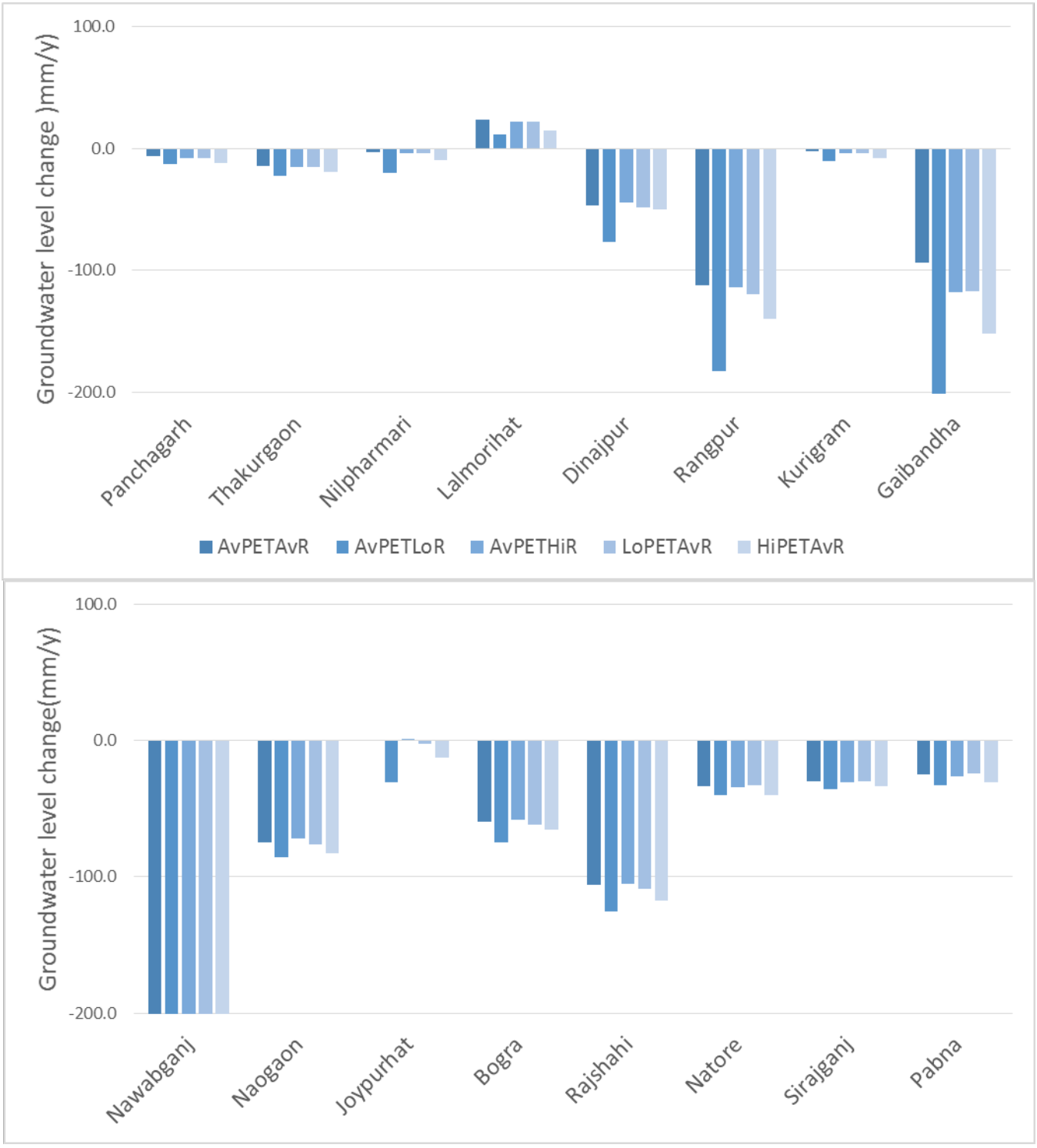

Figure 6.20: Simulated groundwater level trend for the 5 climate scenarios

7 DISCUSSION

Four different modelling approaches were used in the SDIP II Bangladesh project to analyse major water balance components of 16 districts of northwest Bangladesh. Two approaches using MIKE SHE models and MODFLOW model for analysing integrated SW-GW balance and saturated zone water balance respectively are described in this report. Another district-scale lumped water balance model was used to assess the impact of agricultural development and climate scenarios in the companion report (Mainuddin et al. 2021). A separate assessment based on remote sensing data was used to analyse the dynamics and trends in actual evapotranspiration of the districts of the northwest. While each of these studies focussed on specific objectives, assessment of some or all components of groundwater balance were included as part of the analyses. This provided the opportunity to analyse the water balance components from each modelling study in light of the findings from the other studies to explore similarities, differences and uncertainties.

The ETa time series obtained for the 16 districts from the MIKE SHE model simulations are shown in Figure 7.2. The dynamics and the mean ETa obtained from MIKE SHE simulations matches well with the estimates from the water balance and remote sensing estimates in the companion studies (Peña -Arancibia et al. 2020, Peña-Arancibia et al. 2021a) shown in Figure 7.1. It is noteworthy that in every year ETa has two distinct peaks corresponding to the cropping seasons.

The long-term average annual gross recharge values obtained from the MIKE SHE and MODFLOW (median of simulations) models for the 16 districts and the whole northwest region are compared in Figure 7.3. It is noteworthy that these values compare well, especially at the regional level. While these fluxes are presented here as obtained from the modelling results, the main objective of the MODFLOW model was not to investigate these fluxes and their trends. Instead, the key focus of the MODFLOW modelling work was the simulation of groundwater storage changes. Nonetheless, comparable results in fluxes between models using different approaches to represent the processes improve confidence in these model predictions.

Similarly, the sum of ETg and groundwater extraction obtained from the MODFLOW model for the 16 districts are compared to the irrigation water demand obtained from the MIKE SHE model in Figure 7.4. It is noteworthy that these estimates compare reasonably well for most districts. The volume of groundwater extraction estimated by the MODFLOW and MIKE SHE models are compared to corresponding estimates from companion studies (and Kirby et al, 2014) in Figure 7.5. Ahmed et al (2014) using remote sensing data and SEBAL model, estimated net groundwater use in the northwest Bangladesh region in 2010 as 10,500 Mm3. Despite large differences in the way the flow processes are represented in the different models, the cumulative volumes of the recharge and irrigation water use compare reasonably well across these methods and studies. Some differences exist between the estimates, especially at the district scale, and are indicative of the prediction uncertainties of these components.

Figure 7.1: Comparison of ETa estimates from water balance and remote sensing approaches (Jorge et al, 2020)

It is noteworthy that every year estimated ETa has two distinct peaks corresponding to the cropping seasons.

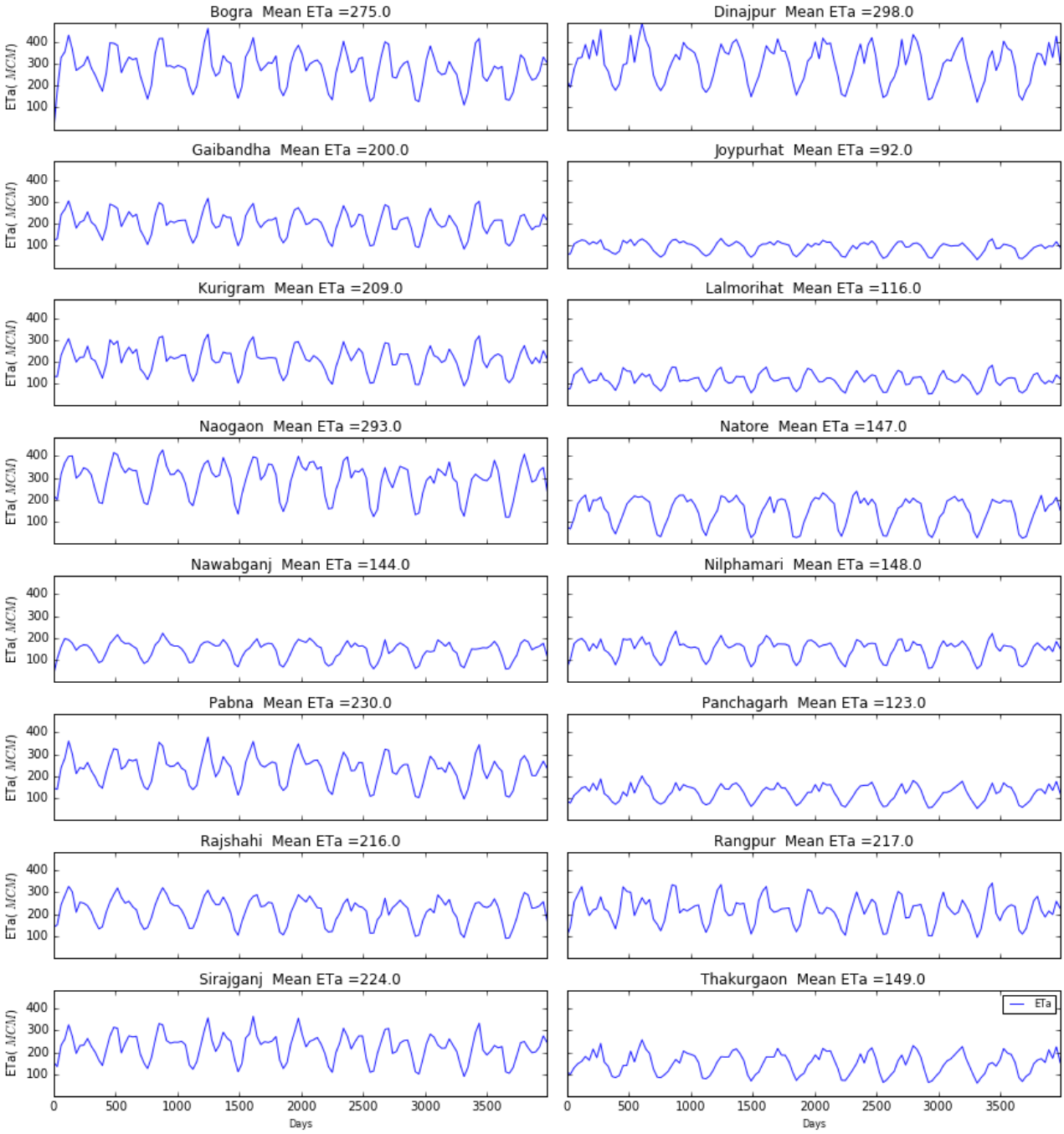

Figure 7.2: Actual evapotranspiration flux simulated for the northwest districts by the MIKE SHE model

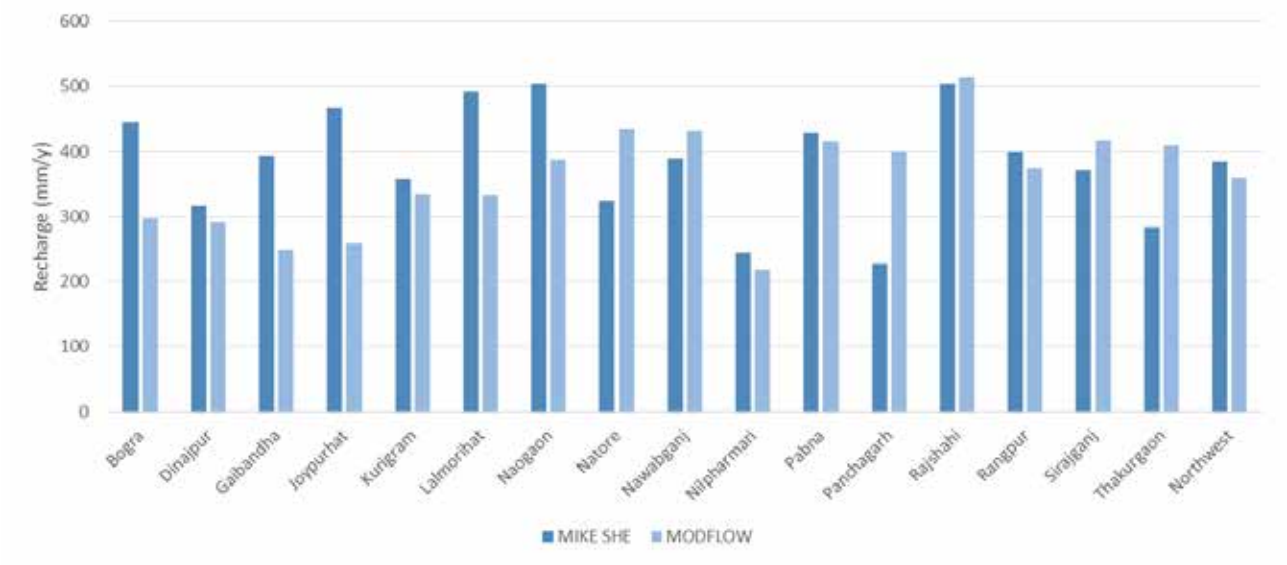

Figure 7.3: Comparison of long-term average recharge values used for districts in the calibrated MIKE SHE and MODFLOW models

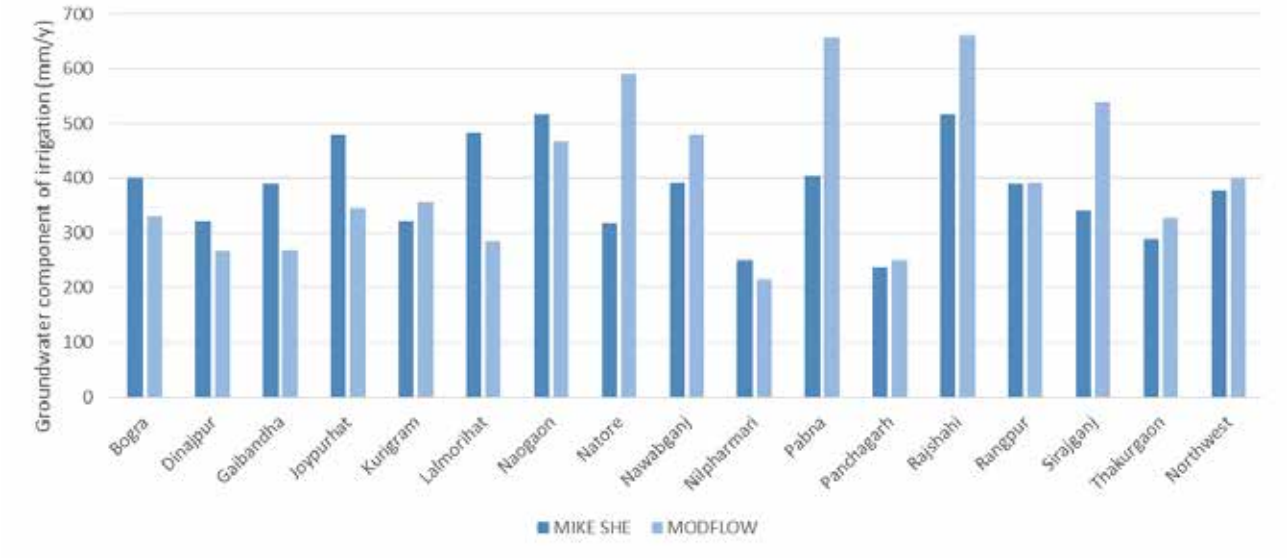

Figure 7.4: Comparison of groundwater component of irrigation as represented in the MIKE SHE and MODFLOW models

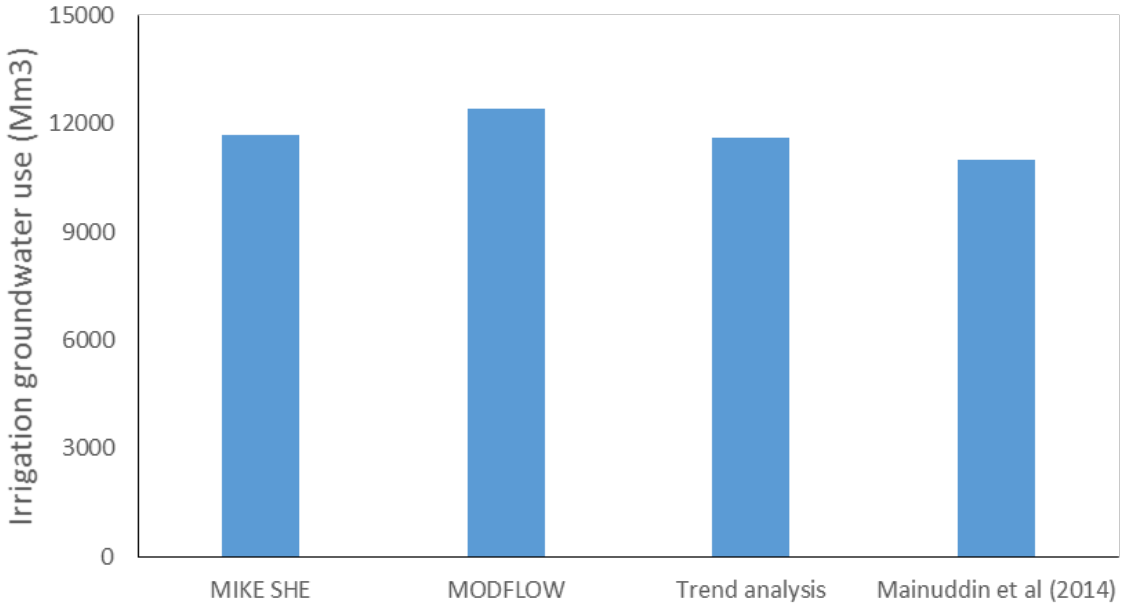

Figure 7.5: Comparison of volume of irrigation groundwater use estimated by different studies

While comparability of groundwater fluxes estimated by different studies improves confidence in these water balance components, it should be noted that all the modelling studies used only groundwater levels to constrain respective models; hence, large uncertainties in the values of individual flux components are still possible. While the data-worth of the groundwater head observations in constraining individual flux components are low, these observations provided valuable information for meaningful simulation of groundwater storage changes between 1985 and 2016 which was the key prediction of the MODFLOW model.

7.1.1 RECHARGE AND GROUNDWATER CONTRIBUTIONS TO ETA

Long-term average recharge obtained from the groundwater balance analysis using the first initial conceptualisation of the model is given in Table 7.1. This is the gross recharge as the groundwater contribution to ETa is represented separately in this model conceptualisation. The gross recharge is also expressed as percentage of rainfall. The total groundwater contribution to ETa, comprising the sum of pumping and ETg, is also shown in the table and is also expressed as percentage of ETa in Table 7.1.

Table 7.1: Annual average gross recharge and ETg estimated using the first model conceptualisation in comparison with the rainfall and ETa

DISTRICT	P (RAINFALL) (MM/Y)	ETA (MM/Y)	RECHARGE (MM/Y)	ETG (MM)	RECHARGE (% P)	ETG (% ETA)
Bogra	1750	1140	297	329	17	29
Dinajpur	1999	1063	291	268	15	25
Gaibandha	1966	1082	249	269	13	25
Joypurhat	1731	1122	259	344	15	31
Kurigram	2543	1078	335	358	13	33
Lalmonirhat	1957	986	333	285	17	29
Naogaon	1543	1111	387	468	25	42
Natore	1547	1085	435	589	28	54
Nawabganj	1456	1094	432	479	30	44

District	P (rainfall) (mm/y)	ETa (mm/y)	Recharge (mm/y)	ETg (mm)	Recharge (% P)	ETg (% ETa)
Nilphamari	2171	1003	218	215	10	21
Pabna	1466	1031	417	657	28	64
Panchagarh	2404	1023	399	251	17	25
Rajshahi	1428	1122	514	661	36	59
Rangpur	2262	1073	374	391	17	36
Sirajganj	1764	1107	417	540	24	49
Thakurgaon	2331	1080	410	328	18	30
Northwest	1895	1075	360	402	20	37

It is noteworthy that gross recharge varies from 13 to 36% of rainfall in the northwest with an average value of 20% of rainfall. The recharge estimates are significantly higher than average in districts like Rajshahi and Nawabganj where groundwater extraction has increased significantly in the past. This is indicative of increased recharge induced by lowering of water table. Such areas may have attained the maximum of recharge potential. Other areas may have the opportunity for further groundwater development.

The estimates of recharge and pumping obtained from the second model conceptualisation are expressed as percentage of rainfall and ETa in Table 7.2. As groundwater contribution to ETa is not separately represented in this model, net recharge values are estimated by this approach. Average net recharge is 9% of rainfall with values ranging between 3 and 23 % in different districts.

Table 7.2: Annual average recharge and pumping obtained from the second model conceptualisation

District	P (rainfall) (mm/y)	ETa (mm/y)	Recharge (mm)	Pumping (mm)	Recharge (% P)	Pumping (% ETa)
Bogra	1750	1140	77	104	4	9
Dinajpur	1999	1063	117	105	6	10
Gaibandha	1966	1082	62	100	3	9
Joypurhat	1731	1122	216	271	13	24
Kurigram	2543	1078	145	187	6	17
Lalmonirhat	1957	986	179	116	9	12
Naogaon	1543	1111	194	228	13	20
Natore	1547	1085	248	425	16	39
Nawabganj	1456	1094	198	242	14	22
Nilphamari	2171	1003	148	135	7	13
Pabna	1466	1031	137	191	9	18
Panchagarh	2404	1023	166	76	7	7
Rajshahi	1428	1122	323	309	23	28
Rangpur	2262	1073	264	299	12	28
Sirajganj	1764	1107	196	302	11	27
Thakurgaon	2331	1080	125	87	5	8
Northwest	1895	1075	175	199	9	18

7.1.2 CHANGES IN LONG-TERM AVERAGE GROUNDWATER STORAGE

Probabilistic simulations using the MODFLOW model indicated that groundwater storage is very likely to be declining at an average rate of −6.4 mm/year across the northwest region. This corresponds to an average groundwater level decline of about 85 mm/year across the northwest. The highest rates of groundwater storage decline were predicted for the districts of Nawabganj, Naogaon and Rajshahi.

The probabilistic simulations showed that groundwater storage in Nawabganj, Naogaon and Rajshahi could be declining at the rate of −12.5, −10.6 and −8.9 mm/year respectively. These levels of storage decline indicate drop in groundwater level at a rate of −167, −141 and −119 mm/y respectively for these districts. The companion water balance study (Mainuddin et al. 2021) also identified these three districts in the same order as having the highest groundwater level decline in northwest region.

Such groundwater level decline is often considered as caused by groundwater pumping that has increased manyfold in the northwest for Boro rice cultivation. However, the modelling analysis in this and other companion studies shows that it is not such a simple cause and effect relationship. Increased pumping across the region does have the potential to increase the rate of groundwater level decline as indicated by the Scenario B. However, recharge potential in most parts of the northwest is high and hence increased pumping results in increased recharge, both the diffuse recharge from rainfall and from the rivers. Scenario analysis corresponding to linearly increasing pumping over the 30 years indicated increase in the recharge from rivers corresponding to increased pumping. While not explicitly modelled in MODFLOW model, similar increase in diffuse recharge is also expected in several districts especially in areas where water table is shallow. Shallow water table results in large amounts of rejected recharge and hence lowering of water table by pumping before the monsoons have potential for reducing the rejected recharge.

The companion study (Mainuddin et al, 2021) shows that rainfall has decreased in most of the districts between 1985 and 2016. The recharge simulated in the MODFLOW model corresponds to this and indicates a small declining trend in all districts. Decreasing recharge together with increased pumping could be contributing to declining groundwater storage especially in areas like the Barind tract where recharge is limited by the soil and other topographic characteristics.

7.1.3 CHANGES IN SHORT-TERM GROUNDWATER LEVELS IN RESPONSE TO IRRIGATION WATER USE

Management option modelling with MIKE SHE considered groundwater level changes in the Barind area covered by the four districts Panchgarh, Thakuragaon, Dinajpur and Joypurhat in response to future groundwater development and rainfall patterns. THree options considered rainfalls comprising 50% (Option 0 corresponding to average year) , 80% (Option I corresponding to dry year) and 95% (Option II corresponding to extreme dry year) dependable rainfall conditions. The future groundwater development scenario considered all cultivable areas used for water intensive Boro rice cultivation. The average conditions (Option 0) indicated that the groundwater level is between 2.5 and 13 m bgl across most of the areas and falls below suction limit in some areas during summer season. Increased groundwater used for irrigation under more limited rainfall availability of 80% dependable rainfall would result in summer water levels declining further by 2 m in the selected. However, water levels were found to recover back during monsoon with 80% dependable rainfall. But water levels can decline further and do not recover under the extreme dry conditions.

These analyses indicate that groundwater levels are dependent significantly on the annual replenishment from the rainfall recharge and levels can rapidly change if the rainfall pattern and amounts change.

Boro rice expansion solely depends on groundwater use for irrigation and such extensive use during drought years can potentially deplete the resource.

As large volumes of groundwater are extracted every year, variability and change in recharge pattern caused by climate change could significantly affect access and availability of groundwater.

7.1.4 PUMPING-INDUCED GROUNDWATER LEVEL DECLINE

Increased pumping from deep tube wells drilled for Boro rice irrigation is often attributed as the cause of groundwater level decline, especially in the districts like southern districts of the northwest. On an average, Boro rice cultivation increased by 1665 % in the districts of northwest between 1985 and 2016. While estimated ETa shows very small increasing trends in some districts, a remarkable increase is not observable across the region (Mojid et al, 2021a). This is potentially because Boro rice would have replaced vegetation that was also transpiring at high rates. While consumptive use has not increased, the amount of pumping for Boro rice cultivation could have increased significantly in the last three decades.

While pumping is not metered, the increase in the number of tube wells in the region certainly indicate that groundwater extraction has increased.

7.1.5 TRENDS IN EXTRACTED GROUNDWATER VOLUME

At district level, 4 different trends in groundwater extraction were revealed:

- insignificantly increasing trend for 6 districts – Rajshahi, Natore, Dinajpur, Gaibandha, Panchagarh, Rangpur
- insignificantly decreasing trend for 4 districts – Naogaon, Chapai Nawabganj, Pabna, Sirajganj
- significantly (p £ 0.05) increasing trend for 4 districts – Kurigram, Lalmonirhat, Nilphamari, Thakurgaon
- significantly (p £ 0.05) decreasing trend for 2 districts – Bogura[1], Joypurhat.

For comparison, volumes of groundwater extraction trends and their significance levels for four districts with different categories of groundwater extraction trends are illustrated in Figure 7.6. Sen's slope provided in the figure gives a robust estimate of the linear trend in the time series data.

[1] Noting that the Shibganj upazila of Bogura district shows a constant groundwater extraction trend

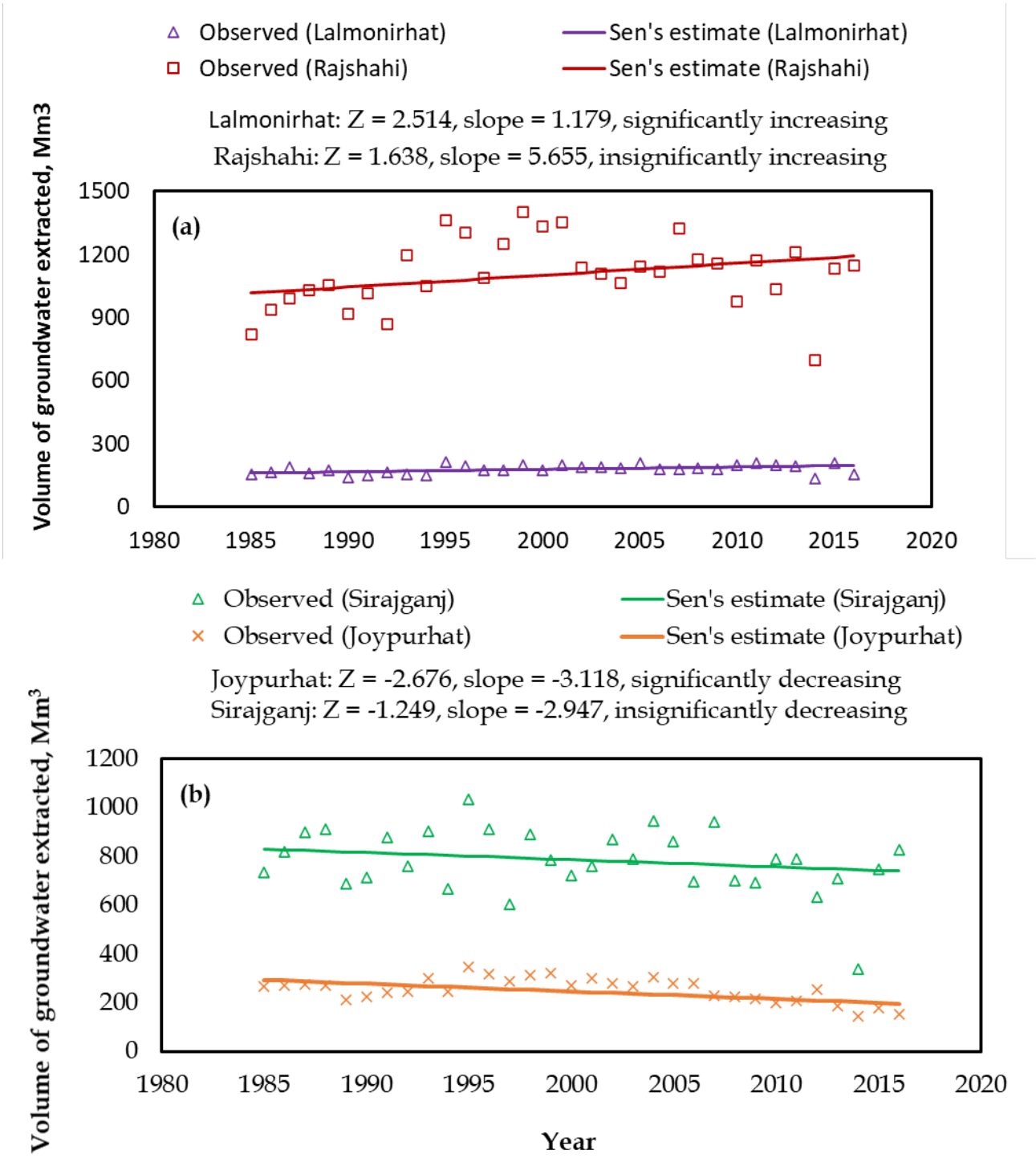

Figure 7.6: Illustration of significant and insignificant trend-types of the annual groundwater extraction volume in (a) Lalmonirhat and Rajshahi districts, and (b) Joypurhat and Sirajganj districts

Figure 7.7 illustrates the volume of groundwater extracted in Rajshahi and Rangpur districts over the 32 years from 1985 to 2016. It is observed that the extraction of groundwater decreased over the period in Rajshahi district but increased in Rangpur district. With regard to the volume of groundwater extracted in Rajshahi district, it dropped from 7,339 Mm^3 in 1985 to 6,702 Mm^3 in 2016, showing an insignificant annual decreasing rate of 0.3 %. On the other hand, the extraction of groundwater volume in Rangpur district increased from 4,192 Mm^3 in 1985 to around 4,986 Mm^3 in 2016, showing an insignificant annual increasing rate of 0.6 %.

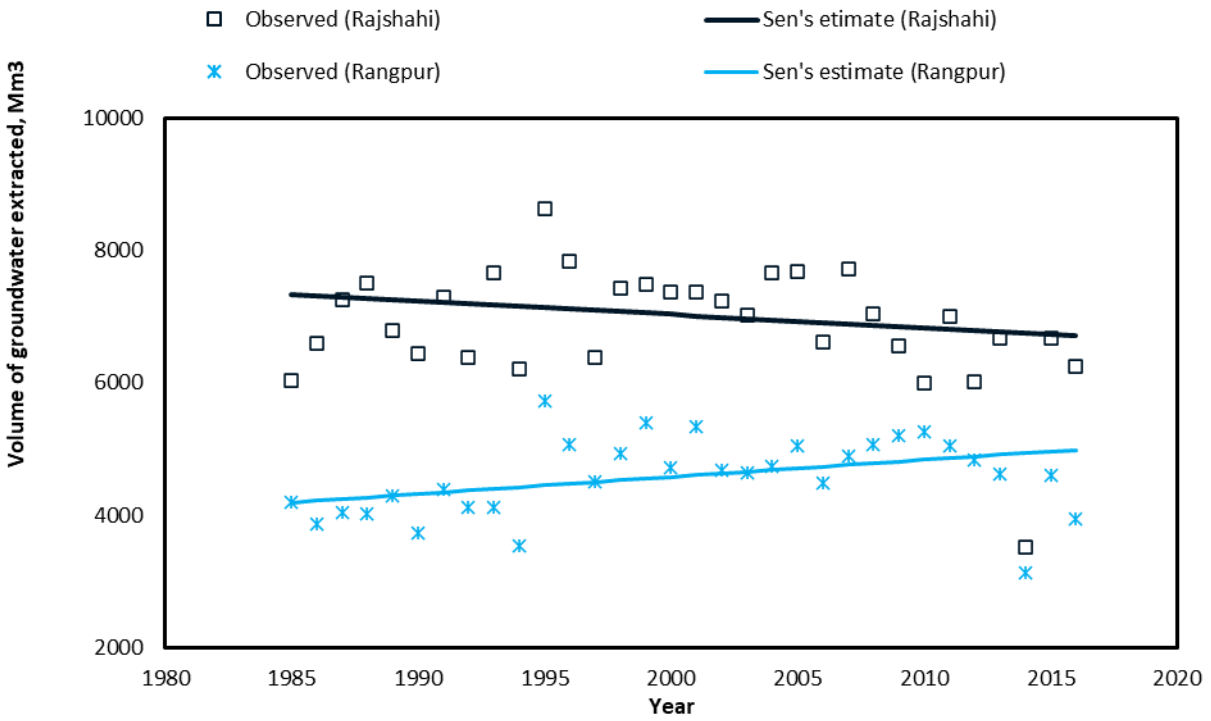

Figure 7.7: Trend of groundwater extraction volume in Rajshahi and Rangpur divisions

When the entire NW region is considered as a single zone, the overall extraction volume of groundwater revealed an insignificant increasing trend (Figure 7.8). The extracted volume of groundwater was 11,536 Mm^3 in 1985 and increased to 11,684 Mm^3 in 2016 (annual rate 0.04%). The estimated volume of extracted groundwater is comparable to that of Kirby et al. (2014) who estimated the volume of groundwater use for irrigation from the regional water balances as 11,000 Mm^3 in the NW.

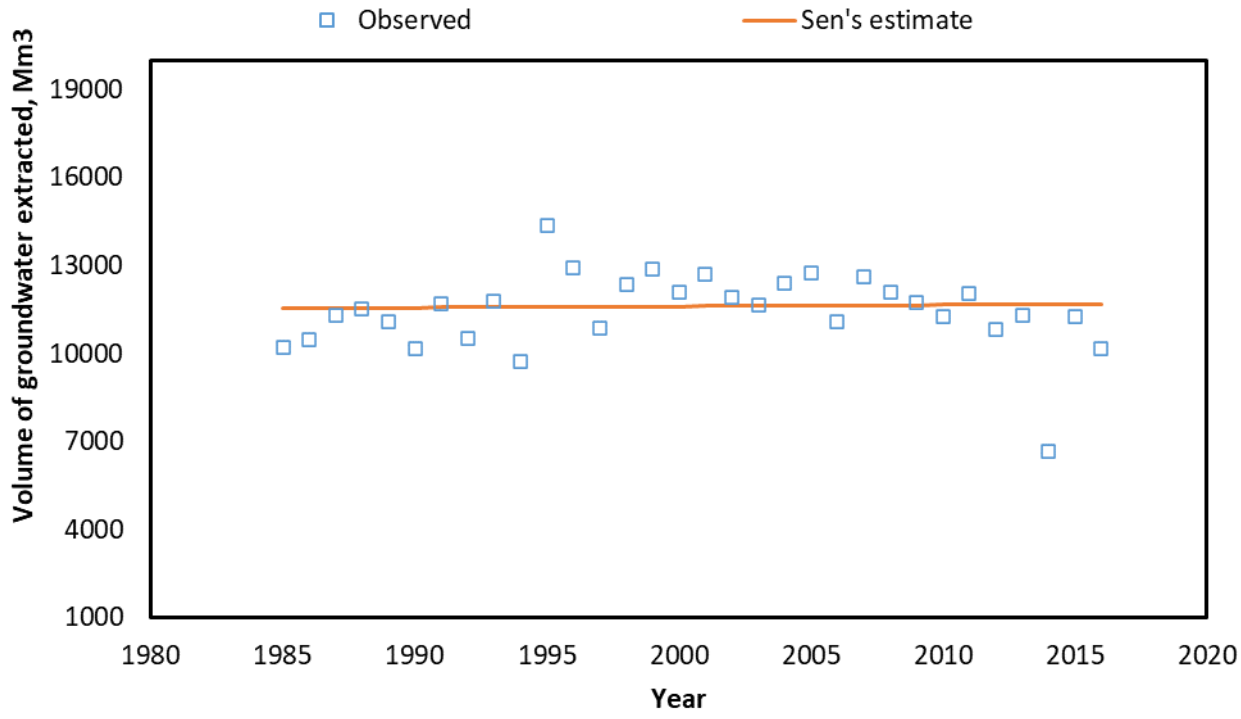

Figure 7.8: Overall trend of groundwater extraction volume over 1985–2016 in the north-west region of Bangladesh

As discussed in the companion studies (Peña-Arancibia et al. 2021a), increased pumping without a remarkable increase in the ETa in some districts indicates the possibility that the excess water pumped

beyond the ET requirement is not part of the consumptive water use (Mainuddin et al. 2020). Given the nature of paddy cultivation with standing water, it is very likely that a significant portion of the water is returned to the aquifer as irrigation return (Rushton et al. 2020).

Scenario B simulations were undertaken to test whether an increasing trend in pumping can explain the groundwater level decline that is observed in many bores in the northwest. This scenario explored linear increase in pumping corresponding to up to 50 % in ETa in all districts between 1985 and 2016 (Scenario B). It assumed that full recharge potential is achieved in the region and thus additional recharge was not induced due to excess pumping. The root mean square error of simulated heads increased to 3.5 m (as compared to 2.8 m for the base case). This indicates that 50% increase in the net groundwater usage is unlikely to have occurred across all districts.

The results of this scenario were analysed for trends in predicted water levels in the observation bores in comparison with the predicted water levels for the base scenario. Simulations indicated that a large number of bores would have experienced steeper decline in groundwater levels than observed, should net groundwater use increased by 50% over the last 30 years. We found that generally the observed trends in water level were better mimicked by the base case (scenario A) that did not consider increase in net pumping over the years. The simulations showed that a linear increase in pumping over the 30-year period without a corresponding increase in recharge would result in steeper decline in water levels in many bores. Examples of bores for which linearly increasing net pumping scenario worsens the match to the observed trend are shown in Figure 7.9. The analyses revealed that simulation of increase in net pumping was not necessary to match the observed declining trends in majority of the bores. While actual pumping may have increased across most of the areas, this would have been accompanied by increase in induced recharge and irrigation return resulting in no major significant increase the net groundwater discharge.

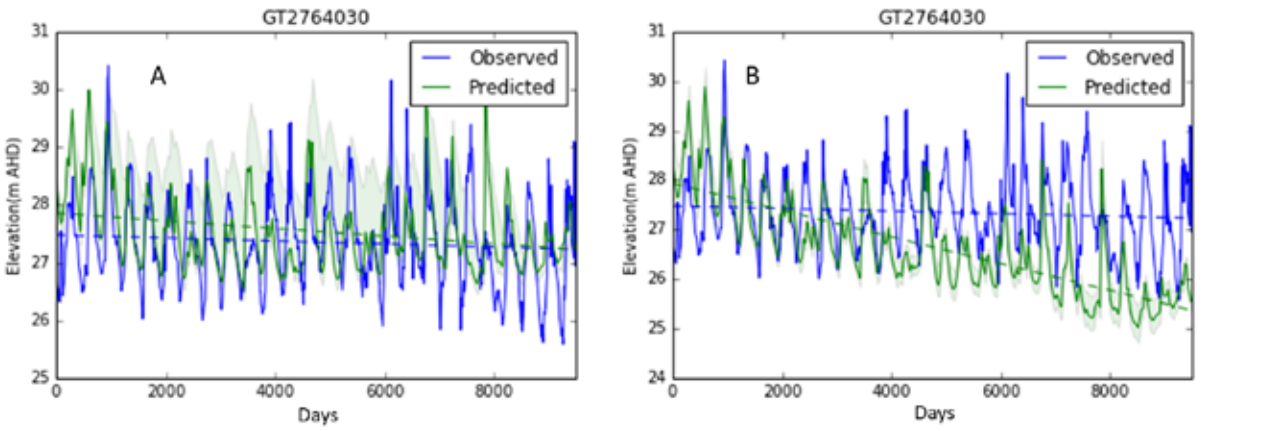

Figure 7.9: Examples of bores for which scenario B worsen the match to the observed trend in comparison to base scenario (shaded area shows the uncertainty bands in predicted groundwater heads)

However, the simulated water level trend in a few bores improved when linear increase in pumping was considered. As an example, Figure 7.10 shows one bore in Rajshahi district, where consideration of linear increase in pumping improved the match between observed and simulated trend in water levels. This could be representative of areas where potential maximum recharge have been achieved and thus increased pumping directly results in groundwater level decline.

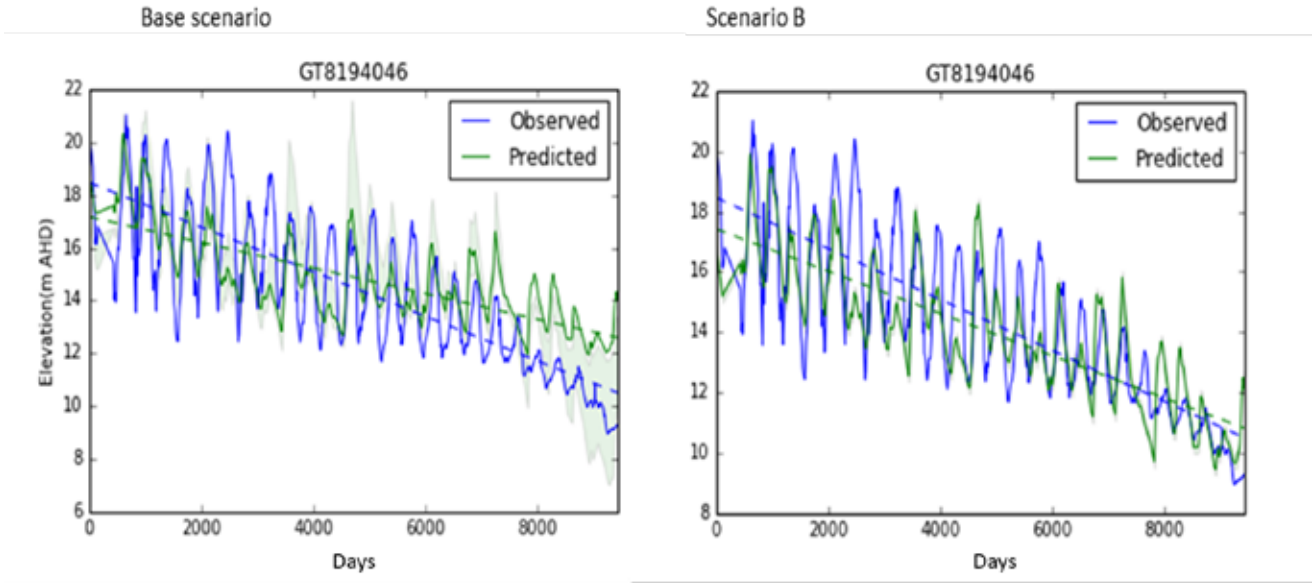

Figure 7.10: Example of a groundwater bore for which scenario B simulation improves the match with observed trend (the shaded area shows the uncertainty bands in simulated groundwater heads)

8 CONCLUSION

Groundwater modelling analyses were undertaken to investigate groundwater balance and storage changes in the northwest region of Bangladesh. Integrated water balance analysis using MIKE SHE models informed that on an average 50% of the total water influx into the northwest region through rainfall and irrigation exists the system as evapotranspiration. The remainder contributes to other water balance components including net recharge into groundwater, drainage into surface water network and small amounts of lateral flow.

Groundwater balance analysis was undertaken using flow modelling and uncertainty analysis of the saturated zone using a water balance model built using the MODFLOW code. The analysis indicated that over the historical long term period (1985 to 2016), an average of 20% of the rainfall entered the aquifer as gross recharge annually. Owing to the shallow groundwater level in most areas, a significant share of that recharge contributed directly to ETa by means of uptake from the root zone or shallow pumping. The long-term average net recharge from rainfall was estimated as 9 % of the annual average rainfall. In addition to this, a significant amount of water enters the aquifer through recharge from rivers. Gross and net recharge were estimated to be significantly higher than average in districts like Nawabganj, Naogaon and Rajshahi where groundwater extractions have been high. This is likely because of the lowering of water levels due to pumping, inducing additional recharge than occurring under natural conditions. While parts of these districts may have achieved potential maximum recharge, other areas may have potential opportunity for more induced recharge. Groundwater contribution to consumptive use was estimated between 35% and 37 % of the ETa by the MIKE SHE and MODFLOW models.

Probabilistic simulations using the calibrated model indicated that groundwater storage across the northwest region is likely declining at a rate of −1.5 mm/y resulting in the likelihood of decline of groundwater levels at an average rate of −19 mm/y. An alternate conceptual model considering the net values of recharge and discharge indicated that the average groundwater storage loss could be potentially as much as −6.4 mm/y corresponding to an average groundwater level decline of −85 mm/y across the region. The highest rates of groundwater storage decline were simulated for the districts of Nawabganj, Rajshahi and Naogaon with groundwater level declines in Nawabganj as high as −250 mm/y in pockets where specific yield is low. Current groundwater use is likely to be unsustainable in such pockets.

While pockets of significant over-exploitation exist, simulation analysis shows that increased pumping does not cause long-term groundwater storage depletion consistently in all areas within the northwest. In areas where the maximum recharge potential is achieved, pumping could directly result in groundwater mining and storage loss. This could be true in areas, especially in the Barind tract, within the districts of Nawabganj, Naogaon and Rajshahi where long-term storage depletion is relatively high.

Modelling of groundwater levels using MIKE SHE models indicated that increased future groundwater use for Boro rice cultivation could cause deepening of water table in the summer months, beyond the suction limit resulting in groundwater access problems. However, that is not necessarily indicative of unsustainable use as water table would recover in such areas by recharge from the monsoon rains. But simulations do indicate that such extensive use of groundwater in drought-like conditions could result in groundwater mining.

Pumping management and conjunctive management strategies could be adopted for more sustainable management. Replacing groundwater use with surface water where possible can decrease the long-term storage depletion. Modelling analysis showed that increased pumping could potentially increase recharge from the rivers in many districts. Such responses indicate potential for conjunctive management.

Appendix A MIKE SHE MODELLING APPROACH

A.1 TECHNICAL BACKGROUND OF INTEGRATED MIKE SHE-MIKE 11 MODELLING

Natural hydrologic systems as well hydrologic problems are very complex. It is found that the integrated MIKE 11-MIKE SHE includes the entire complex processes in the land phase of the hydrologic cycle:

- Precipitation (rain or snow)
- Evapotranspiration, including canopy interception
- Overland sheet flow
- Channel flow
- Unsaturated sub-surface flow
- Saturated groundwater flow

The selected MIKE SHE-MIKE 11 is a physically-based, spatially-distributed, finite difference, integrated surface water and groundwater model. The detail description of the various module of MIKE SHE and the equation used in the MIKE SHE model is describe in the following section.

A.1.1 CHANNEL AND OVERLAND FLOWS

MIKE SHE, coupled with MIKE 11, is capable of modelling open channel flow using the kinematic wave, diffusive wave, and dynamic wave approximation. MIKE 11 supports any level of complexity and offers simulation engines that cover the entire range from simple Muskingum routing to the higher order dynamic wave formulation of the Saint-Venant equations. MIKE 11 can simulate a full range of structures (dams, weirs, culverts, gates, etc) in its solution domain.

When the net rainfall rate exceeds the infiltration capacity of the soil, water is ponded on the ground surface. This water is available as surface runoff/overland flow, to be routed down-gradient towards the river system.

Overland flow is simulated using the diffusive wave approximation and special provisions are available in MIKE SHE for flow routing between the overland flow plane and channels that depend on channel bank geometry and user selected flooding options. Using rectangular coordinates in horizontal plane, the conservation of mass is given by

$$\frac{\partial h}{\partial t} + \frac{\partial}{\partial x}(uh) + \frac{\partial}{\partial y}(vh) = i \qquad (1)$$

and the momentum equations are given by

$$S_{fx} = S_{ox} - \frac{\partial h}{\partial x} - \frac{u}{g}\frac{\partial u}{\partial x} - \frac{1}{g}\frac{\partial u}{\partial t} - \frac{qu}{gh} \qquad (2a)$$

$$S_{fy} = S_{oy} - \frac{\partial h}{\partial y} - \frac{v}{g}\frac{\partial v}{\partial y} - \frac{1}{g}\frac{\partial v}{\partial t} - \frac{qy}{gh} \qquad (2b)$$

where, $h(x, y)$ is the flow depth; $u(x, y)$ and $v(x, y)$ are the flow velocities in *x*- and *y*-directions, respectively; $i(x, y)$ is the net input into overland flow (net rainfall less infiltration); S_{fx} and S_{fy} are the friction slopes in the *x*- and *y*-directions, respectively; S_{ox} and S_{oy} are the slope of the ground surface in x- and y-directions, respectively; g is the gravitational constant; q is the discharge per unit width. Equations (1), (2a) and (2b) are known as St. Venant equations and when solved yield a fully dynamic description of shallow (two-dimensional) free surface flow. If we drop the last three terms of the momentum equations, we are ignoring momentum losses due to local and convective accelerations and lateral inflows, the remaining terms of the equations constitute the diffusive wave approximation. If the depth of flow does not vary significantly between adjacent cells, the fourth term may be dropped further, the resulting equations are called kinematic wave approximation.

Overland flow is simulated using the diffusive wave approximation and special provisions are available in MIKE SHE for flow routing between the overland flow plane and channels that depend on channel bank geometry and user selected flooding options.

In MIKE SHE, a river is typically considered to be a line located between model grid cells. The river-aquifer exchange is calculated from both sides of the river, depending on the head gradient. This is valid if the river width is small relative to the model cells. Otherwise, an area-inundation flooding approach is to be adopted. Thus, during low flow conditions, when the river is narrow (less than one grid size) and water flow is confined to the main river channel, the river-aquifer exchange method is adopted. If the area-inundation option is used, MIKE SHE calculates distributed surface water stages by comparing the simulated MIKE 11 water level with topographic elevations. In this case, surface water is treated as normal ponded water, which implies that surface water exchange can take place through the normal unsaturated zone infiltration, otherwise, through the normal overland-saturated zone exchange.

A.1.2 UNSATURATED FLOW, RAINFALL AND EVAPOTRANSPIRATION

MIKE SHE utilizes three methods to simulate flow in the unsaturated zone but assumes that flow is vertical in all three methods. The basis for this assumption is that the flow is primarily vertical at the scale typically simulated with MIKE SHE (catchment scale).

Once infiltrated water enters the surficial aquifer, the 3D ground water equations take over. Two of the available unsaturated zone methods in MIKE SHE are: the full Richard's equation and a simplified Richard's equation that neglects capillary tension.

The full and simplified Richard's equation methods use real soil properties and soil moisture-relationships that can be developed using Brooks and Corey or Van Genuchten relationships. The third method, which is a simplified wetland module, useful for areas with a shallow groundwater table, uses a linear relationship between depth to the water table and average soil moisture content and a linear infiltration equation.

The driving force for transport of water in the unsaturated zone is $h = z + \psi$ where, h is the hydraulic head, ψ is the pressure head (–ve in unsaturated zone), and z is the position head with respect to datum (+ve downward).

The volumetric flux is then obtained from Darcy's law:

$$q = - K(\psi) \frac{\partial h}{\partial z} \qquad (3)$$

Where, $K(\psi)$ is the unsaturated hydraulic conductivity. Assuming that the soil matrix is incompressible and the soil water has a constant density, the one-dimensional continuity equation yields the tension-based Richards equation as follows:

$$\frac{\partial}{\partial z}\left[K(\psi)\left(\frac{\partial \psi}{\partial z}+1\right)\right]=C(\psi)\frac{\partial \psi}{\partial t}+R(z) \quad (4)$$

Where, $C(\psi)$ ($=\partial q/\partial \psi$) is the soil water capacity obtained from the slope of the soil moisture retention curve; $R(z)$ is the root extraction sink term.

Solution of the above Richards equation requires the knowledge of the characteristics curves $K(\psi)$ and $C(\psi)$ or $\theta(\psi)$. The root extraction term when integrated over the entire root zone depth equals the total actual evapotranspiration. Direct evaporation from the soil is calculated only for the first node below the ground surface.

As unsaturated zone extends from the ground surface to the water table, the vertical flow is determined by the boundary conditions at each end of the grid column. The upper boundary condition is either a constant flux condition (Neuman) within each time step determined by rainfall rate on the ground surface, or, a constant head condition (Dirichlet) within each time step determined by level of ponded water on the ground surface; these conditions switch between them depending on infiltration capacity and rainfall rate. The lower boundary, on the other hand, in most cases is a pressure boundary determined by water table elevation. The initial conditions for ψ are generated by MIKE SHE assuming an equilibrium soil moisture/pressure profile with no-flow. The equilibrium profile is calculated assuming zero pressure at the water table and decreasing linearly in the unsaturated zone up to ψFC (ψ field capacity) and then remains constant for all nodes above that point. The assumption is that the flow is almost zero at moisture contents below field capacity. The method assumes that the soil profile is divided into discrete computational nodes; as a general guideline, one should choose a finer spatial resolution in the top nodes and coarser resolution in the bottom nodes.

Interception and evapotranspiration can be simulated in combination with the full or simplified Richard's equation unsaturated zone modules using an empirical evapotranspiration module (Kristensen and Jensen, 1975). If the wetland unsaturated zone module is used, evaporation is determined using a top-down approach (interception storage, detention storage, unsaturated zone, and groundwater) until potential evaporation is satisfied, if possible, or water levels are below a specified seasonally- and spatially-varying evapotranspiration extinction depth.

A.1.3 SATURATED FLOW

MIKE SHE includes a 3D saturated zone model in a heterogeneous aquifer with shifting conditions between unconfined and confined conditions. The spatial and temporal variations of the dependent hydraulic head are described mathematically by the non-linear Boussinesq equation. The geology is described in terms of layers or lenses with attached hydraulic properties. Properties can be specified either on a cell-by-cell basis or by property zones defined by polygons or grid-code files. MIKE SHE allows grid-independent geology specification, which allows changing the horizontal or vertical mesh quickly.

The governing flow equation for three-dimensional saturated flow is:

$$\frac{\partial}{\partial x}\left(K_x\frac{\partial h}{\partial x}\right)+\frac{\partial}{\partial y}\left(K_y\frac{\partial h}{\partial y}\right)+\frac{\partial}{\partial z}\left(K_z\frac{\partial h}{\partial z}\right)=S_s\frac{\partial h}{\partial t}+Q \quad (5)$$

where, K_x, K_y, and K_z are the hydraulic conductivities along the x, y and z axes assumed parallel to the principal directions of anisotropy of the domain; Q is the source/sink term; S_s is the specific storage coefficient stitches between confined and unconfined conditions of the aquifer.

Boundary conditions are specified for each computational layer. MIKE SHE supports traditional groundwater boundary conditions and offers large flexibility in terms of spatial and temporal variation of boundary conditions. Boundary conditions may be specified on a cell-by-cell basis, but typically it is more convenient to attach boundary conditions to geometric features such as polygons (lakes), lines (rivers) or points (pumps, injections, drains). A lake could, for instance, be a polygon with an attached water level time series and leakage coefficient. Similar to the meteorological time-series data, boundary time-series data may be specified in separate time-series files that include different and non-equidistant time steps. MIKE SHE automatically synchronizes all time-series data thus, eliminating tedious time-series pre-processing. Simulation time steps and stress periods may be specified independent of input time series.

The MIKE SHE allows for flow through drains in the soil, to simulate intermediate hydrograph response (interflow) in regional modelling. The drainage flow may also be used to simulate relatively fast surface runoff for cases where the space resolution of the individual grid squares is too large to represent small scale variations in the topography. MIKE SHE gives opportunity for routing drainage water to local depressions, rivers or model boundaries.

The overland, unsaturated, and saturated zone modules and MIKE 11 are explicitly coupled which allows the time step of each component to be determined based on the response time of the component processes. The explicit coupling allows simulations to be tailored to particular problems but requires extreme diligence to ensure that mass balance errors do not occur. Special provisions are available in MIKE SHE to adjust the time step during a simulation based on changes in input fluxes (i.e. rainfall). The rainfall time step can vary from 15 minutes to one hour to one day, and a mix of time steps is possible. Thus, one-day time steps can be used for most of the period, with a one-hour time step during critical rainfall periods.

A.1.4 SOIL DATABASE

MIKE SHE comes with a database of various soils and typical crops for different climatic regions of the world. The soil database includes a number of pedo-transfer functions that link suction, water content and hydraulic conductivity, but also allows the user to specify soil properties in a tabular format. Soil profiles are easily distributed in space using soil maps. Land-use is described in terms of vegetation types combined with impervious/semi-impervious areas. Vegetation types and impervious/semi-impervious areas may be spatially distributed using land-use maps. Crop rotation is made easy by defining a date-of-establishment and then specifying a link to the crop type in the crop database. MIKE SHE comes with a database of typical crops in different climatic regions. Users may edit the database, add vegetation types to the database or create a new database from scratch.

A.1.5 DEVELOPMENT OF A CONCEPTUAL MODEL

The first step in the procedure of modelling is the development of a conceptual model of the problem. The conceptual model consists of a set of assumptions that reduce the real problem and the real domain to simplified versions that are acceptable in view of the objectives of the modelling and of the associated management problem. The conceptual model must include the main features and driving forces of the hydrological system and be suitable for implementation in the mathematical model. The set of assumptions that represent our simplified perception of the project are:

- general hydrological skill and experience
- knowledge about the local hydrogeological system
- an analysis of available field data
- soft data such as interviews, information about special local features for instance flooding/water logging of certain areas during wet seasons, etc.

The most important aspect of the conceptual model is perhaps development of a geologic model. A geologic model is described in terms of layers, lenses and hydraulic properties. Other important aspects of the conceptual model development are:

- which river/canals to include
- how to describe the drainage networks that are not included in the river model
- identifying the boundary conditions
- determining the horizontal and vertical discretization.

Appendix B MODEL DOMAINS OF THE 4 MIKE SHE MODELS

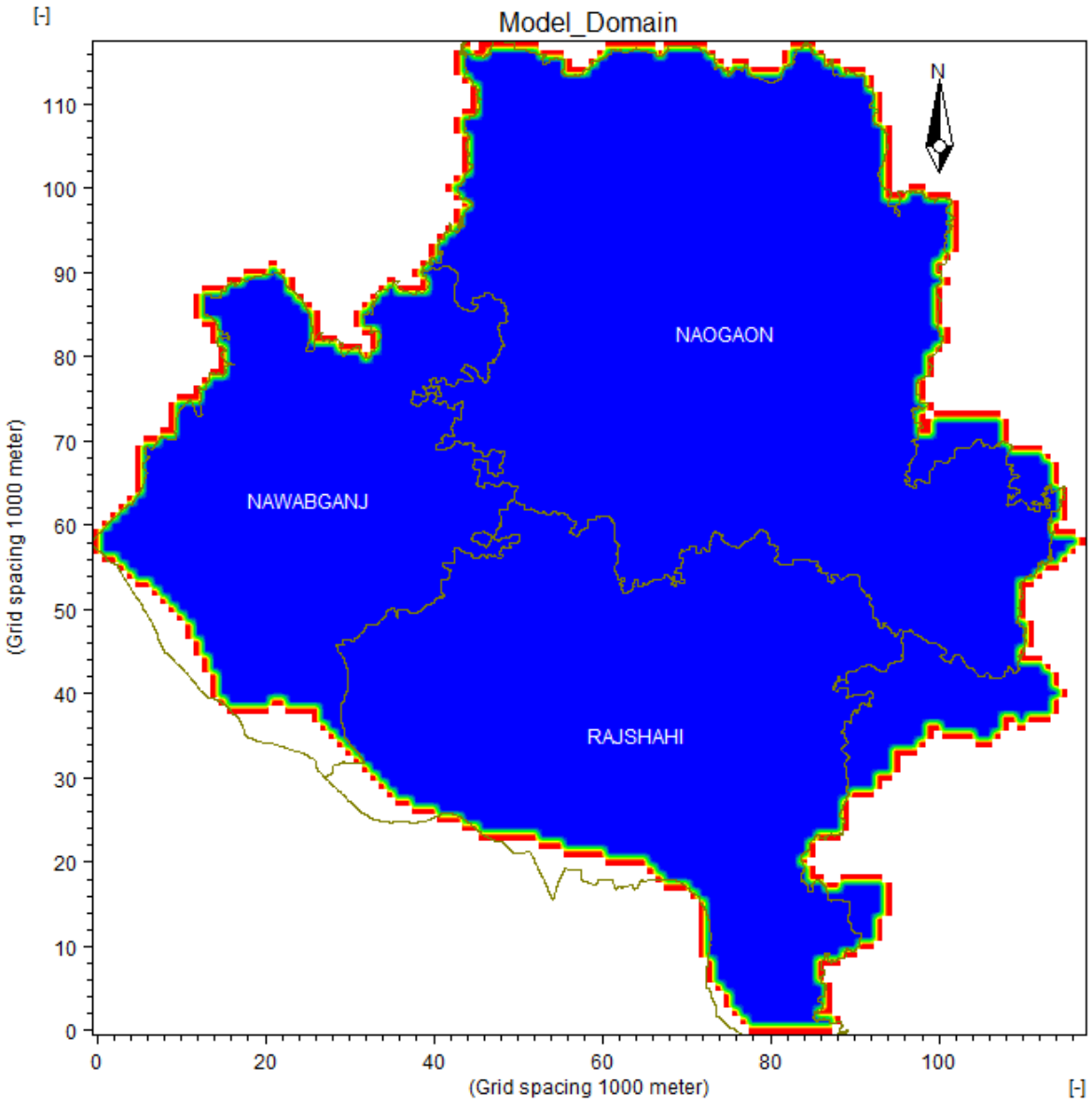

Figure B.1: Domain of the Barind model

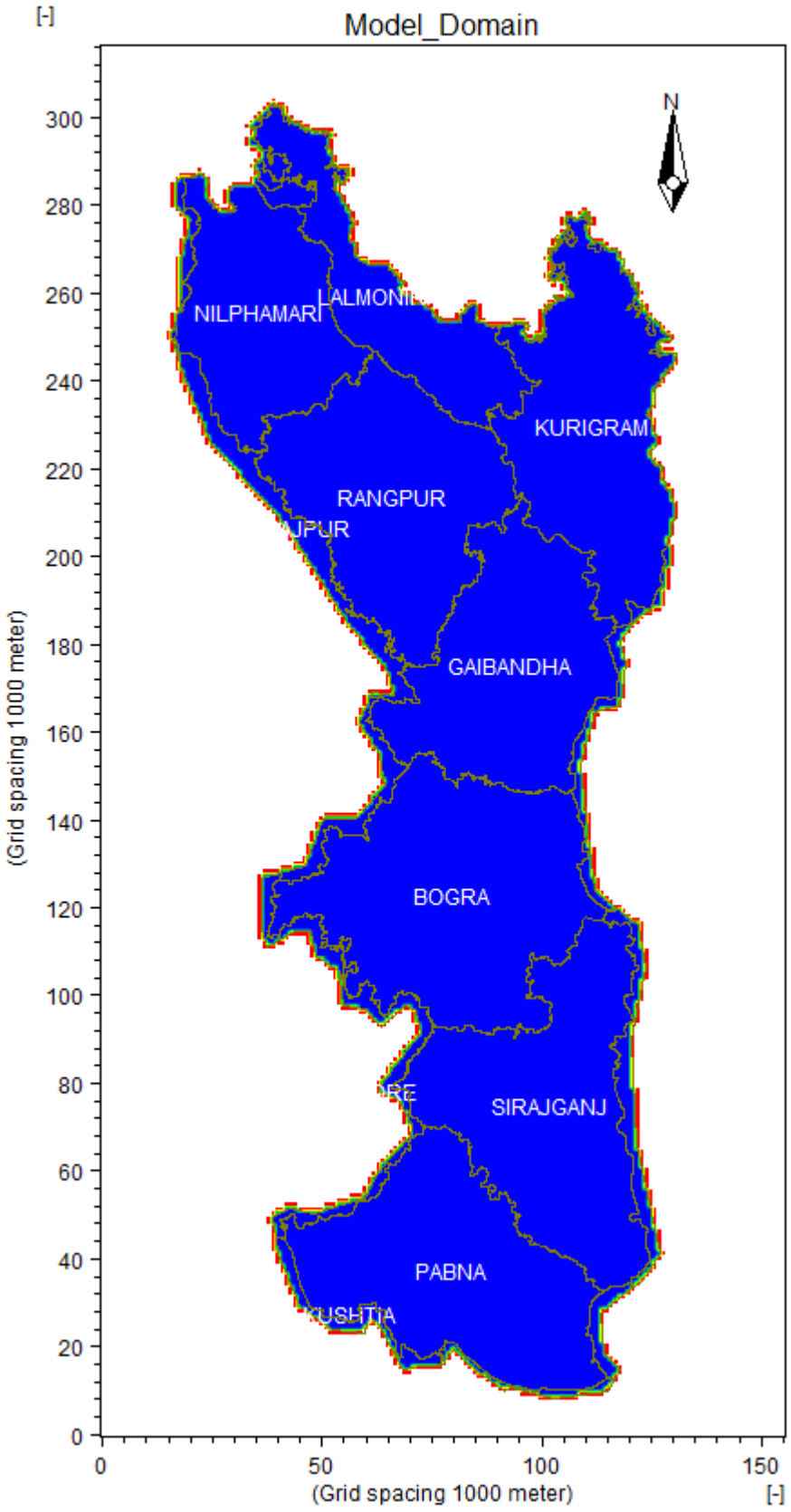

Figure B.2: Domain of the 8-district model

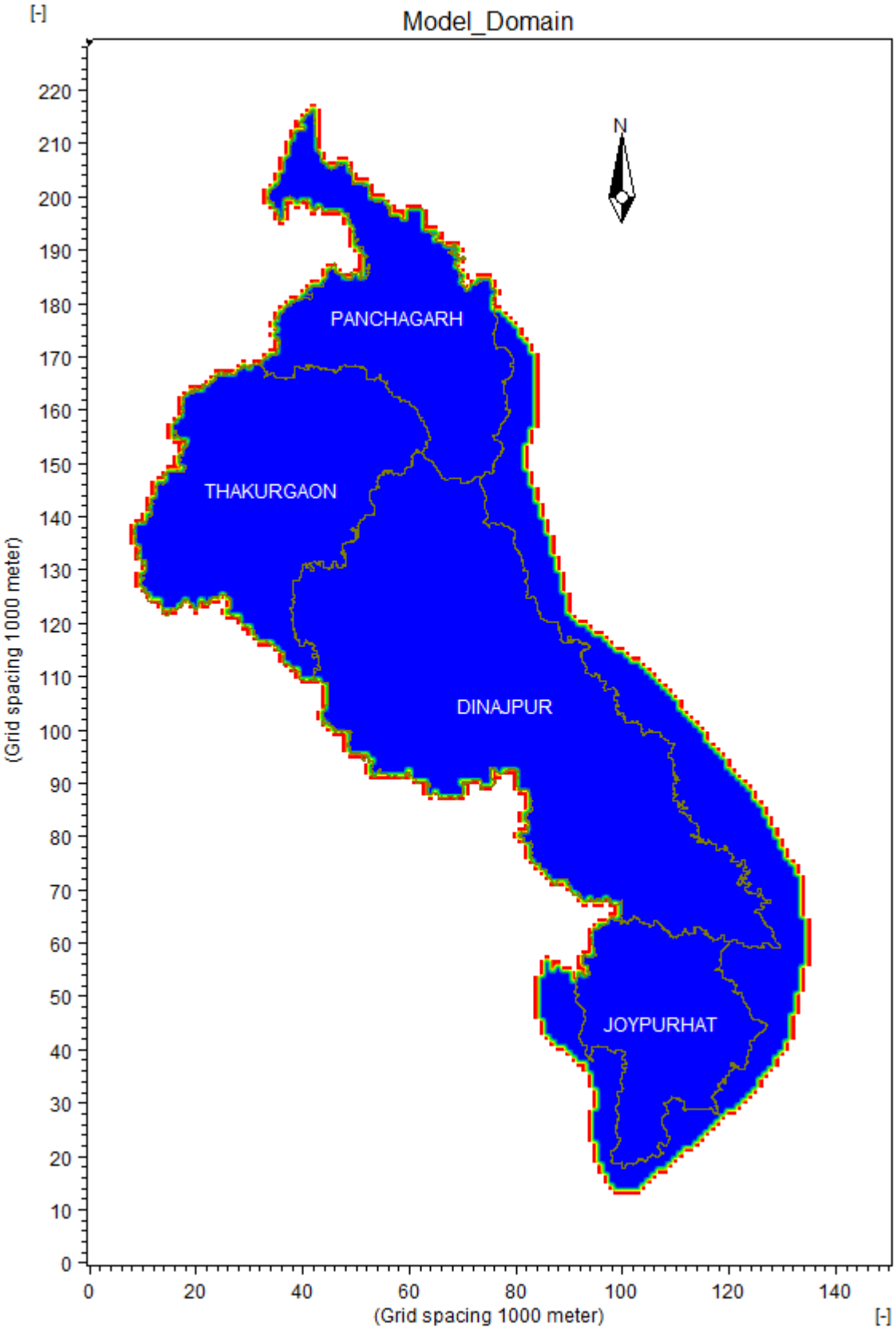

Figure B.3: Domain of the 4-district model

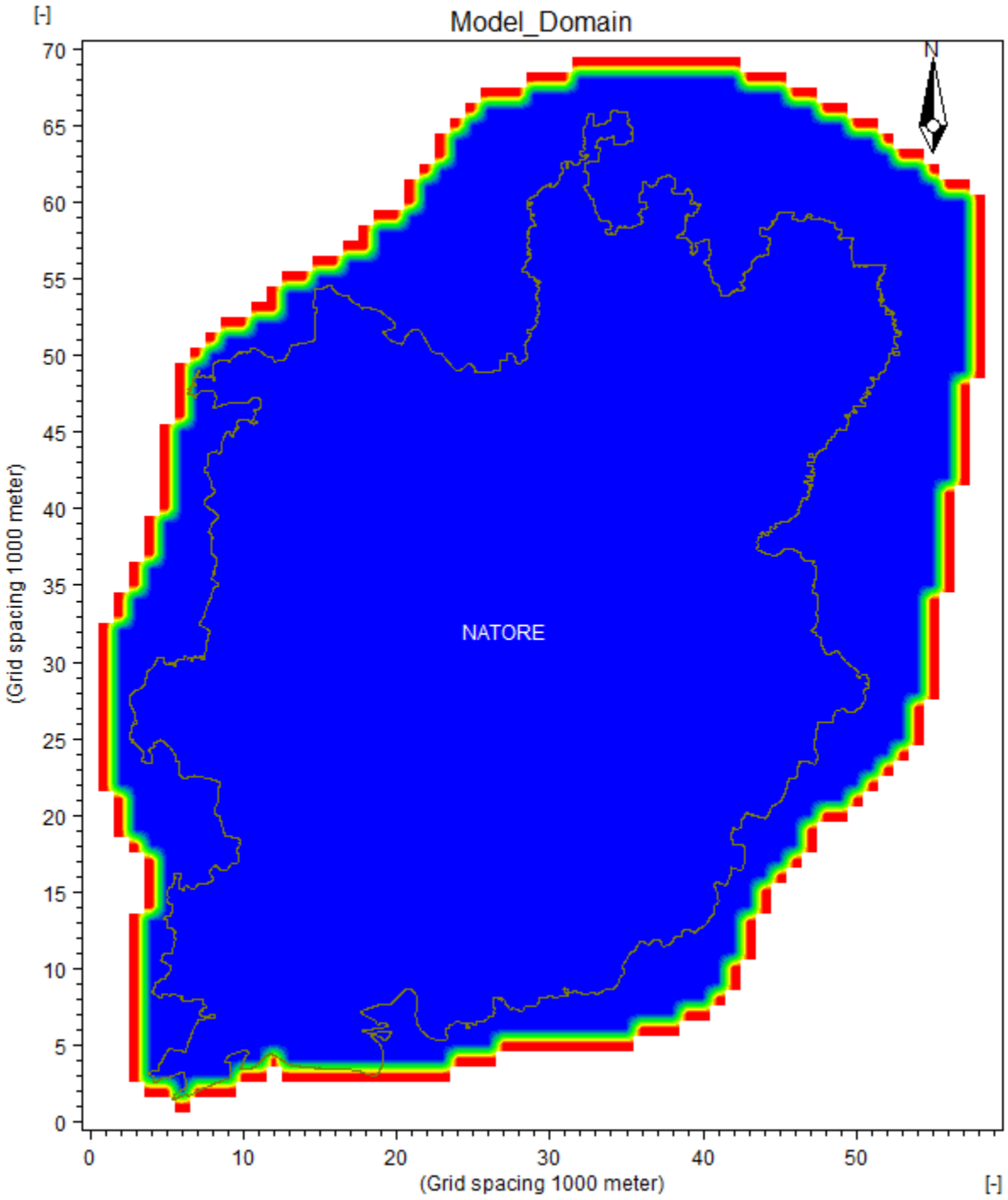

Figure B.4: Domain of the Natore model

Appendix C DIGITAL ELEVATION MODELS

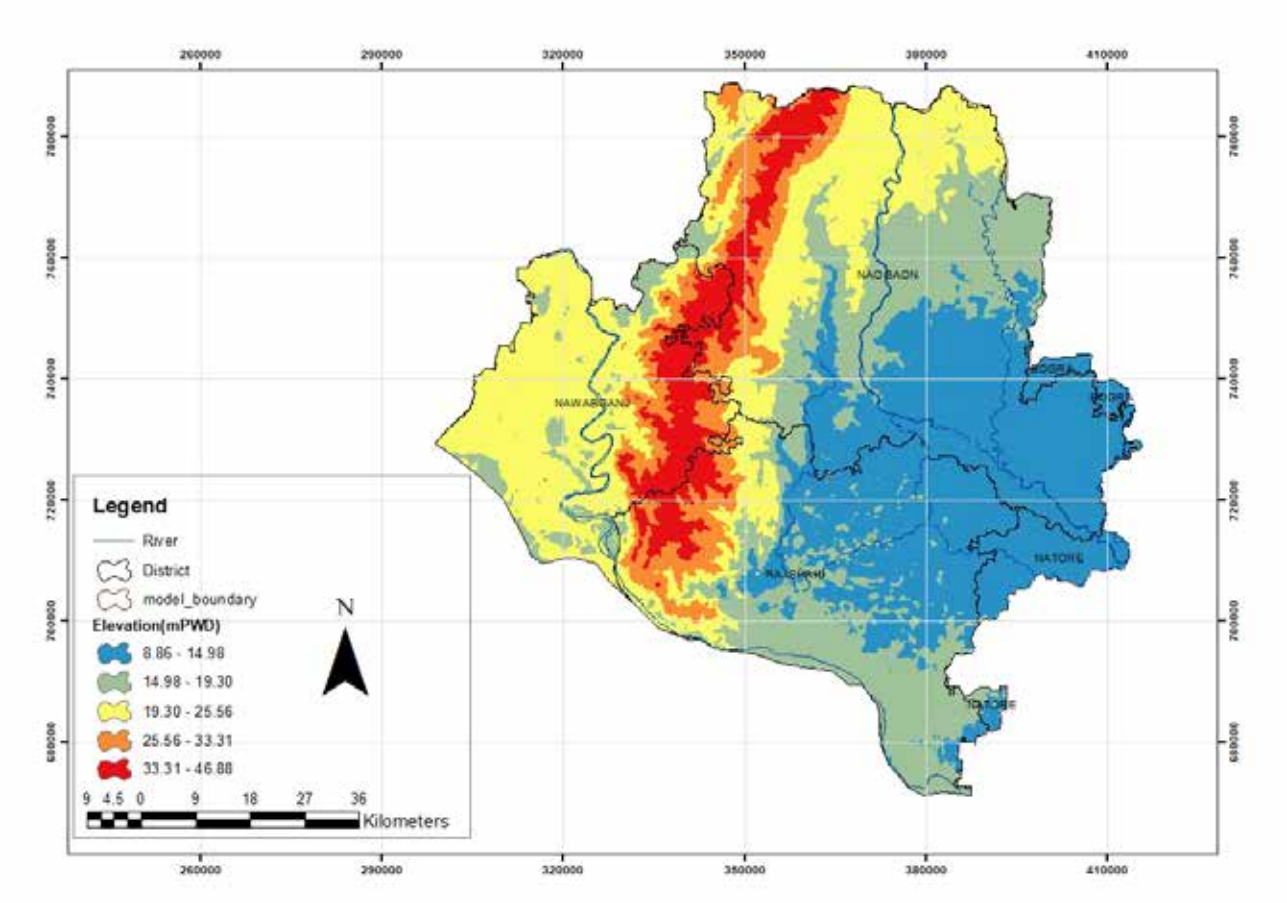

Figure C.1: Digital Elevation Model (DEM) of the Barind model area

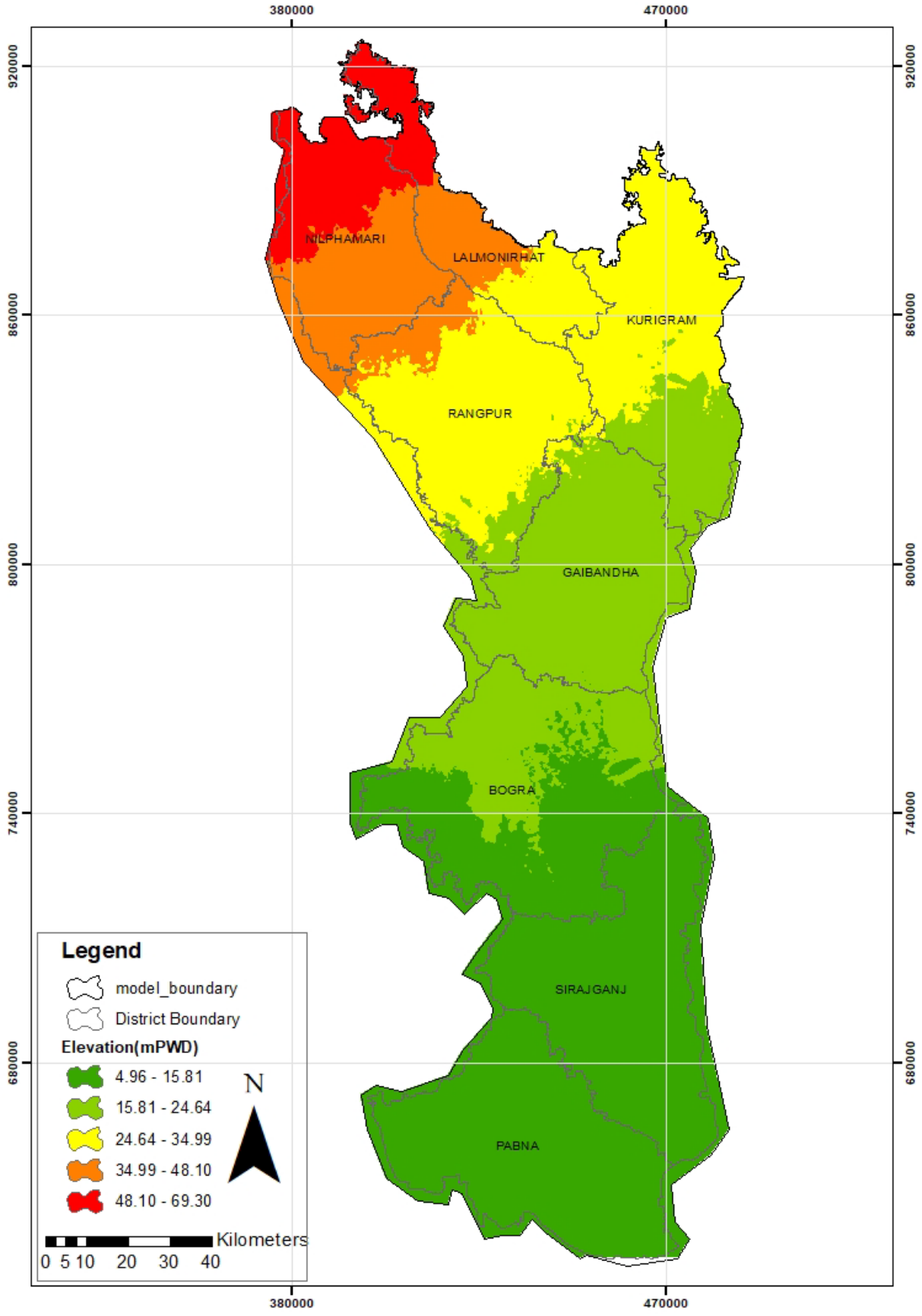

Figure C.2: Digital Elevation Model (DEM) of the 8-district model

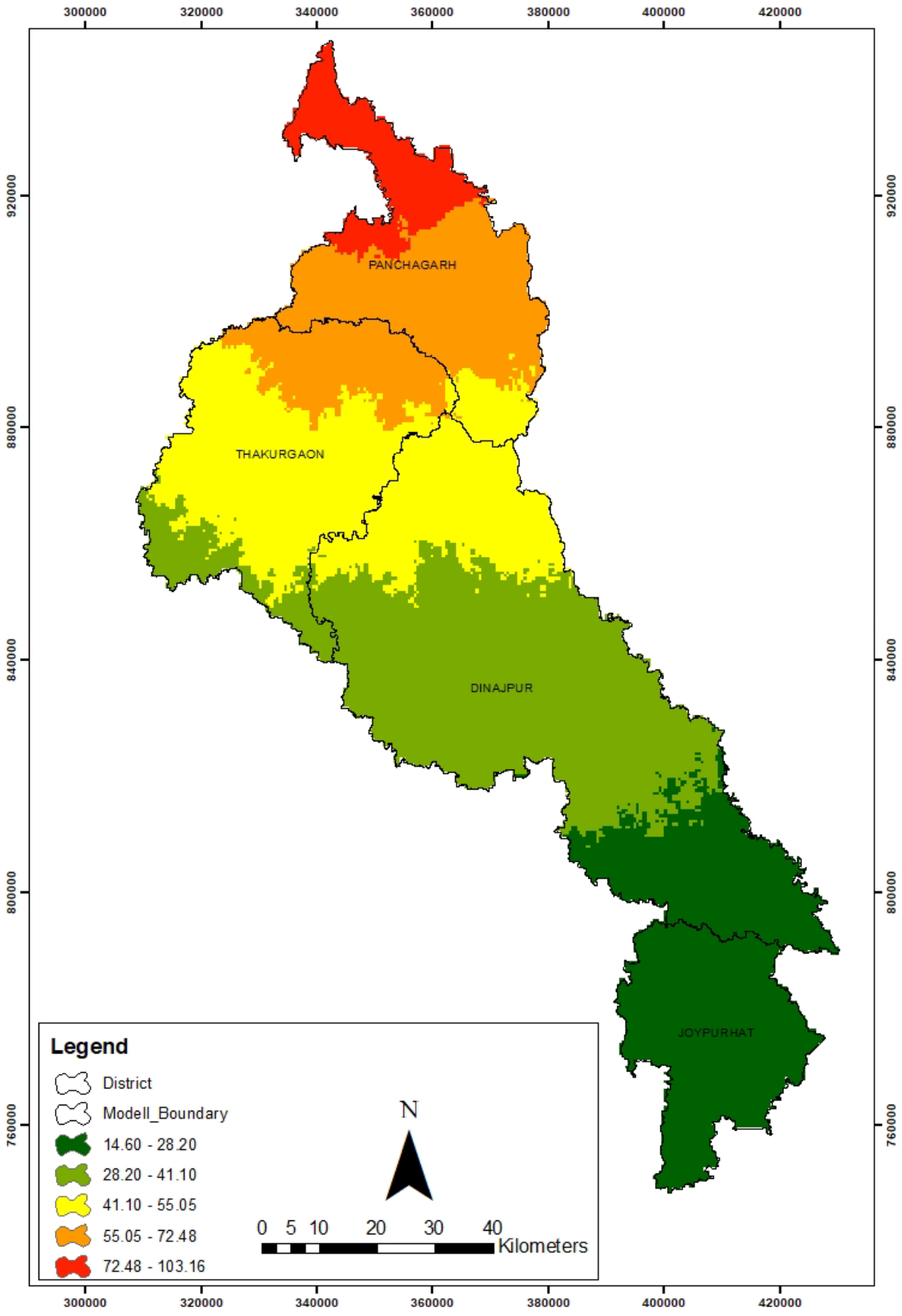

Figure C.3: Digital Elevation Model (DEM) of the 4-district model

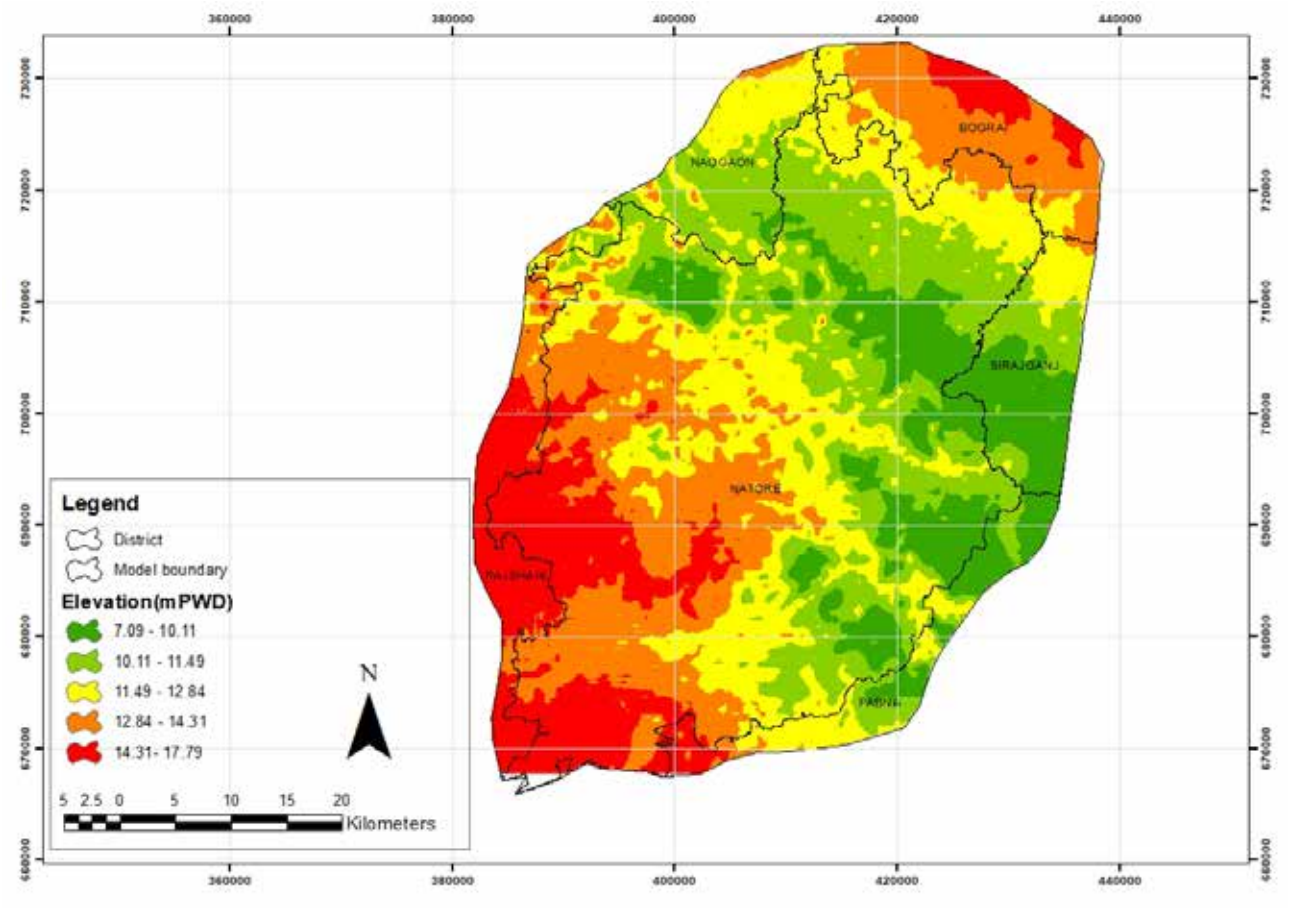

Figure C.4: Digital Elevation Model (DEM) of the Natore model

Appendix D PRECIPITATION DATA AND THIESSEN POLYGONS

Table D.1: List of rainfall stations used in the model

SL_No	Station_Name	Station_ID	Latitude	Longitude
1	Tentulia	CL220	26.56	88.38
2	Pirganj	CL203	25.38	89.35
3	Panchagarh	CL197	26.40	88.52
4	Phulbari	CL201	25.54	88.92
5	Pirgacha	CL202	25.65	89.43
6	Mahipur	CL188	25.87	89.13
7	Rangpur	CL206	25.76	89.28
8	Ruhea	CL209	26.27	88.42
9	Saidpur	CL210	25.78	88.92
10	Mithapukur	CL186	25.58	89.31
11	Sundarganj	CL218	25.55	89.53
12	Hilli (Hakimpur)	CL175	25.31	88.99
13	Thakurgaon	CL221	26.09	88.43
14	Ulipur	CL222	25.68	89.68
15	Dalia	CL226	26.16	89.02
16	Setabganj	CL213	25.84	88.46
17	Debiganj	CL166	26.14	88.68
18	Patgram	CL200	26.40	88.98
19	Badarganj	CL153	25.66	89.05
20	Bagdogra(Nilphamari)	CL154	25.96	88.96
21	Gaibandha(Bhawaniganj)	CL156	25.32	89.55
22	Bhithargarh	CL157	26.43	88.54
23	Bhurangamari	CL159	26.14	89.65
24	Boda	CL161	26.23	88.58
25	Kaunia	CL178	25.76	89.40
26	Ghoraghat	CL164	25.29	89.24
27	Lalmanirhat	CL183	25.89	89.40
28	Dimla	CL167	26.14	88.97
29	Dinajpur	CL168	25.68	88.62
30	Gobindaganj	CL171	25.12	89.40
31	Kaliganj	CL177	26.05	88.97
32	Khansama	CL179	25.94	88.69
33	Kantanagar	CL180	25.81	88.64
34	Kurigram	CL182	25.84	89.61
35	Chilmari	CL163	25.56	89.68
36	Nawabganj	CL196	25.49	89.09

SL_No	Station_Name	Station_ID	Latitude	Longitude
37	Sujanagar	CL38	23.91	89.48
38	Atghoria	CL1	24.06	89.20
39	Ullapara	CL40	24.31	89.59
40	Taras	CL39	24.44	89.37
41	Shazadpur	CL35	24.21	89.58
42	Sirajganj	CL34	24.39	89.73
43	Raiganj	CL29	24.48	89.61
44	Pabna	CL25	23.98	89.30
45	Chatmohar	CL7	24.20	89.21
46	Joari	CL16	24.31	89.27
47	Ishurdi	CL15	24.12	89.09
48	Gurudaspur	CL14	24.36	89.17
49	Faridpur Banuaripara	CL12	24.15	89.40
50	Bera	CL4	24.01	89.65
51	Manda	CL185	24.81	88.67
52	Chapai-Nawabganj	CL195	24.61	88.24
53	Nazipur (Patnitala)	CL192	25.07	88.77
54	Naogaon	CL191	24.89	88.91
55	Joypurhat	CL520	25.07	89.02
56	Dubchanchia	CL169	24.91	89.18
57	Sherpur_Bogra	CL33	24.64	89.39
58	Nandigram	CL22	24.58	89.26
59	Natore	CL23	24.38	88.96
60	Shibganj (Bogra)	CL216	24.95	89.34
61	Bogra	CL6	24.83	89.46
62	Sardah	CL212	24.29	88.78
63	Sapahar	CL211	25.09	88.60
64	Bholahat	CL158	24.90	88.22
65	Dhunot	CL11	24.71	89.55
66	Rohanpur	CL208	24.87	88.36
67	Rajshahi	CL205	24.38	88.49
68	Puthia	CL204	24.33	88.84
69	Godagari	CL172	24.45	88.38
70	Shibganj(Rajshahi)	CL215	24.68	88.19
71	Tanore	CL219	24.64	88.46
72	Sapahar	CL211	25.09	88.60
73	Nachole	CL190	24.76	88.41
74	Badalgachi	CL152	24.99	88.92
75	Mohadebpur	CL187	24.89	88.78
76	Atrai Ahsanganj	CL3	24.61	89.00
77	Nithpur	CL194	24.99	88.45

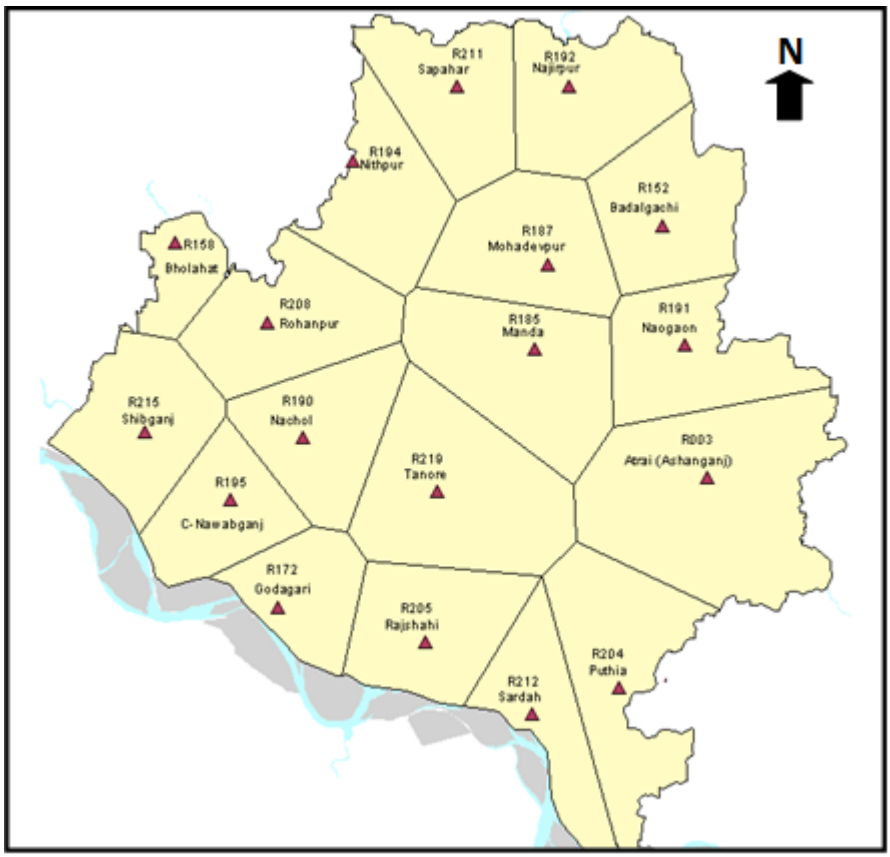

Figure D.1: Thiessen polygons for rainfall stations of the Barind model area

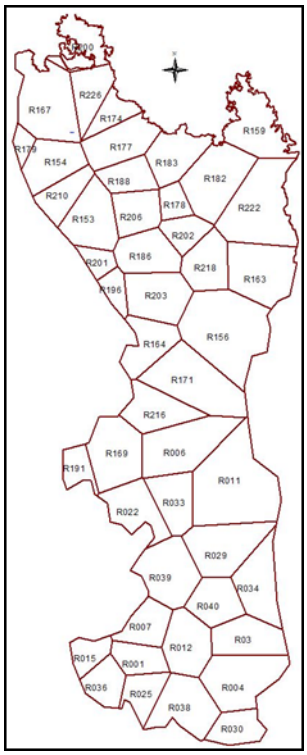

Figure D.2: Thiessen polygons for rainfall stations of the 8-district model area

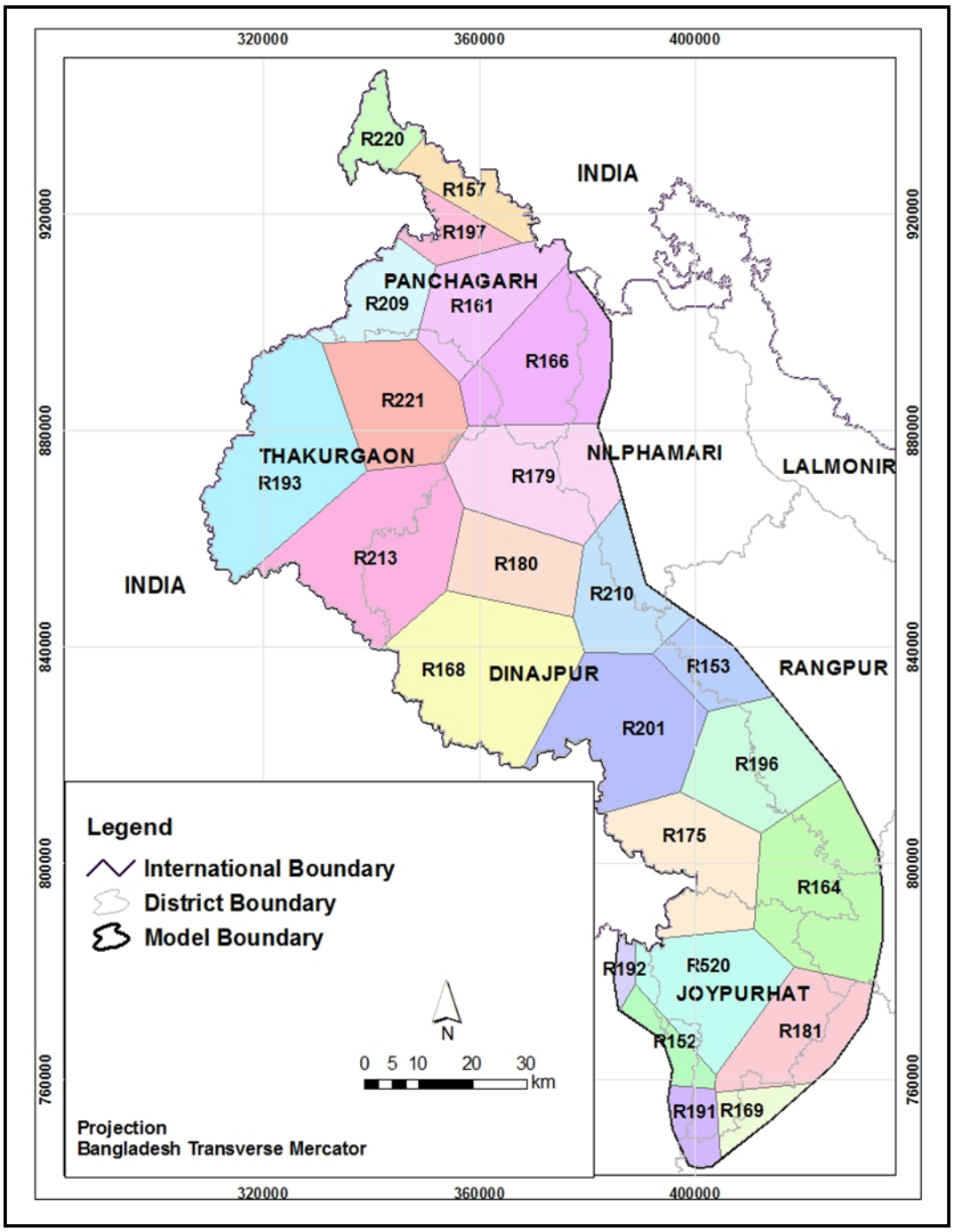

Figure D.3: Thiessen polygons for rainfall stations of the 4-district model area

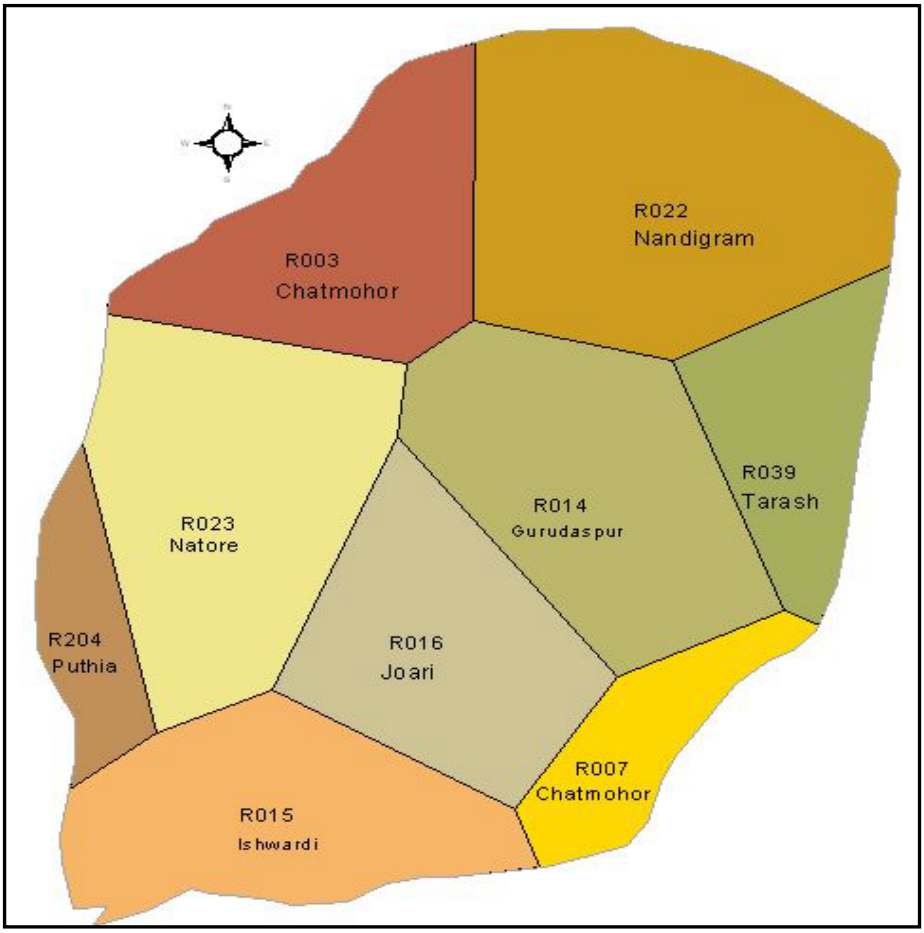

Figure D.4: Thiessen polygons for rainfall stations of the Natore model area

Appendix E HYDRO-STRATIGRAPHIC CROSS-SECTIONS

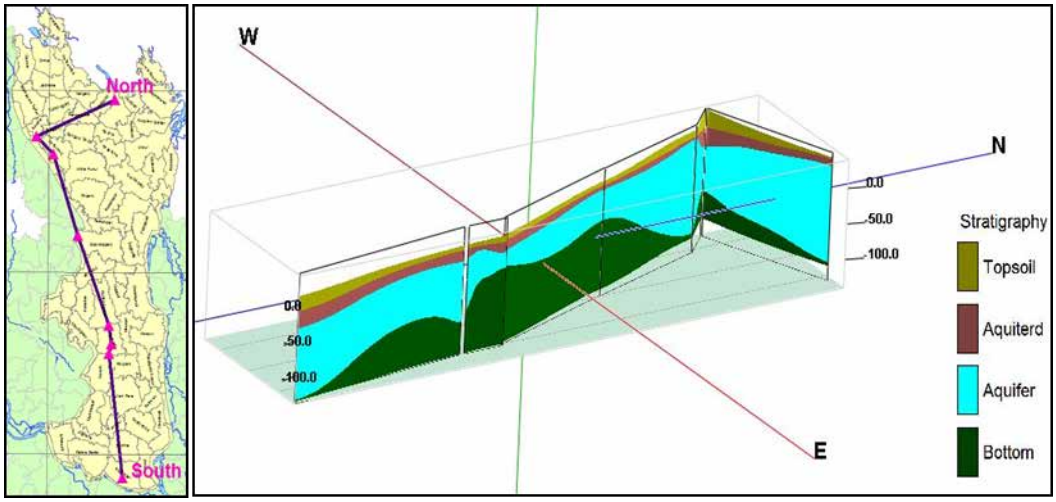

Figure E.1: Hydro-stratigraphic cross-section of the 8-district model area

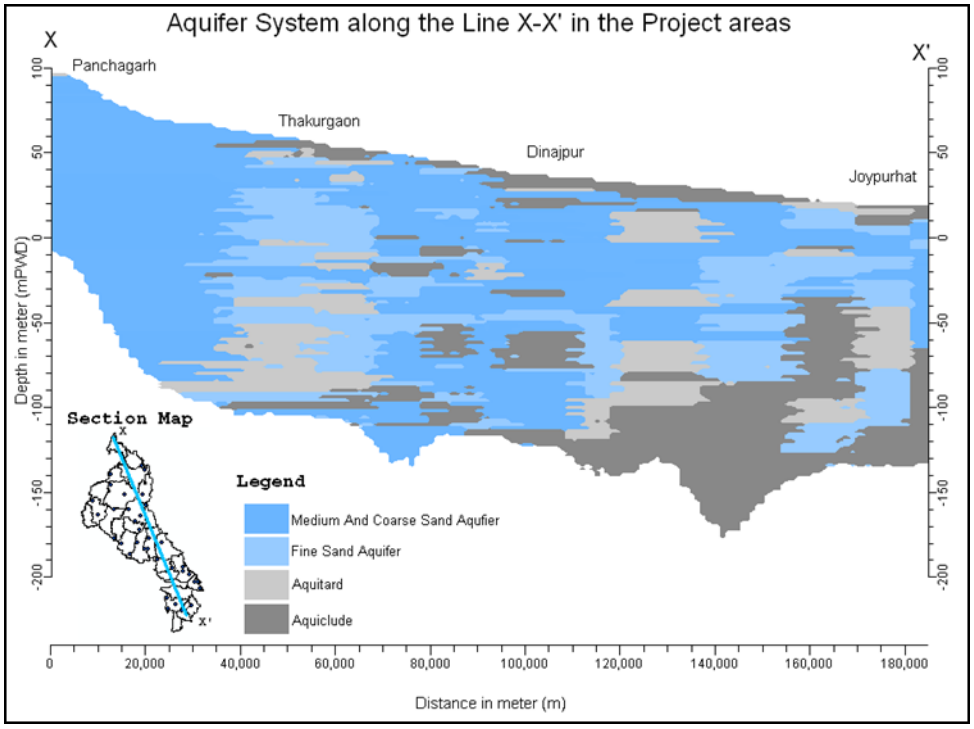

Figure E.2: Hydro-stratigraphic cross-section of the 4-district model area

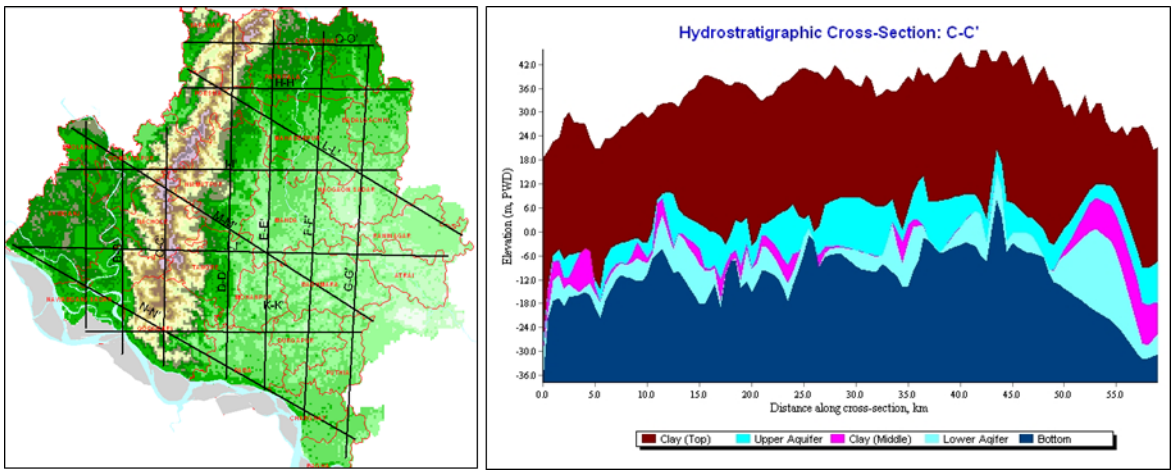

Figure E.3: Hydro-stratigraphic cross-section of the Barind model area

Appendix F INITIAL AND BOUNDARY CONDITIONS

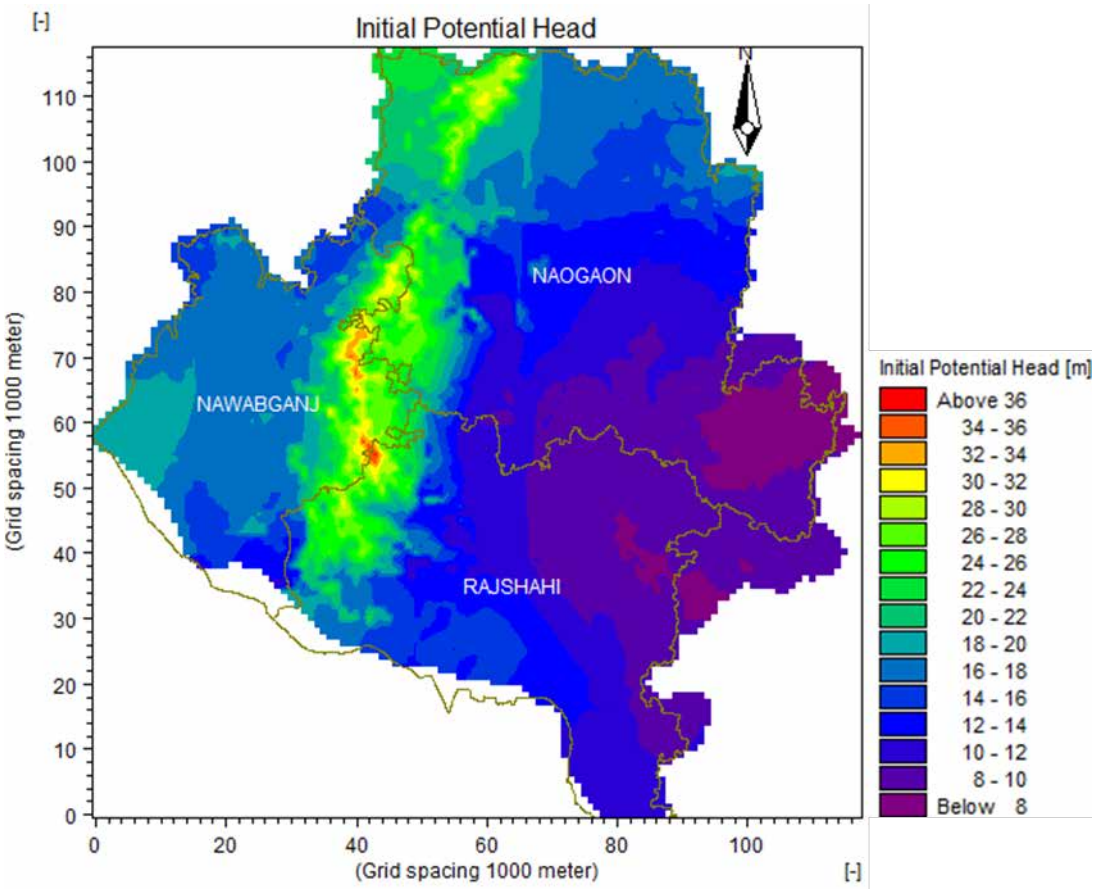

Figure F.1: Initial potential head of the Barind model area

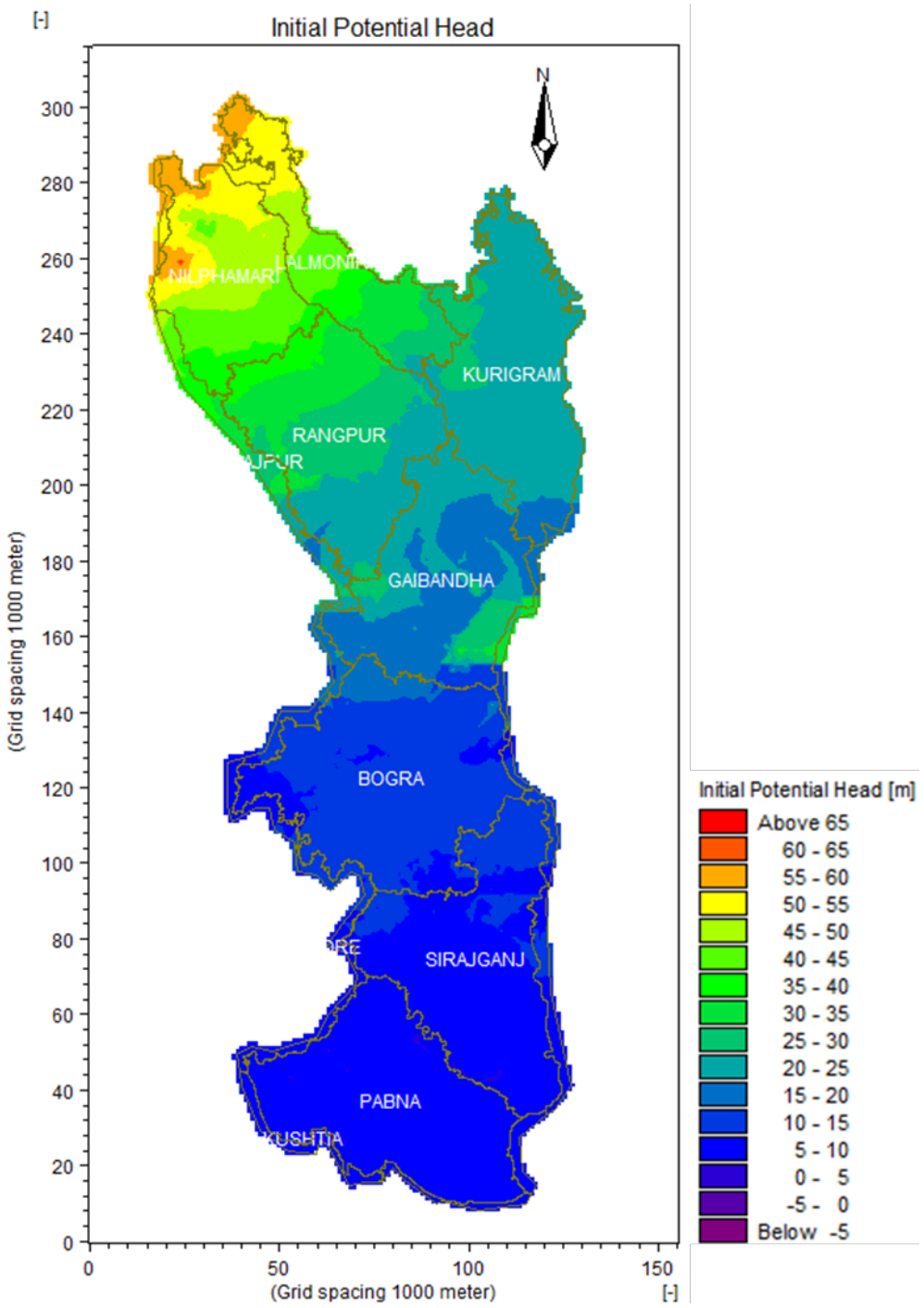

Figure F.2: Initial potential head of the 8-district model area

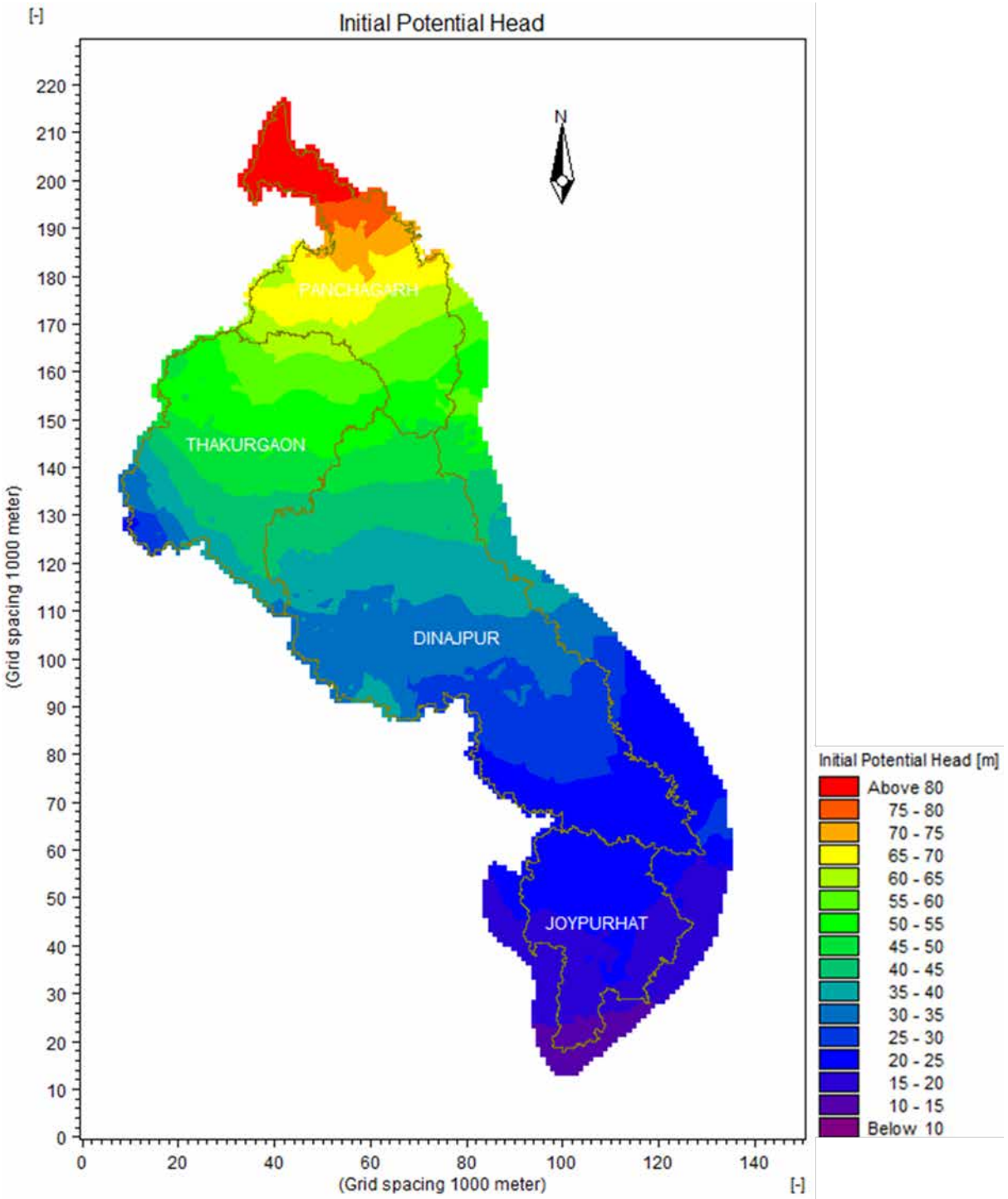

Figure F.3: Initial potential head of the 4-district model area

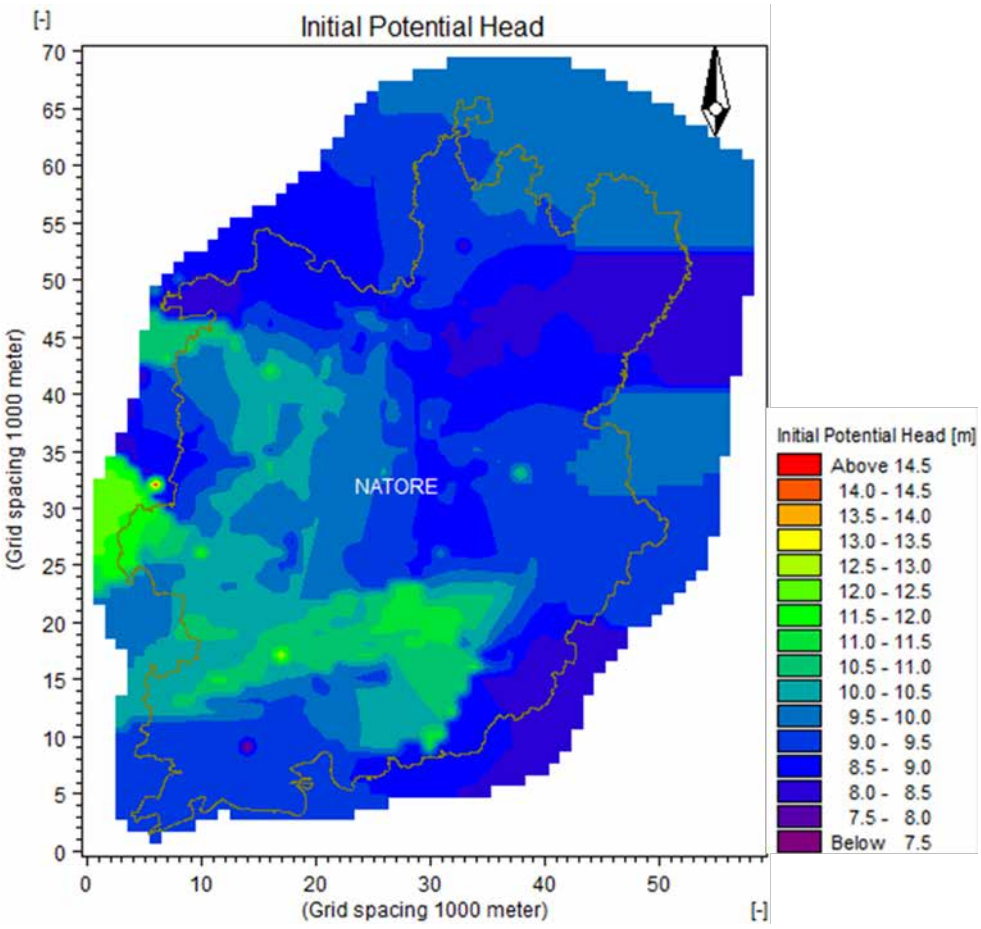

Figure F.4: Initial potential head of the Natore model area

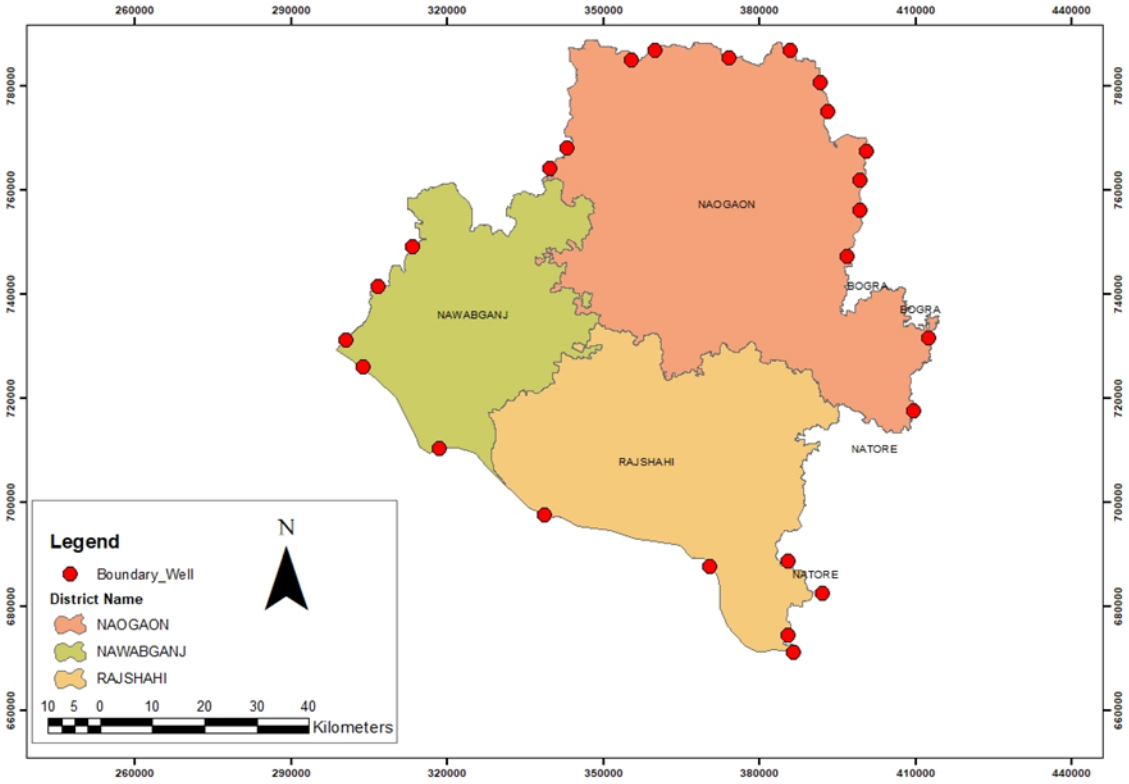

Figure F.5: Location of boundary wells of the Barind model

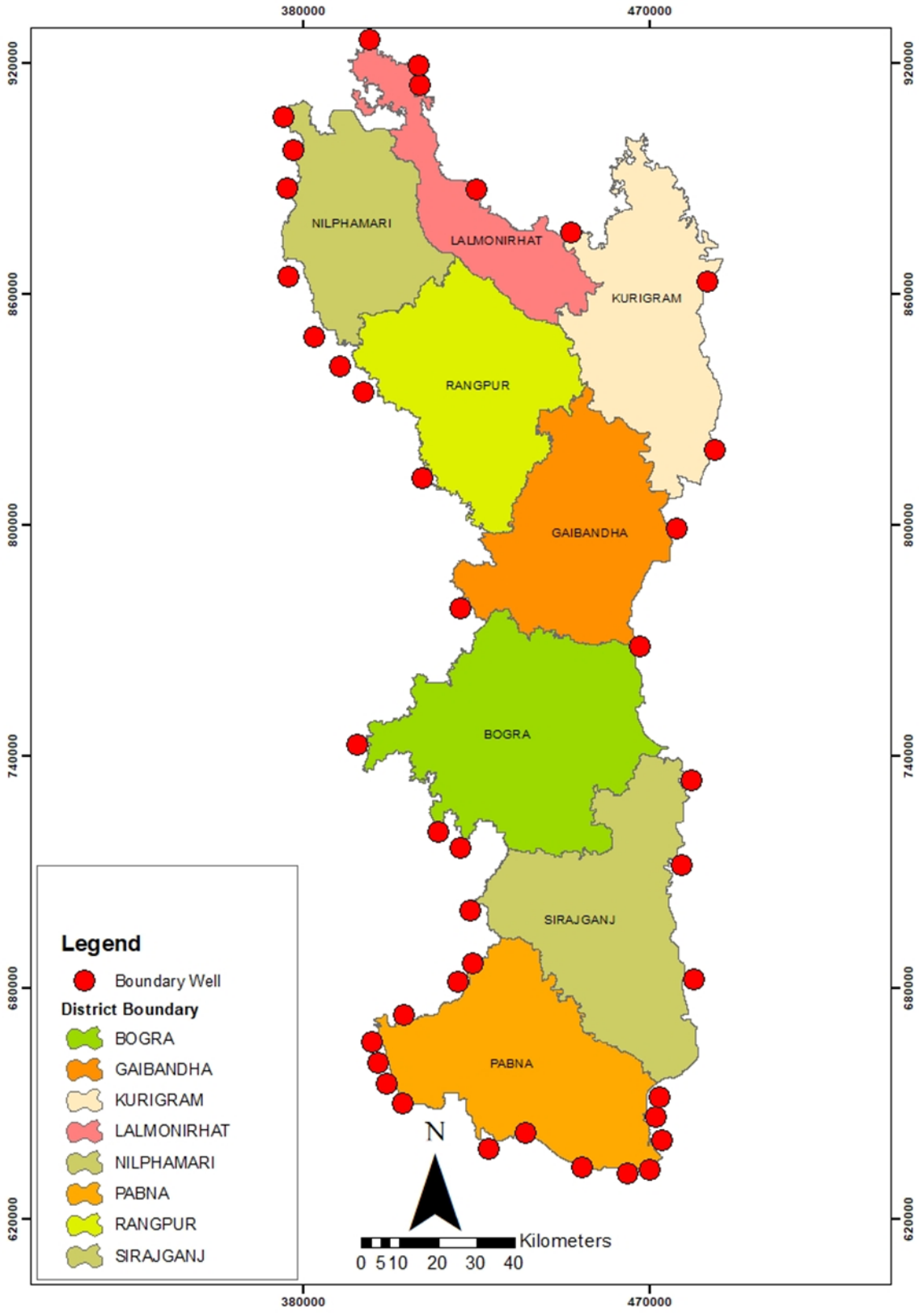

Figure F.6: Location of boundary wells of the 8-district model

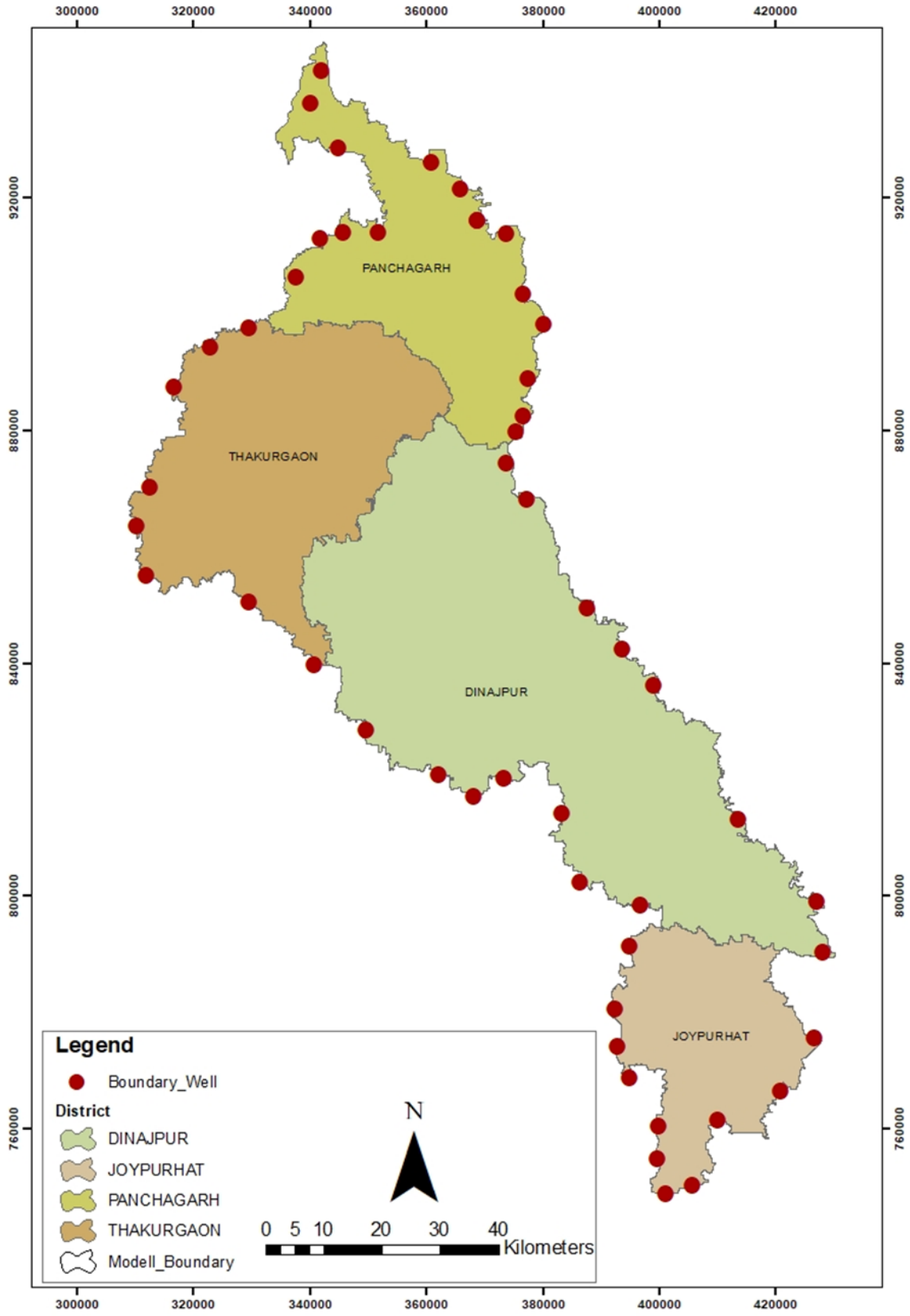

Figure F.7: Location of boundary wells of the 4-district model

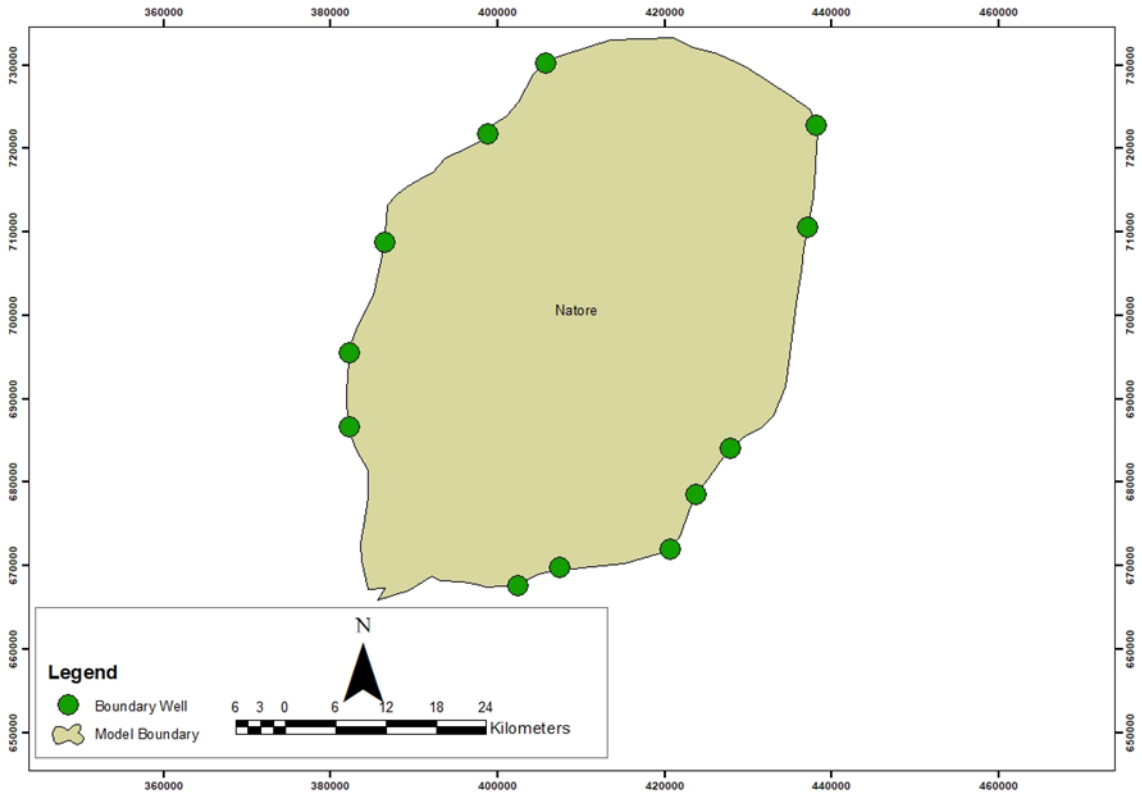

Figure F.8: Location of boundary wells of the Natore model

Appendix G OBSERVATION BORE LOCATIONS

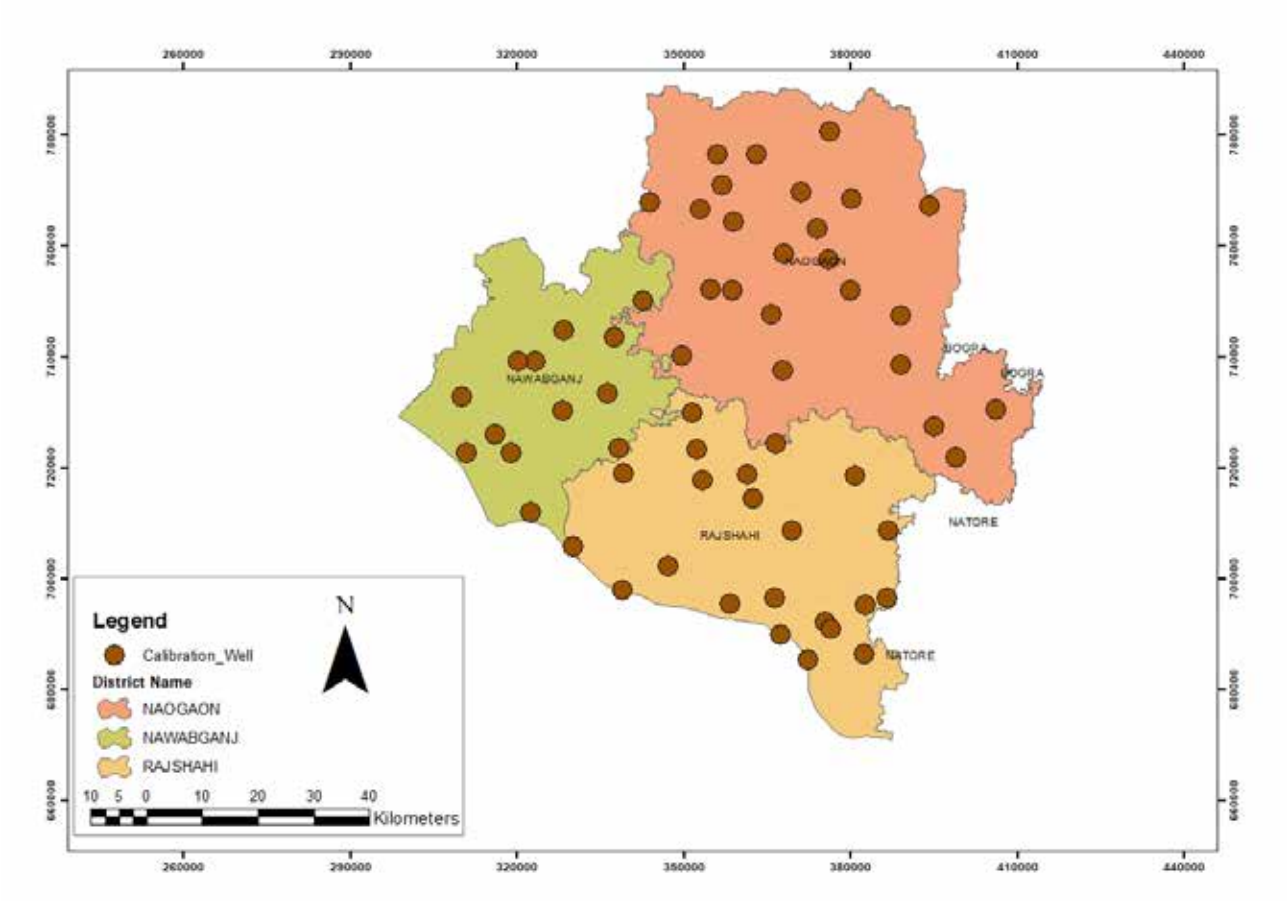

Figure G.1: Location of calibration wells of the Barind model

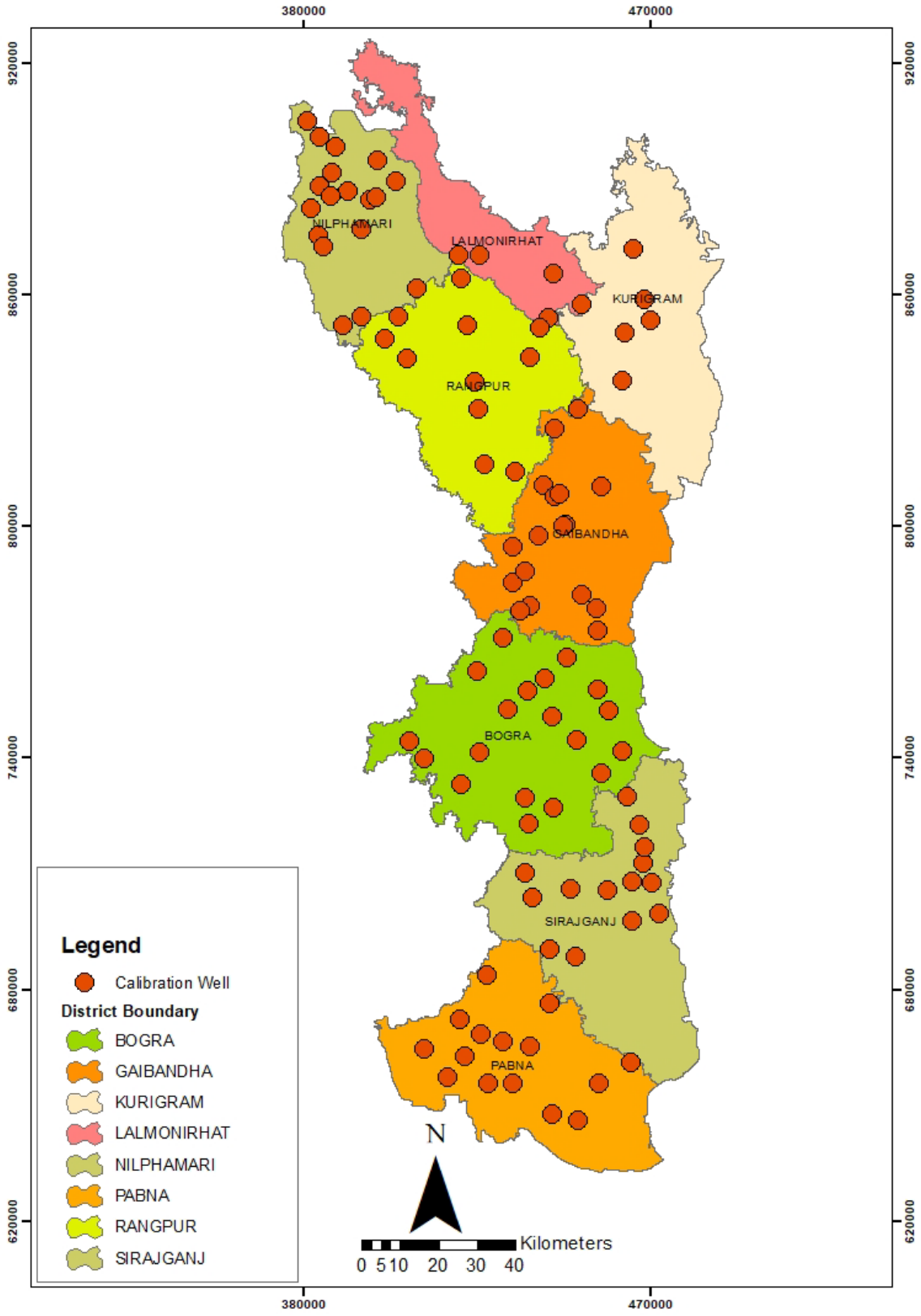

Figure G.2: Location of calibration wells of the 8-district model

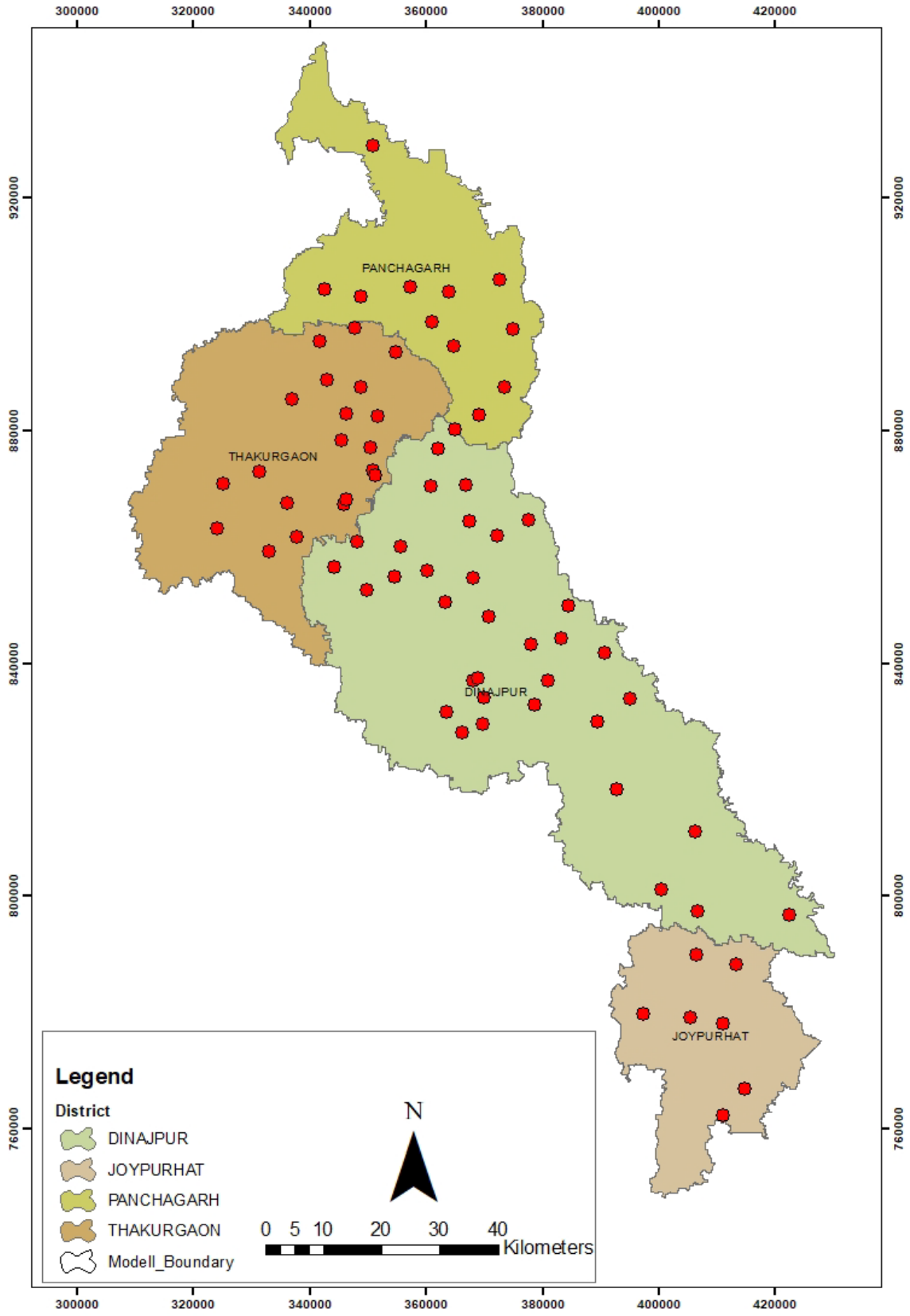

Figure G.3: Location of calibration wells of the 4-district model

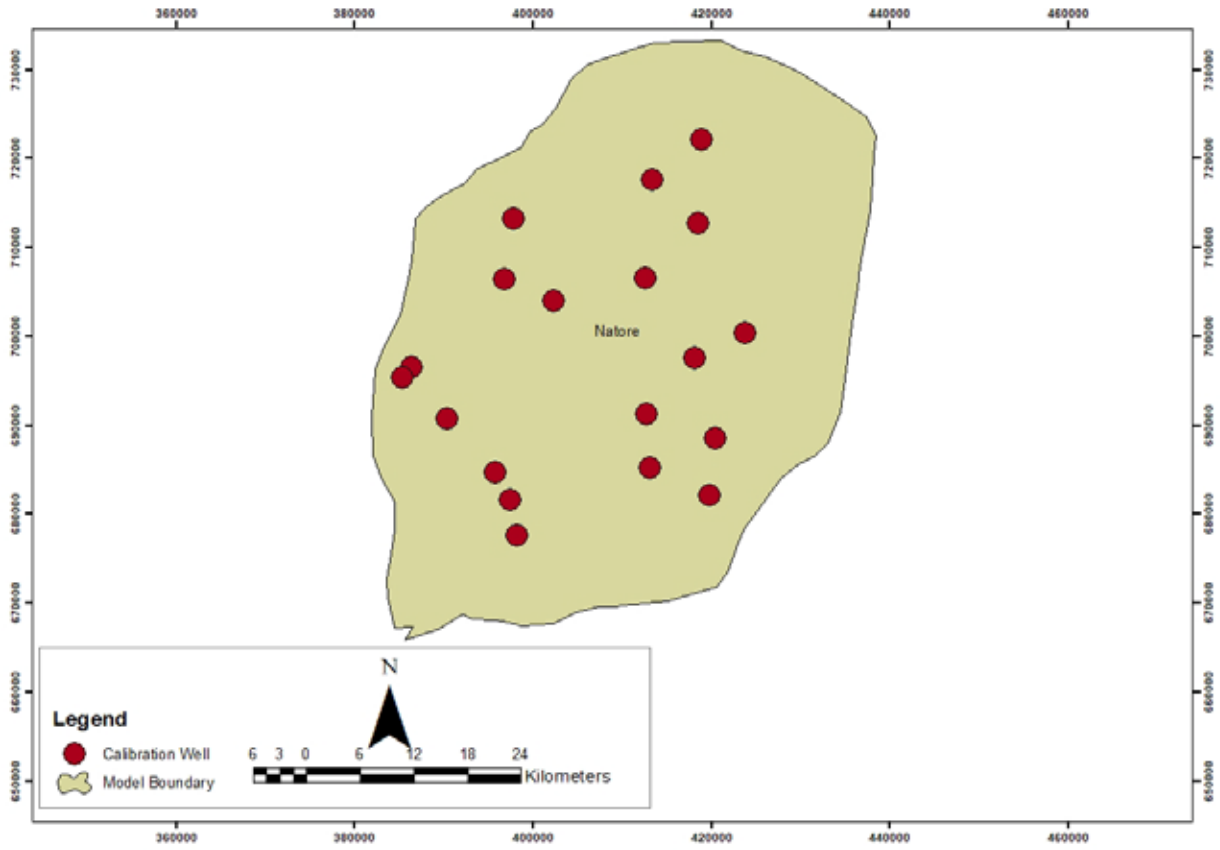

Figure G.4: Location of calibration wells of the Natore model

Appendix H CALIBRATED HYDRAULIC PROPERTIES

H.1 CALIBRATED HYDRAULIC CONDUCTIVITY

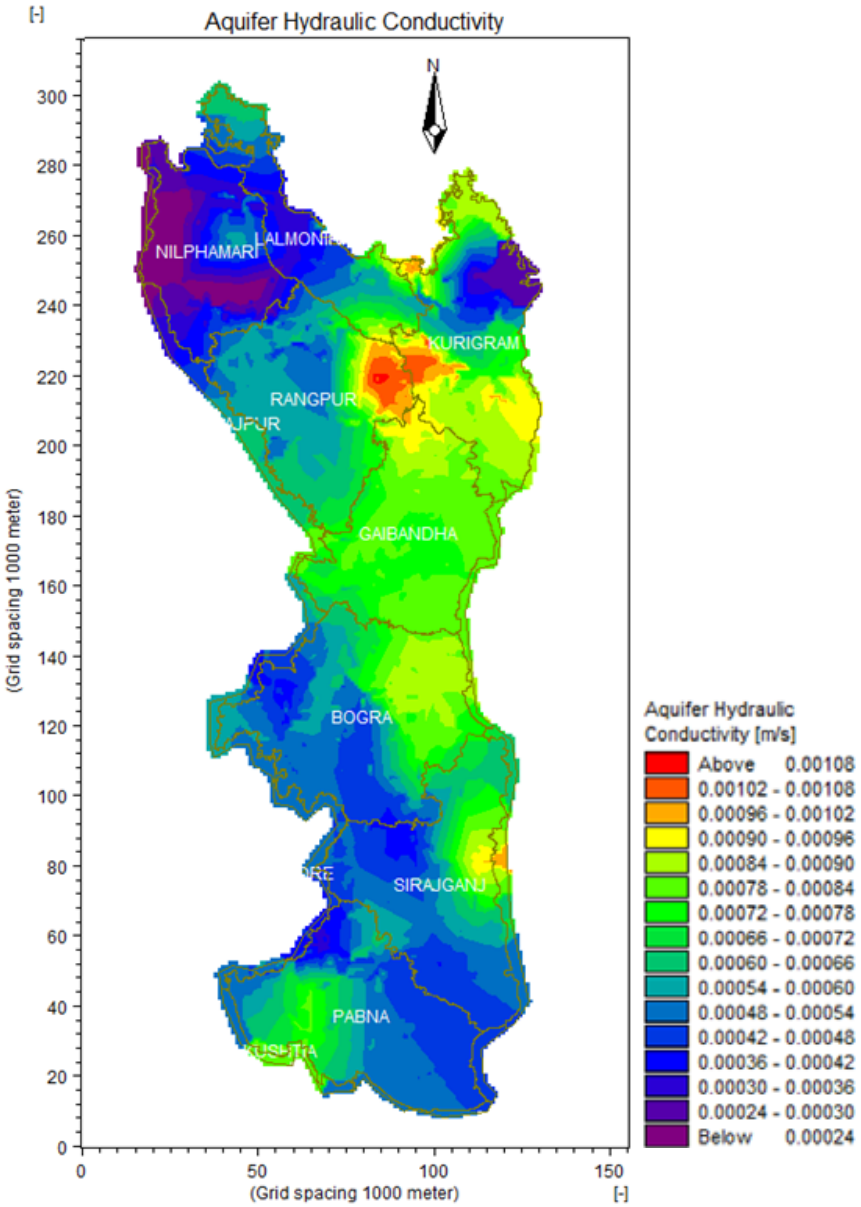

Figure H.1: Map of calibrated hydraulic conductivity in the aquifer layers of the 8-district model areas

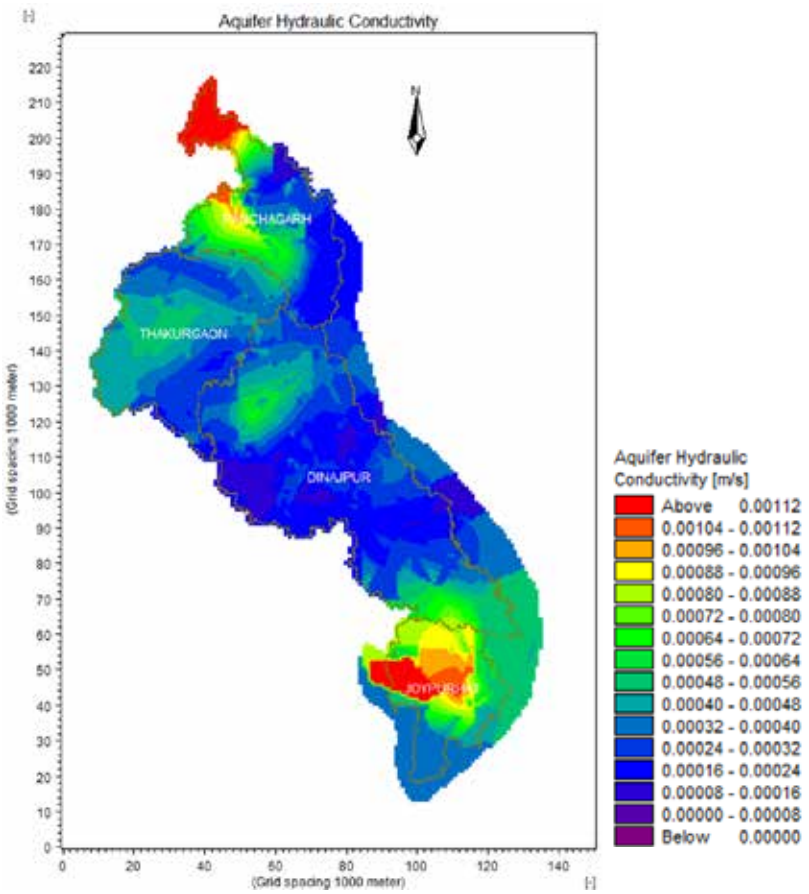

Figure H.2: Map of calibrated hydraulic conductivity in the aquifer layers of the 4-district model area

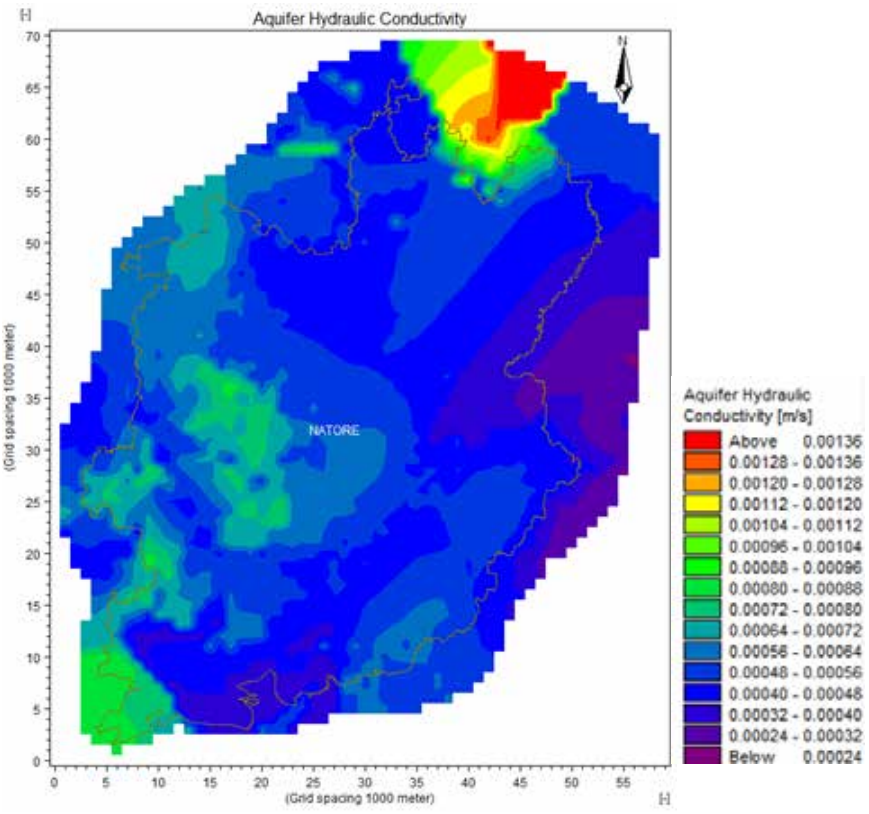

Figure H.3: Map of calibrated hydraulic conductivity in the aquifer layers of the Natore model areas

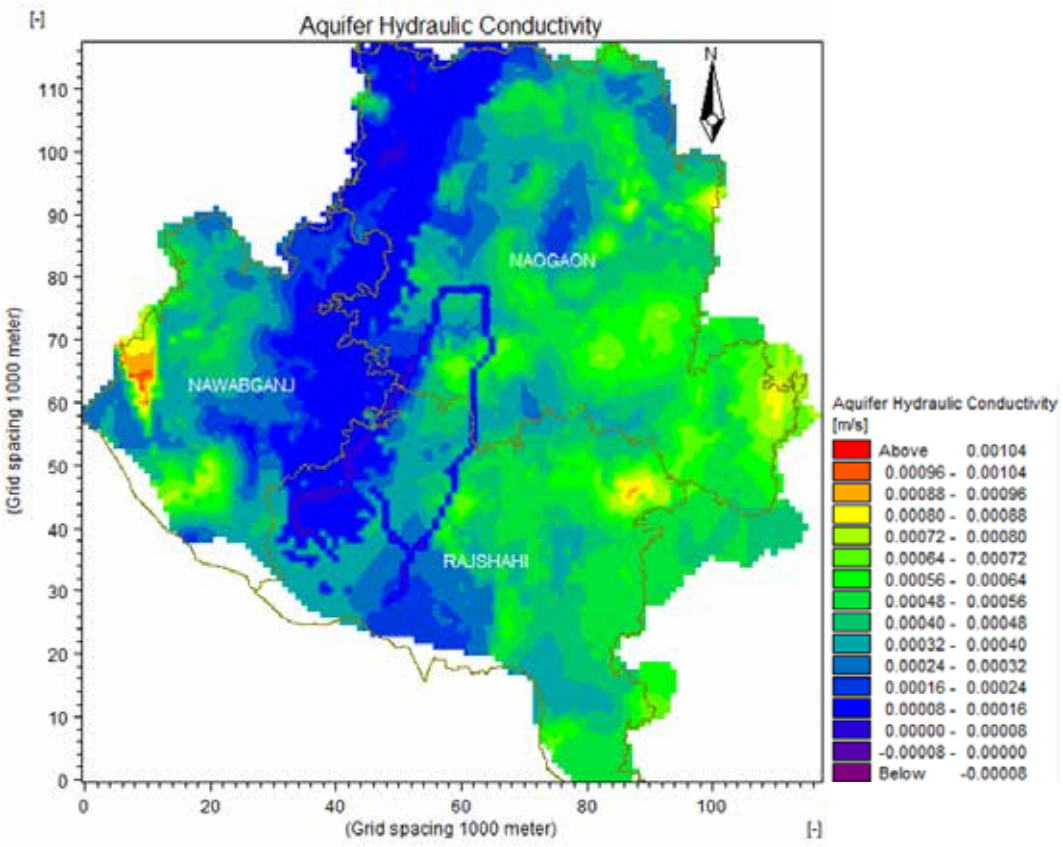

Figure H.4: Map of calibrated hydraulic conductivity in the aquifer layers of the Barind model areas

H.2 SPECIFIC YIELD

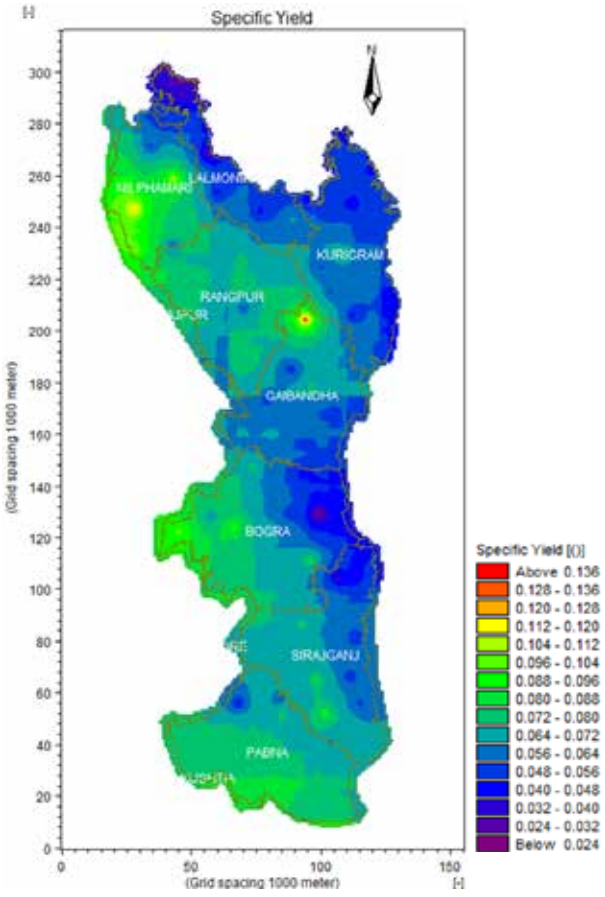

Figure H.5: Map of specific yield across the 8-district model area

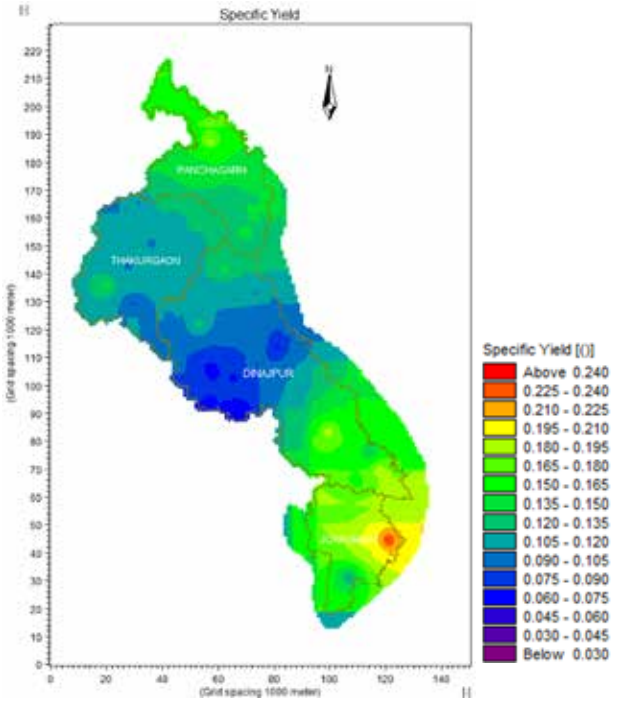

Figure H.6: Map of specific yield across the 4-district model area

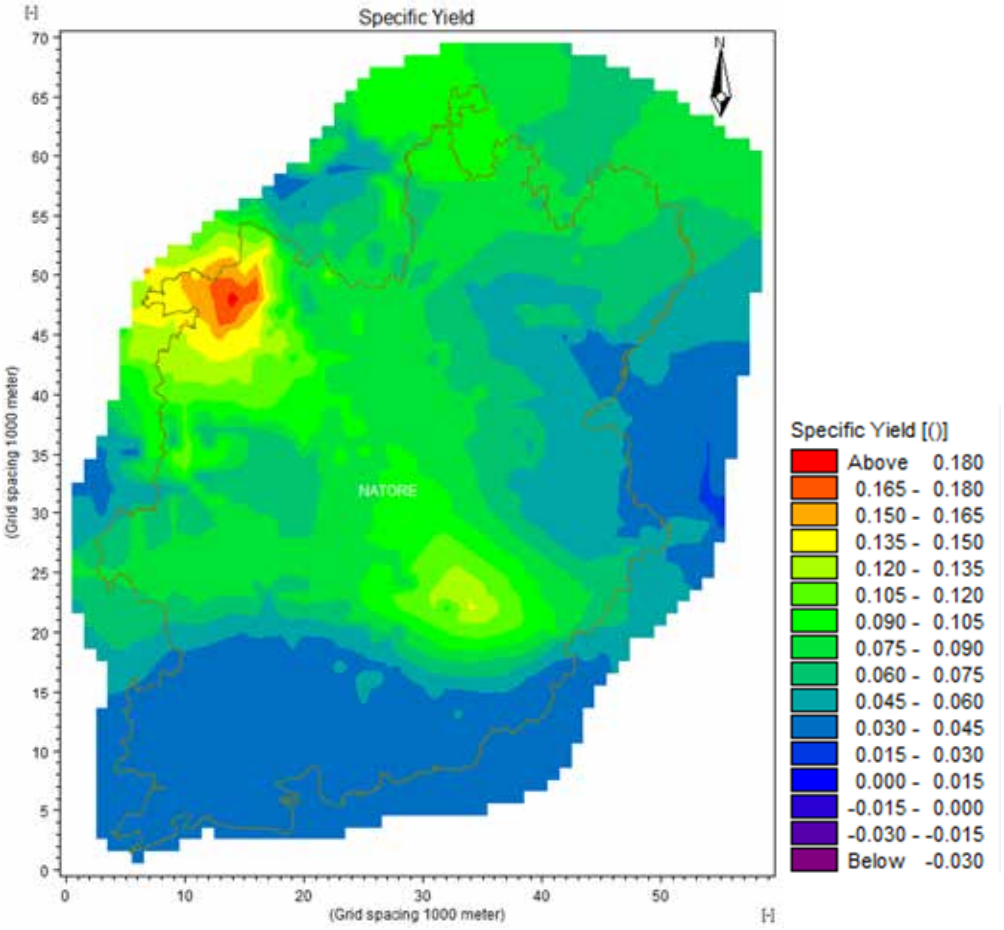

Figure H.7: Map of specific yield across the Natore model area

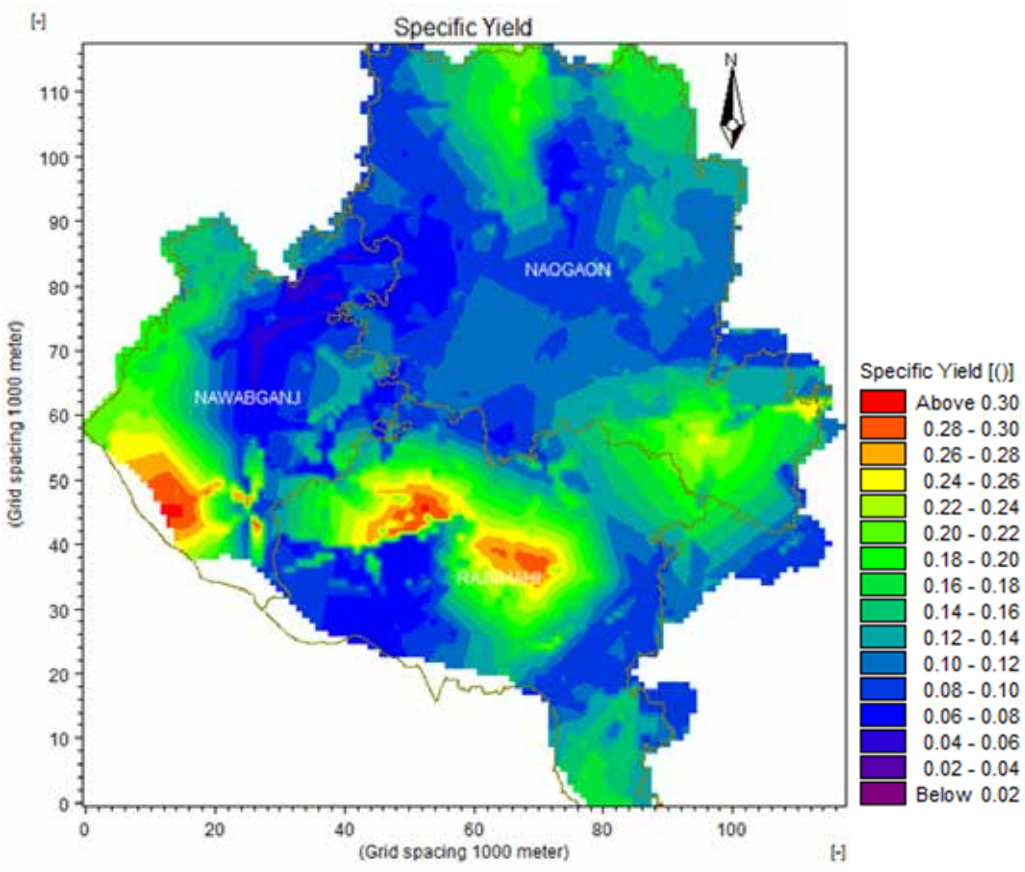

Figure H.8: Map of specific yield across the Barind model area

Appendix I SENSITIVITY ANALYSIS

I.1 SENSITIVITY ANALYSIS FOR THE 8-DISTRICT MODEL AREA

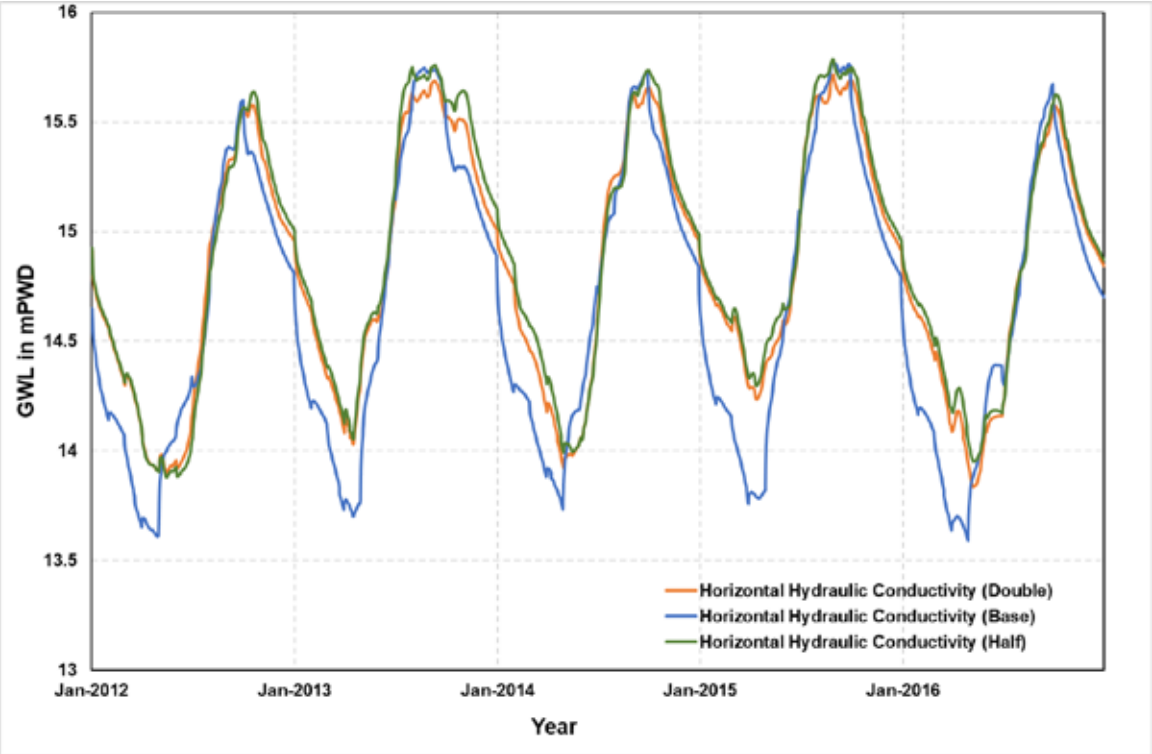

Figure I.1: Sensitivity analysis for horizontal conductivity (double, half and base) of GT1095026

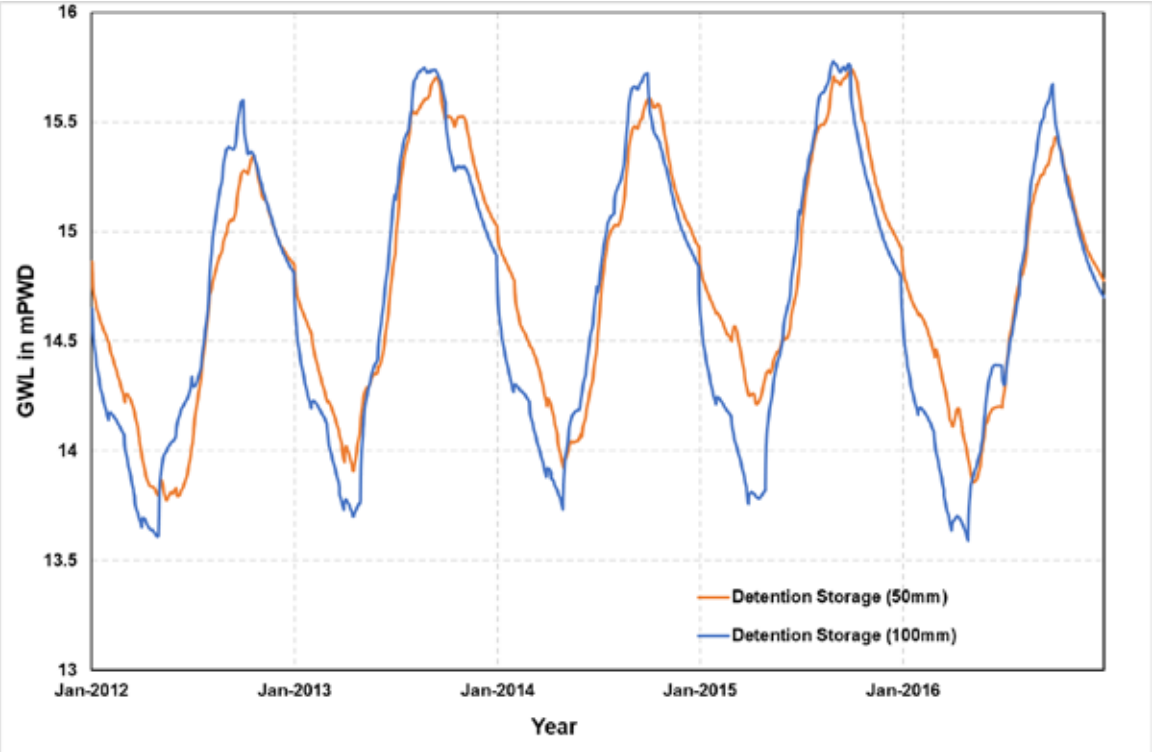

Figure I.2: Sensitivity analysis for detention storage (50 mm and 100 mm) of GT1095026

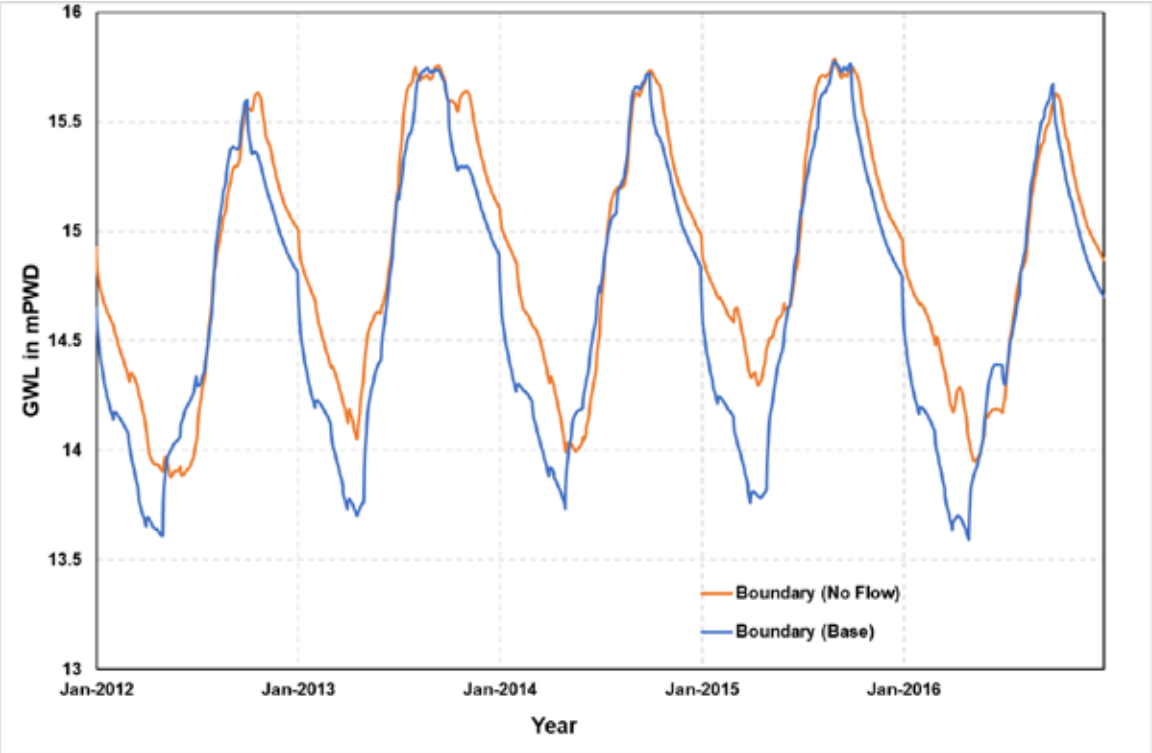

Figure I.3: Sensitivity analysis for boundary conditions (no flow and base) of GT1095026

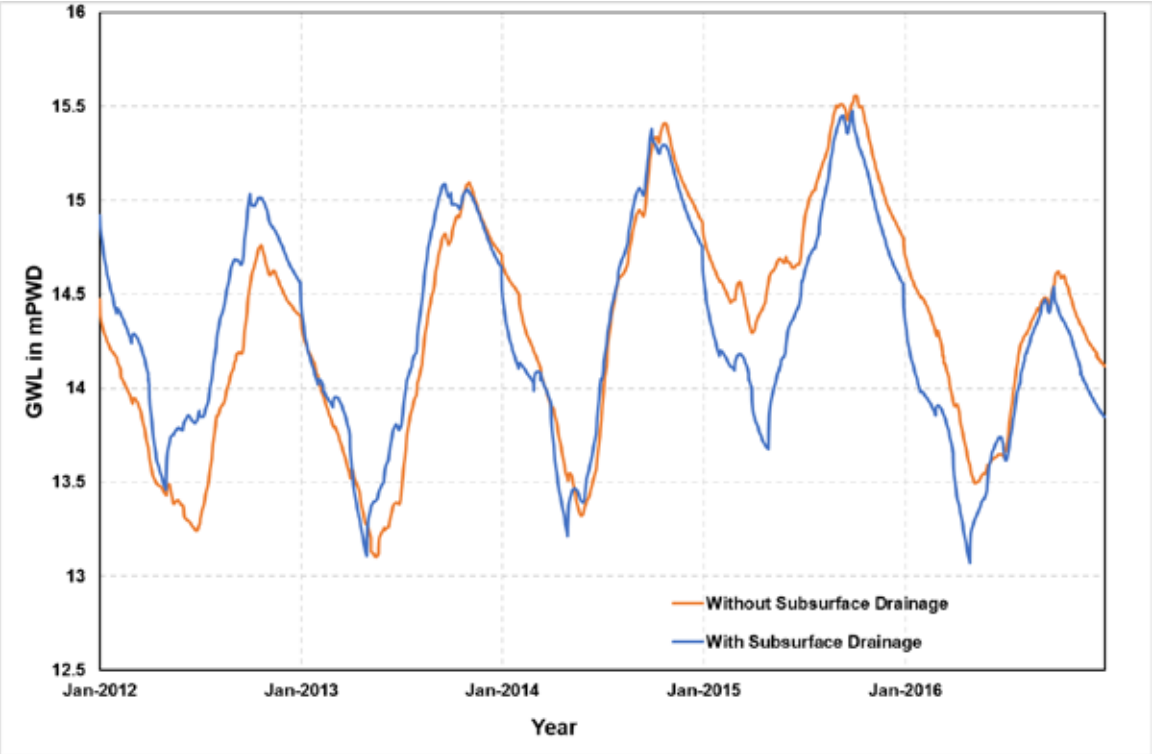

Figure I.4: Sensitivity analysis for subsurface drainage (with and without) of GT1020005

I.2 SENSITIVITY ANALYSIS FOR THE 4-DISTRICT MODEL AREA

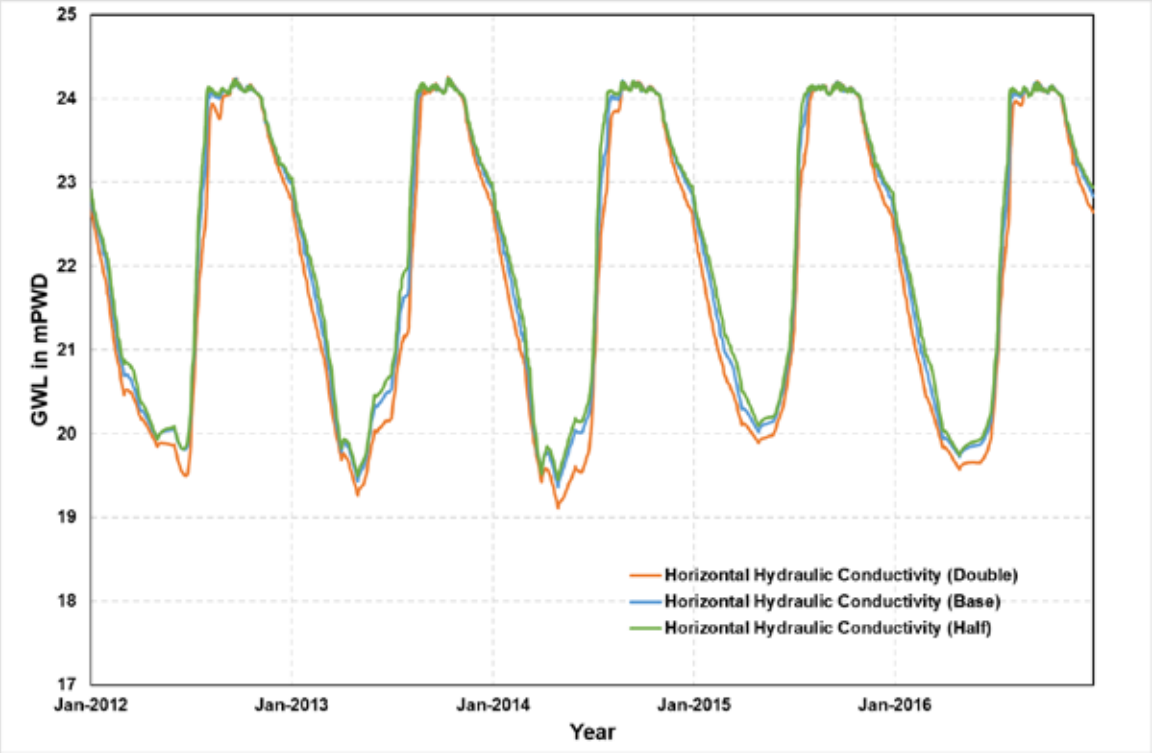

Figure I.5: Sensitivity analysis for horizontal conductivity (double, half and base) of GT2747022

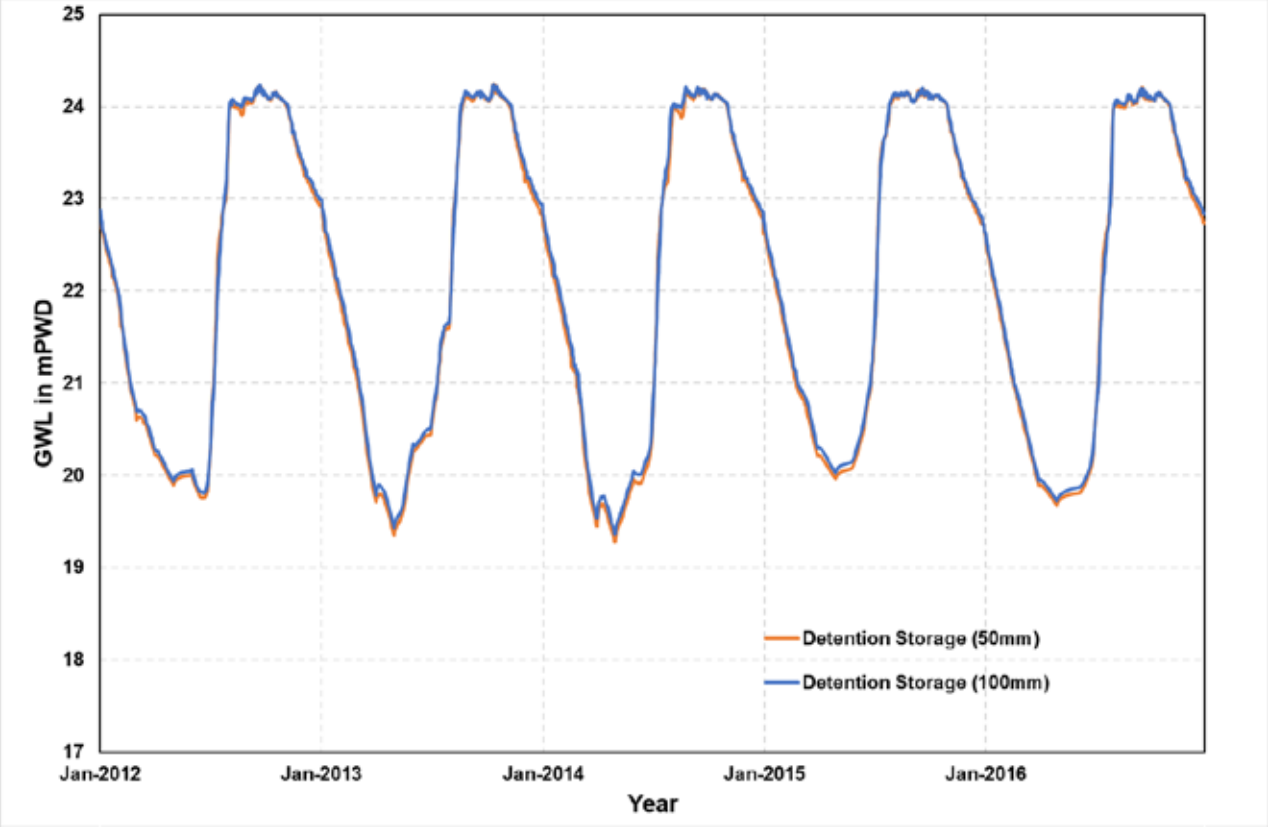

Figure I.6: Sensitivity analysis for detention storage (50 mm and 100 mm) of GT2747022

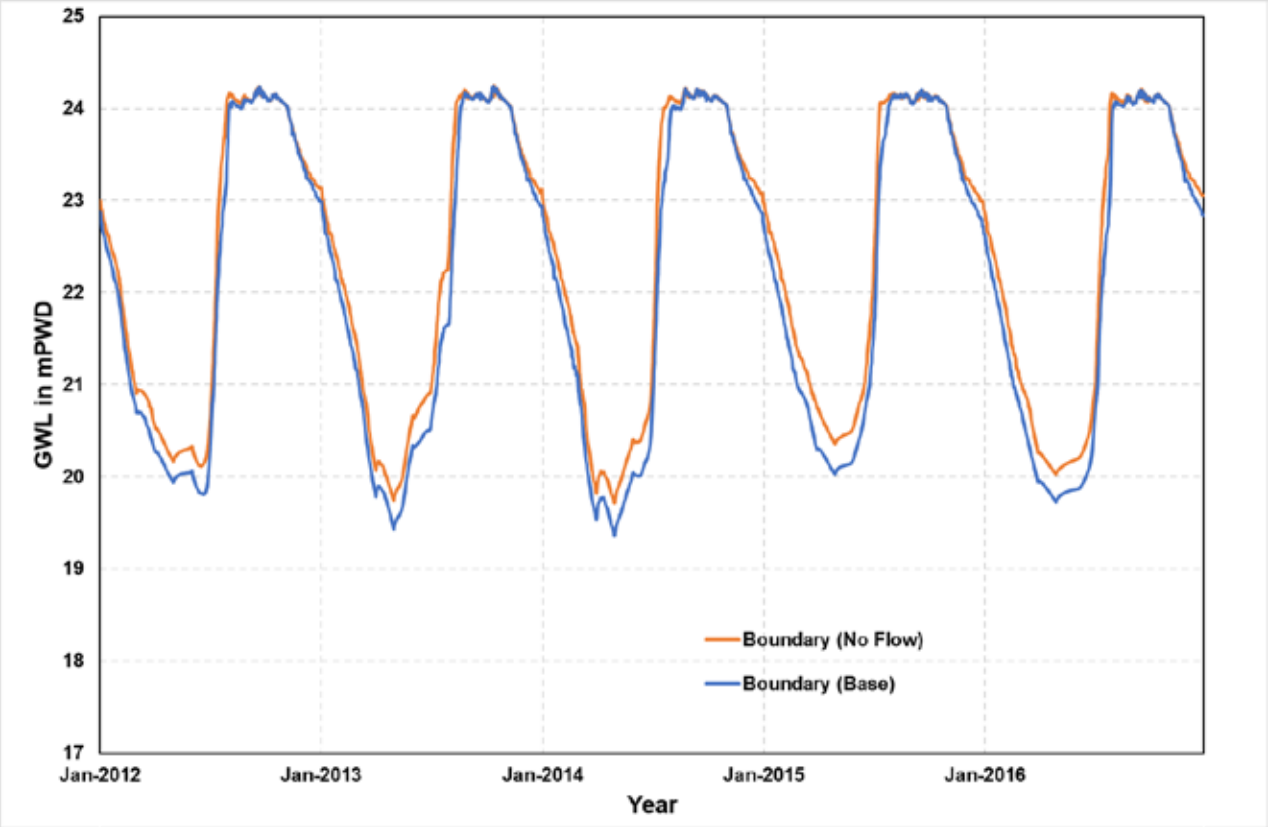

Figure I.7: Sensitivity analysis for boundary condition (no flow and base) of GT2747022

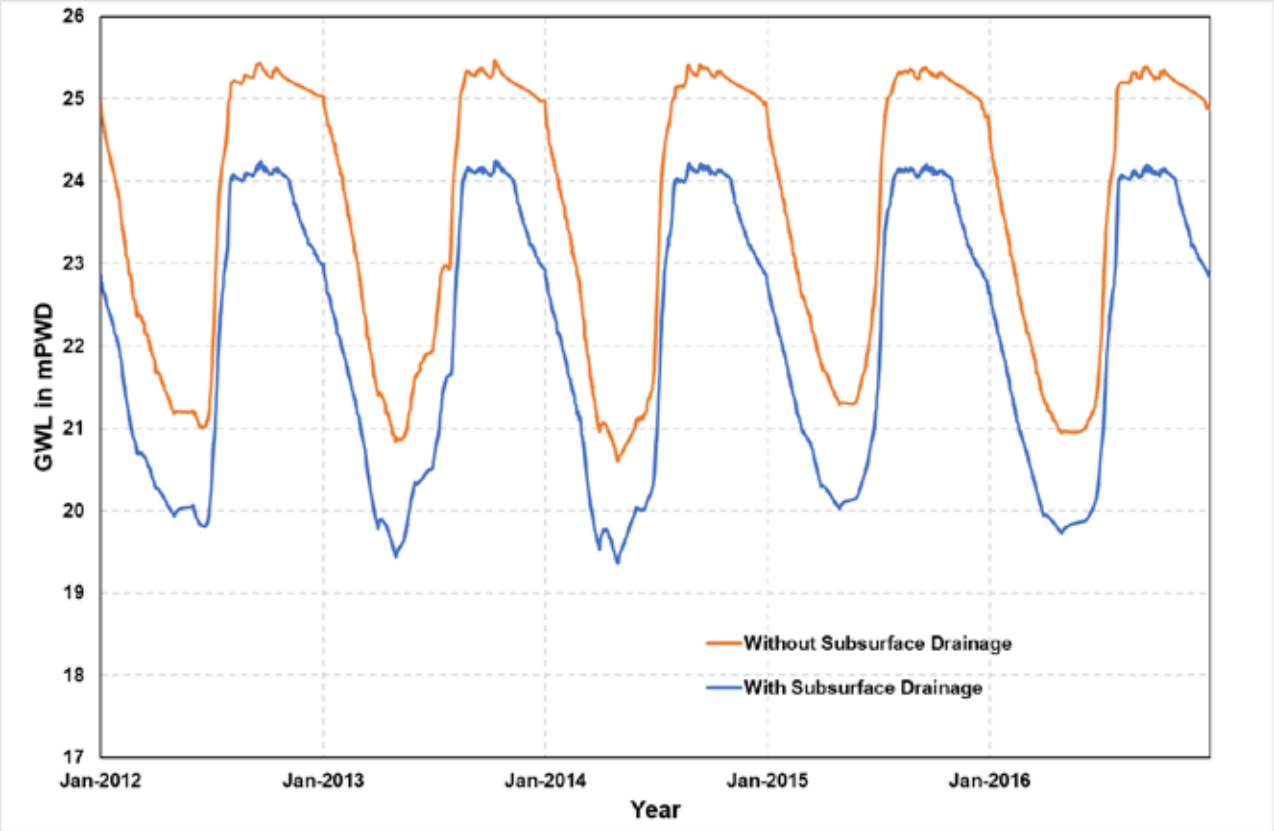

Figure I.8: Sensitivity analysis for subsurface drainage (with and without) of GT2747022

I.3 SENSITIVITY ANALYSIS FOR THE NATORE MODEL AREA

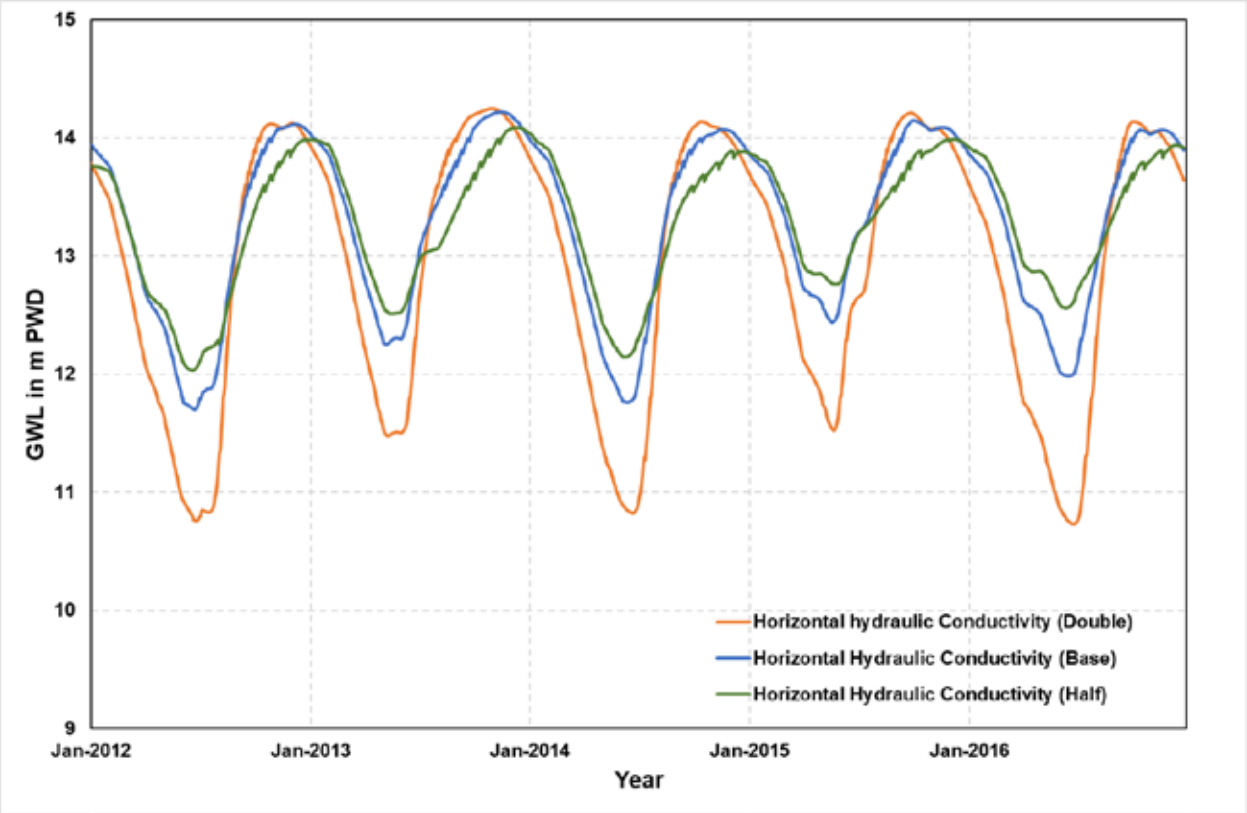

Figure I.9: Sensitivity analysis for horizontal conductivity (double, half and base) of GT6909501

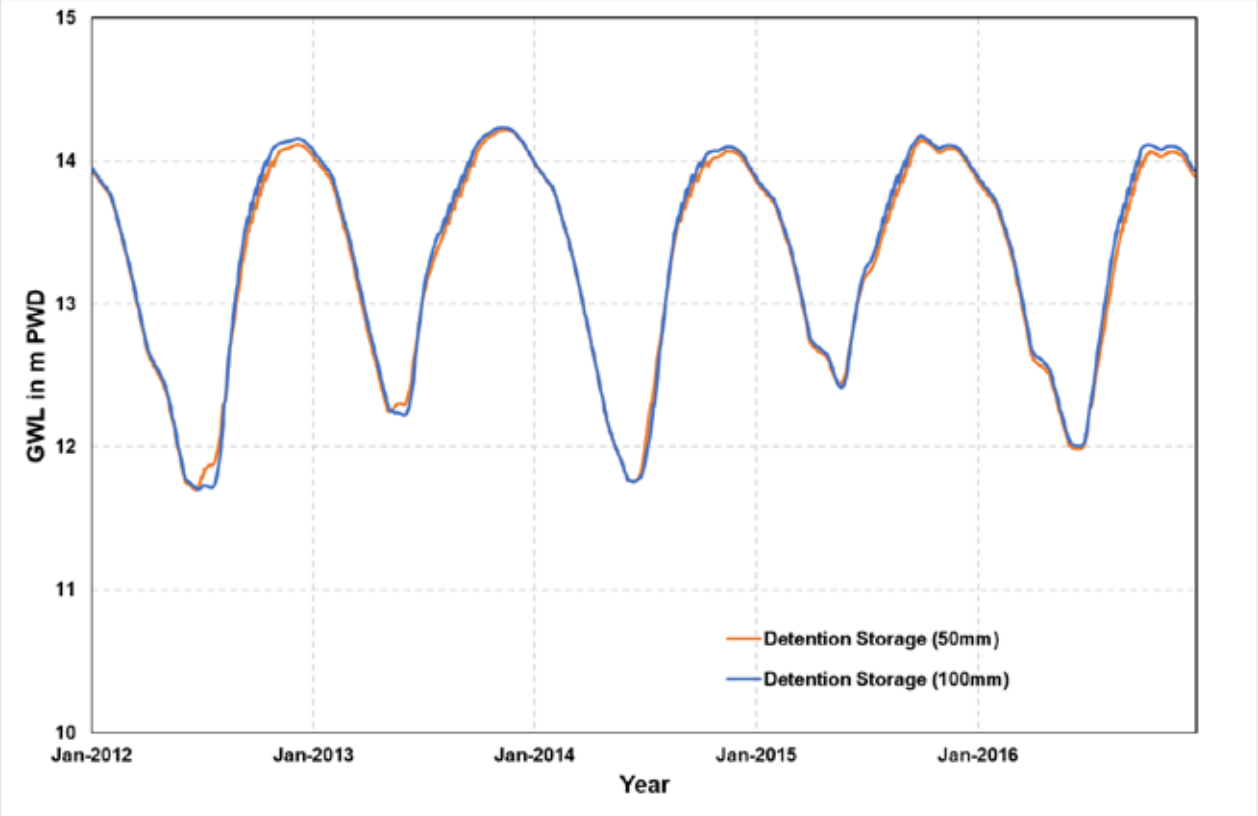

Figure I.10: Sensitivity analysis for detention storage (50 mm and 100 mm) of GT6909501

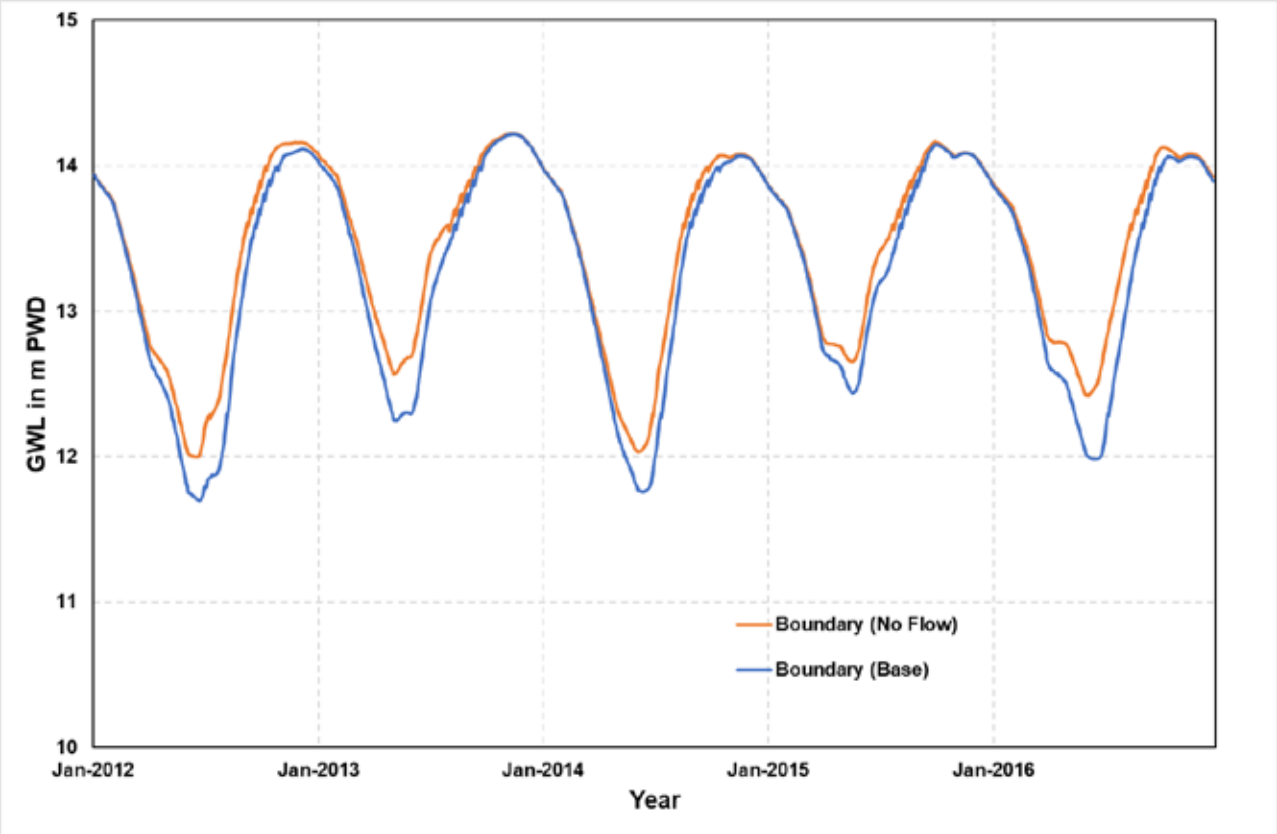

Figure I.11: Sensitivity analysis for boundary condition (no flow and base) of GT6909501

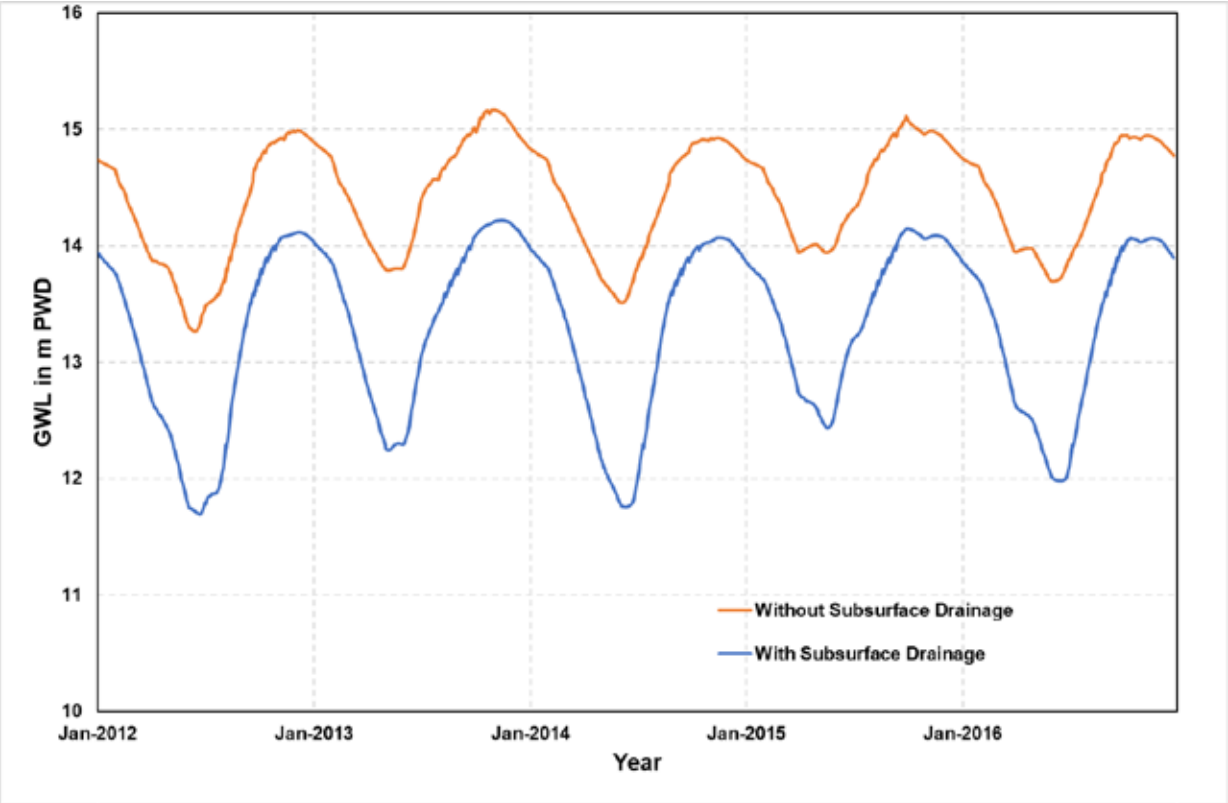

Figure I.12: Sensitivity analysis for subsurface drainage (with and without) of Gt6909501

I.4 SENSITIVITY ANALYSIS FOR THE BARIND MODEL AREA

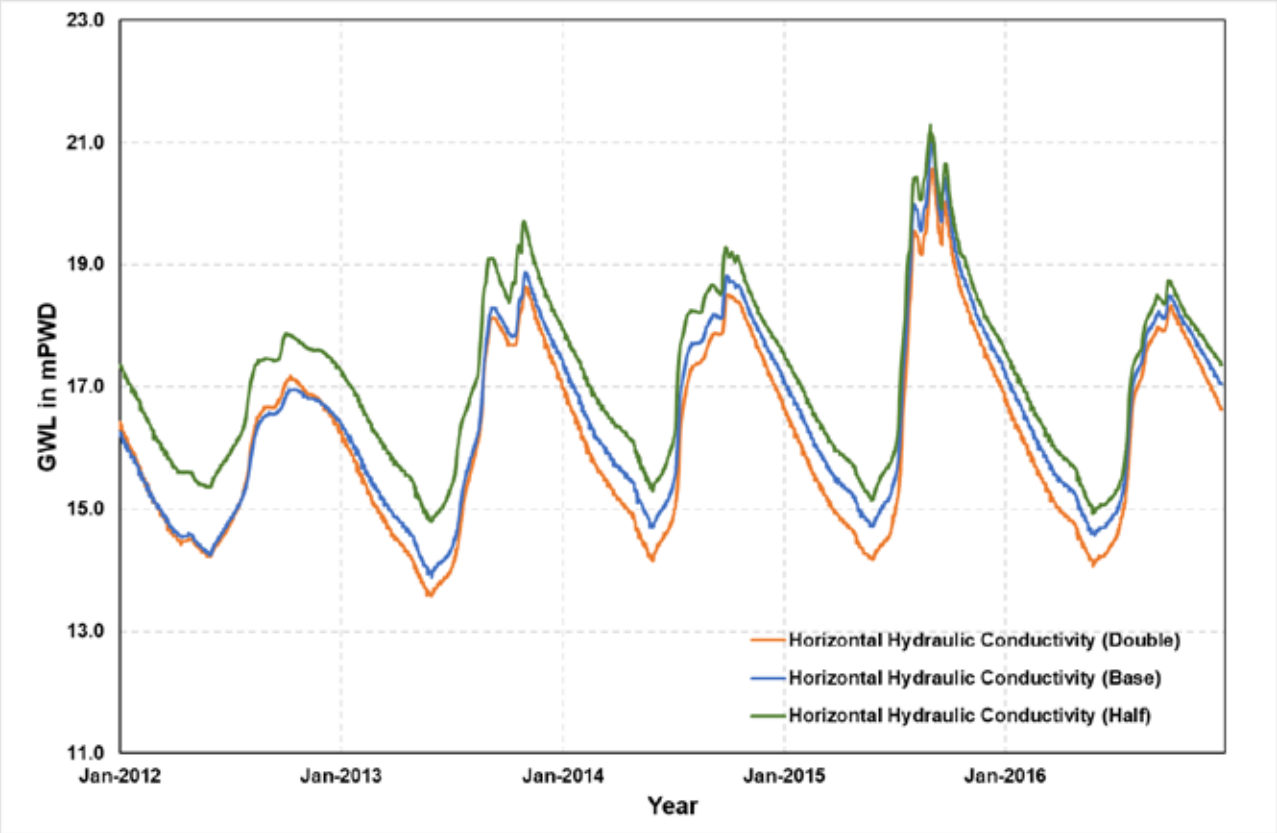

Figure I.13: Sensitivity analysis for horizontal conductivity (double, half and base) of GT7088023

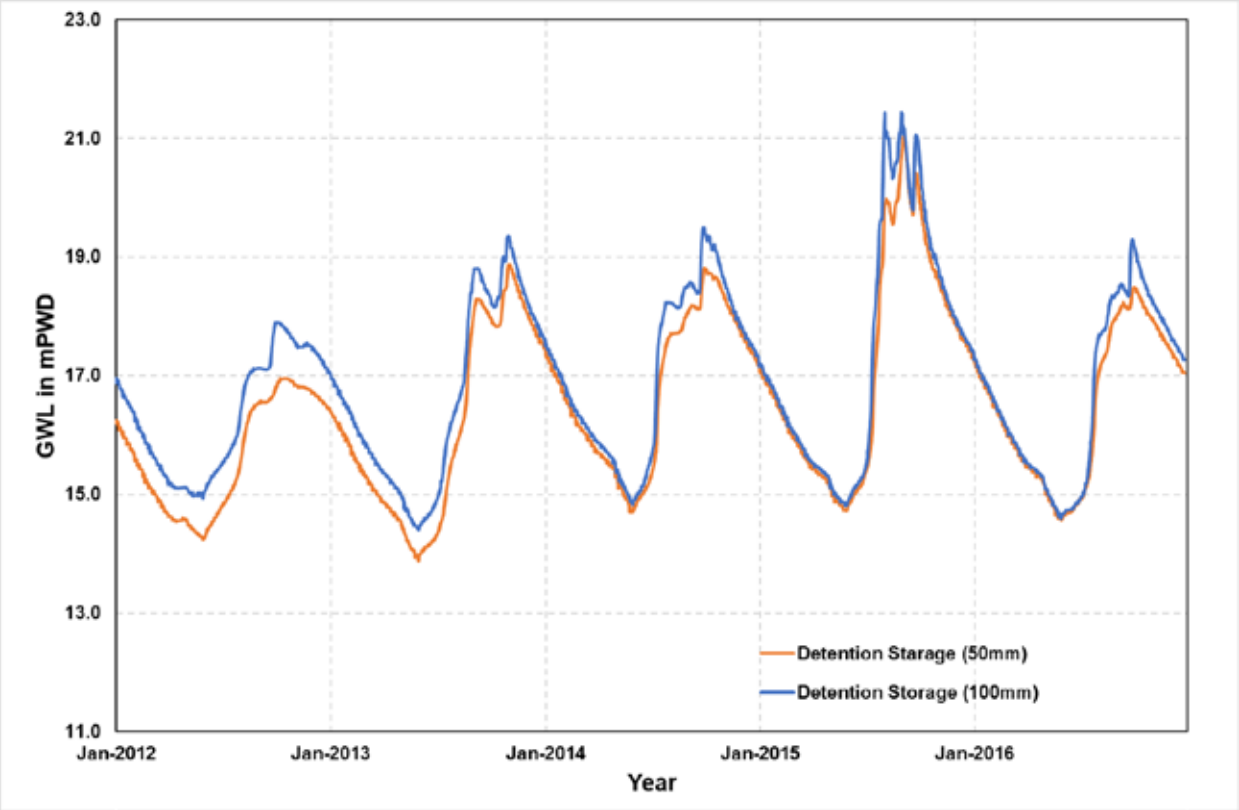

Figure I.14: Sensitivity analysis for detention storage (50 mm and 100 mm) of GT7088023

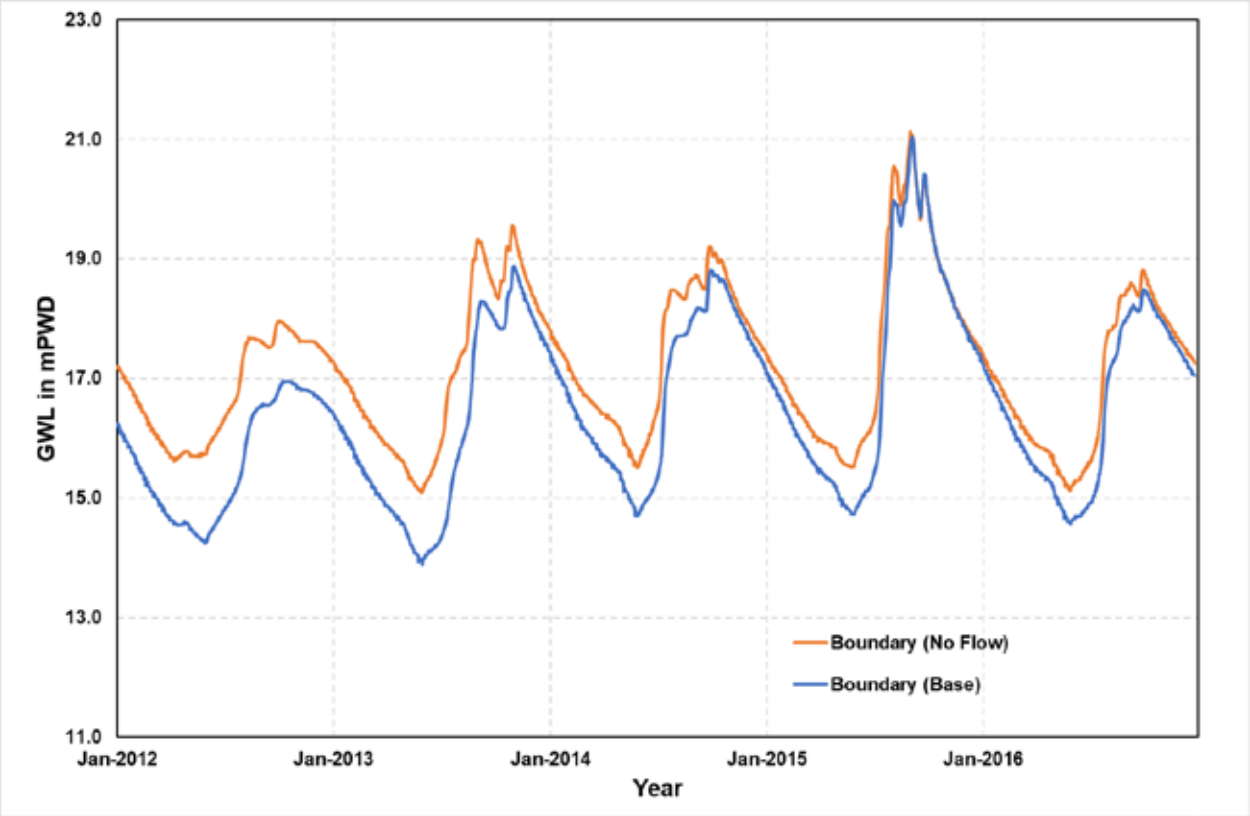

Figure I.15: Sensitivity analysis for boundary condition (no flow and Base) of GT7088023

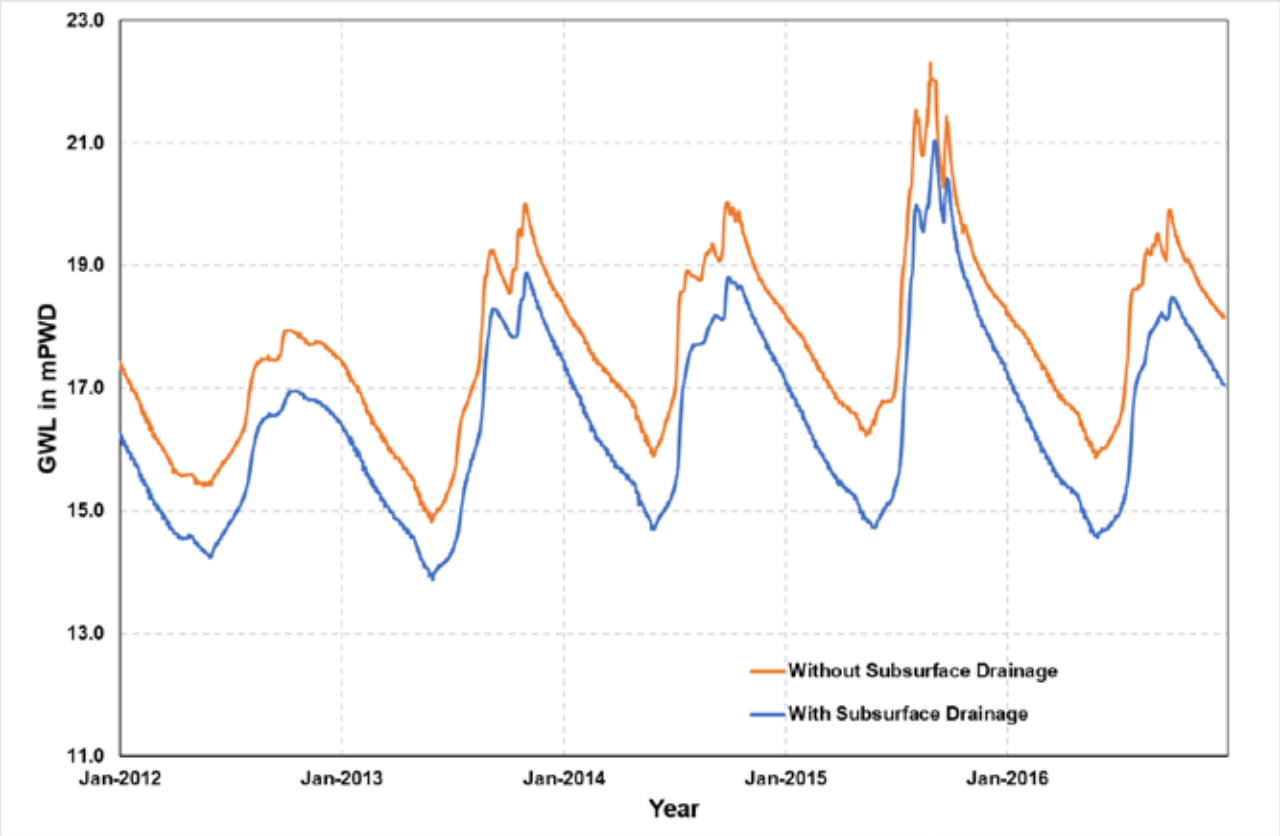

Figure I.16: Sensitivity analysis for subsurface drainage (with and without) of GT7088023

Appendix J WATER BALANCE FOR THE DISTRICTS

The comprehensive water balance components across the unsaturated and saturated zones obtained from the MIKE SHE model are shown in this appendix. These are lumped water balance estimates over the period 2005 to 2016. The analyses of annual average storage changes for the saturated zone were computed using the MODFLOW model developed for the saturated zone.

J.1 WATER BALANCE: PABNA DISTRICT (2005–2016)

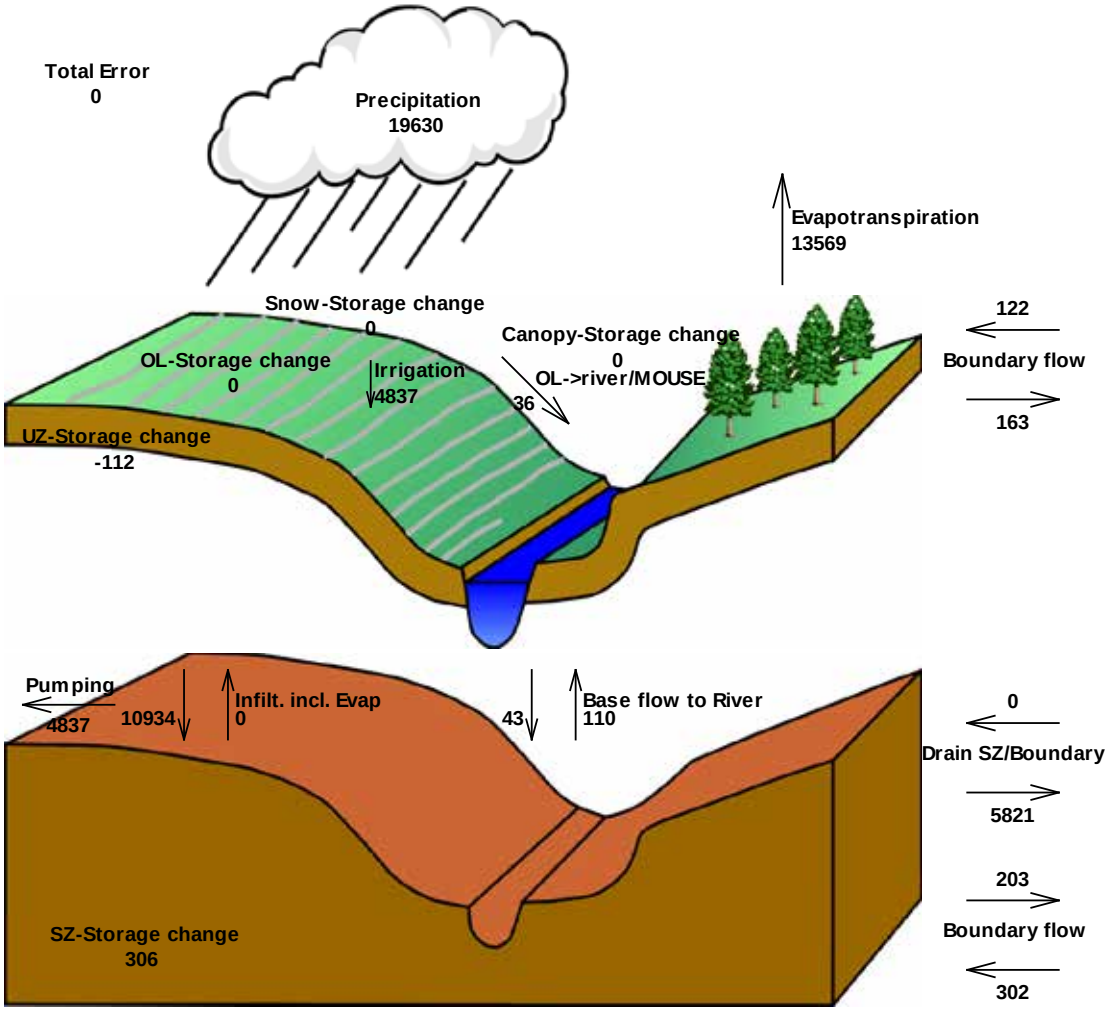

Figure J.1: Water balance (in mm) for the period 04 January 2005 to 31 December 2016 for Pabna district

Table J.1: Water balance for the period 04 January 2005 to 31 December 2016 for Pabna District

Components	Unsaturated Zone(UZ)		Saturated Zone (SZ)		River System		GW Recharge/Discharge	
	Inflow	Outflow	Inflow	Outflow	Inflow	Outflow	Recharge	Discharge
	(mm)	(mm)	(mm)	(mm)	(mm)	(mm)	(mm)	(mm)
Rainfall	19630	—	—	—	—	—	—	—
Evapotranspiration(ET)	—	13569	—	—	—	—	—	—
Abstraction	—	—	—	4837	—	—	—	—
Irrigation	4837	—	—	—	—	—	—	—
Capilary rise & ET from SZ to UZ	0	—	—	0	—	—	—	—
Deep Percolation from UZ to SZ	—	10934	10934	—	—	—	10934	0
Boundary Flow	122	163	302	203	—	—	99	0
Base Flow	—	—	43	110	110	43	0	67
Overland flow to river	—	36	—	—	36	—	—	—
Drain flow to river	—	—	0	0	0	0	0	0
OL storage Change	0	0	—	—	—	—	—	—
Drain SZ/Boundary	—	—	0	5821	—	—	0	5821
Total	**24589**	**24702**	**11279**	**10971**	**146**	**43**	**11033**	**5888**
Net Balance= Inflow-Outflow	**-113**		**308**		**103**		**5145**	
Explanation	**Inflow/Outflow of SZ**		**Change in Storage**		**River/Aquifer Interaction**		**Annual Recharge /Discharge**	

J.2 WATER BALANCE: BOGRA DISTRICT (2005–2016)

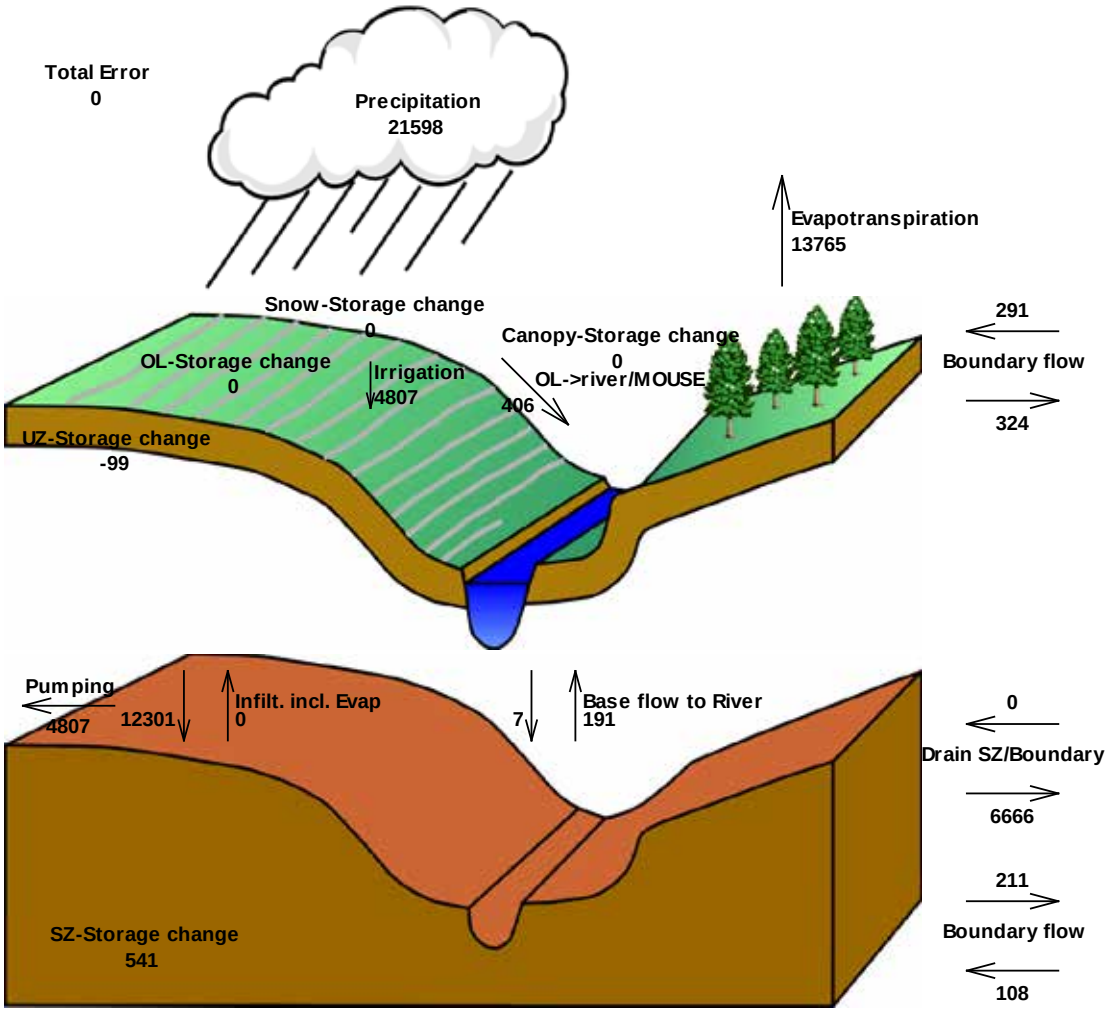

Figure J.2: Water balance (in mm) for the period of 04 January 2005 to 31 December 2016 for Bogra district

Table J.2: Water balance for the period 04 January 2005 to 31 December 2016 for Bogra district

Components	Unsaturated Zone(UZ)		Saturated Zone (SZ)		River System		GW Recharge/Discharge	
	Inflow	Outflow	Inflow	Outflow	Inflow	Outflow	Recharge	Discharge
	(mm)	(mm)	(mm)	(mm)	(mm)	(mm)	(mm)	(mm)
Rainfall	21598	—	—	—	—	—	—	—
Evapotranspiration(ET)	—	13765	—	—	—	—	—	—
Abstraction	—	—	—	4807	—	—	—	—
Irrigation	4807	—	—	—	—	—	—	—
Capilary rise & ET from SZ to UZ	0	—	—	0	—	—	—	—
Deep Percolation from UZ to SZ	—	12301	12301	—	—	—	12301	0
Boundary Flow	291	324	108	211	—	—	0	103
Base Flow	—	—	7	191	191	7	0	184
Overland flow to river	—	406	—	—	406	—	—	—
Drain flow to river	—	—	0	0	0	0	0	0
OL storage Change	0	0	—	—	—	—	—	—
Drain SZ/Boundary	—	—	0	6666	—	—	0	6666
Total	**26696**	**26796**	**12416**	**11875**	**597**	**7**	**12301**	**6953**
Net Balance= Inflow-Outflow	**-100**		**541**		**590**		**5348**	
Explanation	**Inflow/Outflow of SZ**		**Change in Storage**		**River/Aquifer Interaction**		**Annual Recharge /Discharge**	

J.3 WATER BALANCE: GAIBANDHA DISTRICT (2005–2016)

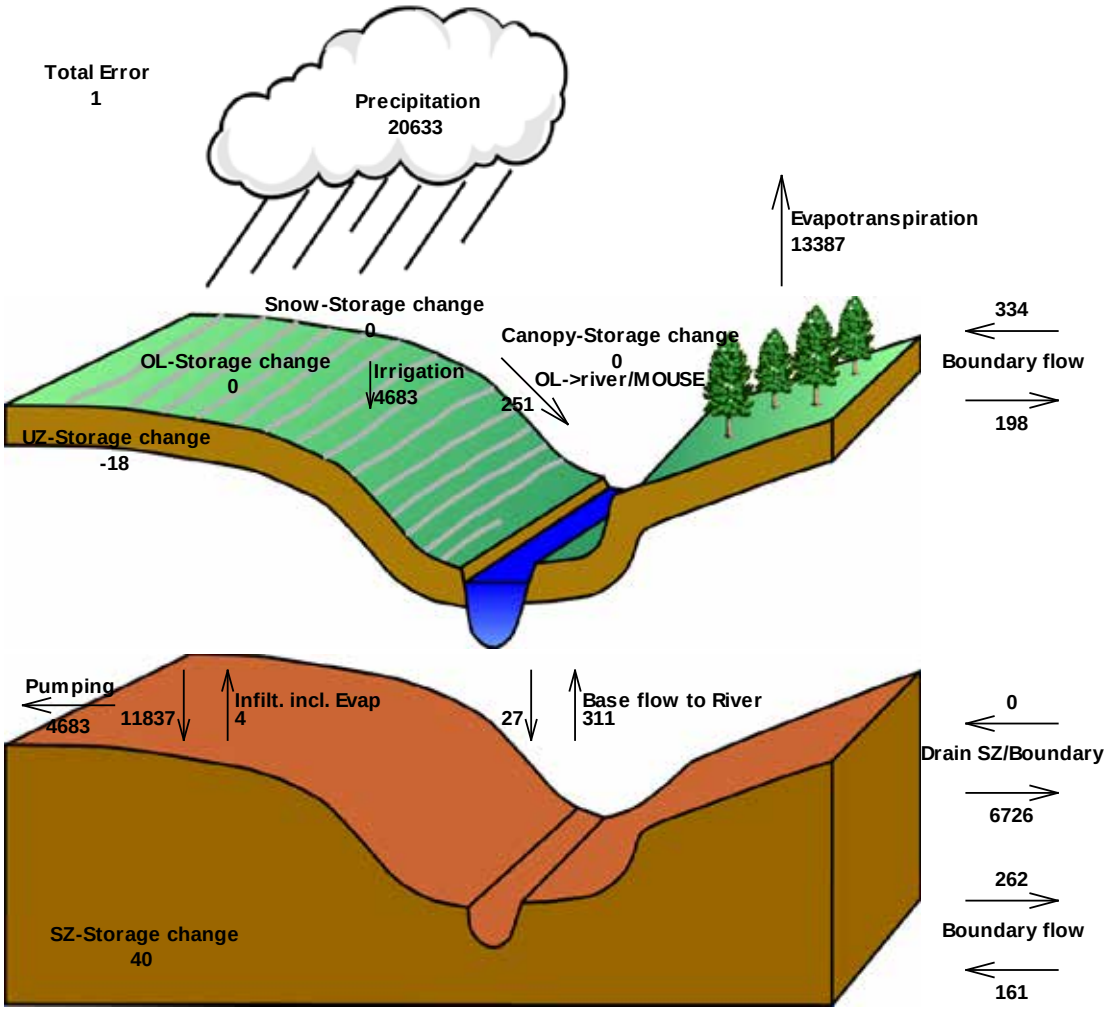

Figure J.3: Water balance (in mm) for the period 04 January 2005 to 31 December 2016 for Gaibandha district

Table J.3: Water balance for the period 04 January 2005 to 31 December 2016 for Gaibandha district

Components	Unsaturated Zone(UZ)		Saturated Zone (SZ)		River System		GW Recharge/Discharge	
	Inflow	Outflow	Inflow	Outflow	Inflow	Outflow	Recharge	Discharge
	(mm)	(mm)	(mm)	(mm)	(mm)	(mm)	(mm)	(mm)
Rainfall	20633	—	—	—	—	—	—	—
Evapotranspiration(ET)	—	13387	—	—	—	—	—	—
Abstraction	—	—	—	4683	—	—	—	—
Irrigation	4683	—	—	—	—	—	—	—
Capilary rise & ET from SZ to UZ	4	—	—	4	—	—	—	—
Deep Percolation from UZ to SZ	—	11837	11837	—	—	—	11833	0
Boundary Flow	334	198	161	262	—	—	0	101
Base Flow	—	—	27	311	311	27	0	284
Overland flow to river	—	251	—	—	251	—	—	—
Drain flow to river	—	—	0	0	0	0	0	0
OL storage Change	0	0	—	—	—	—	—	—
Drain SZ/Boundary	—	—	0	6726	—	—	0	6726
Total	**25654**	**25673**	**12025**	**11986**	**562**	**27**	**11833**	**7111**
Net Balance= Inflow-Outflow	**-19**		**39**		**535**		**4722**	
Explanation	**Inflow/Outflow of SZ**		**Change in Storage**		**River/Aquifer Interaction**		**Annual Recharge /Discharge**	

J.4 WATER BALANCE: KURIGRAM DISTRICT (2005–2016)

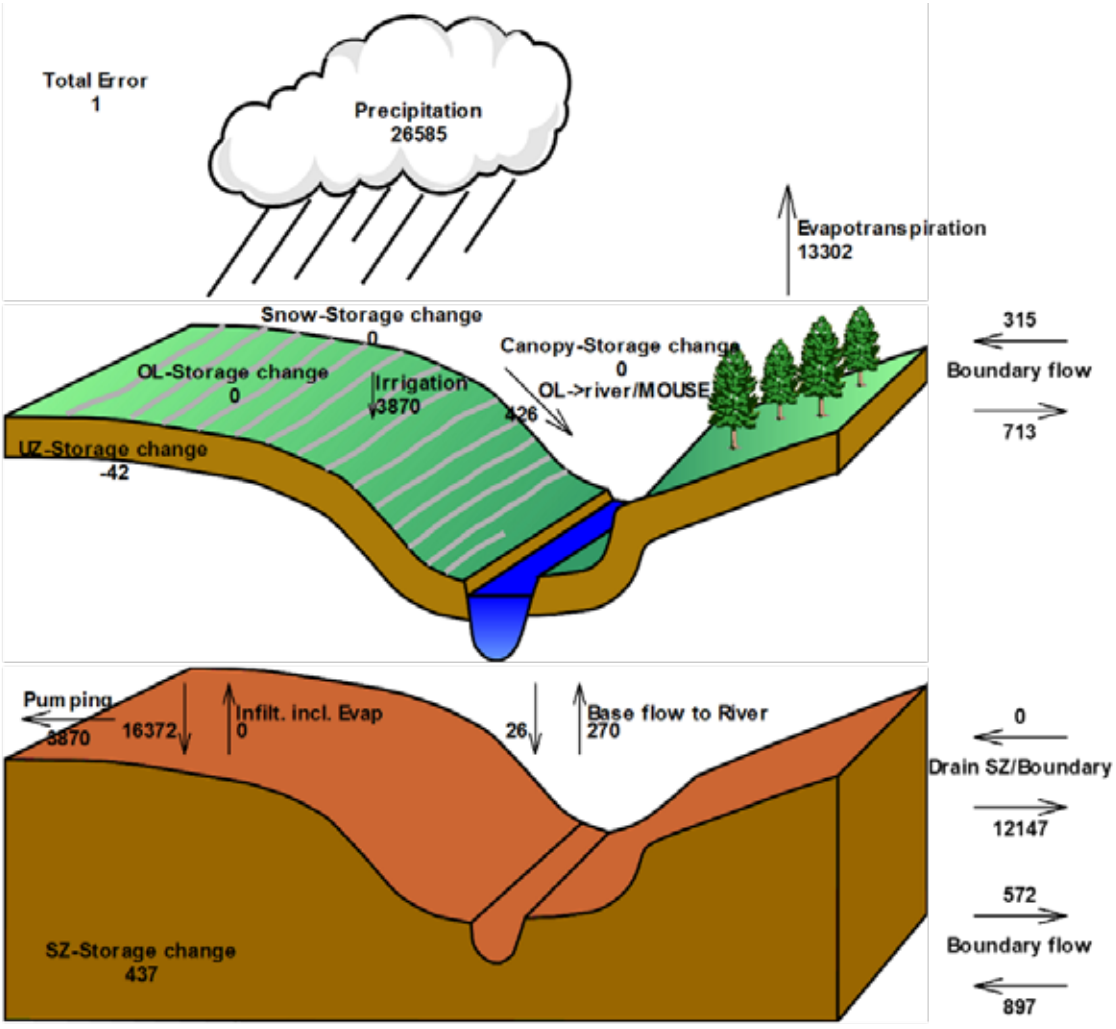

Figure J.4: Water balance (in mm) for the period 04 January 2005 to 31 December 2016 for Kurigram district

Table J.4: Water balance for the period 04 January 2005 to 31 December 2016 for Kurigram district

Components	Unsaturated Zone(UZ)		Saturated Zone (SZ)		River System		GW Recharge/Discharge	
	Inflow	Outflow	Inflow	Outflow	Inflow	Outflow	Recharge	Discharge
	(mm)	(mm)	(mm)	(mm)	(mm)	(mm)	(mm)	(mm)
Rainfall	26585	—	—	—	—	—	—	—
Evapotranspiration(ET)	—	13302	—	—	—	—	—	—
Abstraction	—	—	—	3870	—	—	—	—
Irrigation	3870	—	—	—	—	—	—	—
Capilary rise & ET from SZ to UZ	0	—	—	0	—	—	—	—
Deep Percolation from UZ to SZ	—	16372	16372	—	—	—	16372	0
Boundary Flow	315	713	897	572	—	—	325	0
Base Flow	—	—	26	270	270	26	0	244
Overland flow to river	—	426	—	—	426	—	—	—
Drain flow to river	—	—	0	0	0	0	0	0
OL storage Change	0	0	—	—	—	—	—	—
Drain SZ/Boundary	—	—	0	12147	—	—	0	12147
Total	**30770**	**30813**	**17295**	**16859**	**696**	**26**	**16697**	**12391**
Net Balance= Inflow-Outflow	**-43**		**436**		**670**		**4306**	
Explanation	**Inflow/Outflow of SZ**		**Change in Storage**		**River/Aquifer Interaction**		**Annual Recharge /Discharge**	

J.5 WATER BALANCE: LALMONIRHAT DISTRICT (2005–2016)

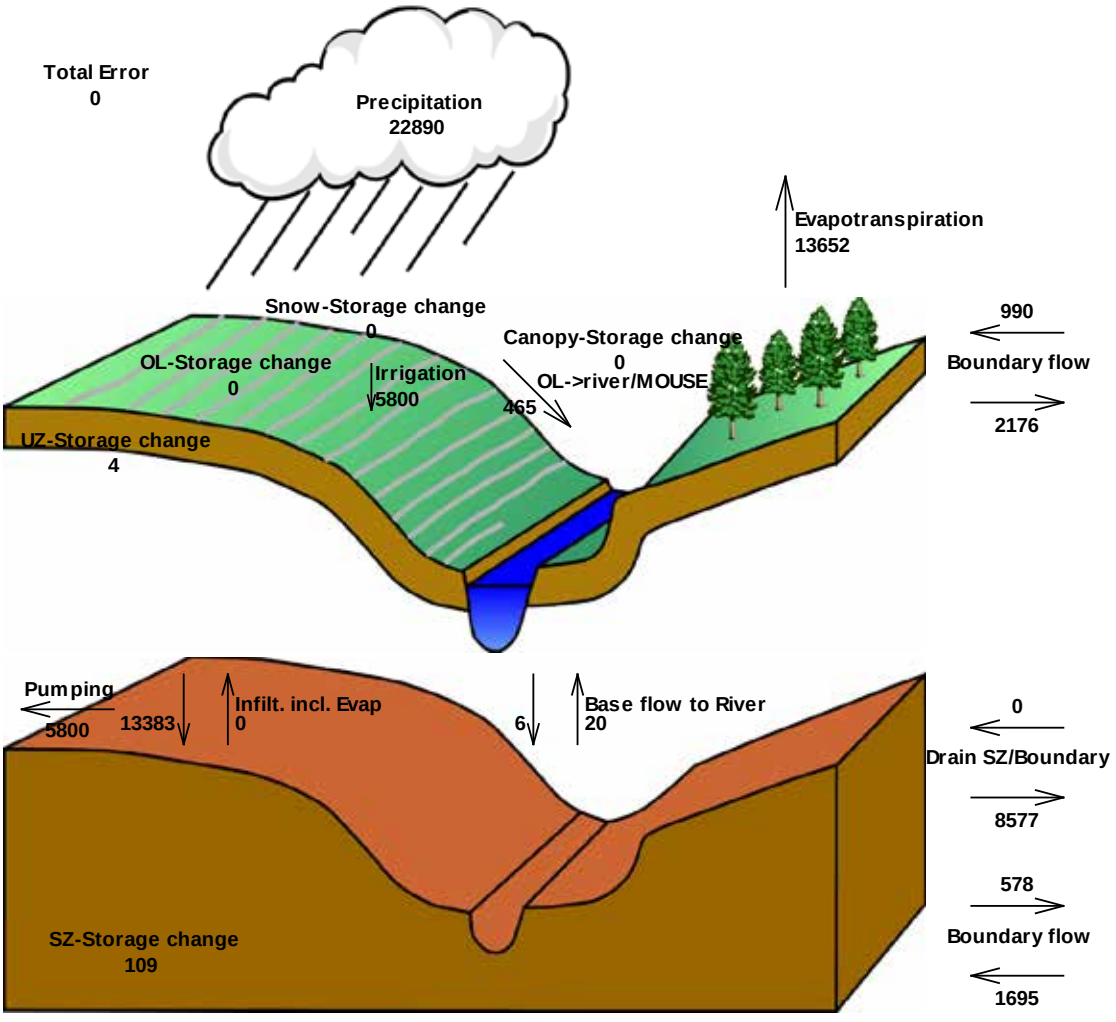

Figure J.5: Water balance (in mm) for the period 04 January 2005 to 31 December 2016 for Lalmonirhat district

Table J.5: Water balance for the period 04 January 2005 to 31 December 2016 for Lalmonirhat district

Components	Unsaturated Zone(UZ)		Saturated Zone (SZ)		River System		GW Recharge/Discharge	
	Inflow	Outflow	Inflow	Outflow	Inflow	Outflow	Recharge	Discharge
	(mm)	(mm)	(mm)	(mm)	(mm)	(mm)	(mm)	(mm)
Rainfall	22890	—	—	—	—	—	—	—
Evapotranspiration(ET)	—	13652	—	—	—	—	—	—
Abstraction	—	—	—	5800	—	—	—	—
Irrigation	5800	—	—	—	—	—	—	—
Capilary rise & ET from SZ to UZ	0	—	—	0	—	—	—	—
Deep Percolation from UZ to SZ	—	13383	13383	—	—	—	13383	0
Boundary Flow	990	2176	1695	578	—	—	1117	0
Base Flow	—	—	6	20	20	6	0	14
Overland flow to river	—	465	—	—	465	—	—	—
Drain flow to river	—	—	0	0	0	0	0	0
OL storage Change	0	0	—	—	—	—	—	—
Drain SZ/Boundary	—	—	0	8577	—	—	0	8577
Total	**29680**	**29676**	**15084**	**14975**	**485**	**6**	**14500**	**8591**
Net Balance= Inflow-Outflow	**4**		**109**		**479**		**5909**	
Explanation	**Inflow/Outflow of SZ**		**Change in Storage**		**River/Aquifer Interaction**		**Annual Recharge /Discharge**	

J.6 WATER BALANCE: NILPHAMARI DISTRICT (2005–2016)

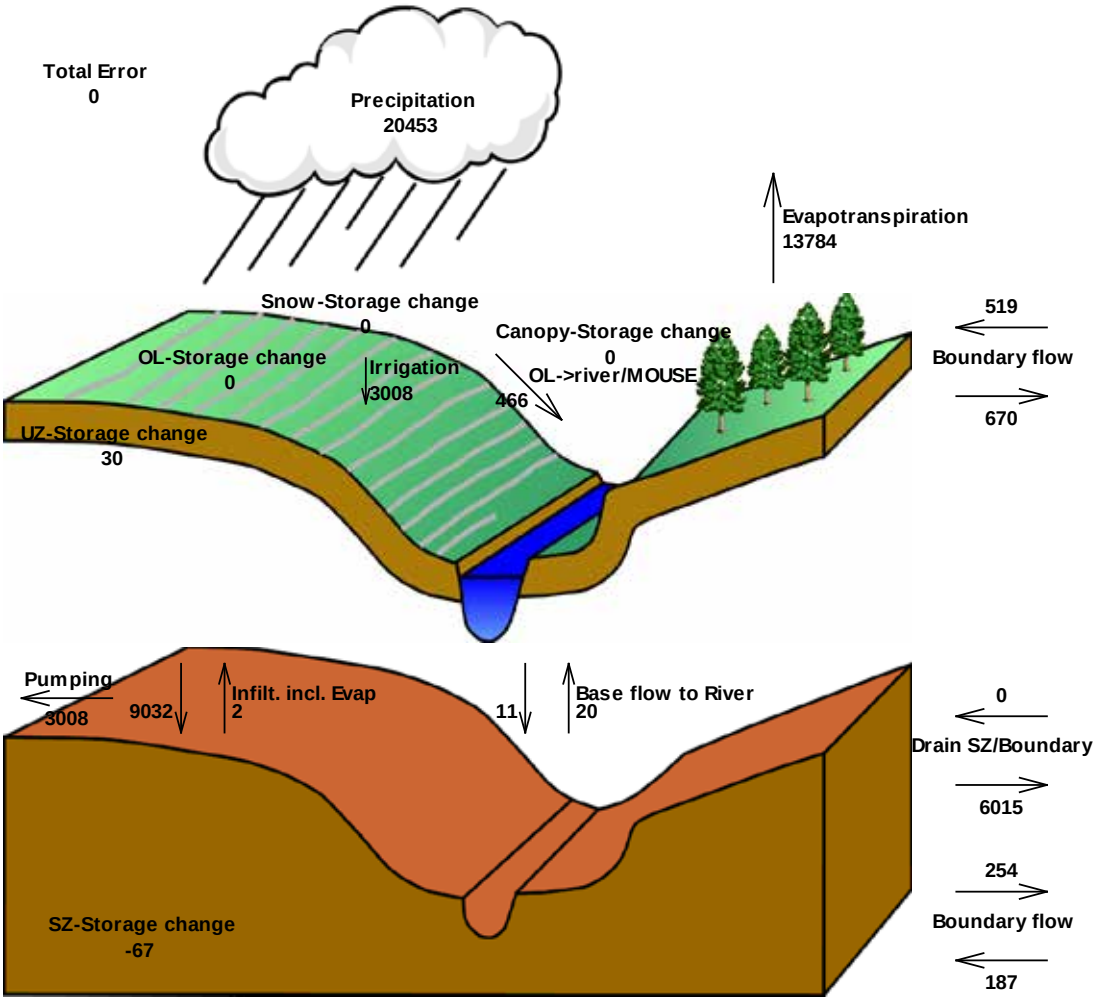

Figure J.6: Water balance (in mm) for the period 04 January 2005 to 31 December 2016 for Nilphamari district

Table J.6: Water balance for the period 04 January 2005 to 31 December 2016 for Nilphamari district

Components	Unsaturated Zone(UZ)		Saturated Zone (SZ)		River System		GW Recharge/Discharge	
	Inflow	Outflow	Inflow	Outflow	Inflow	Outflow	Recharge	Discharge
	(mm)	(mm)	(mm)	(mm)	(mm)	(mm)	(mm)	(mm)
Rainfall	20453	—	—	—	—	—	—	—
Evapotranspiration(ET)	—	13784	—	—	—	—	—	—
Abstraction	—	—	—	3008	—	—	—	—
Irrigation	3008	—	—	—	—	—	—	—
Capilary rise & ET from SZ to UZ	2	—	—	2	—	—	—	—
Deep Percolation from UZ to SZ	—	9032	9032	—	—	—	9030	0
Boundary Flow	519	670	187	254	—	—	0	67
Base Flow	—	—	11	20	20	11	0	9
Overland flow to river	—	466	—	—	466	—	—	—
Drain flow to river	—	—	0	0	0	0	0	0
OL storage Change	0	0	—	—	—	—	—	—
Drain SZ/Boundary	—	—	0	6015	—	—	0	6015
Total	**23982**	**23952**	**9230**	**9299**	**486**	**11**	**9030**	**6091**
Net Balance= Inflow-Outflow	**30**		**-69**		**475**		**2939**	
Explanation	**Inflow/Outflow of SZ**		**Change in Storage**		**River/Aquifer Interaction**		**Annual Recharge /Discharge**	

J.7 WATER BALANCE: RANGPUR DISTRICT (2005–2016)

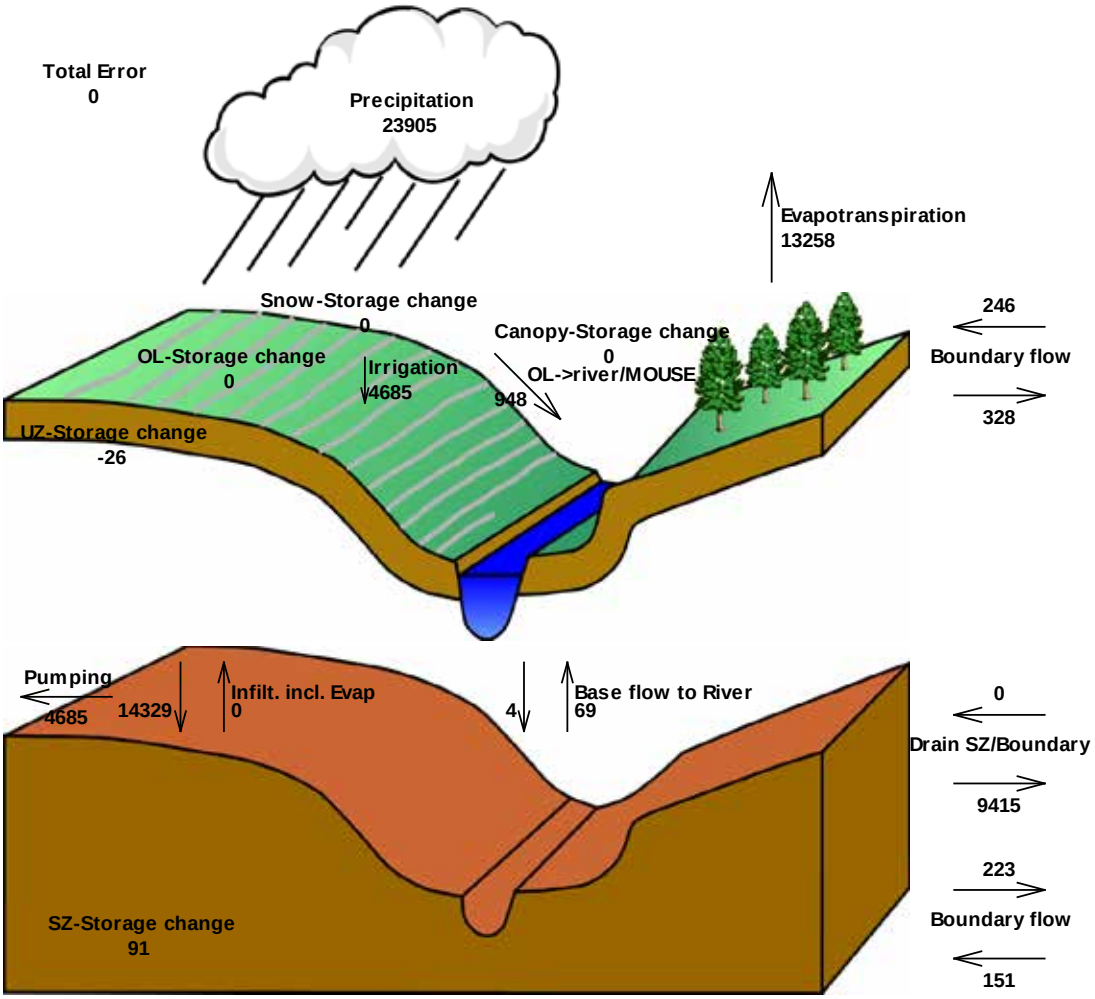

Figure J.7: Water balance (in mm) for the period 04 January 2005 to 31 December 2016 for Rangpur district

Table J.7: Water balance for the period 04 January 2005 to 31 December 2016 for Rangpur district

Components	Unsaturated Zone(UZ)		Saturated Zone (SZ)		River System		GW Recharge/Discharge	
	Inflow	Outflow	Inflow	Outflow	Inflow	Outflow	Recharge	Discharge
	(mm)	(mm)	(mm)	(mm)	(mm)	(mm)	(mm)	(mm)
Rainfall	23905	—	—	—	—	—	—	—
Evapotranspiration(ET)	—	13258	—	—	—	—	—	—
Abstraction	—	—	—	4685	—	—	—	—
Irrigation	4685	—	—	—	—	—	—	—
Capilary rise & ET from SZ to UZ	0	—	—	0	—	—	—	—
Deep Percolation from UZ to SZ	—	14329	14329	—	—	—	14329	0
Boundary Flow	246	328	151	223	—	—	0	72
Base Flow	—	—	4	69	69	4	0	65
Overland flow to river	—	948	—	—	948	—	—	—
Drain flow to river	—	—	0	0	0	0	0	0
OL storage Change	0	0	—	—	—	—	—	—
Drain SZ/Boundary	—	—	0	9415	—	—	0	9415
Total	**28836**	**28863**	**14484**	**14392**	**1017**	**4**	**14329**	**9552**
Net Balance= Inflow-Outflow	**-27**		**92**		**1013**		**4777**	
Explanation	**Inflow/Outflow of SZ**		**Change in Storage**		**River/Aquifer Interaction**		**Annual Recharge /Discharge**	

J.8 WATER BALANCE: SIRAJGANJ DISTRICT (2005–2016)

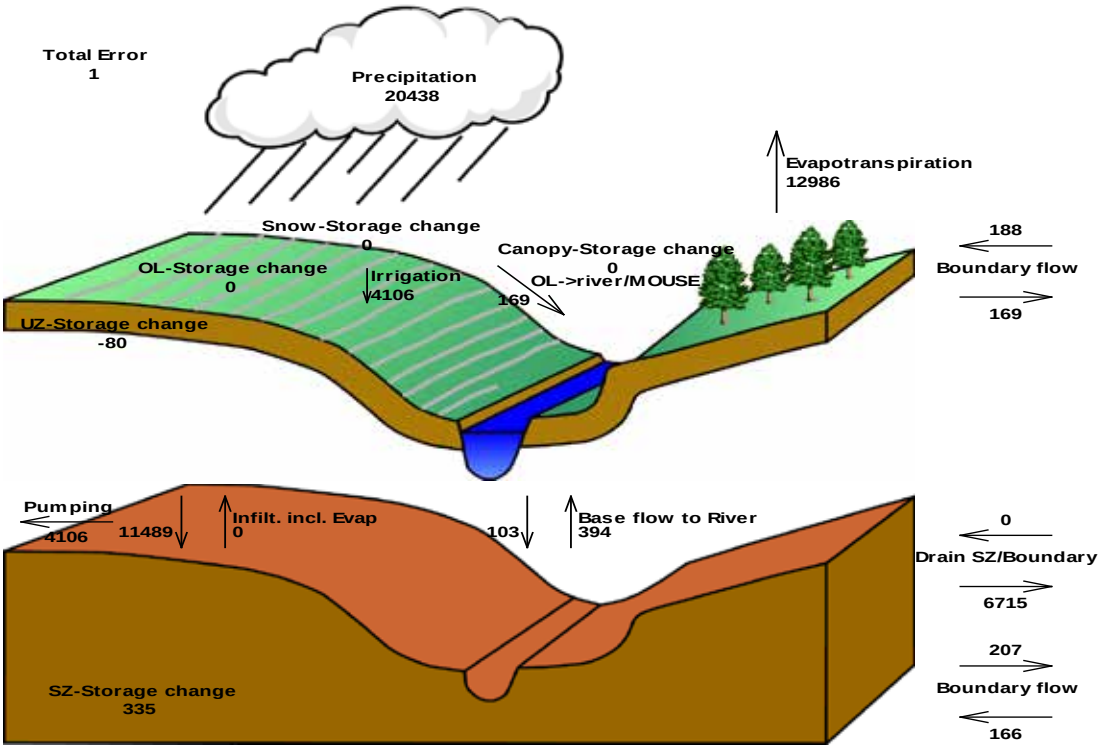

Figure J.8: Water balance (in mm) for the period 04 January 2005 to 31 December 2016 for Sirajganj district

Table J.8: Water balance for the period 04 January 2005 to 31 December 2016 for Sirajganj district

Components	Unsaturated Zone(UZ)		Saturated Zone (SZ)		River System		GW Recharge/Discharge	
	Inflow	Outflow	Inflow	Outflow	Inflow	Outflow	Recharge	Discharge
	(mm)	(mm)	(mm)	(mm)	(mm)	(mm)	(mm)	(mm)
Rainfall	20438	—	—	—	—	—	—	—
Evapotranspiration(ET)	—	12986	—	—	—	—	—	—
Abstraction	—	—	—	4106	—	—	—	—
Irrigation	4106	—	—	—	—	—	—	—
Capilary rise & ET from SZ to UZ	0	—	—	0	—	—	—	—
Deep Percolation from UZ to SZ	—	11489	11489	—	—	—	11489	0
Boundary Flow	188	169	166	207	—	—	0	41
Base Flow	—	—	103	394	394	103	0	291
Overland flow to river	—	169	—	—	169	—	—	—
Drain flow to river	—	—	0	0	0	0	0	0
OL storage Change	0	0	—	—	—	—	—	—
Drain SZ/Boundary	—	—	0	6715	—	—	0	6715
Total	**24732**	**24813**	**11758**	**11422**	**563**	**103**	**11489**	**7047**
Net Balance= Inflow-Outflow	**-81**		**336**		**460**		**4442**	
Explanation	**Inflow/Outflow of SZ**		**Change in Storage**		**River/Aquifer Interaction**		**Annual Recharge /Discharge**	

J.9 WATER BALANCE: THAKURGAON DISTRICT (2005-2016)

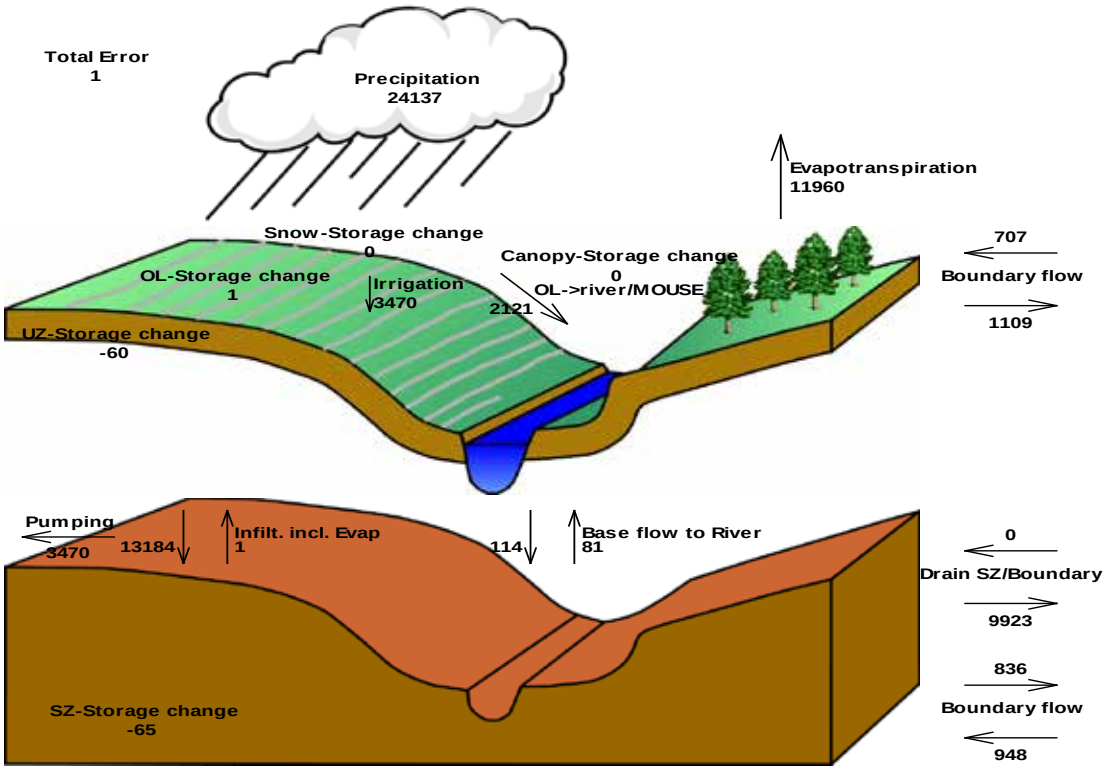

Figure J.9: Water balance (in mm) for the period 03 January 2005 to 31 December 2016 for Thakurgaon district

Table J.9: Water balance for the period 03 January 2005 to 31 December 2016 for Thakurgaon district

Components	Unsaturated Zone(UZ)		Saturated Zone (SZ)		River System		GW Recharge/Discharge	
	Inflow	Outflow	Inflow	Outflow	Inflow	Outflow	Recharge	Discharge
	(mm)	(mm)	(mm)	(mm)	(mm)	(mm)	(mm)	(mm)
Rainfall	24137	—	—	—	—	—	—	—
Evapotranspiration(ET)	—	11960	—	—	—	—	—	—
Abstraction	—	—	—	3470	—	—	—	—
Irrigation	3470	—	—	—	—	—	—	—
Capilary rise & ET from SZ to UZ	1	—	—	1	—	—	—	—
Deep Percolation from UZ to SZ	—	13184	13184	—	—	—	13183	0
Boundary Flow	707	1109	948	836	—	—	112	0
Base Flow	—	—	114	81	81	114	33	0
Overland flow to river	—	2121	—	—	2121	—	—	—
Drain flow to river	—	—	0	0	0	0	0	0
OL storage Change	0	1	—	—	—	—	—	—
Drain SZ/Boundary	—	—	0	9923	—	—	0	9923
Total	**28315**	**28375**	**14246**	**14311**	**2202**	**114**	**13328**	**9923**
Net Balance= Inflow-Outflow	**-60**		**-65**		**2088**		**3405**	
Explanation	**Inflow/Outflow of SZ**		**Change in Storage**		**River/Aquifer Interaction**		**Annual Recharge /Discharge**	

J.10 WATER BALANCE: PANCHAGARH DISTRICT (2005–2016)

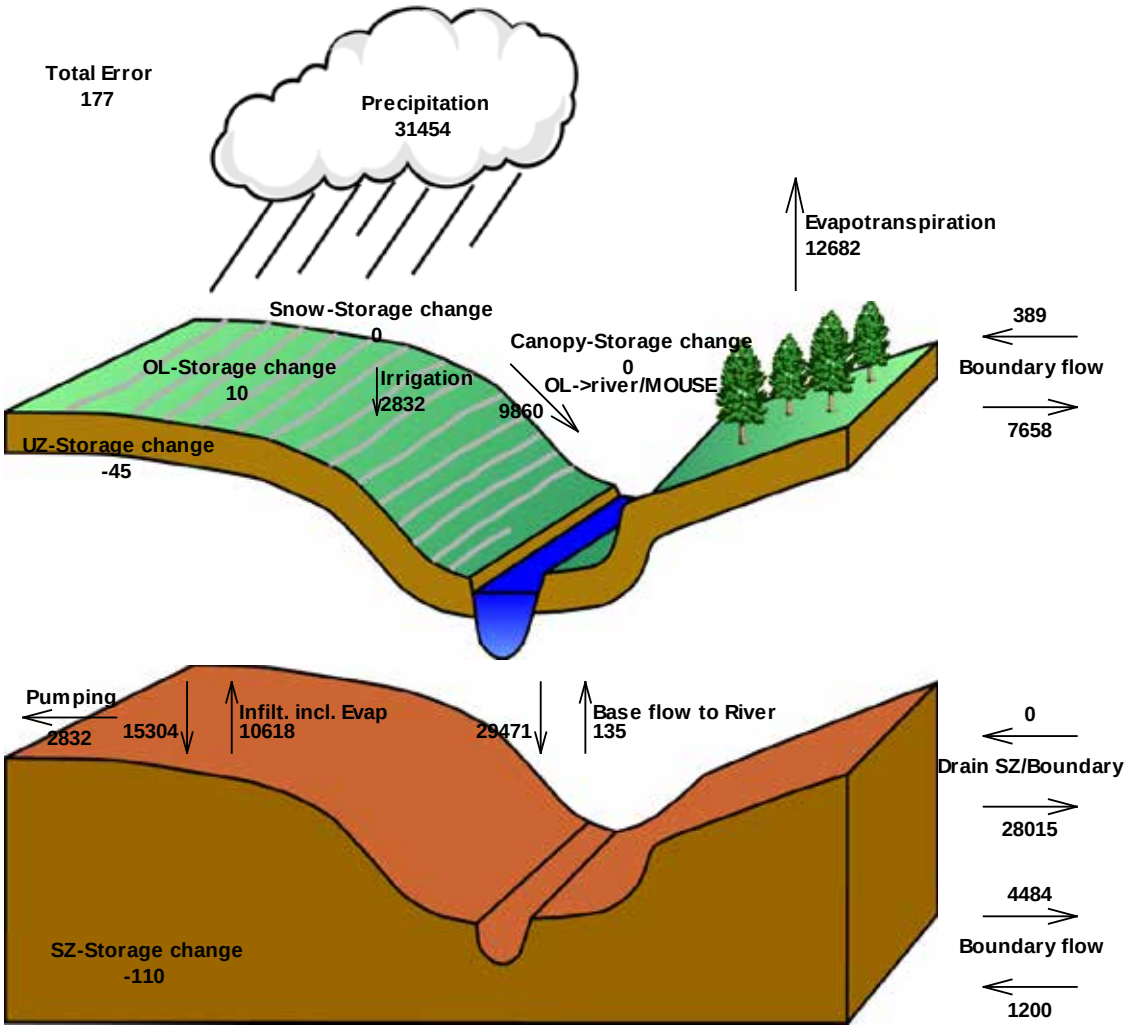

Figure J.10: Water balance (in mm) for the period 03 January 2005 to 31 December 2016 for Panchagarh district

Table J.10: Water balance for the period 03 January 2005 to 31 December 2016 for Panchagarh district

Components	Unsaturated Zone(UZ)		Saturated Zone (SZ)		River System		GW Recharge/Discharge	
	Inflow	Outflow	Inflow	Outflow	Inflow	Outflow	Recharge	Discharge
	(mm)	(mm)	(mm)	(mm)	(mm)	(mm)	(mm)	(mm)
Rainfall	31454	—	—	—	—	—	—	—
Evapotranspiration(ET)	—	12682	—	—	—	—	—	—
Abstraction	—	—	—	2832	—	—	—	—
Irrigation	2832	—	—	—	—	—	—	—
Capilary rise & ET from SZ to UZ	10618	—	—	10618	—	—	—	—
Deep Percolation from UZ to SZ	—	15304	15304	—	—	—	4686	0
Boundary Flow	389	7658	1200	4484	—	—	0	3284
Base Flow	—	—	29471	135	135	29471	29336	0
Overland flow to river	—	9860	—	—	9860	—	—	—
Drain flow to river	—	—	0	0	0	0	0	0
OL storage Change	0	10	—	—	—	—	—	—
Drain SZ/Boundary	—	—	0	28015	—	—	0	28015
Total	**45293**	**45514**	**45975**	**46084**	**9995**	**29471**	**34022**	**31299**
Net Balance= Inflow-Outflow	**-221**		**-109**		**-19476**		**2723**	
Explanation	**Inflow/Outflow of SZ**		**Change in Storage**		**River/Aquifer Interaction**		**Annual Recharge /Discharge**	

J.11 WATER BALANCE: JOYPURHAT DISTRICT (2005–2016)

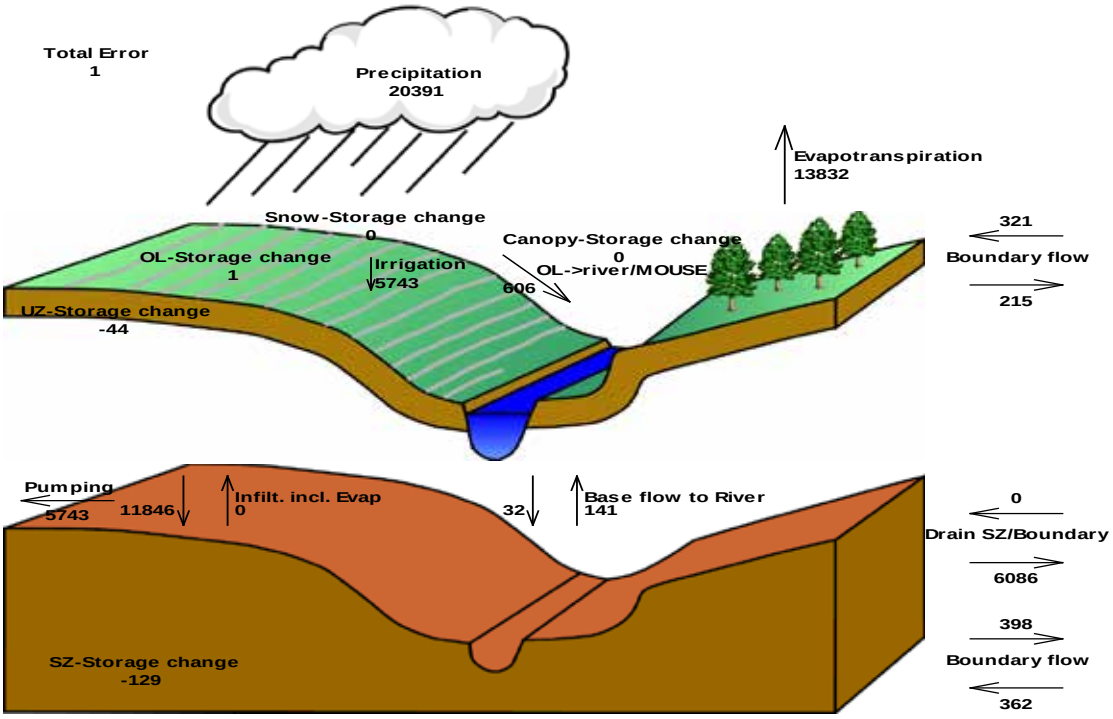

Figure J.11: Water balance (in mm) for the period 03 January 2005 to 31 December 2016 for Joypurhat district

Table J.11: Water balance for the period 03 January 2005 to 31 December 2016 for Joypurhat district

Components	Unsaturated Zone(UZ)		Saturated Zone (SZ)		River System		GW Recharge/Discharge	
	Inflow	Outflow	Inflow	Outflow	Inflow	Outflow	Recharge	Discharge
	(mm)	(mm)	(mm)	(mm)	(mm)	(mm)	(mm)	(mm)
Rainfall	20391	—	—	—	—	—	—	—
Evapotranspiration(ET)	—	13832	—	—	—	—	—	—
Abstraction	—	—	—	5743	—	—	—	—
Irrigation	5743	—	—	—	—	—	—	—
Capilary rise & ET from SZ to UZ	0	—	—	0	—	—	—	—
Deep Percolation from UZ to SZ	—	11846	11846	—	—	—	11846	0
Boundary Flow	321	215	362	398	—	—	0	36
Base Flow	—	—	32	141	141	32	0	109
Overland flow to river	—	606	—	—	606	—	—	—
Drain flow to river	—	—	0	0	0	0	0	0
OL storage Change	0	1	—	—	—	—	—	—
Drain SZ/Boundary	—	—	0	6086	—	—	0	6086
Total	**26455**	**26500**	**12240**	**12368**	**747**	**32**	**11846**	**6231**
Net Balance= Inflow-Outflow	**-45**		**-128**		**715**		**5615**	
Explanation	**Inflow/Outflow of SZ**		**Change in Storage**		**River/Aquifer Interaction**		**Annual Recharge /Discharge**	

J.12 WATER BALANCE: DINAJPUR DISTRICT (2005–2016)

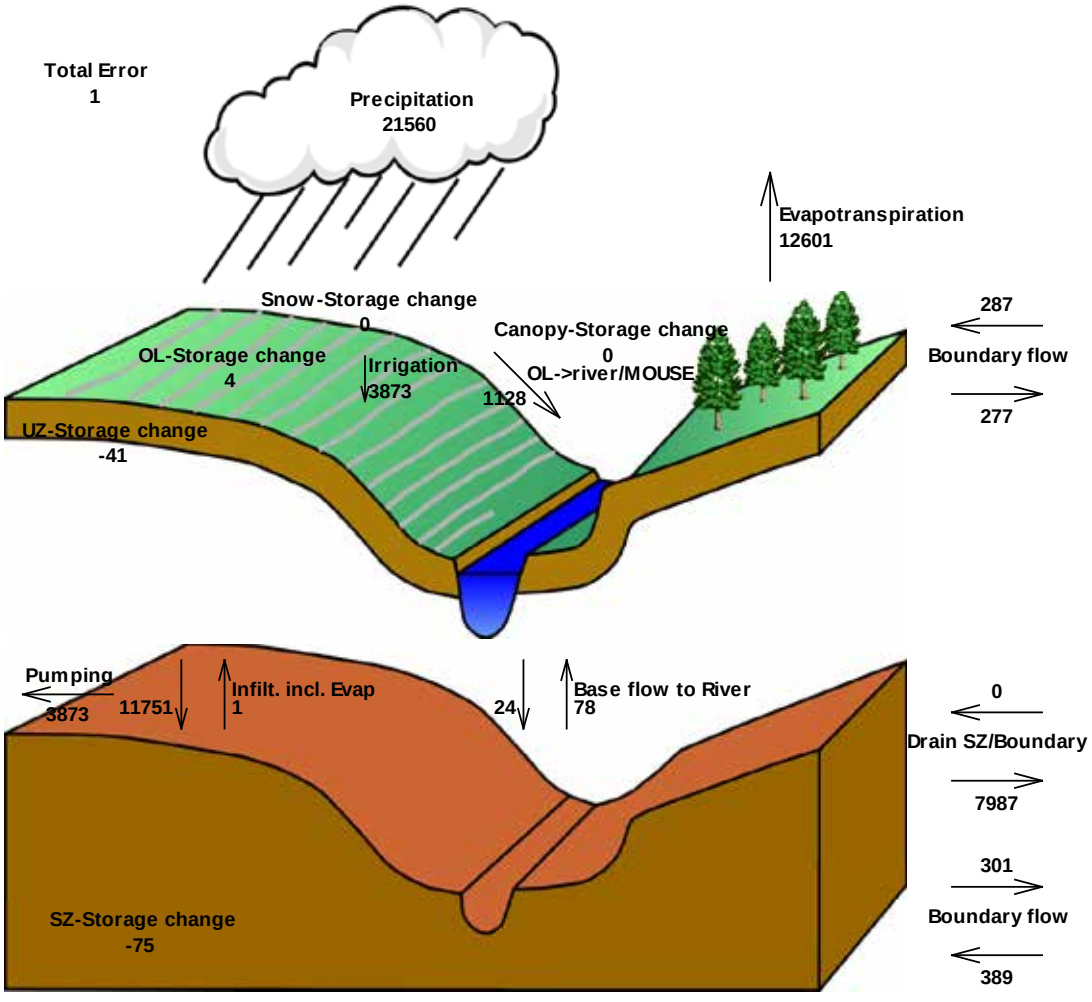

Figure J.12: Water balance (in mm) for the period 03 January 2005 to 31 December 2016 for Dinajpur district

Table J.12: Water balance for the period 03 January 2005 to 31 December 2016 for Dinajpur district

Components	Unsaturated Zone(UZ)		Saturated Zone (SZ)		River System		GW Recharge/Discharge	
	Inflow	Outflow	Inflow	Outflow	Inflow	Outflow	Recharge	Discharge
	(mm)	(mm)	(mm)	(mm)	(mm)	(mm)	(mm)	(mm)
Rainfall	21560	—	—	—	—	—	—	—
Evapotranspiration(ET)	—	12601	—	—	—	—	—	—
Abstraction	—	—	—	3873	—	—	—	—
Irrigation	3873	—	—	—	—	—	—	—
Capilary rise & ET from SZ to UZ	0	—	—	0	—	—	—	—
Deep Percolation from UZ to SZ	—	11751	11751	—	—	—	11751	0
Boundary Flow	287	277	389	301	—	—	88	0
Base Flow	—	—	24	78	78	24	0	54
Overland flow to river	—	1128	—	—	1128	—	—	—
Drain flow to river	—	—	0	0	0	0	0	0
OL storage Change	0	4	—	—	—	—	—	—
Drain SZ/Boundary	—	—	0	7987	—	—	0	7987
Total	**25720**	**25761**	**12164**	**12239**	**1206**	**24**	**11839**	**8041**
Net Balance= Inflow-Outflow	**-41**		**-75**		**1182**		**3798**	
Explanation	**Inflow/Outflow of SZ**		**Change in Storage**		**River/Aquifer Interaction**		**Annual Recharge /Discharge**	

J.13 WATER BALANCE: NATORE DISTRICT (2005–2016)

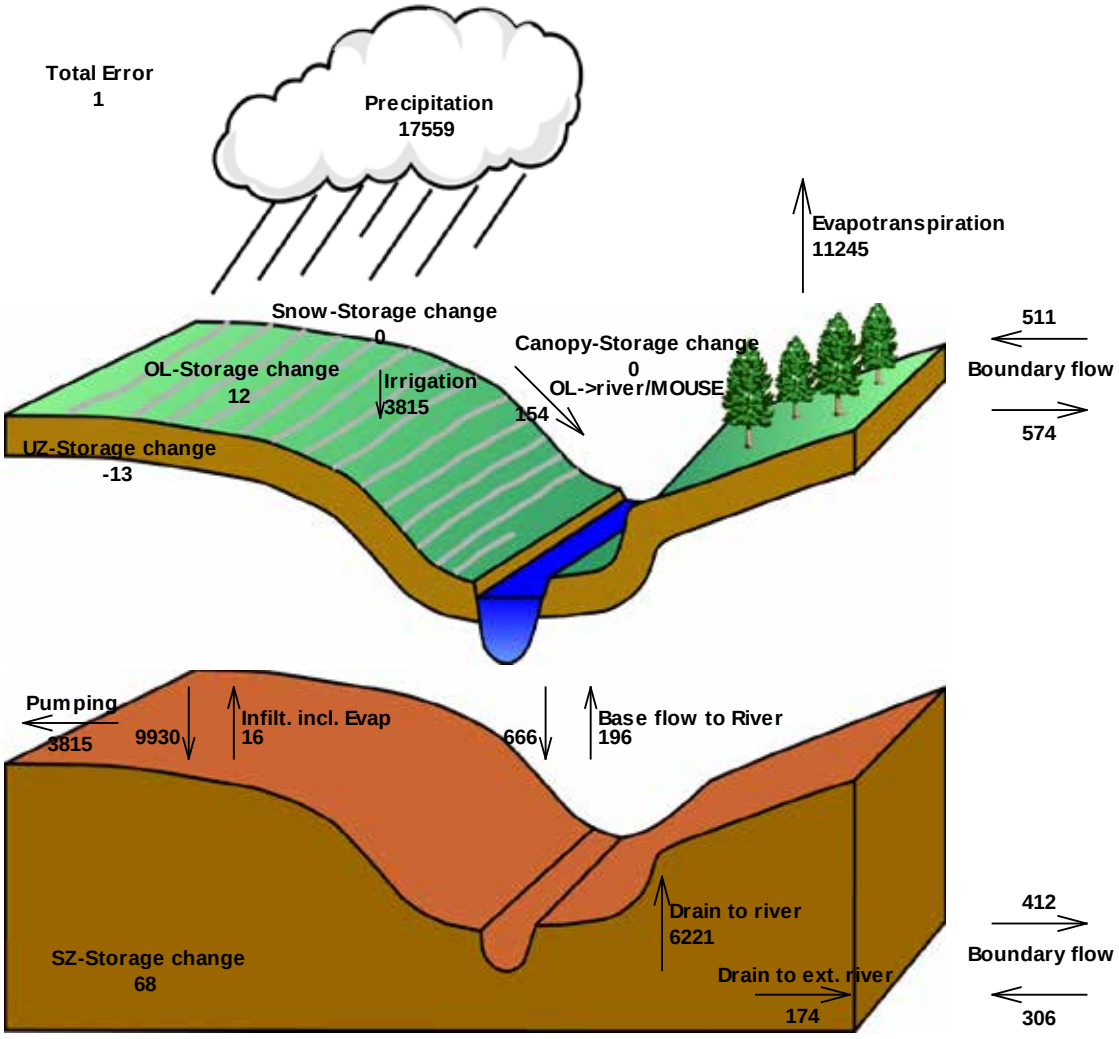

Figure J.13: Water balance (in mm) for the period 01 January 2005 to 31 December 2016 for Natore district

Table J.13: Water balance for the period 01 January 2005 to 31 December 2016 for Natore district

Components	Unsaturated Zone(UZ)		Saturated Zone (SZ)		River System		GW Recharge/Discharge	
	Inflow	Outflow	Inflow	Outflow	Inflow	Outflow	Recharge	Discharge
	(mm)	(mm)	(mm)	(mm)	(mm)	(mm)	(mm)	(mm)
Rainfall	17559	—	—	—	—	—	—	—
Evapotranspiration(ET)	—	11245	—	—	—	—	—	—
Abstraction	—	—	—	3815	—	—	—	—
Irrigation	3815	—	—	—	—	—	—	—
Capilary rise & ET from SZ to UZ	16	—	—	16	—	—	—	—
Deep Percolation from UZ to SZ	—	9930	9930	—	—	—	9914	0
Boundary Flow	511	574	306	412	—	—	0	106
Base Flow	—	—	666	196	196	666	470	0
Overland flow to river	—	154	—	—	154	—	—	—
Drain flow to river	—	—	0	6395	6395	0	0	6395
OL storage Change	0	12	—	—	—	—	—	—
Drain SZ/Boundary	—	—	0	0	—	—	0	0
Total	**21901**	**21915**	**10902**	**10834**	**6745**	**666**	**10384**	**6501**
Net Balance= Inflow-Outflow	**-14**		**68**		**6079**		**3883**	
Explanation	**Inflow/Outflow of SZ**		**Change in Storage**		**River/Aquifer Interaction**		**Annual Recharge /Discharge**	

J.14 WATER BALANCE: RAJSHAHI DISTRICT (2005-2016)

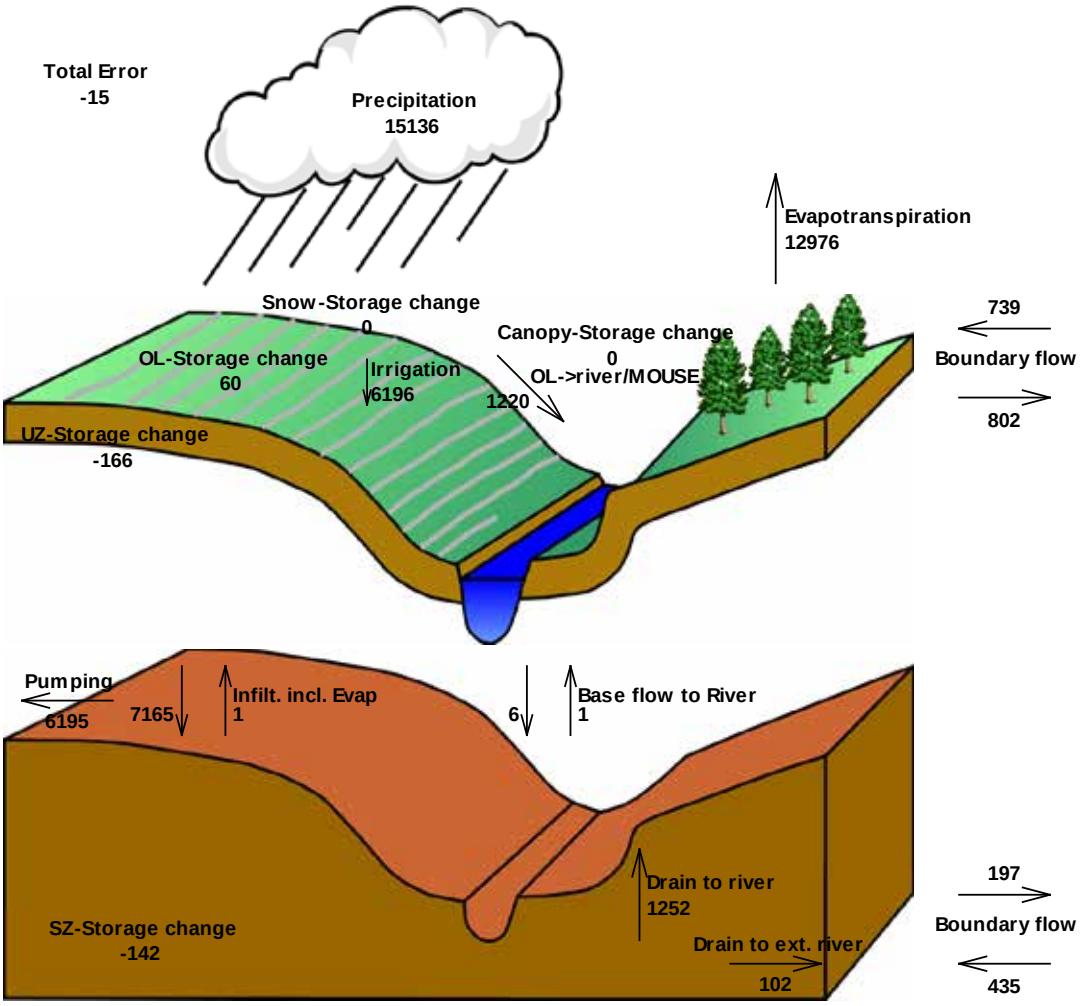

Figure J.14: Water balance (in mm) for the period 07 January 2005 to 26 December 2016 for Rajshahi district

Table J.14: Water balance for the period 07 January 2005 to 26 December 2016 for Rajshahi district

Components	Unsaturated Zone(UZ)		Saturated Zone (SZ)		River System		GW Recharge/Discharge	
	Inflow	Outflow	Inflow	Outflow	Inflow	Outflow	Recharge	Discharge
	(mm)	(mm)	(mm)	(mm)	(mm)	(mm)	(mm)	(mm)
Rainfall	15136	—	—	—	—	—	—	—
Evapotranspiration(ET)	—	12976	—	—	—	—	—	—
Abstraction	—	—	—	6196	—	—	—	—
Irrigation	6196	—	—	—	—	—	—	—
Capilary rise & ET from SZ to UZ	0	—	—	0	—	—	—	—
Deep Percolation from UZ to SZ	—	7165	7165	—	—	—	7165	0
Boundary Flow	739	802	435	197	—	—	238	0
Base Flow	—	—	6	1	1	6	5	0
Overland flow to river	—	1220	—	—	1220	—	—	—
Drain flow to river	—	—	0	1354	1354	0	0	1354
OL storage Change	0	60	—	—	—	—	—	—
Drain SZ/Boundary	—	—	0	0	—	—	0	0
Total	**22071**	**22223**	**7606**	**7748**	**2575**	**6**	**7408**	**1354**
Net Balance= Inflow-Outflow	**-152**		**-142**		**2569**		**6054**	
Explanation	**Inflow/Outflow of SZ**		**Change in Storage**		**River/Aquifer Interaction**		**Annual Recharge /Discharge**	

J.15 WATER BALANCE: CHAPAI NAWABGANJ DISTRICT (2005–2016)

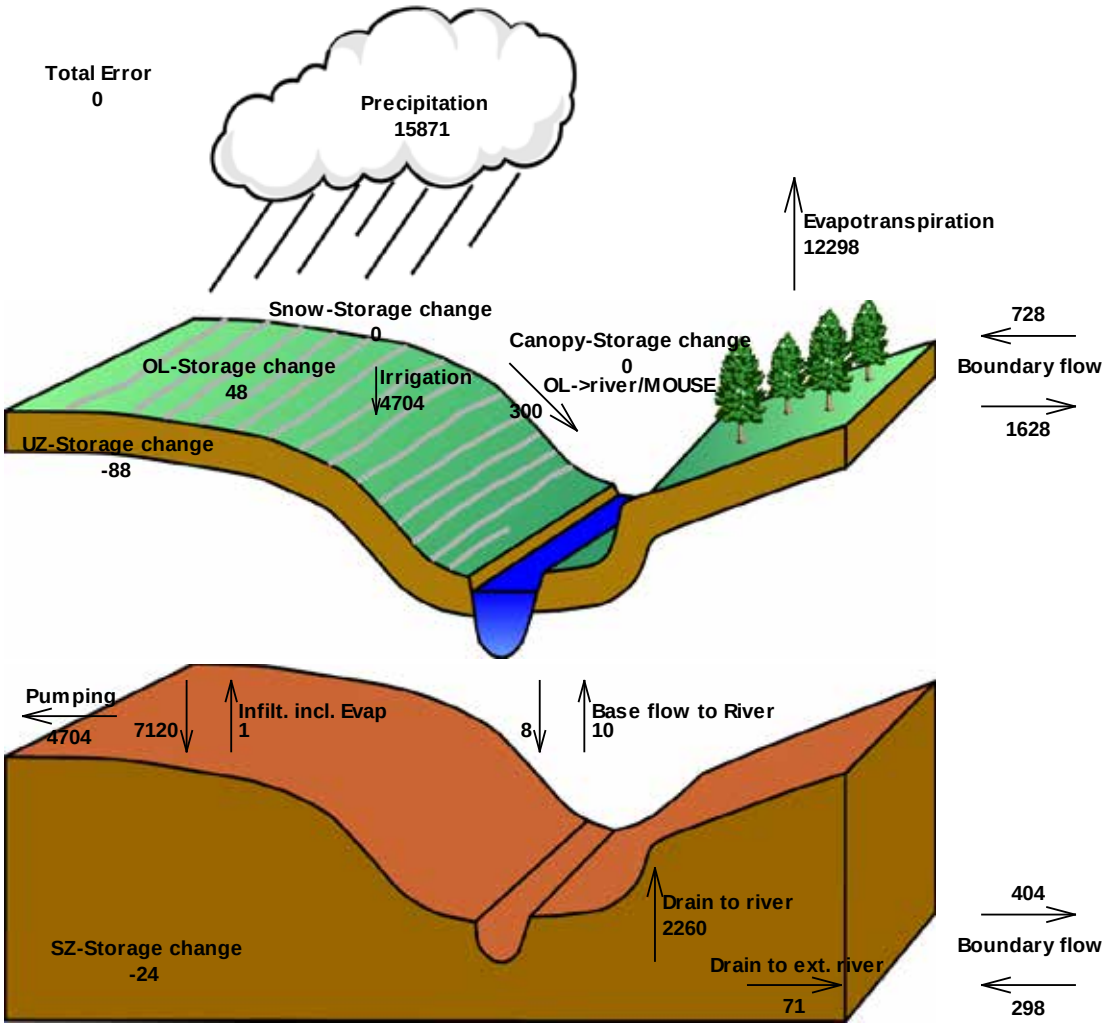

Figure J.15: Water balance (in mm) for the period 07 January 2005 to 26 December 2016 for Chapai Nawabganj district

Table J.15: Water balance for the period 07 January 2005 to 26 December 2016 for Chapai Nawabganj district

Components	Unsaturated Zone(UZ)		Saturated Zone (SZ)		River System		GW Recharge/Discharge	
	Inflow	Outflow	Inflow	Outflow	Inflow	Outflow	Recharge	Discharge
	(mm)	(mm)	(mm)	(mm)	(mm)	(mm)	(mm)	(mm)
Rainfall	15871	—	—	—	—	—	—	—
Evapotranspiration(ET)	—	12298	—	—	—	—	—	—
Abstraction	—	—	—	4704	—	—	—	—
Irrigation	4704	—	—	—	—	—	—	—
Capilary rise & ET from SZ to UZ	1	—	—	1	—	—	—	—
Deep Percolation from UZ to SZ	—	7120	7120	—	—	—	7119	0
Boundary Flow	728	1628	298	404	—	—	0	106
Base Flow	—	—	8	10	10	8	0	2
Overland flow to river	—	300	—	—	300	—	—	—
Drain flow to river	—	—	0	2331	2331	0	0	2331
OL storage Change	0	48	—	—	—	—	—	—
Drain SZ/Boundary	—	—	0	0	—	—	0	0
Total	**21304**	**21394**	**7426**	**7450**	**2641**	**8**	**7119**	**2439**
Net Balance= Inflow-Outflow	**-90**		**-24**		**2633**		**4680**	
Explanation	**Inflow/Outflow of SZ**		**Change in Storage**		**River/Aquifer Interaction**		**Annual Recharge /Discharge**	

J.16 WATER BALANCE: NAOGAON DISTRICT (2005–2016)

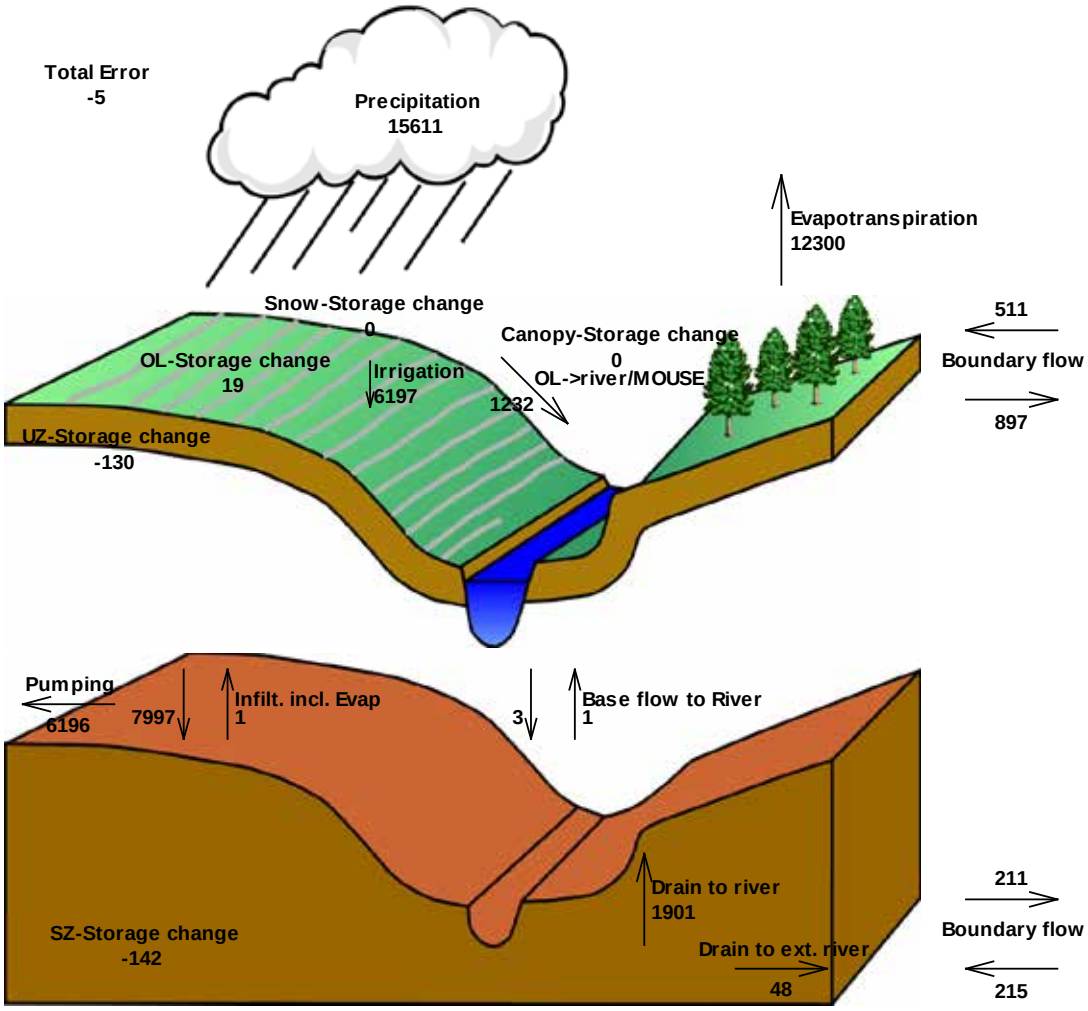

Figure J.16: Water balance (in mm) for the period 07 January 2005 to 26 December 2016 for Naogaon district

Table J.16: Water balance for the period 07 January 2005 to 26 December 2016 for Naogaon district

Components	Unsaturated Zone(UZ)		Saturated Zone (SZ)		River System		GW Recharge/Discharge	
	Inflow	Outflow	Inflow	Outflow	Inflow	Outflow	Recharge	Discharge
	(mm)	(mm)	(mm)	(mm)	(mm)	(mm)	(mm)	(mm)
Rainfall	15611	—	—	—	—	—	—	—
Evapotranspiration(ET)	—	12300	—	—	—	—	—	—
Abstraction	—	—	—	6196	—	—	—	—
Irrigation	6197	—	—	—	—	—	—	—
Capilary rise & ET from SZ to UZ	1	—	—	1	—	—	—	—
Deep Percolation from UZ to SZ	—	7997	7997	—	—	—	7996	0
Boundary Flow	511	897	215	211	—	—	4	0
Base Flow	—	—	3	1	1	3	2	0
Overland flow to river	—	1232	—	—	1232	—	—	—
Drain flow to river	—	—	0	1949	1949	0	0	1949
OL storage Change	0	19	—	—	—	—	—	—
Drain SZ/Boundary	—	—	0	0	—	—	0	0
Total	**22320**	**22445**	**8215**	**8358**	**3182**	**3**	**8002**	**1949**
Net Balance= Inflow-Outflow	**-125**		**-143**		**3179**		**6053**	
Explanation	**Inflow/Outflow of SZ**		**Change in Storage**		**River/Aquifer Interaction**		**Annual Recharge /Discharge**	

REFERENCES

Ahmad MU, Kirby JM, Islam MS, Hossain MJ, Islam MM (2014) Groundwater use for irrigation and its productivity: Status and opportunities for crop intensification for food security in Bangladesh. Water Resour. Manage. 28, 1415–1429

Al-Amin AKMA, Akhter T, Islam AHMS, Jahan H, Hossain MJ, Haque Prodhan MMH, Mainuddin M, Kirby JM (2019) An Intra-household Analysis of Farmers' Perceptions of and Adaptation to Climate Change Impacts: Empirical Evidence from Drought Prone Zones of Bangladesh. Climatic Change. 156: 545–565

Chen Y, Oliver DS (2012) Ensemble randomized maximum likelihood method as an iterative ensemble smoother. *Mathematical Geosciences*, *44*(1), 1-26

Doherty J (2015) *Calibration and uncertainty analysis for complex environmental models*. Brisbane, Australia: Watermark Numerical Computing.

Doorenbos J, Pruitt WO (1984) Crop Water Requirements. FAO Irrigation and Drainage. Paper 24 FAO, Rome

Hodgson GA, Ali R, Turner J, Ahmad M, Dawes W, Masud MS, Hossain MJ, Alam S, Islam MM, Saha GK, Barman TD (2014) Bangladesh Integrated Water Resources Assessment Supplementary Report: Water table trends and associated vertical water balance in Bangladesh. CSIRO, Australia

Hodgson GA, Mojid M, Peña-Arancibia J, Islam MT, Mainuddin M (2021) Groundwater trends in the northwest region of Bangladesh. Technical Report CSIRO, Australia 180pp

IPCC (2014) Summary for policymakers In: Climate Change 2014: Impacts, Adaptation, and Vulnerability Part A: Global and Sectoral Aspects Contribution of Working Group II to the Fifth Assessment Report of the Intergovernmental Panel on Climate Change

Jeuland M, Harshadeep N, Escurra J, Blackmore D, Sadoff C (2013) Implications of climate change for water resources development in the Ganges basin. Water Policy 15:26–50

Kirby JM , Ahmad MD, Mainuddin M, Palash W, Quadir M , Shah-Newaz SM, Hossain MM (2015) The impact of irrigation development on regional groundwater resources in Banglades. Agric Water Manage 159, 264-276

Kirby M, Ahmed M, Mainuddin M, Palash W, Qadir E and Shah-Newaz SM (2014) Bangladesh Integrated Water Resources Assessment, supplementary report: approximate regional water balances A report for the DFAT Australian Aid – CSIRO Research for Development Alliance. CSIRO, Australia

Kirby JM, Mainuddin M, Mpelasoka F, Ahmad MD, Palash W, Quadir ME, Shah-Newaz SM, Hossain MM (2016) The impact of climate change on regional water balances in Bangladesh. Climatic Change 135:481-491 DOI 10 1007/s10584-016-1597-1

Karim F, Mainuddin M, Hasan M, Kirby M (2020) Assessing the Potential Impacts of Climate Changes on Rainfall and Evapotranspiration in the Northwest Region of Bangladesh. Climate 8, 94; doi:10 3390/cli8080094

Karim F, Islam MT, Mainuddin M, Janardhanan S, Islam MM, Masud MS, Kirby M (2021) Surface water modelling in the north west region of Bangladesh A technical report produced by the CSIRO and Institute of Water Modelling. Sustainable Development Investment Portfolio project. CSIRO, Australia

Kristensen KJ, Jensen SE (1975) A model for estimating actual evapotranspiration from potential evapotranspiration. Hydrology Research, 6(3), 170-188

Harbaugh AW (2005) MODFLOW-2005, the U S Geological Survey modular ground-water model -- the Ground-Water Flow Process: U S Geological Survey Techniques and Methods 6-A16

Mainuddin M, Alam MM, Maniruzzaman M, Islam MT, Kabir MJ, Hasan M, Scobie M, Schmidt E (2019) Irrigated agriculture in the northwest region of Bangladesh. CSIRO, Australia

Mainuddin M, Kirby M, Chowdhury RAR, Sanjida L, Sarker MH, Shah-Newaz SM (2014) Bangladesh integrated water resources assessment supplementary report: land use, crop production, and irrigation demand CSIRO: Water for a Healthy Country Flagship

Mainuddin M, Kirby M, Chowdhury RAR, Shah-Newaz SM (2015) Spatial and temporal variations of, and the impact of climate change on, the dry season crop irrigation requirements in Bangladesh Irrigation Sci 33: 107–120

Mainuddin M, Maniruzzaman M, Alam MM, Mojid MA, Schmidt EJ, Islam MT, Scobie M (2020) Water usage and productivity of Boro rice at the field level and their impacts on the sustainable groundwater irrigation in the North-West Bangladesh. Agricultural Water Management 240, 106294 https://doi org/10 1016/j agwat 2020 106294

Mainuddin M, Peña-Arancibia JL, Hodgson G, Kirby JM (2021) The impact of climate change and agricultural development scenarios on district water balances in northwest Bangladesh. Technical report, Sustainable Development Investment Portfolio project. CSIRO, Australia

Masood M, Yeh PJ-F, Hanasaki N, Takeuchi K (2015) Model study of the impacts of future climate change on the hydrology of Ganges–Brahmaputra–Meghna basin. Hydrol Earth Syst Sc 19:747–770

Mojid MA, Mainuddin M, Murad KFI, Kirby JM (2021a) Water usage trends under intensive groundwater-irrigated agricultural development in a changing climate – Evidence from Bangladesh. Agricultural Water Management 251: 106873 https://doi org/10 1016/jagwat 2021 10687

Mojid MA, Aktar S, Mainuddin M (2021b) Rainfall-induced recharge-dynamics of heavily exploited aquifers – a case study in the North-West region of Bangladesh. Groundwater for Sustainable Development 15, 100665 https://doi org/10 1016/j gsd 2021 100665

Mojid MA, Parvez MF, Mainuddin M, Hodgson G (2019) Water table trend—a sustainability status of groundwater development in North-West Bangladesh. Water 11, p 1182, doi:10 3390/w11061182

Moors EJ, Groot A, Biemans H, van Sceltinga CT, Siderius C, Stoffel M, Huggel C, Wiltshire A, Mathison C, Ridley J, Jacob D, Kumar P, Bhadwal S, Gosina A, Collins DN (2011) Adaptation to changing water resources in the Ganges basin, northern India. Environ Sci Pol 14:758–769

MPO (Master Plan Organization) (1987) Groundwater Resources of Bangladesh Technical Report no 5 Master Plan Organization, Dhaka Hazra, USA; Sir M MacDonald, UK; Meta, USA; EPC, Bangladesh

Mulligan M, Fisher M, Sharma B, Xu Z, Ringler C, Mahe G, Jarvis A, Ramirez J, Clanet JC, Ogilvie A, Ahmad MD (2011) The nature and impact of climate change in the Challenge Program on Water and Food (CPWF) basins. Water Int 36:96–124

Peña-Arancibia JL, Mahboob G, Islam T, Mainuddin M, Yu Y, Ibn Murad K, Saha K, Hossain A, Moniruzzaman M, Hodgson G, Kirby JM (2021a) Land cover and cropping system analysis Technical Report South Asia Sustainable Development Investment Portfolio (SDIP) project CSIRO, Australia

Peña-Arancibia JL, Mahboob MG, Islam AFMT, Mainuddin M, Yu Y, Ahmad M, Murad KFI, Saha K, Hossain MA, Moniruzzaman M, Ticehurst C, Kong D (2021b) The Green Revolution from space: Mapping the historic dynamics of main rice types in one of the world's food bowls. Remote Sensing Applications: Society and Environment 21: 100460

Peña-Arancibia JL, Mainuddin M, Ahmad MD, Hodgson G, Murad KFI, Ticehurst C, Kirby JM (2020) Groundwater use and rapid irrigation expansion in a changing climate: hydrological drivers in one of the world's food bowls. Journal of Hydrology, 581, 124300

Rahman MW, Jahan H, Palash MS, Jalilov S, Mainuddin M (2020) An Empirical Investigation of Men's Views of Women's Contribution to Farming in Northwest Bangladesh Sustainability 12: 3521; doi:10 3390/su12093521

Rahman MW, Jahan H, Palash MS, Jalilov S-M, Mainuddin M, Wahid S (2021) Sustaining groundwater Irrigation for Food Security in the Northwest Region of Bangladesh: Socioeconomics, Livelihood and Gender Aspects. South Asia Sustainable Development Investment Portfolio (SDIP) project. CSIRO, Australia

Refsgaard JC, Storm B (1995) MIKE SHE In Computer Models of Watershed Hydrology, 809-846 V Singh, ed Highland Ranch, Colo : Water Resources Publication

Rose S (2009) Groundwater Recharge and Discharge Groundwater 3, 73

Rushton KR, Zaman MA, Hasan M (2020) Monitoring groundwater heads and estimating recharge in multi-aquifer systems illustrated by an irrigated area in north-west Bangladesh. Sust Water Resour Manage 6:22 https://doi org/10 1007/s40899-020-00382-y

WARPO (Water Resources Planning Organization) (2000) National Water Management Plan Project draft development strategy, Ministry of Water Resources, Government of the People's Republic of Bangladesh, Dhaka

White JT, Fienen MN, Barlow PM, Welter DE(2018) A tool for efficient, model-independent management optimization under uncertainty. Environmental modelling & software, *100*, 213-221

Zahid A, Ali MH, Khan M (2016) Evaluation of the aquifer system and groundwater quality of the north-western districts of Bangladesh for development potential. BRAC Univ J 11 (02) http://hdl handle net/10361/8389

Zheng H, Chiew FH, Charles S, Podger G (2018) Future climate and runoff projections across South Asia from CMIP5 global climate models and hydrological modelling. Journal of Hydrology: Regional Studies, 18, 92-109

As Australia's national science agency and innovation catalyst, CSIRO is solving the greatest challenges through innovative science and technology.

CSIRO. Unlocking a better future for everyone.

Contact us

1300 363 400
+61 3 9545 2176
csiroenquiries@csiro.au
www.csiro.au

For further information

CSIRO Land and Water
Sreekanth Janardhanan
Sreekanth.janardhanan@csiro.au
csiro.au/L&W

CSIRO Land and Water
Mohammed Mainuddin
Mohammed.Mainuddin@csiro.au
csiro.au/L&W